

# **A pathological investigation of the frontal lobe in post-stroke dementia and other ageing-related dementias**

Vincent Foster MRes, BSc Hons

Neurovascular Research Group

Institute of Neuroscience

Newcastle University

Campus for Ageing and Vitality

Newcastle upon Tyne

NE4 5PL

Thesis submitted for the degree of Doctor of Philosophy in

Newcastle University

January 2015

## **Abstract**

Approximately 30% of elderly stroke survivors develop post-stroke dementia (PSD). The mechanisms underlying this cognitive decline following stroke are unclear. Vascular pathology is associated with the frontal lobe, damage to which may result in executive dysfunction; a common clinical outcome of PSD. Previous pathological studies in PSD subjects have found that pyramidal neurons in the CA1 region of the hippocampus were particularly vulnerable, with atrophy of these cells associated with cognitive impairment. In this study we test the hypothesis that similar changes in pyramidal neurons in the three prefrontal circuits which control executive function may be related to executive dysfunction. The three circuits are; the dorsolateral prefrontal cortex (dlPFC), anterior cingulate cortex (ACC) and the orbitofrontal cortex (OFC).

Histological and immunohistochemical staining with three dimensional morphometric analysis and quantitative image analysis was carried out in fixed paraffin-embedded prefrontal brain sections from the MRC funded CogFAST study (a long-term prospective study designed to investigate delayed dementia after stroke) as well as frontal brain tissue from aged-matched controls and pathologically defined dementia groups: vascular dementia (VaD), Alzheimer's disease (AD), and those with mixed Alzheimer's disease and vascular dementia (mixed).

Pyramidal neuron volumes were significantly reduced in PSD, VaD, mixed, and AD when compared to aged-controls and post-stroke non demented (PSND) subjects in layer III, with layer V following a similar pattern. The neuronal changes in PSD correlated with global and executive function scores and were associated with markers for mitochondrial function, though did not correlate with tau or amyloid burden. Neuronal volumes in the ACC and the OFC did not significantly vary between groups; however pyramidal neurons within the OFC were significantly smaller in all groups (controls and disease) when compared to controls in dlPFC and ACC. There were no significant changes in pyramidal neuron densities between PSND and PSD in any of the three frontal regions. Analysis of the interneuronal densities revealed no significant differences between inhibitory neurons in PSND and PSD subjects. Pyramidal neuron

volume changes did not appear to be associated with white matter (WM) pathology in post-stroke subjects. These findings suggest that pyramidal neuronal volume loss in the dIPFC is associated with cognitive decline in post-stroke and ageing-related dementia.

The lack of relationship between AD type pathology, WM pathology, or interneuronal changes suggests dysfunction of the pyramidal neurons in the dIPFC play an important role in the development of executive dysfunction in PSD.

## **Acknowledgments**

First and foremost I would like to thank my supervisor, Professor Raj Kalaria for giving me the opportunity to complete a PhD in an area I find so interesting and for his support, knowledge, and encouragement throughout my four years working with him.

I would like to extend my heartfelt thanks and gratitude to Mr. Arthur Oakley who has made my time here as straightforward and painless as it has been. For his help, attitude to research, and unending depths of experience he ensured there was never an obstacle which could not be surmounted.

I would like to thank Dr. Louise Allan for her help and support throughout the writing of this thesis.

I would like to extend my gratitude to Janet Slade, Ross Hall, and Mary Johnson for their unwavering support throughout my time in Newcastle and sharing their boundless expertise with me, and who without I would be forever lost in the lab.

I would like to give special thanks to those who have made my years here not only manageable but also enjoyable. To Dr. Lucy Craggs, Dr. Matthew Burke, Dr. Elizabeth Gemmell, Dr. Rufus Akinyemi, and Dr. Yoshiki Hase who together made up a truly excellent research team. I would also like to give special thanks to Dr. Ahmad Khundakar, whose guidance and expertise using 3D stereology ensured my PhD got off on the right track, and whose advice was always welcome.

I would also like to thank Dr. Yumi Yamamoto for her ingenious invention of the VasCal software. I would also like to thank Alex Giffen, Jack Eklid, Jennifer Horn, Shobana Anpalakhan, Joseph Osman, Andrew Graham and the staff of the Newcastle Brain Tissue Resource for their assistance during my studies.

I would like to thank the Medical Research Council for funding my research as part of the Lifelong Health and Wellbeing Initiative, which supported the Centre for Brain Ageing and Vitality.

Finally I would like to thank my family for their unwavering support, and Fiona Middleton who put up with me, throughout.

## Contents

Chapter 1. Introduction .....	1
1.1. Normal ageing and dementia.....	1
1.1.2. Ageing and stroke .....	2
1.1.3. Stroke and dementia .....	3
1.1.4. Dementia and cerebrovascular disease (CVD) .....	6
1.1.5. Large and small vessel disease .....	7
1.1.6. Alzheimer's disease (AD).....	10
1.1.7. Mixed dementia.....	13
1.2. The prefrontal cortex.....	16
1.2.1. The prefrontal cortex and disease.....	16
1.2.2. Cortical architecture and pyramidal neurons .....	17
1.2.3. The prefrontal circuits.....	21
1.3. The prefrontal cortex circuit and vascular disease.....	24
1.3.1. Interneurons and the inhibition circuits .....	25
1.3.2. Glial cells.....	34
1.4. The cognitive function after stroke (CogFAST) study and it's key findings.....	38
1.4.2. Neuropathological assessment and dementia diagnosis.....	42
1.5. Aims and objectives.....	43
Chapter 2. Methods and Materials.....	44
2.1. Introduction .....	44
2.1. The Cognitive function after stroke (CogFAST) prospective study .....	44
2.1.1. The study design .....	44
2.1.2. Participants from the COGFAST study.....	47
2.2. Demographics of subjects analysed in the study .....	47
2.3. Other participants .....	49
2.4. Tissue acquisition .....	49
2.5. Sectioning and tissue preparation.....	50
2.6. Histological staining .....	52
2.6.1. Haematoxylin and Eosin (H&E).....	52
2.6.2. Cresyl Fast Violet (CFV).....	52
2.6.3. Luxol Fast Blue (LFB).....	53
2.7. Immunohistochemistry (IHC) .....	55
2.7.1. IHC methods .....	55
2.7.2. Fluorescent labelling (double immunofluorescence) .....	56

2.8.	Imaging and image analyses techniques .....	58
2.8.1.	Brightfield microscopy .....	58
2.8.2.	Densitometric image analysis.....	58
2.8.3.	Three dimensional stereology .....	60
2.8.4.	2D analysis of pyramidal neurons .....	64
2.8.5.	Sclerotic index measurements. ....	65
2.9.	Atrophy analysis estimates .....	66
2.9.1.	Myelin index .....	67
2.10.	Golgi-Cox technique .....	69
2.10.1.	Rapid single-section Golgi technique.....	69
2.10.2.	Golgi-Kopsch technique.....	69
2.11.	Statistical analyses .....	70
Chapter 3.	Pyramidal neurons of the prefrontal cortex .....	71
3.1.	Introduction.....	71
3.1.1.	Stereological analysis of the pre-frontal cortex.....	72
3.2.	Methods.....	74
3.2.1.	Subject demographics.....	74
3.2.2.	Three dimensional stereological analysis of neuronal volumes and densities.....	77
3.2.3.	Two dimensional analysis .....	77
3.2.4.	Sclerotic index.....	77
3.2.5.	Immunohistochemistry .....	77
3.2.6.	Fluorescent immunohistochemistry.....	78
3.2.7.	Cortical thickness measurements and atrophy estimates .....	78
3.2.8.	Stroke location analysis.....	78
3.2.9.	Statistical analysis .....	78
3.3.	Results.....	79
3.3.1.	Pyramidal neuronal densities .....	79
3.3.2.	Pyramidal neuronal volumes .....	81
3.3.3.	Two dimensional analysis .....	85
3.3.4.	Correlations with neuropathological findings .....	87
3.3.5.	Clinical features in post-stroke dementia and VaD subjects.....	88
3.3.6.	SMI31/32 positive cells in the dlPFC of post-stroke cases and other dementias .....	88
3.3.7.	Cortical thickness and dlPFC atrophy .....	94
3.3.8.	Comparison of Alzheimer's type pathology between cases. ....	97
3.4.	Discussion .....	99
3.4.1.	3D stereological analysis.....	99
3.4.2.	Neuronal densities.....	99

3.4.3. Neuronal volumes .....	100
3.4.4. Neuronal volumes and cognitive impairment.....	101
3.4.5. Interlaminar correlation.....	102
3.4.6. Comparison of neurofilament markers in post-stroke survivors and other groups.....	103
3.4.7. Neuronal volume loss, cortical thinning and atrophy .....	104
3.4.8. Alzheimer’s type and vascular type pathology in post-stroke dementia and other dementias. ....	105
3.5. Conclusion .....	106
Chapter 4. Non-pyramidal neurons and glial cells within the dorsolateral prefrontal cortex in post-stroke dementia.....	107
4.1. Introduction .....	107
4.1.1. Non-pyramidal neurons and disease.....	107
4.1.2. Glial cells.....	108
4.2. Methods.....	110
4.2.1. Subject demographics.....	110
4.2.2. Three dimensional analysis of non-pyramidal neuron and glial cell densities in layers III and V of the dlPFC. ....	111
4.2.3. Immunohistochemical analysis of interneuronal cell populations in layers III and V the dlPFC .....	111
4.2.4. Statistical analysis .....	112
4.3. Results.....	112
4.3.1. Distribution of non- pyramidal neurons.....	112
4.3.2. Three dimensional stereological analysis of interneuronal densities in pyramidal layers III and V of the dlPFC.....	112
4.3.3. Immunohistochemical analysis of non-pyramidal neurons .....	118
4.3.4. Three dimensional stereological analysis of glial cell density.....	126
4.4. Discussion .....	129
4.4.1. 3D stereological analysis of non-pyramidal neuron density in the dlPFC .....	129
4.4.2. Immunohistological analysis of interneurons in the dlPFC. ....	132
4.5. Conclusions .....	134
Chapter 5. White matter changes in the frontal lobe in post-stroke dementia. ....	135
5.1. Introduction.....	135
5.1.1. Myelin and axons in post-stroke and other dementias. ....	135
5.1.2. Retrograde vs. anterograde neurodegeneration. ....	136
5.1.3. Vascular pathology and frontal white matter. ....	137
5.2. Methods.....	139
5.2.1. Details of subjects used in this study.....	139

5.2.2.	IHC and image analysis .....	140
5.2.3.	Myelin index assessment .....	140
5.3.	Results.....	141
5.3.1.	Myelin Index .....	141
5.3.2.	SMI32 analysis of axonal damage.....	145
5.3.3.	Correcting for myelin loss.....	147
5.3.4.	Adjusted SMI32 staining values .....	147
5.3.5.	Analysis of SMI31 staining in the white matter. ....	150
5.3.6.	Analysis of vascular pathology in the white matter.....	155
5.3.7.	GRP78 staining of oligodendrocytes .....	157
5.4.	Discussion .....	159
5.4.1.	White matter loss.....	159
5.4.2.	Corrected SMI32 as a marker for WM damage.....	160
5.4.3.	SMI31 analysis of frontal WM integrity. ....	161
5.4.4.	Myelin loss as an effective measure of axonal damage and of cognitive function. ....	162
5.4.5.	Vascular pathology in frontal WM.....	162
5.4.6.	GRP78 staining as a marker for oligodendrocyte pathology .....	163
5.5.	Conclusion .....	163
Chapter 6.	Markers of metabolism in the dIPFC .....	165
6.1.	Introduction.....	165
6.1.1.	Neuronal metabolism .....	165
6.2.	Methods.....	170
6.2.1.	Details of subjects used in this study.....	170
6.2.2.	Immunohistochemical analysis.....	171
6.2.3.	Statistics.....	171
6.3.	Results.....	171
6.3.1.	GRP78 staining in layers III and V of the dIPFC.....	171
6.3.2.	COX4 immunoreactivity in pyramidal neurons .....	176
6.3.3.	COX4 positive neurons as a percentage of total pyramidal neuron population. ....	180
6.3.4.	Co-localisation of COX4 and GRP78 .....	182
6.3.5.	Estimation of dendritic arbour.....	185
6.4.	Discussion .....	185
6.4.1.	Analysis of GRP78 in the dIPFC .....	185
6.4.2.	COX4 analysis of pyramidal neuron metabolism.....	186
6.5.	GRP78 and COX4 co-localisation.....	189
6.6.	Golgi analysis of the dendritic arbour.....	190
6.6.1.	Conclusion .....	190



Chapter 7. Discussion.....	191
7.1. Introduction .....	191
7.2. Morphological changes in the dIPFC .....	191
7.2.1. The causes of cognitive dysfunction.....	193
7.2.2. The neurocentric hypothesis for the breakdown of the neurovascular unit .....	193
7.2.3. WM pathology and pyramidal volume change in the frontal lobe	195
7.2.4. Mechanisms for pathology in the dIPFC and cognitive dysfunction .....	196
7.2.5. Cognitive brain reserve. ....	197
7.3. Strengths and limitations of the study .....	198
7.3.1. The CogFAST study.....	198
7.3.2. Additional disease subjects and aged-controls .....	198
7.4. Future directions .....	199
7.4.1. Morphological investigations .....	199
7.4.2. Dendritic arbour and cognition .....	200
7.4.3. Biochemical basis for neuronal dysfunction .....	201
7.4.4. Genomics of the CogFAST cohort.....	201
7.5. Conclusion .....	202
Chapter 8. Appendix.....	204
8.1. Golgi staining.....	204
8.2. Frontotemporal Dementia (FTD).....	206
8.2.1. Three dimensional stereological analysis of the dIPFC in FTD subjects.....	208
8.2.2. Additional analysis of the FTD subjects.....	210
8.3. List of publications .....	210

Figure 1-1 showing the hypothetical model of the ultimate effects of sustained vascular influence during ageing that lead to AD type changes, CAA, and VaD. AD = Alzheimer’s disease, CAA = cerebral amyloid angiopathy, and VaD = vascular dementia adapted from (Kalaria 2002; Roman 2002a). Images adapted from (Okamoto et al. 2012; Gamblin et al. 2003; Johnson et al. 2012) .5

Figure 1-2 showing cortical neuronal connections within the PFC and subcortical areas of the brain. Neuronal connections of layer III largely project to areas within the PFC with few connections to subcortical brain regions in other areas of the circuit. Layer V contributes the majority of subcortical connections making up the circuit. Adapted from (Tekin and Cummings 2002)). .....19

Figure 1-3 showing gross differences between layer III and layer V pyramidal neurons. Graphics adapted from Spruston et al (Spruston 2008). .....20

Figure 1-4 showing the location of the three PFC circuits and their relative functions. PFC = prefrontal cortex, dlPFC = dorsolateral prefrontal cortex, ACC = anterior cingulate cortex, and OFC = orbitofrontal cortex (O. Perry 1993). ....23

Figure 1-5 showing the soma and proximal dendrite-targeting interneurons of the prefrontal cortex (Markram et al. 2004) Red lines = dendrites, blue line = axons, and blue dots = axonal boutons. Markram *et al.*, 2004).....28

Figure 1-6 showing the axon targeting interneuron. Red lines = dendrites, blue line = axons, and blue dots = axonal boutons. Adapted from (Markram et al. 2004).....29

Figure 1-7 showing dendrite and tuft-targeting interneurons. Red lines = dendrites, blue line = axons, and blue dots = axonal boutons. Adapted from (Markram et al. 2004).....30

Figure 1-8 showing the dendrite-targeting neurons in the prefrontal cortex. Red lines = dendrites, blue line = axons, and blue dots = axonal boutons. Adapted from (Markram et al. 2004). .....31

Figure 1-9 showing the distribution of interneuronal subtypes in layers II, III, and V of the prefrontal cortex. Adapted from Markram et al (Markram et al. 2004; Simpson et al. 2007; Chance et al. 2011). .....33

Figure 1-10 demonstrating the mechanism with which oligodendrocytes myelinate axons (Sherman and Brophy 2005). .....36

Figure 2-1 flow chart showing the CogFAST study design adapted from Allan et al (Allan et al. 2011). CT = X-ray computed tomography scan, MMSE = Mini Mental State Exam, CAMCOG = Cambridge Cognitive Examination, AD = Alzheimer's disease, C = degree celsius. ....	46
Figure 2-2 showing the Newcastle University brain map (O. Perry 1993). ....	51
Figure 2-3 showing two frontal sections stained with luxol fast blue. Image 'a' demonstrates a section with intact WM. Image 'b' shows some signs of WM degeneration. ....	54
Figure 2-4 demonstrating p/a staining analysis using the densitometric technique using Mediacybernetics Image Pro software. Histogram-based segmentation is performed, highlighting, in red, all areas immunochemically stained. ....	58
Figure 2-5 a) illustrating frontal lobe regions (O. Perry 1993) and b) image of the nucleator principle for assessing neuronal volumes. ....	62
Figure 2-6 cartoon demonstrating the multi-planed, 3D nature of the stereology technique. ....	63
Figure 2-7 showing a cartoon of a vessel's lumen being assessed the VasCal software. ....	65
Figure 2-8 demonstrating the quartile analysis method for determining myelin index (Ihara et al. 2010). ....	68
Figure 3-1 neuronal densities in the dlPFC, ACC, and OFC. Controls = aged matched controls, PSND = post-stroke no dementia, PSD = post-stroke dementia, VaD = vascular dementia, mixed = mixed vascular and Alzheimer's disease, AD = Alzheimer's disease. * = significance different to ageing controls (p < 0.05). Controls vs mixed layer III and V (p = 0.001, and p = 0.015 respectively), PSD vs mixed layer III and V (p = 0.049, p = 0.028 respectively), Controls vs VaD in layer III (p = 0.023), PSND vs AD in layer III (p = 0.007). ....	80
Figure 3-2 pyramidal neuron volumes in the dlPFC, ACC, and OFC. Controls = aged matched controls, PSND = post-stroke no dementia, PSD = post-stroke dementia, VaD = vascular dementia, mixed = mixed vascular and Alzheimer's disease, AD = Alzheimer's disease. * = significant to controls, ** = significant to controls and PSND (p < 0.05). Controls vs PSD (P = 0.027), VaD (p = 0.012), mixed (p = 0.03), and AD (p = 0.035). PSND vs PSD (p = 0.01), VaD (p = 0.01), mixed (p = 0.004), and AD (p = 0.005) in layer III. In layer V controls vs PSD (p	

= 0.007), VaD (p = 0.002), mixed (p = 0.008), and AD (p = 0.015). PSND vs VaD (p = 0.034). .....	84
Figure 3-3 showing pyramidal neuron volumes in layers III and V in control cases of the dlPFC and OFC. P/A = per area (a count of average pixel content of each neuron). * = significant compared to other brain region (p < 0.05). dlPFC vs OFC layer III (F = 21.457, p = 0.010), layer V (F = 11.096, p = 0.027). .....	86
Figure 3-4 showing significant correlations between pyramidal neuronal volumes in the dlPFC and clinical variables. a) $\sigma = 0.707$ , p = 0.0001), b) $\sigma = 0.500$ , p = 0.021, c) $\sigma = 0.583$ , p = 0.006, and d) $\sigma = 0.444$ , p = 0.044. ....	87
Figure 3-5 showing SMI32 positive pyramidal neurons in layer III of the dlPFC. a) aged-controls, b) PSND c) PSD, d) VaD, e) Mixed, and f) AD. Size bar = 20 $\mu$ m.....	89
Figure 3-6 Showing SMI31 positive neurons in layer III of the dlPFC. a) aged-controls, b) PSND, c) PSD, d) VaD, e) Mixed, and f) AD. Arrows indicates SMI31 positively stained pyramidal neurons. Size bar = 20 $\mu$ m.....	90
Figure 3-7 showing counts for SMI31 positive pyramidal neurons in layer III and V. Controls = aged matched controls, PSND = post-stroke no dementia, PSD = post-stroke dementia, VaD = vascular dementia, mixed = mixed vascular and Alzheimer's disease, AD = Alzheimer's disease. * = significant to PSND. PSND vs PSD (p = 0.004), VaD (P = 0.031).....	91
Figure 3-8 showing counts for SMI32 positive pyramidal neurons in layer III and V. Controls = aged matched controls, PSND = post-stroke no dementia, PSD = post-stroke dementia, VaD = vascular dementia, mixed = mixed vascular and Alzheimer's disease, AD = Alzheimer's disease. * = significant to PSND and PSD. PSND vs mixed (p = 0.004), PSD vs mixed (p = 0.037). ....	92
Figure 3-9 showing correlations (a) relationship between SMI31 staining in layer III vs layer V, (b) SMI32 staining in layer V vs SMI31 staining in layer V, (c) SMI32 staining vs layer III volume in post-stroke non-demented subjects, and (d) SMI31 staining in layer III vs layer V in post-stroke demented subjects. 'a' ( $\sigma = 0.529$ , p = 0.001), 'b' ( $\sigma = $ ), 'c' ( $\sigma = 0.733$ , p = 0.016), 'd' ( $\sigma = 0.259$ , p = 0.020).....	93
Figure 3-10 Cortical atrophy Z scores in the dlPFC. Controls = aged matched controls, PSND = post-stroke no dementia, PSD = post-stroke dementia. ....	96

Figure 3-11 shows fluorescent stained images from the dIPFC layer III of control subjects (A), post-stroke no dementia (B), post-stroke dementia (C), vascular dementia (D), mixed dementia (E), and Alzheimer’s disease (F). Background auto-fluorescence from lipofuscin and red blood cells is evident in all images. Hollow arrows = amyloid plaques (green), solid arrows = hyperphosphorylated tau (red). Scale bar 50µm. ....98

Figure 4-1 showing Nissl stained non-pyramidal neuron densities in control and disease groups in layers III and V of the dIPFC. Blue = Layer III. Green = layer V. Control = aged control, PSND = post-stroke no dementia, PSD = post-stroke dementia, VaD = vascular dementia, Mixed = mixed dementia, AD = Alzheimer’s disease. Controls vs VaD (p = 0.017), Mixed (p = 0.003), AD (p = 0.017). Mixed vs PSND (p = 0.016), PSD (p = 0.009).....114

Figure 4-2 scatter graphs showing significant correlations between non-pyramidal neuronal densities in layers III and V and clinical and morphological variables. a)  $\sigma = 0.133$ , p = 0.021, b)  $\sigma = -0.125$ , p = 0.021, c)  $\sigma = 0.231$ , p = 0.001, d)  $\sigma = 0.818$ , p = 0.05.....115

Figure 4-3 scatter graphs showing significant relationships between non-pyramidal neurons and glial cell density in layer III of the dIPFC in a) control ( $\sigma = 0.755$ , p = 0.007) and b) AD ( $\sigma = 0.758$ , p = 0.011) subjects. ....116

Figure 4-4 bar chart showing non-pyramidal neuron density in control, PSND, and PSD subjects in layer II of the dIPFC. Control = aged control, PSND = post-stroke no dementia, PSD = post-stroke dementia. \* = significance to controls. Controls vs PSND (p = 0.023), PSD (p = 0.006).....117

Figure 4-5 showing parvalbumin (PV), calbindin (CB), and calretinin (CR) positive neurons in layer V of the dIPFC. Solid black arrows = darkly stained neurons, hollow arrows = pale stained neurons. Left column taken at x10 magnification, right side column taken at x40 magnification. Left scale bar = 100µm. Right scale bar = 20µm.....120

Figure 4-6 scatter graphs showing significant correlations between non-pyramidal neuronal density in layer V and clinical variables. PV = parvalbumin, CB = calbindin, CR = calretinin. a)  $\sigma = 0.456$ , p = 0.018, b)  $\sigma = 0.738$ , p = 0.037, c)  $\sigma = 0.406$ , p = 0.017, d)  $\sigma = 0.900$ , p = 0.037. ....125

Figure 4-7 showing non-pyramidal neuron densities in control and disease groups in layers III (blue) and V (green) of the dIPFC. Control = aged control, PSND = post-stroke no dementia, PSD = post-stroke dementia, VaD = vascular

dementia, Mixed = mixed dementia, AD = Alzheimer's disease. VaD vs controls (p = 0.002), PSND (p = 0.003), PSD (p = 0.001), (mixed p = 0.05) in layer III. .... 127

Figure 4-8 showing the correlation between pyramidal neuron volumes and glial cell densities in layer V ( $\sigma = 609$ , p = 0.047). .... 128

Figure 4-9 showing non-pyramidal neuron densities in control and disease groups in layer II of the dlPFC. Control = aged control, PSND = post-stroke no dementia, PSD = post-stroke dementia. No significant differences between groups (p <0.05). .... 128

Figure 5-1 showing the myelin index in the frontal WM of controls and disease subjects. Controls = aged controls, PSND = post-stroke non-demented, PSD = post-stroke dementia, VaD = vascular dementia, Mix = mixed dementia, AD = Alzheimer's disease. \* = significant to controls. † = significant to undamaged myelin. Mean MI: Undamaged myelin = 25, control = 28, PSND = 30, PSD = 34, VaD = 43, mixed = 36, AD = 40. Controls vs VaD (p = 0.034). Undamaged myelin vs VaD (p = 0.001), mixed (p = 0.003), AD (p = 0.002). .... 142

Figure 5-2 showing significant correlations between clinical variables and myelin loss index. a)  $\sigma = -0.320$ , p = 0.02, b)  $\sigma = -0.451$ , p = 0.001, c)  $\sigma = -0.344$ , p = 0.034, d)  $\sigma = -0.516$ , p = 0.001, e)  $\sigma = -0.388$ , p = 0.016, f)  $\sigma = 0.277$ , p = 0.028. .... 144

Figure 5-3 showing SMI32 positively stained axons in the frontal WM. a) aged-controls, b) PSND c) PSD, d) VaD, e) Mixed, and f) AD. Size bar = 20 $\mu$ m. ... 146

Figure 5-4 showing SMI32 staining (blue) and corrected SMI32 staining (green) in controls and disease groups. Controls = aged controls, PSND = post-stroke non-demented, PSD = post-stroke dementia, VaD = vascular dementia, Mix = mixed dementia, AD = Alzheimer's disease. \* = significant to controls. † = significant to mixed dementia. Uncorrected: Controls vs PSND (p = 0.018), VaD (p = 0.041), mixed (p = 0.001). Mixed vs PSD (p = 0.041), and AD (p = 0.005). Corrected: Controls vs PSND (p = 0.014), PSD (p = 0.029), VaD (p = 0.006), mixed (p = 0.001), and AD (p = 0.029). Mixed vs PSND (p = 0.049), PSD (p = 0.034), and AD (p = 0.029). .... 148

Figure 5-5 showing significant correlations between clinical variables and SMI32 frontal WM staining. a)  $\sigma = -0.319$ , p = 0.020, b)  $\sigma = -0.339$ , p = 0.033, c)  $\sigma = 0.296$ , 0.037. .... 149

Figure 5-6 SMI31 positively stained axons in the frontal WM. a) aged-controls, b) PSND c) PSD, d) VaD, e) Mixed, and f) AD. Size bar = 20µm. .... 151

Figure 5-7 showing mean SMI31 staining in the frontal WM of controls and diseased subjects. Controls = aged controls, PSND = post-stroke non-demented, PSD = post-stroke dementia, VaD = vascular dementia, Mix = mixed dementia, AD = Alzheimer’s disease. \* = significant to controls. Controls vs VaD (p = 0.016). .... 153

Figure 5-8 showing significant correlations between SMI31 frontal WM staining and clinical variables. a)  $\sigma = -0.336$ , p = 0.034, b)  $\sigma = -0.301$ , p = 0.034, c)  $\sigma = 0.684$ , p = 0.001, d)  $\sigma = -0.350$ , p = 0.027. .... 154

Figure 5-9 showing frontal vascular pathology in the WM of controls and disease subjects. Controls = aged controls, PSND = post-stroke non-demented, PSD = post-stroke dementia, VaD = vascular dementia, Mixed = mixed dementia, AD = Alzheimer’s disease. SI = sclerotic index, PVS = perivascular space. No significance between groups: WMSI (p = 0.053), PVSWM (p = 0.863)..... 156

Figure 5-10 showing GRP78 staining of the WM in a) AD and b) VaD. Bar = 20µm..... 157

Figure 5-11 showing GRP78 staining in the frontal WM of controls and disease subjects. Controls = aged controls, PSND = post-stroke non-demented, PSD = post-stroke dementia, VaD = vascular dementia, Mix = mixed dementia, AD = Alzheimer’s disease. No significance between groups (p = 0.868). .... 158

Figure 6-1 demonstrating the electron transfer chain in mitochondria (Moncada and Erusalimsky 2002). .... 168

Figure 6-2 showing GRP78 staining of layer III of the dlPFC in PSND (a) and PSD (b). (scale bar = 20µm) ..... 172

Figure 6-3 showing p/a staining of GRP78 in both layers III. Controls = aged controls, PSND = post-stroke non-demented, PSD = post-stroke demented, VaD = vascular dementia, mixed = mixed vascular and Alzheimer’s disease, AD = Alzheimer’s disease. Blue = layer III, Green = layer V, \* = Significant to controls. Control vs PSND (P = 0.036) in layer V..... 173

Figure 6-4 showing GRP78 counts in layers III and V of the dlPFC Controls = aged controls, PSND = post-stroke non-demented, PSD = post-stroke demented, VaD = vascular dementia, mixed = mixed vascular and Alzheimer’s disease, AD = Alzheimer’s disease. Blue = layer III, Green = layer V, \* =

Significant to controls, ° = significant to AD, † PSND. Control vs PSND ( $p = 0.035$ ), PSND vs AD ( $p = 0.005$ ), VaD ( $p = 0.023$ )..... 175

Figure 6-5 showing cytochrome oxidase 4 (COX4) p/a staining. Controls = aged controls, PSND = post-stroke non-demented, PSD = post-stroke demented, VaD = vascular dementia, mixed = mixed vascular and Alzheimer's disease, AD = Alzheimer's disease. \* = Significant to controls. Controls vs PSD ( $p = 0.019$ ), VaD ( $p = 0.028$ ), mixed ( $p = 0.034$ ) in layer III. Controls vs PSND ( $p = 0.019$ ), PSD ( $p = 0.004$ ), VaD ( $p = 0.049$ ), and mixed ( $p = 0.004$ ) in layer V. .... 177

Figure 6-6 showing average COX4 positive pyramidal neuron count in layers III and V of the dlPFC. Controls = aged controls, PSND = post-stroke non-demented, PSD = post-stroke demented, VaD = vascular dementia, mixed = mixed vascular and Alzheimer's disease, AD = Alzheimer's disease. \* = Significant to controls. † = significant to AD. Controls vs PSND ( $p = 0.001$ ), PSD ( $p = 0.013$ ), VaD ( $p = 0.001$ ), and mixed ( $p = 0.001$ ) in layer III. Controls vs PSND ( $p = 0.002$ ), PSD ( $p = 0.002$ ), VaD ( $p = 0.031$ ), mixed ( $p = 0.002$ ), and AD ( $p = 0.019$ ). Mixed vs AD ( $p = 0.044$ ) in layer V. .... 178

Figure 6-7 showing COX4 positive pyramidal neurons in layer V of the dlPFC. a) aged-controls, b) PSND c) PSD, d) VaD, e) Mixed, and f) AD. Solid arrows indicate positively stained pyramidal neurons, hollow arrows indicate negatively stained pyramidal neurons. Size bar =  $20\mu\text{m}$ ..... 179

Figure 6-8 showing COX4 percentage differences of positively stained pyramidal neurons vs GRP78 total counts in layer V of the dlPFC. Controls = aged controls, PSND = post-stroke non-demented, PSD = post-stroke demented, VaD = vascular dementia, mixed = mixed vascular and Alzheimer's disease, AD = Alzheimer's disease. \* = Significant to controls. Controls vs PSND ( $p = 0.006$ ), PSD ( $p = 0.043$ ), VaD ( $p = 0.005$ ), mixed ( $p = 0.010$ )..... 181

Figure 6-9 fluorescent image showing the co-localisation of COX4 antibody (green), and GRP78 (red) in pyramidal neurons in layer V of the dlPFC. Where antibodies are co-localised the image will appear yellow. Blue = DAPI. a) aged-controls, b) PSND, c) PSD, d) VaD, e) Mixed, and f) AD. Open arrows indicate co-localisation of GRP78 and COX4 within pyramidal neurons. White arrows indicate GRP78 positive, COX4 negative pyramidal neurons. Red arrows indicate vessel auto-fluorescence green. Size bar =  $10\mu\text{m}$ ..... 183

Figure 6-10 showing separate fluorescence images for DAPI (c, d), COX4 (e, f), and GRP78 (g, h) in control (left column) and PSD (right column) subjects.



Images 'a' and 'b' show composite of images for control and PSD subjects, respectively. COX4 = green, GRP78 = red, DAPI = blue, co-localisation = blue  
Size bar = 10µm.....184

Figure 8-1 demonstrating the clustering nature of the Golgi-Kopsch technique on pyramidal neurons within layer III the dIPFC. Scale bar = 100µm.....204

Figure 8-2 demonstrating the clustering nature of the golgi-kopsh technique. The section had been counterstained with nissl to demonstrate a specific sub-population of pyramidal neurons within layer III of the dIPFC have been unaffected by the stain. Scale bar = 100µm.....204

Figure 8-3 showing the Golgi techniques uniform staining of blood vessels within the frontal lobe. Scale bar = 100µm.....205

Figure 8-4 showing (a) pyramidal neuronal volumes, and b) pyramidal neuron densities in the dIPFC of FTD subjects in both layers III and V. ....209

Figure 8-5 showing combined layer III and V pyramidal neuronal volume in the dIPFC in FTD subjects. \* = significant compared to controls (p < 0.044). ....209

## List of abbreviations

2D	Two-dimensional
3D	Three-dimensional
4G8	Beta Amyloid (A $\beta$ ) Monoclonal Antibody
ABETA	Amyloid Beta
ACC	Anterior cingulate cortex
AD	Alzheimer's disease
$\alpha$	Alpha
ANOVA	Analysis of variance
APES	Aminopropyltriethoxysilane
APOE	Apolipoprotein E
APP	Amyloid precursor protein
ATP	Adenosine tri-phosphate
BBB	Blood brain barrier
BC	Basket cells
$\beta$	Beta
BPC	Bipolar cells
BtC	Bifurcated cells
bvFTD	Behavioural variant frontotemporal dementia
CA	Cornu Ammonis
CAA	Cerebral amyloid angiopathy
CADASIL	Cerebral autosomal-dominant arteriopathy with subcortical infarcts & leukoencephalopathy
CAMCOG	Cambridge Examination for Mental Disorders in the Elderly
CB	Calbindin
CC	Chandelier cells
CERAD	Consortium to Establish a Registry for Alzheimer's Disease
CFV	Cresyl fast violet
CNS	Central nervous system
CogFAST	Cognitive function after stroke study
COX	Cytochrome oxidase
CR	Calretinin
CSF	Cerebral spinal fluid
CT	Computer tomography
CVD	Cerebral vascular dementia
DAB	3,3'-Diaminobenzidine
dIPFC	Dorsolateral prefrontal cortex
dMBP	Damaged myelin basic protein
DPC	Double bouquet cells
DSM-IV	Diagnostic and Statistical Manual of Mental Disorders, four
ER	Endoplasmic reticulum
ETC	Electron transport chain
EXEC	Executive function
FDT	Fronto-temporal dementia
FTLD	Fronto-temporal l
FT	Fixation time
GABA	$\gamma$ -Aminobutyric acid

γ	Gamma
GM	Grey matter
GRP78	78 kDa glucose-regulated protein
GWAS	Genome-wide association study
IHC	Immunohistochemistry
IOD	Integrated optical density
IQCODE	Informative questionnaire on cognitive decline in the elderly
Parv	Parvalbumin
LACS	Lacunar stroke
LFB	Luxol fast blue
LSD	Least significance difference
LVD	Large vessel disease
MAP	Microtubule-associated protein
MC	Martinotti cells
MI	Myelin index
Mixed	Mixed dementia
MMSE	Mini-mental-state-exam
MRI 3T	Magnetic resonance imaging
MTA	Medial temporal atrophy
NBTR	Newcastle brain tissue resource
NFT	Neurofibrillary tangle
NOS3	Nitric oxide synthase - three
NRG	Neurovascular research group
NVU	Neurovascular unit
OFC	Orbitofrontal cortex
p/a	Per area
PACS	Partial anterior stroke
PBS	Phosphate-buffered saline
PET	Positron emission topography
PMD	Post-mortem delay
POCS	Posterior circulation stroke
PSD	Post-stroke dementia
PSND	Post-stroke non-demented
PS	Post-stroke
PV	Perivascular
PVS	Perivascular space
ROI	Region of interest
SDFTD	Semantic dementia frontotemporal dementia
SEM	Standard error of mean
SI	Sclerotic index
SNP	Single nucleotide polymorphism
SVD	Small vessel disease
TACS	Total anterior circulation stroke
TBS	Tris-buffered saline
Tg	Transgenic
TNF	Tumour necrotising factor
ToM	Theory of mind testing
TSC	Tri-sodium citrate

VaD	Vascular dementia
WCST	Wisconsin card test
WMH	White matter hyperintensities
WML	White matter lesions

# Chapter 1. Introduction

## 1.1. Normal ageing and dementia

Over 35 million people worldwide are living with dementia at an estimated cost of \$604 billion per year (Wimo et al. 2013) putting a significant strain on the economy (Leal et al. 2006). With older age as the single most significant risk factor for developing dementia, an ageing population is only set to exacerbate the problem. Improved healthcare, wealth, and more sanitary living conditions indicate people are living longer and will add to the burden of dementia.

Pathological features of dementia are acquired gradually during normal ageing. Neuronal loss, cortical atrophy, and white matter lesions all occur in individuals, who do not appear cognitively impaired (Brockmann et al. 2013; Marner et al. 2003; de Leeuw et al. 2001; Apaydin et al. 2002; Opris and Casanova 2014), with the hallmarks of specific neurodegenerative diseases such as amyloid  $\beta$  and hyperphosphorylated tau, principal markers of AD, having been reported in abundance in otherwise healthy, cognitively normal adults. This suggests that the brain may have a threshold level which must be surpassed before the pathological burden or additional factors affect the cognitive status of individuals. Risk factors have also been reported in non-demented aged-controls, such as reduced cerebral blood flow, vascular basement membrane thickening, amyloid deposits on vasculature, and impairment of the blood brain barrier (BBB) (Farkas and Luiten 2001; Chen et al. 2011; Kalaria 1996). Some of these vascular changes are consistent with the presence of white matter changes identified as white matter hyperintensities (WMH) on T2-weighted MRI imaging techniques, with up to 100% of those ages 71-80 years of age showing some degree of change (Christiansen et al. 1994; de Leeuw et al. 2001). In addition to vascular pathology, it is not uncommon for cognitively normal elderly healthy individuals to display some form of Alzheimer type pathology with no apparent accompanying cognitive dysfunction (Braak and Braak 1991). Indeed Snowdon et al (Snowdon et al. 1997) found that 40% of those exhibiting Alzheimer pathology above the threshold required for disease diagnosis, remained cognitive intact.

#### 1.1.1.1. ***Cognitive reserve hypothesis***

One reason for the mismatch between clinical diagnosis and pathological brain changes has been attributed to individual cognitive reserves (Barulli and Stern 2013). This theory suggests that individuals may be equally vulnerable to pathological damage but, some may have an increased brain reserve to hold off dementia (Stern et al. 1994). If an individual dies before their respective pathology reaches the reserve threshold then they will remain cognitively intact. However, it is difficult to measure one's cognitive reserve in order to test this theory. Whether this theory plays a role in ageing or not, it is not surprising that elderly individuals with several comorbidities i.e. more than one risk factor, succumb to dementia due to the combined stress that such pathologies will place on any hypothetical cognitive reserve (Allan et al. 2011) .

#### 1.1.2. **Ageing and stroke**

The risk of stroke increases greatly with age (Pendlebury and Rothwell 2009; E. J. Burton et al. 2004) with one third of ischaemic stroke sufferers over the age of 80 (Ly and Maquet 2014), and the Framingham study reporting a 1 in 6 lifetime risk of suffering a stroke (Seshadri et al. 2006). Ischaemic stroke is responsible for two thirds of morbidity and mortality which results from stroke (Ly and Maquet 2014), accounting for 10-12% of deaths in industrialised countries with around 88% attributed to those over 88 years of age (Bonita 1992). Indeed this trend appears to be increasing with the prevalence of stroke in over 75-year olds rising from 9% to 13% between 1994, and 2006 (Scarborough et al. 2009).

Around 80% of strokes are ischaemic and almost all are caused by some type of arterial occlusion, resulting in a reduced flow of blood, nutrients, and oxygen (Kalara and Ballard 2001). The sudden lack of oxygen and nutrients leads to neuronal death, in the affected area, through a combination of hypoxia, hypoglycemia, and glutamate excitotoxicity (Larsen et al. 2006), as part of the ischemic stroke cascade which can continue for a long time after the initial stroke has resolved itself (Dirnagl et al. 1999). Due to this oxidative damage mitochondria within the cell begin to break down and release apoptotic factors, which result in cell death (Sanchez-Gomez et al. 2003). Though this series of events can occur in all tissue deprived of oxygen, neurons are also susceptible

to hypoxia due to their high metabolic turnover (Magistretti 2006; Magistretti and Pellerin 1999).

The infarct area resulting from an ischaemic stroke consists of a central core, which may involve the cortex and/or the WM, of complete infarction which is devoid of functioning components such as neurons, axons, and oligodendrocytes. Surrounding the core is the hypo-perfused penumbra region. This area may in time recover some function as the vasculature recovers (Nedergaard and Dirnagl 2005). Focal ischaemia, as that seen in the ocular occlusions present in stroke tend to result in death for all cells at the epicenter of the infarct with both neurons and glial cells equally affected. In the penumbra cells may be metabolically active, but do not appear mechanistically capable of sending out electrical signals (Nedergaard and Dirnagl 2005). The fate of these neurons and glial cells may decide whether an individual recovers from a stroke or declines into delayed post-stroke dementia. However, once blood flow has been restored there may be a period of stability before the stroke subject begins to develop cognitive dysfunction (Leys et al. 2005).

### **1.1.3. Stroke and dementia**

Post-stroke dementia (PSD) is defined as any type of dementia occurring after stroke, regardless of the underlying pathological cause, including VaD and AD (Leys et al. 2005). It has been estimated that 20% of those over the age of 65 will suffer a stroke, incidentally resulting in a nine-fold increase in the risk of dementia when compared to those who have not suffered a stroke (Kalaria and Ballard 2001), with Savva et al's (Savva et al. 2010) systematic review of sixteen post-stroke epidemiological studies concluding that a history of stroke doubles the risk of dementia in an older population. The risk of cognitive decline after stroke also increases with age (Moroney and Desmond 1997). Delayed cognitive decline, developing a minimum of 3 months post-stroke, has been reported in 35.2% of post-stroke patients compared to 3.8% incidence in controls (Tatemichi et al. 1994) with around 30% of PSD cases show mixed CVD and AD type pathology (Pohjasvaara et al. 1998) and around 10% displaying some form of dementia before first stroke (Pendlebury and Rothwell 2009). Though PSD does not necessarily have to be vascular based (Leys et al. 2005), vascular risk factors have been cited to increase risk for dementia after

stroke, with the presence of microscopic infarcts contributing to dementia (Pascual et al. 2010; Firbank et al. 2012; E. Burton et al. 2003) and silent infarcts having been shown to be independent predictors for developing PSD (Desmond et al. 2000; Henon et al. 2001; Tatemichi 1990). Those who go on to develop dementia have an increased risk of further stroke, suggesting a relationship between the development of dementia and an underlying CVD (Moroney et al. 1997). The importance of stroke alone in the development of PSD has been highlighted. The size, number, and location of lesions appeared to be more significant than the underlying vascular risk factors. Strategic infarcts, i.e. stroke locations which result in dementia regardless of any other lesion or factor (Leys et al. 2005) are associated with PSD. The inferomesial temporal and mesial frontal locations have been suggested as sites where infarcts may result in significant cognitive decline (Leys et al. 2005). Leys et al suggest that vascular lesions have a more prominent role in the development of PSD when a patient is too young to have developed the conventional hallmarks of Alzheimer pathology (Pasquier and Leys 1997). In addition, a number of non-stroke based risk factors were also identified including low education attainment, race, diabetes, medial and temporal lobe atrophy, arterial fibrillation, and leukoaraiosis (Pendlebury and Rothwell 2009). In addition, milder forms of cognitive impairment also exist following stroke, with reports of executive function and attention deficits apparent in stroke survivors without cognitive impairment (Stephens et al. 2004).



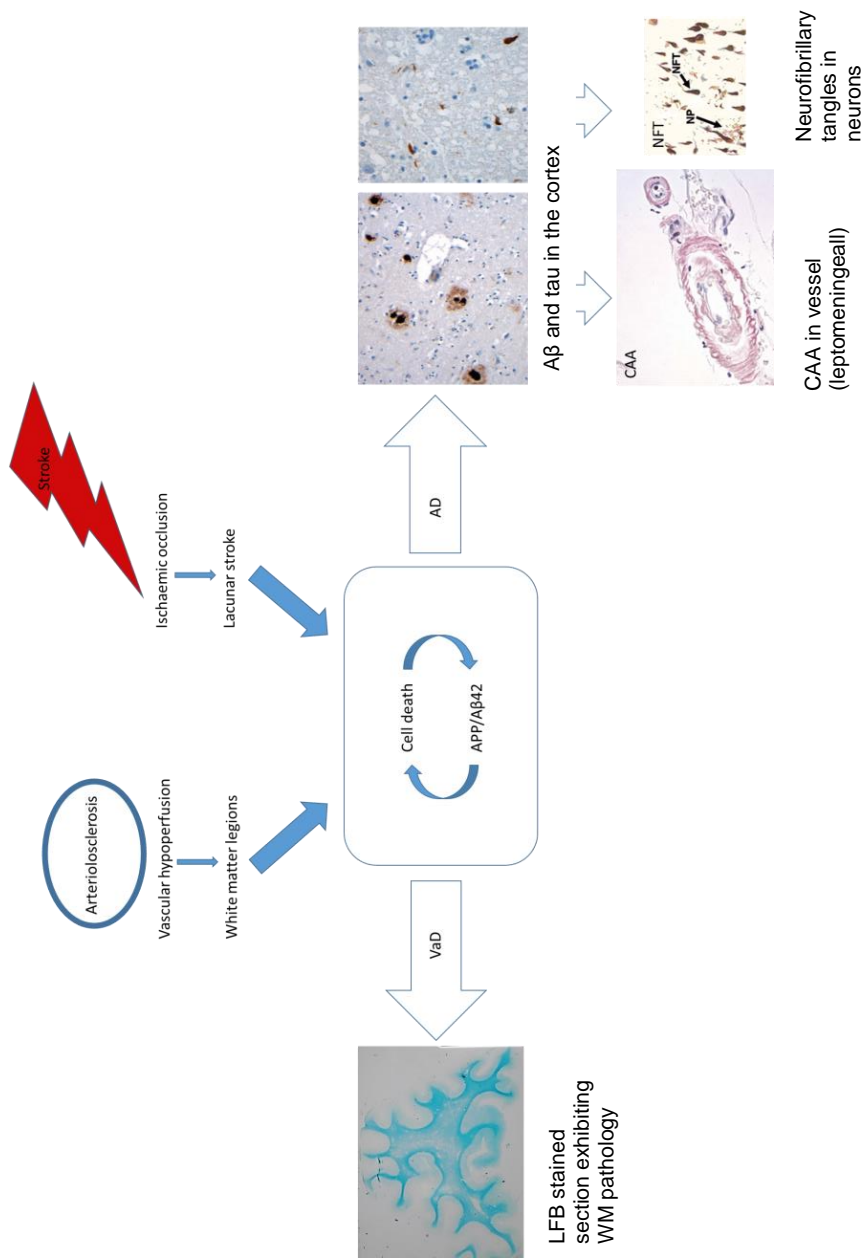


Figure 1-1 showing the hypothetical model of the ultimate effects of sustained vascular influences during ageing that lead to AD type changes, CAA, and VaD. AD = Alzheimer's disease, CAA = cerebral amyloid angiopathy, and VaD = vascular dementia adapted from (Kalaria 2002; Roman 2002a). Images adapted from (Okamoto et al. 2012; Gamblin et al. 2003; Johnson et al. 2012)

#### 1.1.3.1. ***Cerebral Atrophy, metabolism, and stroke***

Subjects with global cerebral atrophy are at increased risk for the development of post-stroke dementia (Leys et al. 2005), with medial temporal atrophy most common in those suffering dementia previous to stroke. The presence of medial temporal atrophy in those with PSD may suggest pre-clinical AD which is exacerbated or exposed by the stroke (Tang et al. 2004), though medial temporal atrophy has been noted in vascular dementia (VaD) (Jobst et al. 1998; Laakso et al. 1996; Fein et al. 2000). Elderly stroke sufferers who remain dementia free but have temporal atrophy develop slower mental speeds and visuospatial tasks. Executive function remained intact in these cases, suggesting no involvement of the frontal lobes (Leys et al. 1998; Henon, Godefroy, et al. 1996). Glucose metabolism was shown to decrease in the frontal lobe in cases with suspected vascular pathology (Haight et al. 2013) and the temporal lobes of those suffering AD suggesting decreased neuronal function in areas shown to exhibit atrophy (Pascual et al. 2010; Jagust et al. 1991).

#### 1.1.4. **Dementia and cerebrovascular disease (CVD)**

Cerebrovascular disease (CVD) plays an important role in the development of dementia with the risk of CVD increasing with age in association with cognitive decline (Kalaria and Ballard 2001). The brain accounts for around 2% of the body mass, yet requires over 20% of the body's total blood and oxygen (Kalaria 2010). This makes the brain extremely vulnerable to changes in the vasculature which could affect this supply. Mounting evidence from pathological, neuroimaging and clinical studies indicates a strong link between CVD and the onset of VaD. VaD is the second most common form of age-related dementia, accounting for between 36% and 67% of cases (Roman 2002a). This vascular pathology results in ischaemic damage and hypoperfusion which acts to deprive neurons and glial cells of oxygen and trophic factors, resulting in their damage or death (Zlokovic 2011; Majno and Joris 1995; Dirnagl et al. 1999; Nedergaard and Dirnagl 2005). Clinical features can develop insidiously over a period of years with pathology either developing as cognitive impairment in later in life or detected at autopsy, so any long standing changes may mask the original underlying causes (Farrall and Wardlaw 2009), or can appear as a sudden

stepwise decline as a result of more severe infarcts having an instant impact of cognition (Roman et al. 2002).

#### 1.1.5. **Large and small vessel disease**

Cerebrovascular disease can be conveniently grouped into two distinct categories: Large vessel disease (LVD) and small vessel disease (SVD) (Kalara 2012).

##### 1.1.5.1. ***Large vessel disease***

LVD involves the major arteries feeding the brain such as the carotid or the circle of Willis. These large vessels can be affected by atherosclerosis, haemorrhage, thrombotic occlusion, and embolism (up to 50% of ischaemic strokes) which lead to blockage of major arterial territories causing large macroinfarcts which are visible upon gross inspection of the brain (Kalara 2012; Kalara et al. 2004). LVD can result in large volumes of tissue loss, associated with high mortality death, and/or cognitive impairment (Nedergaard and Dirnagl 2005) as a result of delayed neuronal death. In addition, blockage of the internal carotid and/or circle of Willis can also lead to multi-infarct dementia, accounting for 15% of VaD cases (Brun 1994)

##### 1.1.5.2. ***Small vessel disease***

Pathological changes in small vessels are thought to lead to decreases in blood flow, microinfarcts and diffuse white matter changes, which have been identified as substrates for cognitive impairment. The frontal lobe is more vulnerable to vascular pathology and SVD than the temporal (E. Burton et al. 2003; Deramecourt et al. 2012). Severe SVD can result in vascular dementia (VaD) (Jellinger 2013). SVD may result in a more insidious, progressing pathology than the step-wise decline associated with large vessel infarcts/strokes, in which each new event results in a marked decrease in cognitive faculties (Kalara et al. 2004). The most common lesions associated with SVD are vessel wall modifications, such as arteriolosclerosis and CAA, with the frontal lobe more heavily affected (Deramecourt et al. 2012). These pathologies are thought to promote replacement of the vascular smooth muscle with collagen reducing the structural integrity of the vessel that are causal in lacunar and micro infarcts [lesions under 2cm (Kalara 2012)]. Arteriolosclerosis is the result of hyalinosis and degradation of smooth muscle cells, followed by the continuing concentric

accumulation of collagen and fibroblasts and ultimately a decrease of the vessel lumen. This decreased lumen may result in restricted blood flow, creating a chronic ischaemic environment in the surrounding tissue. This occurs most commonly in the small vessels of the WM as well as cortical grey matter (Craggs et al. 2013; Lammie 2000). Craggs et al reported an increase in the sclerotic index of vessels of deep and cortical WM in cases with SVD and CADASIL (a condition characterised by SVD) when compared to cognitively normal controls (Craggs et al. 2013). These changes affect the ability of the vessel to dilate and contract resulting in potential haemodynamic irregularity and loss of auto-regulation through disruption of the perivascular nerve plexi (Craggs et al. 2013; Kalaria 2010), and may lead to subsequent pathologies such as microinfarcts detectable at MRI (E. Burton et al. 2003; E. J. Burton et al. 2004; Firbank et al. 2012).

Microinfarcts (a minuscule area of necrosis resulting from sudden insufficiency of arterial or venous blood supply) are found in both cortical and subcortical regions, most probably signifying underlying microvascular pathology.

Microinfarcts are associated with cognitive impairment and their presence predicts a poor outcome in elderly individuals with CVD independent of Alzheimer's pathology (Vinters et al. 2000; Ballard et al. 2000; Kalaria et al. 2004). Another outcome of an occlusion are lacunar infarcts which are indicative of severe ischaemic damage resulting in a small area of necrosis leaving behind a cavity (lacuna). Combined, microinfarcts and lacunar infarcts are associated with over 50% of VaD cases (Esiri et al. 1999; Kalaria et al. 2004). Strategic infarcts refer to perfusion loss in a specific, cognitively important area of the brain, which may result in severe cognitive impairment relative to a similar sized infarct affecting a less critical part of the brain as mentioned earlier (Roman 2002b).

#### 1.1.5.3. ***Neuroimaging studies***

Neuroimaging studies have correlated changes in the white matter with cognitive dysfunction. Additionally frontal lesions have been associated with executive dysfunction (E. Burton et al. 2003). White matter hyperintensities (WMH) on T2 weighted MRI have long been associated as a pathological substrate of SVD and VaD (Kalaria and Ballard 1999; Tang et al. 2004; O'Brien et al. 2003) with WMH more prominent in the frontal lobe. The inefficient

vasculature leading to a chronic hypoxic state is thought to result in a loss of myelin and damage to the axonal tracts forming the cortico-cortico and cortico-subcortical connections within the brain (Kalaria and Ihara 2013). This hypoxic state is also thought to damage oligodendrocytes, cells which are responsible for repairing the myelin sheath. These cells are activated after mild to moderate ischaemic injury, however the prolonged hypoxic state is thought to lead to damage of the oligodendrocyte's precursor cells which no longer retain the ability to compensate for the myelin loss resulting in long term WM damage (Ihara et al. 2010).

#### 1.1.5.4. ***The blood brain barrier***

Gradual damage to the cerebral endothelium, which makes up the blood brain barrier (BBB) as a result of small vessel pathology may compromise the protective nature of the network of capillaries. The BBB plays a key role in the neurovascular unit and helps maintain an optimal environment for neurons and other cells to function. Breakdown of the vessel walls may result in the unregulated movement of macromolecules and fluid across the barrier into the brain with several studies linking the breakdown of the BBB to the development of cognitive impairment (Alafuzoff et al. 1983; Elovaara et al. 1987; Blennow et al. 1995; Wada 1998) with VaD sufferers more affected than those of AD suggesting a vascular link to cognitive decline. This is further supported by the correlation between WML and BBB permeability (Skoog et al. 1998; Wardlaw et al. 2003; Farrall and Wardlaw 2009). However, BBB dysfunction has been linked to amyloid levels in the cerebral spinal fluid, with those developing dementia having a higher CSF to serum albumin ratio than those without (Skoog et al. 1998; Blennow et al. 1990; Hampel et al. 1995). These studies suggest BBB dysfunction may be associated with both AD and VaD in elderly demented subjects, suggesting reduced selectivity of the permeability of the BBB. This increased permeability may result in increased flow of potentially harmful substrate entering the brain, disrupting neurons and other cells. The increase in CSF amyloid may signal the beginnings of the much-heralded amyloid cascade (Kalaria 2010; J. A. Hardy and Higgins 1992).

#### 1.1.5.5. ***Cerebral amyloid Angiopathy***

The insidious buildup of amyloid  $\beta$  ( $A\beta$ ) (a protein associated with AD and ageing) in the vessel walls is known as cerebral amyloid angiopathy (CAA)

(Grinberg and Thal 2010; Attems et al. 2011). Amyloid is transported through the perivascular space as a clearance mechanism. A breakdown in this mechanism may result in a buildup of A $\beta$ -40, and to a lesser extent 42, within the vessels basement membrane causing CAA (Weller et al. 2009; Kalaria 1992). The accumulation of A $\beta$  within the vasculature may lead to degeneration of the vessel wall, lowering perfusion and resulting in micro infarctions and haemorrhage (Kalimo et al. 2002; Knudsen et al. 2001).

#### 1.1.6. Alzheimer's disease (AD)

AD is the most common form of dementia, affecting around 10% of the population over the age of 75 (Jellinger 2002; Jorm and Jolley 1998). Clinically, AD is characterised by short term memory loss, impairments to spatial memory, which continue to deteriorate as the disease progresses (Thind and Sabbagh 2007). Memory loss results in pathology localized in the medial temporal, hippocampal areas. As the disease advances, involvement of the frontal lobes (Braak and Braak 1991) can result in executive dysfunction (Braak and Braak 1996; Braak et al. 1998; Braak and Braak 1998). At post-mortem the major pathological hallmarks of AD are amyloid-beta (A $\beta$ ) plaques, neurofibrillary tangles (NFTs), neuropil threads, and neuritic plaques (Braak and Braak 1991; Khachaturian 1985; J. A. Hardy and Higgins 1992).

One of the primary features of AD are extracellular cortical amyloid  $\beta$  plaques (A $\beta$ ), formed mainly of cortical A $\beta$ 42 (Montine et al. 2012) and to a lesser extent A $\beta$ 40 peptides. Amyloid  $\beta$  formed by the cleavage of APP by proteolytic enzymes  $\alpha$ ,  $\beta$ , and  $\gamma$  secretase. However A $\beta$ -40 and 42 are more likely to be formed when APP is cleaved by the  $\beta$  or the  $\gamma$  secretases at (Donmez et al. 2010). It has been shown that increasing the activation of ADAM 10, the gene encoding alpha secretase, can reduce the level of A $\beta$  produced due to alternative cleavage of the APP (Donmez et al. 2010). In addition, mutations within presenilin 1 and 2, a sub-protein of  $\gamma$ -secretase have been associated with increased amyloid production in familial AD (J. Hardy 1997). Age-related vascular pathology is thought to contribute the decrease in clearance of amyloid  $\beta$  (Kalaria 2010) resulting aggregation of the proteins, developing originally in

the neocortex and hippocampus before spreading to other areas of the brain in a well characterized manner as the disease progresses (Thal et al. 2002).

Several gene mutations have been associated with the production of amyloid. It has been shown that mutations within the gene coding for presenilin, part of the  $\gamma$ -secretase complex, are correlated with increased A $\beta$ 42 production, whilst specific mutations in the APP gene itself have been found to aid the subsequent folding capabilities of the A $\beta$  peptides produced through its cleavage. Though these mutations point towards a strong argument for the role of amyloid in AD it must be stated that familial cases of AD, such as those which present with mutations, represent only around 0.1% of all AD cases (Ertekin-Taner 2010). The majority of AD sufferers belong to a group known as sporadic AD. Whilst a range of specific gene mutations and SNPs have been reported in studies such as GWAS (Ertekin-Taner 2010) by far the most important risk factor in developing AD is age, though there exists a range of factors which may predispose an individual to developing AD.

Apolipoprotein (APO) E is a class of apolipoprotein essential for the catabolism of triglyceride rich lipoproteins. ApoE exists in 3 isoforms: Apo E2, E3, and E4. Those expressing one or two alleles of the apolipoprotein epsilon 4 have a significantly increased risk of developing AD (Walter 2012; Kalaria 2002), however, this is not a prerequisite for developing AD as 40% of AD sufferers do not possess the APOE  $\epsilon$ 4 allele at all.

The second neuropathological hallmark of AD is the presence of intracellular neurofibrillary tangles (NFTs) which consist of large entanglements of hyperphosphorylated tau protein (Goedert 1996; Alonso et al. 2008). Under normal conditions tau is a soluble microtubule-associated protein, with its role in stabilising the structure of cells, primarily aiding the stability of axonal microtubules. As part of its role all tau within a system is in a continuous flux between phosphorylation and non-phosphorylation (Iqbal et al. 2010; Alonso et al. 2008). In AD the tau protein becomes hyperphosphorylated leading to the formation of neurofibrillary tangles consisting of paired and single filaments within individual neurons. These large tangles are thought to either possess neurotoxic (gain-of-function) properties, damaging the neuron from within, or mechanistically disrupting the neuron by physically taking up large amount of

internal space (Mandelkow and Mandelkow 1998). Tau may also interact with amyloid in the form of neuritic plaques, A $\beta$  plaques surrounded by degenerating axons and dendrites containing hyperphosphorylated tau (Nelson et al. 2012; Montine et al. 2012).

The amyloid cascade hypothesis, a theory tying the two pathologies together, places amyloid burden at the core of AD progression, leading to NFT formation, has been a key focus for research (J. A. Hardy and Higgins 1992; Lamb 1997; Joseph et al. 2001). However, support for the theory is slowly beginning to wane. Braak et al showed that severity of clinical AD did not correlate with the amyloid pathology seen at post-mortem with high amyloid pathology also being reported in the brains of cognitively normal elderly individuals. The relationship between amyloid and tau has also been questioned, with each pathological substrate progressing differently (Ohm et al. 1995; Braak and Braak 1991).

CAA as mentioned previously is associated with up to 98% of AD patients (Jellinger 2002). Affected vessels present with thickened walls, with some presenting with microaneurysms and fibroid necrosis (Masson et al. 2000; Jellinger 2002). It is believed to be produced by the smooth muscle cells, which synthesis A $\beta$ -40 intracellularly. This protein then aggregates extracellularly into fibrils which result degeneration of the smooth muscle cell. This degeneration results in haemodynamic changes and rupturing of the blood vessels (Coria and Rubio 1996; Alonzo et al. 1998).

AD is also associated with reduced cholinergic neurotransmission, nicotinic acetylcholine receptors, and synaptic loss (Masliah 1995, 1998; Maelicke 2001; Crow et al. 1984; E. K. Perry et al. 1981), and cortical, ventricular, and white matter atrophy (Firbank et al. 2007; E. Burton et al. 2003; Chan et al. 2001). Neuronal or synaptic loss is thought to be the ultimate cause of the cognitive decline in AD though it is uncertain whether plaques and/or tangles are the cause of this loss or are just a by-product of an underlying pathology, such as CVD (Breteler 2000; Mann et al. 1988; Skoog et al. 1999; Maelicke 2001) .

Primarily, research into preventative treatments for AD has focused on A $\beta$  aggregate clearance mechanisms. However, attempts to develop suitable treatment against A $\beta$  accumulation have been unsuccessful (Karran et al. 2011). Treatments focused on alleviating the symptoms of AD have been



relatively more successful. Current drugs target the cholinergic and glutamatergic neurotransmission pathways, which have been shown to improve symptoms, though the neuroprotective role of such interventions is debatable (Mangialasche et al. 2010; Takeda et al. 2006; Bullock 2002). It is possible that current drug targets for the treatment of AD are focused on the end product of the disease and that in order to prevent disease progression, earlier interventions are needed. With this aim, early detection of AD may be helpful. Imaging with positron emission tomography (PET) with Pittsburgh Compound-B has linked amyloid  $\beta$  deposition with decreased glucose metabolism in the brain, providing a reliable imaging technique for detection of AD (Klunk et al. 2004). Perhaps more promisingly, Mapstone et al have developed a method for detecting AD 2-3 years before symptoms appear by the analysis of blood-borne phospholipids as a biomarker (Mapstone et al. 2014). However, without current treatments the usefulness of such early detection remains limited.

#### **1.1.7. Mixed dementia**

Mixed dementia is the diagnosis of two disease states both contributing to cognitive decline in an individual, in which the absence of one of the diseases would still result in dementia. The most common form of mixed dementia consists of AD and VaD (Kalaria and Ballard 1999). Indeed, 60-90% of those who exhibit clinical AD are found to have some form of CVD at post mortem (Kalaria 2002) and 60% of older patients with AD present with incomplete white matter infarctions (Roman et al. 2002) suggesting an underlying vascular component.

Historically a clinical diagnosis of 'pure' VaD is only established in subjects with cerebrovascular pathology and dementia in the absence of other dementia type pathologies (Erkinjuntti 1994). However, neuropathological examination of those thought to be suffering from AD have shown extensive CVD pathology, which thought to dramatically exacerbate dementia symptoms (Kalaria and Ballard 1999; Kalaria 2002, 2010). It is now widely acknowledged that due to the overlap of the two pathologies that the number of mixed VaD/AD cases is hugely underestimated (Leys et al. 2005; Skoog et al. 1999; Kalaria and Ballard 1999; Pascual et al. 2010). Additionally, a study conducted by Hulette et al

found the incidence of 'pure' VaD to be very uncommon (Hulette et al. 1997), with between 30-50% of mixed cases incorrectly diagnosed as VaD (Gold et al. 1997). It has also been shown that AD pathology occurs more often in subjects with CVD than in a normal ageing population, with some VaD subjects bearing other AD pathology such as cholinergic neuronal deficits (Kalaria and Ballard 1999) suggesting a shared aetiology between the two pathologies. Conversely, clinically diagnosed VaD subjects, at post-mortem, are frequently found to show AD type pathology (Kalaria 2002; Kalaria et al. 2004). Studies have also found amyloid accumulation around vessels correlating with hypoperfusion suggesting CVD may trigger AD type pathology (Sojkova et al. 2008; Huang et al. 2012). A causal link between AD pathology and VaD has been gleaned from Tg mouse studies. These studies suggest auto-regulation of the vasculature fails with amyloid accumulation, with vascular changes appearing in advance of neurodegeneration or A $\beta$  deposits (Iadecola 2004). This interplay between CVD and AD pathologies is also evident in the number of risk factors shared between the two pathologies, including hypertension, atrial fibrillation, and coronary artery disease (Kalaria 2002; Gorelick 2004) which suggests a CVD link between the two diseases (Table 1-1). The Nun study, a continuing longitudinal study examining the onset of AD in a cohort of 678 Roman Catholics nuns, revealed that well characterised individuals who were clinically diagnosed with AD performed worse on cognitive tests when displaying higher volumes of lacunar infarcts, whilst presenting with fewer NFTs, suggesting synergistic involvement of vascular pathology in AD suffers (Snowdon et al. 1997). In addition to shared risk factors, stroke has been shown to aggravate AD pathology (Kalaria 2002; Kokmen et al. 1996; Henon, Durieu, et al. 1996), with the ischaemic event potentially exacerbating already underlying AD pathology (Kalaria 2002; Cumming and Brodtmann 2011). It has been suggested that reduced glucose metabolism, resulting in increased activation of the glycogen synthase kinase-3 $\beta$  pathway, along with down regulation of the O-GlcNAcylation may suggest a viable, vascular mechanism for the abnormal hyperphosphorylation of tau in AD and other neuropathies (Deng et al. 2009).

Shared Risk factors between AD  
and VaD

---

Age  
Low education  
Hypertension/hypotension  
Hypercholesterolaemia  
hyperhomocysteinaemia  
Hyperlipidaemia  
Carotid-artery wall thickness  
APOEε4 allele  
Diabetes mellitus  
Traumatic brain injury  
Smoking  
Obesity  
Stroke  
Atrial fibrillation

**Table 1-1 showing the shared risk factors of AD and VaD. Adapted from (Kling et al. 2013; Gorelick 2004)**

## **1.2. The prefrontal cortex**

The prefrontal cortex contains three separate, yet interconnecting circuits responsible for specific aspects of memory, executive function, and social behaviour: the dorsolateral prefrontal cortex (dlPFC), the anterior cingulate cortex (ACC), and the orbitofrontal cortex (OFC) (Figure 1-4). Two other circuits: the motor circuit and the oculomotor circuit also make up the frontal cortex circuitry; though have little or no impact on executive functions (Tekin and Cummings 2002). These executive functions allow the organism to interact adaptively with environmental cues and stimuli. Each circuit takes its name from either its region of origin (i.e. the dorsolateral prefrontal cortex), or its primary function (i.e. motor circuit) (Lichter and Cummings 2001; Tekin and Cummings 2002).

Each of the three frontal circuits shares a similar cortico-subcortical framework, originating in the PFC before projecting to respective aspects of the striatum before reaching the globus pallidus and substantia nigra, pen-ultimately connecting to the thalamus before the circuit is completed by reverting back the PFC (Figure 1-2)(Tekin and Cummings 2002). Though several regions are shared between circuits the general connection remains separate throughout the majority of the circuit, a quality necessary for performance of individual processes and tasks. Much of what is known about the function of these circuits is through loss of function studies.

### **1.2.1. The prefrontal cortex and disease**

Essentially the role of each circuit is to connect the evolutionary younger prefrontal cortex with the more ancient subcortical areas such as the limbic system. These connections are crucial for working memory, processing for tasks and problem solving. By utilising the executive functionality of the PFC against the memories stored in the limbic system it allows for the brain to employ previous experiences against newer stimuli. Studies into the significance of lesions located in specific areas have helped elucidate the roles each of these circuits play. When measuring attention, working memory and visual processing functions via the Wisconsin Card shuffling test (WCST) patients with lesions in the dlPFC performed worse than those with lesions in

the OFC or indeed those with no lesions (Grafman et al. 1990) suggesting the dlPFC has a greater involvement in performing such tasks when compared to the OFC. Indeed several other studies have found deficits in WCST in dlPFC lesioned individuals compared to non-lesioned controls (Barcelo and Knight 2002; Eslinger and Grattan 1993; Bornstein and Sigman 1986). When verbal dexterity is tested through use of the Phonemic Verbal Fluency test in which individuals must say as many words beginning with a given letter, or within a specific category as they can, it was found that those with frontal lobe lesions produced fewer words than those without (Bornstein and Sigman 1986; Butler et al. 1993), and those with lesions in the left frontal hemisphere performed worse still (Stuss et al. 1998; Baldo et al. 2001) revealing a lack of ability to utilise stored information in regards to a current task. A similar trend was found in individuals tested using the Stroop colour word interference test with those suffering left-side frontal lesions performing worse than controls or right-side lesion suffers (Perret 1974; Stuss et al. 2001).

### **1.2.2. Cortical architecture and pyramidal neurons**

Cortical grey matter is divided into different layers with each containing a specific subset and distribution of neurons, glia, and other cells (Mountcastle 1997). The prefrontal cortex is divided into 6 layers with layer I (one) originating near the pial surface running through to VI adjacent to the WM. Though each area, the dlPFC, OFC, and ACC, maintains this basic layered structure, each region exhibits certain specificity, which must be taken into account when selecting areas for analysis (Khundakar et al. 2011b). The cytoarchitecture of the dlPFC is highly regimented, differentiated uniformly into the six layers of the granular isocortex. Conversely the OFC and ACC exhibit a more heterogeneous agranular limbic cortex, whilst still following the six-layered organization (Khundakar et al. 2011a; Khundakar et al. 2011c).

Layer III and V, referred to as the external and internal pyramidal layers respectively, contain a very high proportion of pyramidal neurons in relation to other layers (Spruston 2008). Pyramidal neurons are responsible for long-range projections between cortices which are facilitated by their long axons. Pyramidal neurons are not all identical, varying between regions, but share several characteristics (Figure 1-2). Pyramidal neurons are relatively large, glutamatergic neurons, identifiable due to their distinctive pyramidal shape and

large apical dendrite extended towards the pial surface (Tekin and Cummings 2002). The lone axon emanating from the base of the neurons has a high number of branches, making many excitatory, glutamatergic connections as it travels along its length (Spruston 2008). Projections originating from pyramidal neurons in layer III are thought to form intra-regional connections, whereas projections from layer V typically span further distances throughout the brain forming inter-cortical connection from the frontal cortices to other areas of the cortex as well as subcortical regions (Tekin and Cummings 2002; Khundakar et al. 2009). Some of these connections are thought to be bidirectional allowing information and feedback to be shared between regions. Specifically, the ACC and the OFC have projections to the temporal lobe, with a series of intricate connections with the amygdala. Ghashghaei et al reported modest connections between the amygdala and the lateral PFC suggesting minimum interaction between the two regions (Ghashghaei and Barbas 2002).

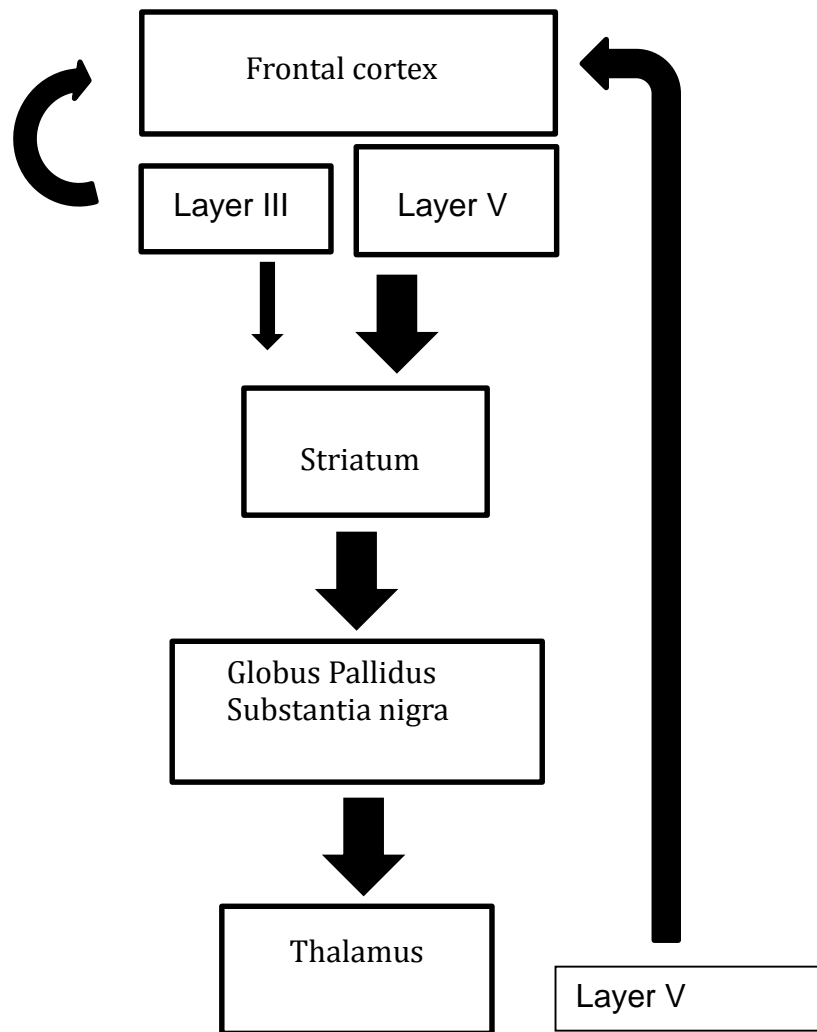


**Figure 1-2 showing cortical neuronal connections within the PFC and subcortical areas of the brain. Neuronal connections of layer III largely project to areas within the PFC with few connections to subcortical brain regions in other areas of the circuit. Layer V contributes the majority of subcortical connections making up the circuit. Adapted from (Tekin and Cummings 2002)).**

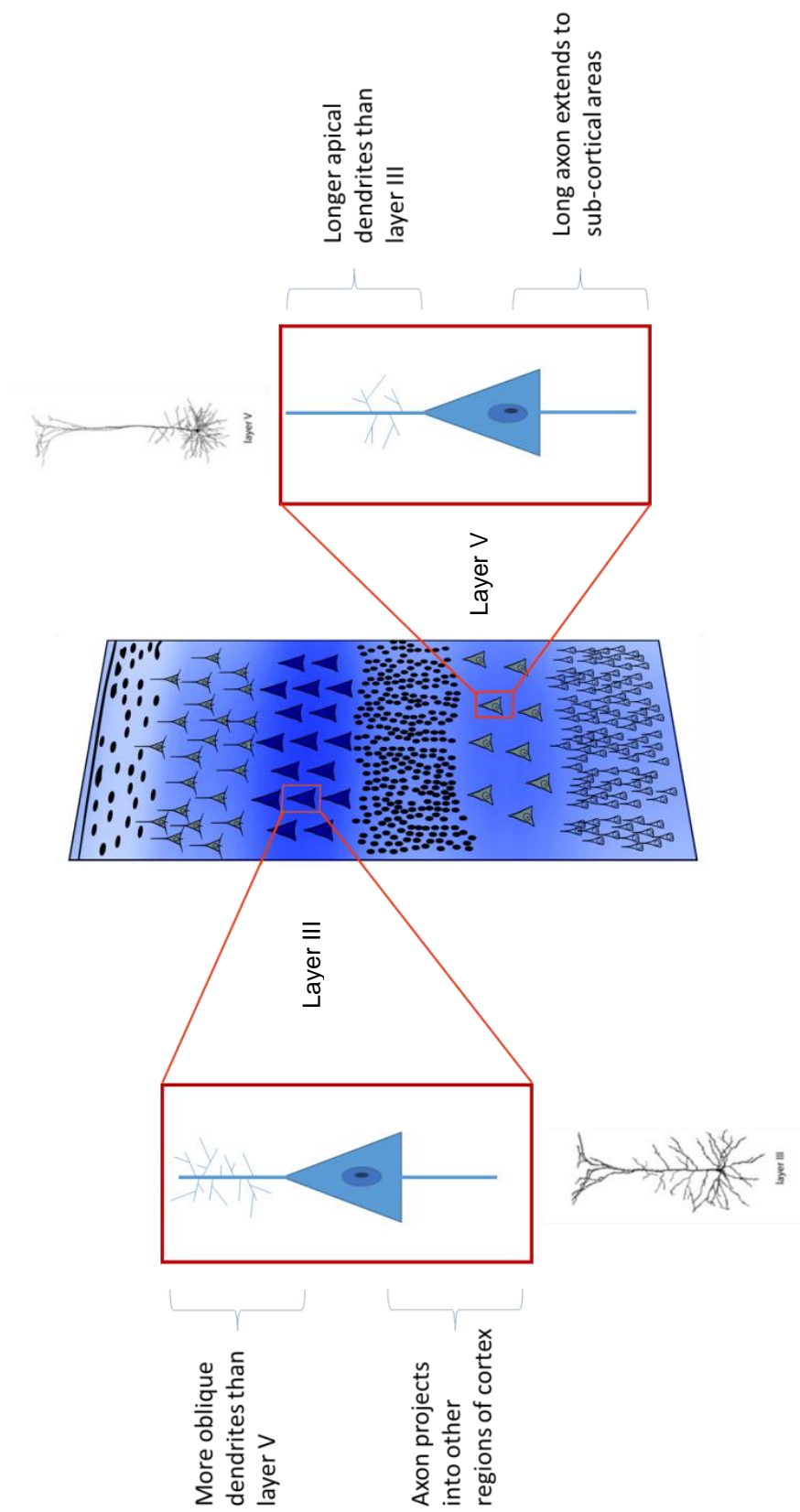


Figure 1-3 showing gross differences between layer III and layer V pyramidal neurons. Graphics adapted from Spruston et al (Spruston 2008).



### 1.2.3. The prefrontal circuits

- The dlPFC originates in Brodmann areas 9 and 46 (Figure 1-4) before projecting to the dorsolateral aspect of the caudate. It is involved mainly in executive function: the integration of processes such as working memory, problem solving and planning. Those suffering dysfunction of the dlPFC display impaired reasoning and lack mental flexibility. They lack the ability to maintain attention and appropriately focus on given tasks, being easily distracted, and requiring constant direction from examiners. They also demonstrated poor verbal fluency. The dlPFC appears to have modest connections with the limbic system (Ghashghaei and Barbas 2002). This executive dysfunction is a principle factor in dementias, in which subcortical circuits such as the dlPFC are thought to be affected. Additionally, those with lesions in the dlPFC struggle recalling long term memory based information for use in current tasks suggesting a dysfunctional link with the temporal lobe (Tekin and Cummings 2002).
- The ACC, primarily located in Brodmann area 24, is notoriously heterogeneous with different aspects of the region commanding distinctively different roles (Gittins and Harrison 2011). The ACC concerns itself with the motivation of behaviour, with distinct lack of motivation being associated with dysfunction in this area. Indeed in some cases of bilateral lesioned individuals display akinetic mutism: a condition characterised by extreme apathy, indifference to pain, hunger or thirst. They may also struggle to understand new concepts or creative thought processes (Tekin and Cummings 2002).
- The OFC possesses the strongest association with the limbic system sharing intricate bidirectional neuronal connections with the amygdala (Ghashghaei and Barbas 2002), as well as connection to the hypothalamus, and other hippocampal formations. This role introduces an emotional tone to outside stimuli, with the OFC connecting environmental cues to the subcortical limbic system (Lichter and Cummings 2001). Damage or degeneration to this circuit can lead to

personality changes i.e. emotional liability and behavioural disinhibition, lacking judgment and empathy (Tekin and Cummings 2002).

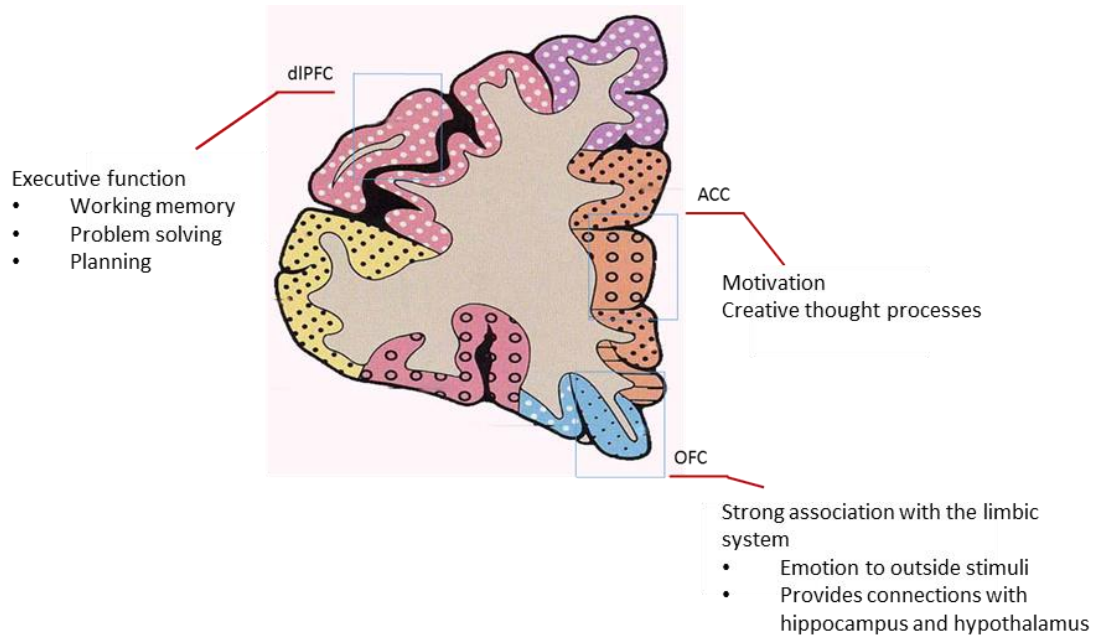


**Figure 1-4 showing the location of the three PFC circuits and their relative functions. PFC = prefrontal cortex, dIPFC = dorsolateral prefrontal cortex, ACC = anterior cingulate cortex, and OFC = orbitofrontal cortex (O. Perry 1993).**

### 1.3. The prefrontal cortex circuit and vascular disease

Executive dysfunction has been suggested as a predictor for VaD in post-stroke cases (Roman and Royall 1999; Pohjasvaara et al. 2002). The frontal lobe is particularly vulnerable to vascular-based pathology. Deramecourt et al reported over 89.6% of demented cases had presence of SVD in the frontal lobe. Arteriolosclerosis was the most common pathological substrate present for 87.3% of SVD sufferers with higher pathology located in the frontal lobes when compared the temporal lobes (Deramecourt et al. 2012).

Clinical symptoms between different diseases can lend valuable insight to underlying pathological processes. Whereas AD sufferers may relinquish memory and language functions, indicative of temporal lobe atrophy, those with VaD express loss of executive functions; attention, and planning as vascular pathology initially localises in the frontal lobe, disrupting the ganglio-thalamo-cortical circuits (Kalaria 2002; Roman and Royall 1999) .

Frontal pathology can also cause non-cognitive symptoms which can overlap with cognitive features. Alexopoulos et al proposed that vasculature changes to the frontal lobe might result in depression in what they called the vascular depression hypothesis (Alexopoulos et al. 1997). Depression is linked to stroke, WMH, and hypertension (Teodorczuk et al. 2007) - similar risk factors associated with dementia. Indeed patients suffering from post-stroke depression have been found to suffer executive dysfunction (Leeds et al. 2001; Pohjasvaara et al. 2002). This link between vascular pathology and the frontal lobe functions cannot be ignored, indeed the cognitive dysfunction observed in vascular depressed cases paralleled the cognitive changes of those suffering VaD (Sultzer et al. 1993; Alexopoulos et al. 1997), suggesting vascular pathology disrupts vital cortico-cortico, cortico-subcortical circuits. Damage to the striato-pallido-thalamo-cortical pathways is common in CVD (Fujikawa et al. 1993; Coffey et al. 1990; Krishnan et al. 1988), which may result from direct damage to the OFC, dlPFC, or ACC.

Furthermore Burton et al reported significantly higher white matter lesions in the frontal lobe of post-stroke patients correlating with executive function and attention deficits and a result of lesion damage to the frontal circuits (E. Burton et al. 2003). Indeed, attention is most susceptible to disruption, and may be the

first cognitive function to decline (Pasquier and Leys 1997). WMH within the frontal lobe detected via MRI have long been associated with microvascular changes thought to affect executive functions in the 'healthy' population (DeCarli et al. 1995; O'Brien et al. 2002) with WMH severity linked to cognitive speeds and executive dysfunction in those suffering VaD suggesting WM damage affects the connectivity between these subcortical regions (Cohen et al. 2002).

Age related changes to the integrity and structure in frontal WM have been linked to the disruption of the frontal subcortical circuits and is thought a result of vascular micropathology (Kalaria 2010). WM lesions are often seen in the elderly via MRI scans in anything between 5-90% of patients with some reporting higher incidence of WMH in women, with evidence that these WMH are a result of PVS and relate directly to cognitive dysfunction through disruption of the PFC circuits (de Leeuw et al. 2001). Indeed it has been shown that patients with increased vascular pathology at MRI have decreased glucose metabolism in the frontal cortex (Pascual et al. 2010). In addition, patients with lacuna infarcts displayed significantly reduced glucose metabolism in the dorsolateral prefrontal cortex which correlated with cognitive dysfunction (Reed et al. 2004). This trend has also been reported with those of suffering cardiovascular disease, as discussed, a known risk factor for VaD (Kuczynski et al. 2009).

### **1.3.1. Interneurons and the inhibition circuits**

The excitatory activity of the pyramidal neurons within the prefrontal cortex is mediated by a parallel counter system controlled by a sub-population of GABAergic interneurons. Interneurons are arranged in the cortex in layers, similar to their excitatory counterparts.

Though the vast majority of neurons within the neocortex are pyramidal neurons, accounting for 70-80% (DeFelipe and Farinas 1992), the remaining neurons are a collection of inhibitory interneurons, which utilise the  $\gamma$ -aminobutyric acid (GABA) as their transmitter, in lieu of the excitatory transmitter-glutamate (Markram et al. 2004). Interneurons have a range of varied synaptic and physiological characteristics. Though the overwhelming majority of

interneurons are inhibitory they receive both excitatory and inhibitory signals via their dendritic arbours.

Biochemically interneurons can be characterised based on the heterogeneous expression of one or more of three specific calcium-binding proteins:

Parvalbumin positive, calbindin positive, and calretinin positive (Table 1-2).

Parvalbumin and calbindin positive cells are thought to act as endogenous buffers in certain neurons with calretinin acting as a template for preplate neurons (Markram et al. 2004).

Interneurons can be distinguished from pyramidal neurons primarily due the lack of a large triangular soma, the presence of aspiny dendrites, the morphology of which are highly variable between interneurons and not useful in defining the specific sub-types of interneuronal species, and for the absence of the large apical dendrite which is so distinctive of pyramidal neurons (Spruston 2008; Markram et al. 2004). Each cell type will have an axonal arbourisation specific to the cell domain, layer or cortical column being targeted. To this end, based on axonal morphology interneurons can be placed into three functional groups: axon-targeting (with the interneuron exhibiting an editing role in relation to the target cell's excitability), soma and proximal dendritic targeting (allowing presynaptic neurons to control the gain/intensity of the action potential leaving the neuron), and distal dendritic and tuft-targeting (for control of local dendritic innervation) (DeFelipe 1997). Interneuron targeting of dendrites allow for control and influence of dendritic processing and the synaptic inputs (Markram et al. 2004).

Unlike pyramidal neurons, the inhibitory effect of interneurons is rarely felt outside the local cortical area, as interneurons do not project to distant brain regions. Interneuronal connections can however project to nearby layers and cortical columns effecting a local inhibitory response, sometimes called the 'local circuit neuron' (Letinic et al. 2002) and can again be broken up into three sub-groups: intralaminar-intracolumnar, interlaminar-intracolumnar, and interlaminar-intercolumnar (Markram et al. 2004).

#### 1.3.1.1. ***Type of Interneurons***

As well as those broad chemical-based distinctions, it is possible to further classify interneurons into 5 broad sub-types:

**Basket cells (BC):** BCs are a class of soma and proximal dendritic interneuron (Gilbert 1993; Y. Wang et al. 2002; Marin-Padilla 1969) accounting for around 50% of all inhibitory neurons in the neocortex. In this role they can adjust the gain of the integrated synaptic responses. It is the converging nature of several of these cells around pyramidal neurons which give them the basket-shaped appearance from which their name derives. Basket cells can be histologically identified through their expression of one of two calcium binding proteins: parvalbumin, and calbindin. Basket cells can be further classified dependent on their axonal and dendritic morphologies: large basket cells, small basket cells, and nest basket cells.

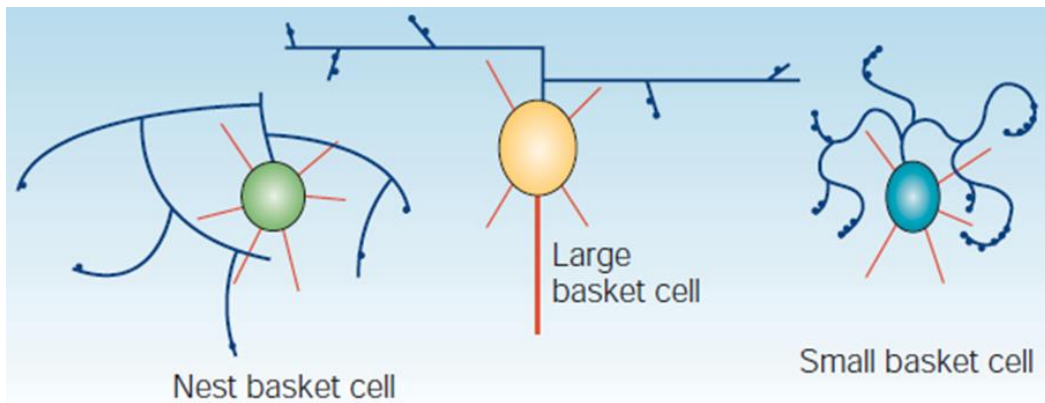


**Figure 1-5 showing the soma and proximal dendrite-targeting interneurons of the prefrontal cortex (Markram et al. 2004) Red lines = dendrites, blue line = axons, and blue dots = axonal boutons. Markram et al., 2004)**



**Chandelier cells (CC):** These are axon targeting interneurons which influence the output of a pyramidal neuron, fine-tuning or nullifying inputs from other, dendritic or soma targeting interneurons (Buhl et al. 1994), and are found in cortical layer II through VI, expressing both PV and CB (Markram et al. 2004).

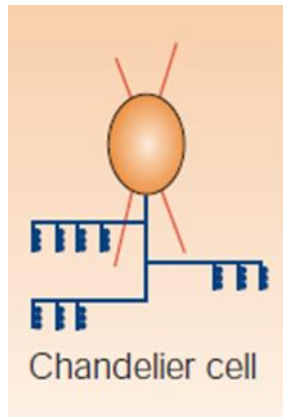


Figure 1-6 showing the axon targeting interneuron. Red lines = dendrites, blue line = axons, and blue dots = axonal boutons. Adapted from (Markram et al. 2004).

**Martinotti cells (MC):** These are unusual as they do not necessarily fall into the classic interneuronal sub-types as described. MCs may target several aspects of pyramidal neurons in layers and columns not immediately local to their area. MCs reside in layers II to IV but their axons project into layers I where they exact most their influence. Interestingly, MCs not only project away from their original layer but also across cortices influencing action potentials in neighbouring cortical columns. MCs target multiple domains of the target neuron such as both distal and proximal dendrites and peri-somatic dendrites and somata. MCs have been known to express both CB and CR.

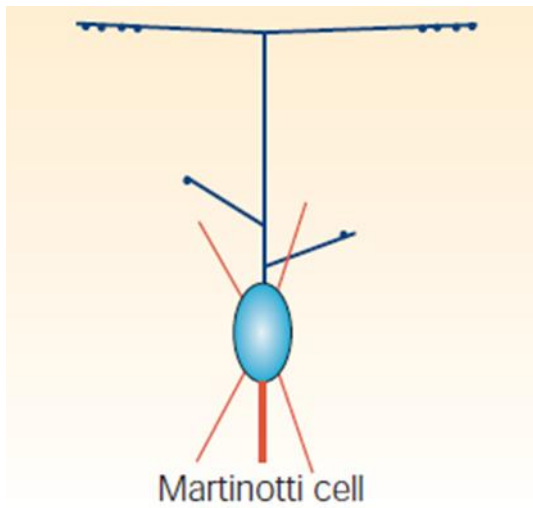


Figure 1-7 showing dendrite and tuft-targeting interneurons. Red lines = dendrites, blue line = axons, and blue dots = axonal boutons. Adapted from (Markram et al. 2004)

**Bipolar cells (BPC):** BPC axons can project across all layers and have either excitatory or inhibitory properties. Due to their low bouton density they contact and therefore influence relatively few neurons when compared to their other interneuronal counterparts. They tend to target the basal dendrite of pyramidal neurons expressing mainly CR (Markram et al. 2004).

**Double bouquet cells (DBC):** DBCs are located in layers II through V (fig 9) and, like BP, target and inhibited basal dendrites of pyramidal neurons as a class of dendritic targeting cells. DBC express both CB and CR (Markram et al. 2004).

**Bitufted cells (BtC):** Though possessing a dendritic arbour less extensive than that of BPCS, and DBCs, BtC project mostly into other layers. A class of dendritic targeting cell, they can influence the input received by pyramidal neurons. BtC cells express CB and CR (Markram et al. 2004).

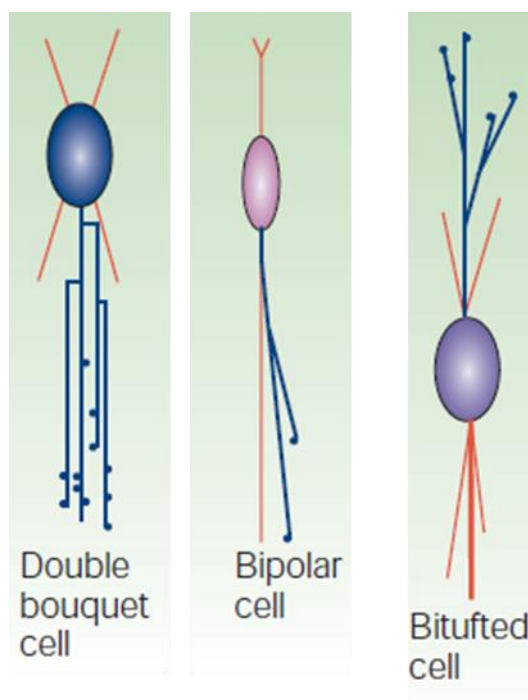


Figure 1-8 showing the dendrite-targeting neurons in the prefrontal cortex. Red lines = dendrites, blue line = axons, and blue dots = axonal boutons. Adapted from (Markram et al. 2004).

The most common type of interneuron in both later II/III and V are large basket cells. In layer II/III this is followed by net basket cells, and Martinotti cells in layer V (Figure 1-9) (Markram et al. 2004).

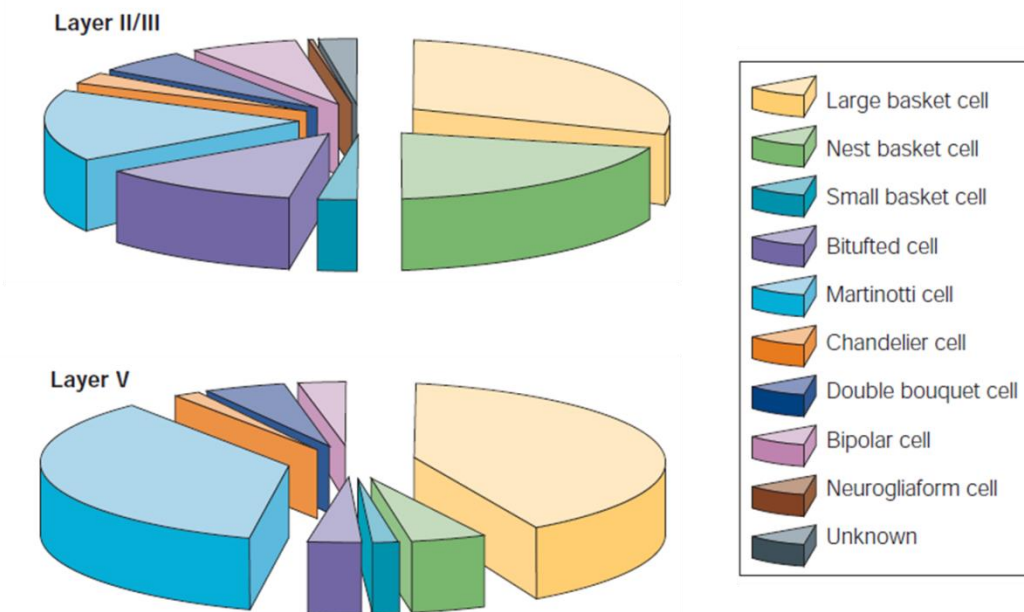


Figure 1-9 showing the distribution of interneuronal subtypes in layers II, III, and V of the prefrontal cortex. Adapted from Markram et al (Markram et al. 2004; Simpson et al. 2007; Chance et al. 2011).

Interneuronal subtypes	PV	CB	CR
Large basket cell	x	x	
Nest basket cell	x	x	
Small basket cell	x	x	
Chandelier cell	x	x	
Martinotti cell		x	x
Bipolar cell			x
Double bouquet cell		x	x
Bitufted cell		x	x

Table 1-2 showing interneuronal subtypes and their respective immunohistochemical reactivity. Adapted from Markram et al (Markram et al. 2004). PV = parvalbumin, CB = calbindin, CR = calretinin.

### 1.3.2. **Glial cells**

Though pyramidal neurons form the vast majority of connections between regions of the brain, and interneurons are thought to keep check of these excitatory cells - glial form a major component of the central nervous system (CNS). Glial cells are an umbrella term representing a range of non-neuronal cells types from: astrocytes, oligodendrocytes and microglia (Nedergaard and Dirnagl 2005). There is not enough research focused on the role glial cells may play in the development of PSD, but as will be shown below, glial cells may play important roles in cognitive impairment and dementia.

#### 1.3.2.1. ***Astrocytes, the neurovascular unit, and stroke***

Astrocytes form part of the neurovascular unit (NVU) (Nedergaard and Dirnagl 2005; Hawkins and Davis 2005) controlling the supply of blood and nutrients to neurons dependent on their metabolic requirements, through the selective uptake of nutrients through their endfeet and control over vessel diameter (Simard et al. 2003; Nedergaard et al. 2003; Koehler et al. 2009). Following ischaemic injury astrocytes have a major role in controlling ion and water homeostasis (Leis et al. 2005; Dienel and Hertz 2005; Kimelberg 2005) in addition to supplying much needed trophic factors and scavenging reactive oxygen species (ROIs) (Trendelenburg and Dirnagl 2005). Astrocytes act as a sponge for excess glutamate and potassium ions which result from a stroke. Large numbers of glutamate transports are present in the glial cell's membrane and act to protect the brain from excitotoxicity due to high concentration of antioxidants such as glutathione and ascorbic acid which protect against the ROS produced after an ischaemic event (Danbolt 2001). Lack of glutamate modulation due to astrocytic damage leading to increased excitotoxicity may be another pathway to neuronal dysfunction (C. M. Anderson and Swanson 2000). Astrocytes may be particularly vulnerable to the ageing process (Kalaria 2010) with changes to the astrocytic endfeet reported in ageing brains (Kalaria 1996), becoming more profound in those suffering neurodegenerative disease, exhibiting degenerated microvascular (Moody et al. 2004). The dysfunction of astrocytes may lead to a breakdown of the neurovascular unit, resulting in a failure in communication between neuronal activity and metabolism and blood

and nutrient flow. This would leave neurons in an undesirable state and may ultimately lead to neuronal dysfunction and death. Additionally, astrocytes are a major store for glycogen within the brain which is used to supply neurons with glucose in periods of high neuronal activity (A. M. Brown and Ransom 2007; Schousboe et al. 2010).

Furthermore, in hypoxic environments and AD subjects, astrocytes have been shown to have increased reactivity, suggesting angiogenic signals are increased in these conditions in an attempt to counter the stroke/vascular damage and AD pathology (Kalaria et al. 1998; Burke et al. 2014).

#### 1.3.2.2. ***Glial cells and white matter***

Oligodendrocytes are responsible for axonal myelination within the white matter of the CNS, and make up almost half of the total volume of the WM (Nave 2010b, 2010a; Alberdi et al. 2005; Pfeiffer et al. 1993). Oligodendrocytes extend a composition layer of protein and lipid which is wrapped around the nearby axon (Sherman and Brophy 2005; Nave 2010b) (Figure 1-10). This sheath insulates the axon and enables salutatory conduction (or impulse propagation) along the length of the axon allowing action potentials to travel at speeds up to 100x faster than in un-myelinated tracts (Nave 2010a).

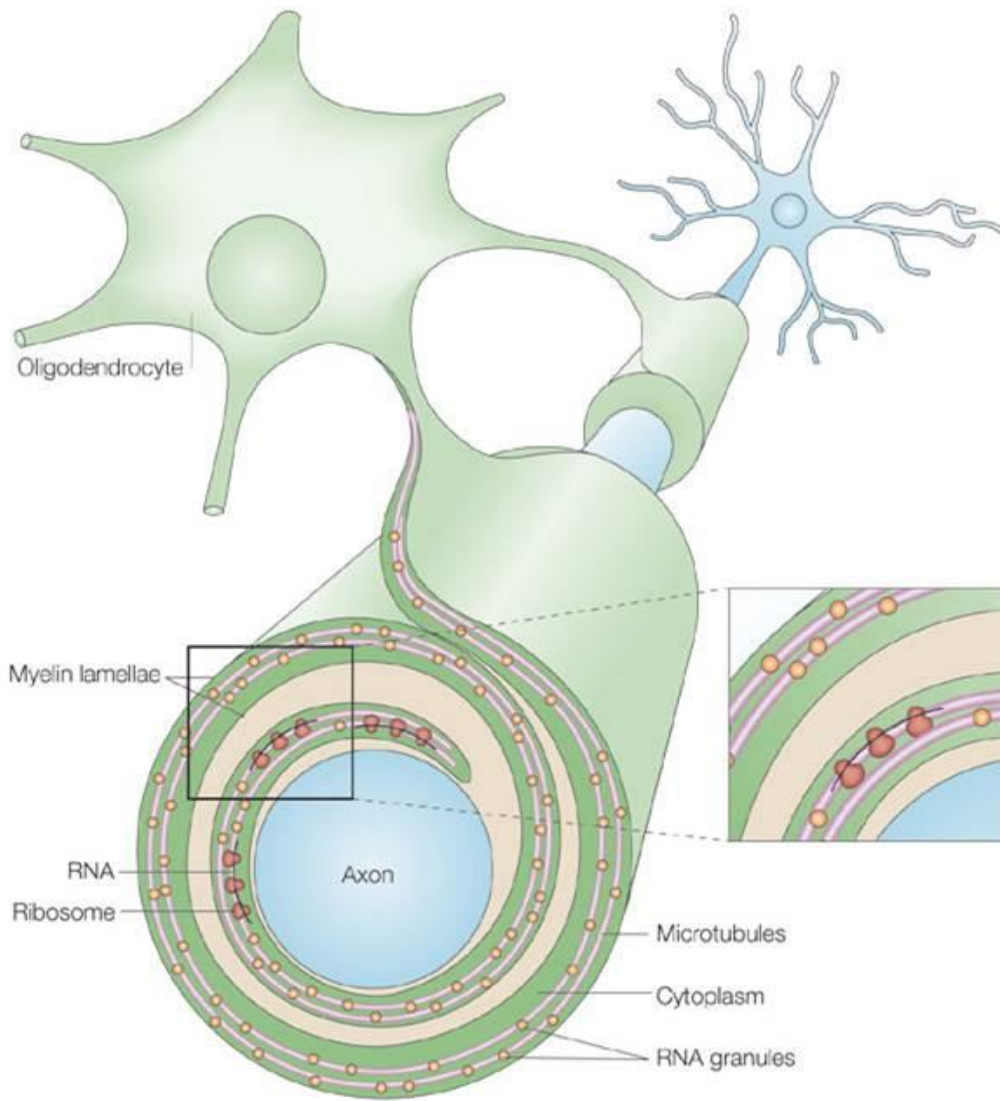


**Figure 1-10 demonstrating the mechanism with which oligodendrocytes myelinate axons (Sherman and Brophy 2005).**



Damage to oligodendrocytes may result in reduced myelination in the WM, slowing action potentials and leading to the potential dysfunction of axonal connections between neurons, disrupting neuronal circuit communications and ultimately cognitive dysfunction. Additionally, damage to oligodendrocytes may lead to Wallerian degeneration, in which break down of the axonal white matter results in the retrograde damage to neurons in the grey matter (Nedergaard and Dirnagl 2005; Nedergaard et al. 2003; Cook and Wisniewski 1973; Mack et al. 2001).

Due to the expression of NMDA receptors and glutamate channels oligodendrocytes are the most vulnerable of the glia to hypoxic and excitotoxic insults resulting from ischaemic damage (Alberdi et al. 2005; Nedergaard and Dirnagl 2005) . This may play a significant role in stroke, CVD, and neurodegenerative disease, with loss of oligodendrocyte function as a result of oxidative stress and mitochondrial dysfunctions (Danbolt 2001; Sanchez-Gomez et al. 2003).

It has been proposed that axons regeneration following a pathological insult is impeded by the formation of a 'glial scar', made up of activated astrocytes and proteoglycans. The glial scar creates a barrier which prevents the potential reformation and reconnection of axons within the WM and are believed to be a major part in the failure of regeneration within the WM (Silver and Miller 2004). Oligodendrocyte dysfunction has also been associated with the development of cognitive dysfunction (Cook and Wisniewski 1973; Giaume et al. 2007; Ihara et al. 2010)

#### 1.3.2.3. ***Microglia and immunoresponse in the brain***

The third most common type of glia are microglia which make up about 20% of the total glial cell population (Gehrmann and Kreutzberg 1994), inhabiting the brain parenchyma. Microglia form the major immune response system within the BBB as the CNS' resident immunocompetent cell (Kreutzberg 1996). Microglia have a complex network of processes which are in contact with neurons, vessels and other glial cells to continuously monitor their local environment (Nimmerjahn et al. 2005; Fetler and Amigorena 2005). Insults to the brain increase the level activated microglia, stimulating the release of a

range of cytokines and chemokines (Nedergaard and Dirnagl 2005). The microglia create a tight network to seal off the damaged area establishing a barrier between healthy and injured tissue (Davalos et al. 2005; Giulian et al. 1994).

Brain inflammation, a pathological substrate of several diseases including stroke, can also result in glial cell proliferation, increasing the numbers of astrocytes and microglia and up-regulation of inflammatory markers, such as interleukin 1 beta, and TNF $\alpha$  in a phase known as reactive gliosis (Rouach et al. 2002; Giulian et al. 1994) which may result in increased excitotoxicity which can lead to BBB dysfunction, increased neurotoxicity within the brain (Nedergaard and Dirnagl 2005) and in extreme circumstances may result in a glial scar (as described previously). Microglia have also been implicated in AD, aggregating around amyloid plaques, possibly in an attempt to clear A $\beta$ , suggesting microglia may play a key role in AD and in potential therapeutic interventions in the future (Bolmont et al. 2008).

It is unknown how these cells play a role in PSD. The intricate relationship between glial cells, neurons, axons, and vessels may be an important aspect of the neurovascular unit and cortical connections. Any disruption to this complex association may result in severe consequences for cognitive health.

#### **1.4. The cognitive function after stroke (CogFAST) study and it's key findings**

The cognitive function after stroke (CogFAST) study was a MRC funded prospective, unique, longitudinal study centred in Newcastle and designed to investigate the long-term pathological processes which may account for the development of dementia in stroke survivors (Allan et al. 2011).

Over 50% of patients experienced improvements in cognition following a stroke (Ballard et al. 2003). Of the 355 subjects recruited into the study 176 had died within a mean follow-up time of 5.76 years, with a median survival time of 6.72 years from the incident stroke. The three most significant univariate risk factors for death after stroke included the subject having suffered a previous disabling stroke, the number of cardiovascular risk factors, and a low CAMCOG executive function score (Table 1-3). When looking at multivariate risk factors as

predictors of death: older age, a history of smoking, and occurrence of previous strokes all increased risk of death (Allan et al. 2011) (Table 1-3).

During a period of 1346 person-years 85 of the 355 participants had developed post-stroke dementia with an incidence of 6.32 cases in every 100 person years, with 39.5 percent of subjects having developed PSD after 7 years. Risk factors for developing PSD included low scoring in follow-up tests such as CAMCOG, the presence of more than one cardiovascular risk factors, and having suffered a previous stroke (Table 1-3). Mean survival time from baseline stroke did not significantly differ between those who developed PSD and those who remained cognitively stable. The majority of PSD cases fulfilled the currently used criteria for vascular dementia, with no typical distinction of vascular pathology seen between cases. Tau pathology was greater in those which developed PSD, whilst also exhibiting a higher proportion of microinfarcts (Allan et al. 2011), with stroke survivors suffering from impairments to working memory and reduced executive function when compared to non-demented controls (Ballard et al. 2003).

Genetic studies on the CogFAST cohort have revealed a single nucleotide polymorphism in the endothelial nitric acid synthase (NOS3) gene (codon 298) increased the risk of dementia in post-stroke subjects, possibly as a result of a reduction in nitric oxide production and cerebral perfusion (Morris et al. 2011). MRI imaging showed the left/right medial atrophy score was greater in subjects with PSD than those who were cognitively unimpaired. Cognitive scoring, as measured using baseline CAMCOG score, significantly correlated with atrophy scores. In turn CAMCOG scores significantly differed between PSD and PSND subjects. PSD subjects exhibited higher frequencies of Braak stage III or higher when compared to PSND (Allan et al. 2011).

#### 1.4.1.1. ***Imaging studies***

MRI studies showed medial temporal atrophy predicted subsequent decline in CAMCOG memory scores, though no such relationship was found between cognition and baseline white matter hyperintensities and no significant difference was found between those who remained cognitively stable and those who would go on to develop PSD. However, global atrophy scores, assessed 2 years post stroke, showed ventricular enlargement correlated with both medial

temporal atrophy (MTA) and total WMH (a marker for vascular/ischaemic pathology). Significant correlation between WMH and reduced cognition suggests a greater involvement in vascular pathology two years post-stroke (Firbank et al. 2012; Firbank et al. 2007). Firbank et al reported memory loss was related to both baseline memory and medial temporal atrophy but not WMH volume, suggesting a greater involvement of Alzheimer type pathology than vascular pathology in late-onset post-stroke dementia (Firbank et al. 2007). In addition, decreased pyramidal neuronal volume has been reported in both hippocampal subfields CA1 and CA2 of PSD subjects when compared to PSND and controls, with this apparent atrophy correlating with both global cognitive function scores and memory function, in post-mortem tissue (Gemmell et al. 2012).

Further studies found increased WMH in all key areas of the brain of stroke subjects. In particular correlations between total and frontal WMH and cognitive function such as attention and processing speeds (E. Burton et al. 2003). Other areas of the brain also appear significant in the development of post-stroke with Infarcts in the putamen correlating with memory impairment. Interestingly, arterial spin labeling MRI 3T imaging revealed cerebral blood flow in global grey and white matter was significantly reduced in post-stroke demented cases when compared to controls (Firbank et al. 2011).

Risk factors	Death	PSD
Age	yes	yes
CAMCOG <80	yes	yes
Number of CV risk factors:		
1 or 2	yes	no
≥3	yes	yes
Previous Stroke	yes	yes
Smoking	yes	yes
Ischaemic heart disease	no	yes
Camcog total exec. Function	yes	yes
Geriatric depression score	yes	yes

**Table 1-3 showing the relationship between risk factors and relative risk of death and dementia. Adapted from (Allan et al. 2011). CAMCOG = Cambridge Cognitive Examination, CV = Cardiovascular, exec = Executive function**

#### **1.4.2. Neuropathological assessment and dementia diagnosis**

All cases in the brain bank undergo a standardised clinical assessment. Dementia is therefore established independently of the pathological findings. After death, stroke survivors and VaD, AD and mixed dementia subjects who came to autopsy underwent a macroscopic and microscopic pathology assessment with standardised protocols (Ihara et al. 2010; Kalaria et al. 2004). General neuropathological assessment of the brain structure, and assessment of infarcts was performed by experienced neuropathologists using haematoxylin and eosin with any infarcts <5mm classified as a microinfarct. CERAD rating of neuritic plaques and Braak staging for tau progression was performed using standard silver impregnation procedures and immunohistochemical techniques respectively. Distribution and burden of vascular amyloid was also noted in each case to assess the level of cerebral amyloid angiopathy. Subjects were diagnosed as AD if they presented with CERAD score of moderate-severe and a Braak score of V-VI with limited present of vascular pathology. VaD was diagnosed if subject's brain showed evidence of vascular pathology such as: small vessel disease, cystic infarcts, lacuna infarcts, microinfarcts, or leukoaraiosis which were deemed severe enough to contribute to result in dementia in the absence of neurodegenerative disease. In cases where vascular pathology deemed substantial enough to lead to a diagnosis of VaD in addition to moderate-severe Alzheimer's pathology a diagnosis of mixed dementia was chosen.

CogFAST cases underwent an additional global vascular assessment, which 4 brain regions were examined for vascular lesion severity. A total vascular score out of 20 was given, made up of the interregional - subscores for each area: Frontal (/6), temporal (/6), hippocampal (/4), and the basal ganglia (/4). Each rating was based on the level of arteriolosclerosis, CAA, perivascular hemosiderin leakage, perivascular space dilation, myelin loss, and cortical infarct burden present in each respective region (Deramecourt et al. 2012)

This information, along with clinical data, was used to assign a final diagnosis of AD, VD, or mixed dementia.

### **1.5. Aims and objectives**

The study described in this thesis had two primary aims:

- i) to study and identify any morphological and immunohistochemical differences in the prefrontal grey and white matter between post-stroke demented and post-stroke non-demented subjects, and compare these to aged-matched controls and other ageing related-dementias in an attempt to elucidate any potential pathological differences which may explain why some individuals decline into dementia and others do not.
- ii) to identify any mechanistic changes in the prefrontal cortex which may be related to the clinical and pathological findings associated with PSD, or associated with a protective role in PSND.

Each of the following experimental chapters will focus on a different aspect of pathology in an attempt to achieve the above aims.

- Hypothesis I: Pyramidal neuronal volumes within the dlPFC, the ACC, and the OFC would show reduced neuronal volume in post-stroke demented and other age-related dementia subjects when compared to aged-controls and non-demented post-stroke survivors (Chapter 3).
- Hypothesis II: The interaction between the excitatory system (primarily pyramidal neurons), the inhibitory system (interneurons), and glial cells will be related to the development of dementia (Chapter 4).
- Hypothesis III: White matter pathology, concerning axons, myelin and oligodendrocytes within the prefrontal cortex will relate to pyramidal neuron volume change and cognitive impairment resulting from stroke (Chapter 5).
- Hypothesis IV: Reduced metabolism in the grey matter within the prefrontal cortex will correlate with pyramidal neuron volume changes and pathology in the WM (Chapter 6).

## Chapter 2. Methods and Materials

### 2.1. Introduction

This chapter offers detailed descriptions of the materials and methods used throughout this study.

#### 2.1. The Cognitive function after stroke (CogFAST) prospective study

##### 2.1.1. The study design

From October 1999 to July 2001 over 700 elderly stroke patients >75 years of age were screened from representative hospital-based stroke registers in Tyneside and Wearside. Subjects suffering from post-stroke dementia before the stroke, or within 3 months post-stroke were excluded from the study as well as those who suffered from any disability which may affect their ability to complete necessary assessments such as: aphasia or hemiparesis affecting the hand used for writing. 355 individuals were recruited into the study (Table 2-1 & Figure 2-1).

Baseline characteristic	n
Number of subjects	355
Age (SD)	80 (4.10)
Gender - male (%)	184 (51.8)
Total CAMCOG score (%) <80	50 (14.1)
average MMSE (SD)	25.9 (2.8)
Hypertension (%)	193 (54.4)
APOE ε4, one copy (%)	64/273 (23.4)
Previous stroke (%)	104 (29.3)

**Table 2-1 showing the baseline characteristics of post-stroke survivors in the CogFAST cohort. Adapted from Allan et al (Allan et al. 2011)**

The Diagnostic and Statistical Manual of Mental Disorders IV criteria (DSM-IV 1994) was used to define dementia status. Annual neuropsychometric follow-up testing was used to assess cognitive deficit and dementia using the Mini Mental State Examination (MMSE), a 30-point questionnaire, with a score of <24



indicating dementia (Blake et al. 2002). The Cambridge Examination for Mental Disorders of the Elderly (CAMCOG), a standardized pen and pencil test, with a maximum score of 107 was used to assess global cognition (e.g. memory (/27), orientation (/10), attention (/7), perception (/11), and executive function (/28)). Subjects scoring <80 falling into the 'demented' category (Huppert et al. 1995). The Bristol Activities of Daily Living scale (Bucks and Haworth 2002) and the Sheffield Language-Screening test (Blake et al. 2002) were used to assess the subjects ability to perform day to day tasks and for assessing language skills, respectively.

The incident dementia was recorded at follow up using the DSM-IV. These formed the two groups, which were compared in this study (Allan et al. 2011). Participants were invited to donate their brains to the NBTR. Those who donated their brain at death were given a clinical diagnosis of post-stroke non-demented (PNSD), or demented (PSD). To date 88 subjects have donated their brains for research.

### Recruitment and screening

706 subjects are originally recruited.

- Recruited from the North East
- $\geq 75$  years
- Stroke confirmed via CT

### Baseline assessment at 3 months after initial stroke

355 subjects eligible to continue study

Clinical and neuropsychological assessments:

- Medical history is taken along with blood samples and cardiovascular risk factors.
- Cognitive testing: MMSE, CAMCOG, and Bristol activities of daily living scale are used to screen for dementia, global cognition and other sub-scores of cognitive function such as executive functions and memory.

### Annual follow-up

- CAMCOG, clinical dementia rating and risk factors for dementia are conducted on an annual basis
- Relative improvement or decline is carefully recorded.

### Brain donation and neuropathological assessment

88 subjects have donated their brains to date

- Neuropathological assessment of all brain donated is conducted at autopsy by neuropathologist..
- Clinicopathological consensus meeting decided final diagnosis of subject.
- Brain tissue blocked and alternatively fixed and embedded in paraffin wax or frozen in  $-80^{\circ}\text{C}$  freezer

**Figure 2-1** flow chart showing the CogFAST study design adapted from Allan et al (Allan et al. 2011). CT = X-ray computed tomography scan, MMSE = Mini Mental State Exam, CAMCOG = Cambridge Cognitive Examination, AD = Alzheimer's disease, C = degree celsius.

### **2.1.2. Participants from the COGFAST study**

Three hundred and fifty five stroke patients  $\geq 75$  years of age were recruited into the CogFAST study. Stroke was defined according to the World Health Organization definition. Twenty participants were assessed at a maximum of 3 months post stroke to test cognitive state.

Participants were excluded if they declined participation, died or withdrew from the study before completing the baseline neuropsychological evaluation, had a disability precluding neuropsychological evaluation (e.g. visual impairment, aphasia, hemiparesis affecting the hand used for writing), had an MMSE score (Folstein et al. 1975) less than 24, or had a diagnosis of dementia according to DSM IV criteria. The assessment was repeated annually during a follow up period of 5-8 years.

The CogFAST cohort provided the post-stroke subjects for this study and is described in detail in the previous chapter. To assess the cognitive status of those taking part in the study, subjects were subjected to an initial battery of examinations.

## **2.2. Demographics of subjects analysed in the study**

Details of subject demographic are given in Table 3-1. The mean age at death and post-stroke survival times were not significantly different between groups thus dementia and executive dysfunction were the only features separating PSND and PSD (Table 3-1). Dementia was determined at the mean time of 7.6 months before death. There were no significant differences in the location of stroke, or in the burden of vascular pathology between the PSND and PSD groups (Table 3-2). Both Alzheimer's disease and mixed dementias showed significantly higher tau and amyloid pathology when compared to all other groups.

All cases	No of cases	Age, years (range)	Sex (female)	FT, weeks (range)	PMD, hours (range)	CERAD (range)	Braak (range)	Frontal vascular score (range)
Control	28	81.5 (71-98)	15	11.2 (2-46)	34.8 (12-98)	n/a	2 (1-4)	n/a
PSND	10	83.3 (78-88)	3	3.8 (1-20)	37.9 (11-76)	1.6 (0-2)	2.3 (1-4)	4.5 (1)
PSD	11	87.1 (80-98)	7	2 (1-3)	40.3 (17-99)	1.3 (0-3)	2.6 (1-4)	4.3 (3-6)
VaD	15	83.8 (71-97)	8	5.1 (2-12)	46.3 (13-74)	1 (0-2)	2.2 (1-4)	5 (4-6)
Mixed	14	83.9 (72-94)	5	5.7 (1-27)	35.5 (9-69)	3 (1-3)	5.4 (4-6)	4 (2-5)
AD	17	85.6 (76-96)	6	7.6 (1-26)	38.6 (6-94)	3 (3)	5.4 (4-6)	1 (1)
FTD	4	71.5 (64-77)	2	n/a	n/a	n/a	n/a	n/a

**Table 2-2 showing the demographics of subjects investigated in this study. Controls = aged matched controls, PSND = post-stroke no dementia, PSD = post-stroke dementia, VaD = vascular dementia, mixed = mixed vascular and Alzheimer's disease, AD = Alzheimer's disease. FT = fixation time, PMD = post-mortem delay. Frontal vascular score (scored out of 6). Age (F = 1.146, p = 0.342, FT (F = 0.519, p = 0.759), PMD (F = 0.449, p = 0.844), CERAD (F = 9.134, p = 0.001), Braak (F = 24.75, p = 0.001), Frontal vascular score (F = 3.262, p = 0.016).**

### **2.3. Other participants**

Brains from non-CogFAST groups (aged-controls, VaD, mixed, and AD) were obtained on request from the Newcastle Brain Tissue Resource (NBTR). These were collected from other prospective clinical studies conducted within the institute. For the initial stereological study, serial cases were selected based on quality of the frontal lobe and availability of tissue due the requirement of a relatively large amount of tissue in this type of analysis. For immunohistochemical investigations cases were selected based on short fixation time and post-mortem delay. This was aided by additional cases which had become available from the NBTR.

### **2.4. Tissue acquisition**

Tissue was obtained from the NBTR, Institute of Neuroscience, Newcastle University. Ethical approval was granted by Newcastle upon Tyne Hospitals Trust ethics committees for use of post-mortem brain tissue in medical research. Neuropathological diagnosis and observations were transcribed from post-mortem reports. After post-mortem examination, brains from subjects in the CogFAST study were cut in 1cm thick coronal slices and sub-dissected into blocks; of which one hemisphere was fixed in 10% buffered formalin and the other was frozen at -80°C. Standard protocols for fixation, sub-dissection and processing were used for all brains. After fixation, blocks were dehydrated in alcohol and cleared xylene and embedded in paraffin wax.

Cases used in the project were prepared and cut with sufficient quantity and quality of frontal tissue available for the methodology to be used. During the course of the project, additional consecutive cases became available and these were added in later chapters. Cases were excluded if there were significant lesions in the prefrontal cortex, such as a large infarct, which precluded examination using the methods proposed. Control cases were excluded if there was a history of myocardial infarction or those who had died from another CVD cause.

The total number of brains evaluated for the project was 99 (25x controls, 10x PSND, 11x PSD, 15 VaD, 14x mixed, 17x AD, and 4x FTD). Cases from this sample were selected for individual parts of the project based upon their

suitability for the methodology, for example, only cases with shorter fixation times were used for IHC studies. In each study, there were no differences between age ( $F = 1.146$ ,  $p = 0.342$ ), fixation time ( $F = 0.519$ ,  $p = 0.759$ ) or post mortem delay times ( $F = 0.499$ ,  $p = 0.844$ ) between any group regardless of the cases selected.

## **2.5. Sectioning and tissue preparation**

Sections were cut from paraffin embedded coronal blocks including areas 9, 11, and 24 containing the dlPFC, OFC, and ACC respectively, where possible between coronal levels 4-8 according to the Newcastle Brain Map (Figure 2-5). Cutting was performed using a Shandon FinesseE+ rotary microtome.

To increase the adhesiveness of slides to tissue sections, clean slides were immersed in acetone for 5 minutes before being added to 2% APES (3 aminopropyl triethoxysilane) solution in acetone for 5 minutes. Slides were then washed in distilled water, removing excess APES solution, before slides were dried in oven at 45°C.

The sections were adhered to the slide and then dewaxed through two rounds of xylene submersion lasting 10 minutes each before being rehydrated through decreasing concentration of alcohol baths sitting in 100%, 95%, 75%, and 50% alcohol/water mix for 1 minute each.

Following each staining protocol, each section was then dehydrated by bringing the slides through 95% ethanol for 1 minute and two changes of 100% ethanol for 2 minutes each. Sections were then placed in two changes of xylene for a minimum of two minutes each. Cover slips were then applied using DPX and a mounting medium.

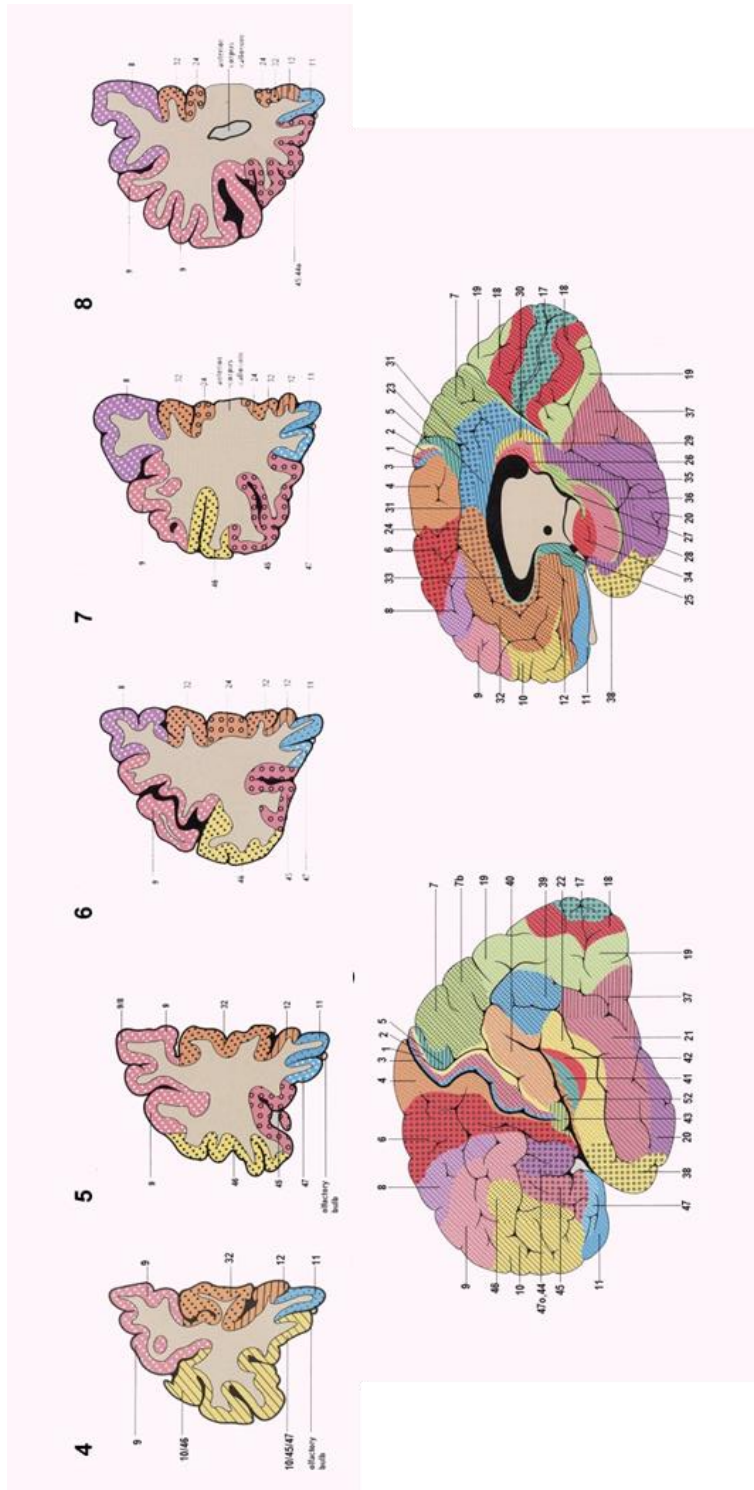


Figure 2-2 showing the Newcastle University brain map (O. Perry 1993).

## **2.6. Histological staining**

### **2.6.1. Haematoxylin and Eosin (H&E)**

H&E was used to visualise arterioles and blood vessels, as well as cell nuclei in blue, and eosinophilic structures in shades of red, orange and pink, in the dIPFC. Sections were dewaxed in xylene (Fisher Scientific, UK) and rehydrated in distilled water for 1 minute. Sections were then immersed in haematoxylin solution [5g haematoxylin (Sigma Aldrich, UK), 0.5g sodium iodate (BDH, USA), 40ml glacial acetate (BDH, USA), 300ml glycerine (Fisher Scientific), and 700ml distilled water] for 3 minutes. Sections were then washed in tap water before being dipped in 1% acid alcohol for 40 seconds before a second wash in tap water. Sections were then immersed in eosin [10g eosin (Sigma Aldrich, UK), 0.25g erythrosin B (Sigma Aldrich, UK), 1000ml 20% ethanol (Fisher Scientific, UK)] for 3 minutes. Excess eosin was washed off with tap water before section was differentiated in 95% ethanol. Slides were then checked under microscope and compared to previously stained sections for consistency.

### **2.6.2. Cresyl Fast Violet (CFV)**

CFV staining was used to visualise the soma, nuclei and the nucleolus of pyramidal and non-pyramidal neurons and glial cells. Thirty  $\mu\text{m}$  sections were cut for use in 3D stereological analysis, and dewaxed in 2 changes of xylene for 5 and 10 minutes respectively. Sections were placed in 100% ethanol for 1 minute before being rehydrated in 95% ethanol for 1 minute. Sections were then placed in 1% acid alcohol for 5 minutes before being rinsed in three changes of deionised water. Sections were incubated in CFV solution for 10 minutes at 60°C in the oven, before being removed from the oven and let cool for a further 10 minutes. Sections were then differentiated in 95% alcohol until the background was a pale purple, before sections were dehydrated in one change of 95% and two changes of 100% ethanol and mounted with cover slips in DPX (Merk, UK). Staining consistency was checked under the microscope and compared to a previously stained section. CFV solution was made up using between 25-50mls (0.2% w/v CFV in deionised water) in 500mls deionised



water and 500mls acetate buffer, pH 4.5 (13.5mls acetate, 23.5g sodium acetate, and 2000mls deionised water).

### **2.6.3. Luxol Fast Blue (LFB)**

LFB was used to visualise the myelinated axons in the WM of the dIPFC. As a copper phthalocyanine dye LFB is attracted to the lipoproteins making up the myelin sheath, staining them blue. Tissue sections were dewaxed in xylene and rehydrated in 95% ethanol before being incubated for 2 hours in LFB stain (1g of luxol fast blue and 5mls of 10% acetic acid in 1000mls of 95% alcohol) at 60°C. Sections were then cooled for 10 minutes before being washed in 70% alcohol for 1 minute. Sections were then differentiated in 4 cycles of; 1 minute distilled water, 10 seconds in  $\text{LiCoO}_3$ , and 1 minute in 70% ethanol. If grey matter remained blue after 4 complete cycles, additional cycles were performed until the cortex appeared colourless. Sections were then immersed in distilled water before being counterstained with CFV solution (0.1% CFV in 1% acetic acid) for 2 minutes at room temperature. Sections were then washed in distilled water and differentiated in 95% ethanol before being compared under microscope to previously stained sections for consistency.

a)



b)

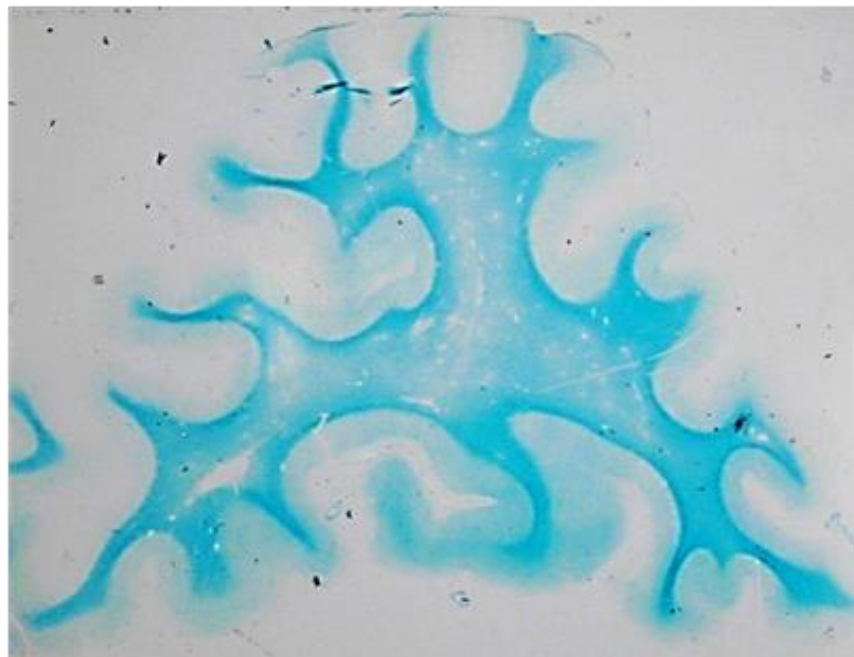


**Figure 2-3 showing two frontal sections stained with luxol fast blue. Image 'a' demonstrates a section with intact WM. Image 'b' shows some signs of WM degeneration.**

## 2.7. Immunohistochemistry (IHC)

### 2.7.1. IHC methods

Paraffin wax embedded sections were dewaxed in two changes of xylene (5 and 10 minutes, respectively) before being rehydrated in 3 changes of alcohol (100%, 95%, and 75%) before being placed in deionised water. 600mls of 10% tri sodium citrate solution (BDH, USA) (60mls TSC to 540mls water) were then brought to boil in the microwave at high power. Once brought to boil, any evaporated water was replaced and sections were added. Sections and TSC solution were again brought to boil. Once boiling the power was switched from high to medium-high power for 11 minutes. Sections and TSC were then left to cool for 20 minutes. Sections were then quenched in 500mls of tris-buffered saline with triton (TBS-T) [12g Tris (Fisher Scientific, UK), 81g NaCl (Fisher Scientific), 7mls Concentrated hydrochloric acid, and 20mls triton (Sigma Aldrich, UK)], and 15mls hydrogen peroxide (H<sub>2</sub>O<sub>2</sub>) (Fisher Scientific, UK) for 15 minutes. After quenching, the sections were washed in TBS-T buffer with 3 changes of 3 minutes each to remove any H<sub>2</sub>O<sub>2</sub>. Sections were then placed on IHC rack and blocked (15µl of serum for every 1mls of buffer). The amount of buffer used was based on the amount needed to suitably cover the section. Non-specific binding was blocked with horse serum (anti-mouse primary), goat serum (anti-rabbit primary), or rabbit serum (anti-goat primary). Block was left to incubate with section for 30 minutes at room temperature. Excess block was then removed from the section, but not washed, and the primary antibody was added. The amount of primary antibody used was dependent on individual protocol. Bovine serum albumin (BSA) was added to the primary antibody at a ratio of 1:300. Sections were then left to incubate at 4°C overnight. The following day, sections were washed in TBS-T with three washes. Sections were then incubated for 30 minutes with secondary antibody (5µl of secondary – targeted at the host animal the primary antibody originated, and 15ul of block, for every 1mls of buffer), followed by a wash of three three-minute changes of TBS-T. Sections were then incubated with tertiary antisera ABC solution (1 drop of A and 1 drop of B for every 2.5mls of buffer for 30 minutes, followed by three three-minute washes in TBS-T. Immunocomplexes were visualised using

diaminobenzidine (DAB) (Sigma Aldrich, UK) (100mls DAB and 267ul H<sub>2</sub>O<sub>2</sub> in 400mls of buffer).

Sections were then washed, dehydrated through 75%-100% ethanol, placed in two changes of xylene for 5 minutes, and mounted using DPX (Merk, UK).

### **2.7.2. Fluorescent labelling (double immunofluorescence)**

Ten µm sections were dewaxed as previously described. In addition to the antigen retrieval steps previously described, sections were placed in formic acid for 4 hours at room temperature. As sections were to be dual stained with two different primary antibodies they were blocked with both goat and horse antibody, as previously described, and washed. Sections were then incubated with both sets of primary antibody overnight. Following another wash phase, sections were then incubated with Dylight fluorescent secondary antibodies (Rabbit- red 550 and mouse- green 488) (Vectalabs, UK) for 45 minutes (all fluorescent staining was performed in the dark, with sections covered with aluminium foil to prevent bleaching of the antibody), followed by another wash phase. Sections were then mounted with Vectashield (Vecta Labs, UK) mounting solution with DAPI staining. All staining was performed in PBS buffer at a pH of 7.5. Sudan black was used to reduce the auto-fluorescence of lipofuscin, with care not to remove too much Dylight fluorescence.

Antibody	Target	Manufacturer	Species	Concentration
4G8	Amyloid $\beta$ , APP	Signet	Mouse (MAb)	1:1000
AT8	Hyperphosphorylated tau	Invitrogen	Rabbit (MAb)	1:2000
Calbindin	Calcium-binding proteins	Sigma	Mouse (MAb)	1:2000
Calretinin	Calcium-binding proteins	Sigma	Rabbit (PAb)	1:1000
COX4	Cytochrome oxidase IV	Abcam	Mouse (MAb)	1:200
Parvalbumin	Calcium-binding proteins	Sigma	Mouse (MAb)	1:1000
GRP78	Glucose-regulated protein	Abcam	Rabbit (PAb)	1:2000
SMI31	Phosphorylated neurofilaments	Alpha center	Mouse (MAb)	1:50,000
SMI32	Phosphorylated neurofilaments	Convance	Mouse (MAb)	1:1000

**2-3 table showing list of antibodies and methods used in this study. All normal horse serum blocked at 5%. MAb = monoclonal antibody, PAb = polyclonal antibody. Secondary antibody concentration 0.5%.**

## **2.8. Imaging and image analyses techniques**

### **2.8.1. Brightfield microscopy**

Images from stained sections were captured on either a Zeiss Axioplan 2 or an AX10 microscope, with an infinity 2 camera at a magnification determined by the type of stain used and type of analysis to be performed. The number of images subsequently taken was sufficient to provide a suitable illustration of the sample area (between 10 and 15 images).

### **2.8.2. Densitometric image analysis**

Image Pro (Mediacybernetics, USA) was used to assess staining levels in images captured from section. Using the software, measurements of the total area of immunoreactivity as a per area percentage (p/a) could be ascertained. Staining intensity, as measured by integrated optical density (IOD), could also be measured, which assesses the level of staining per pixel.

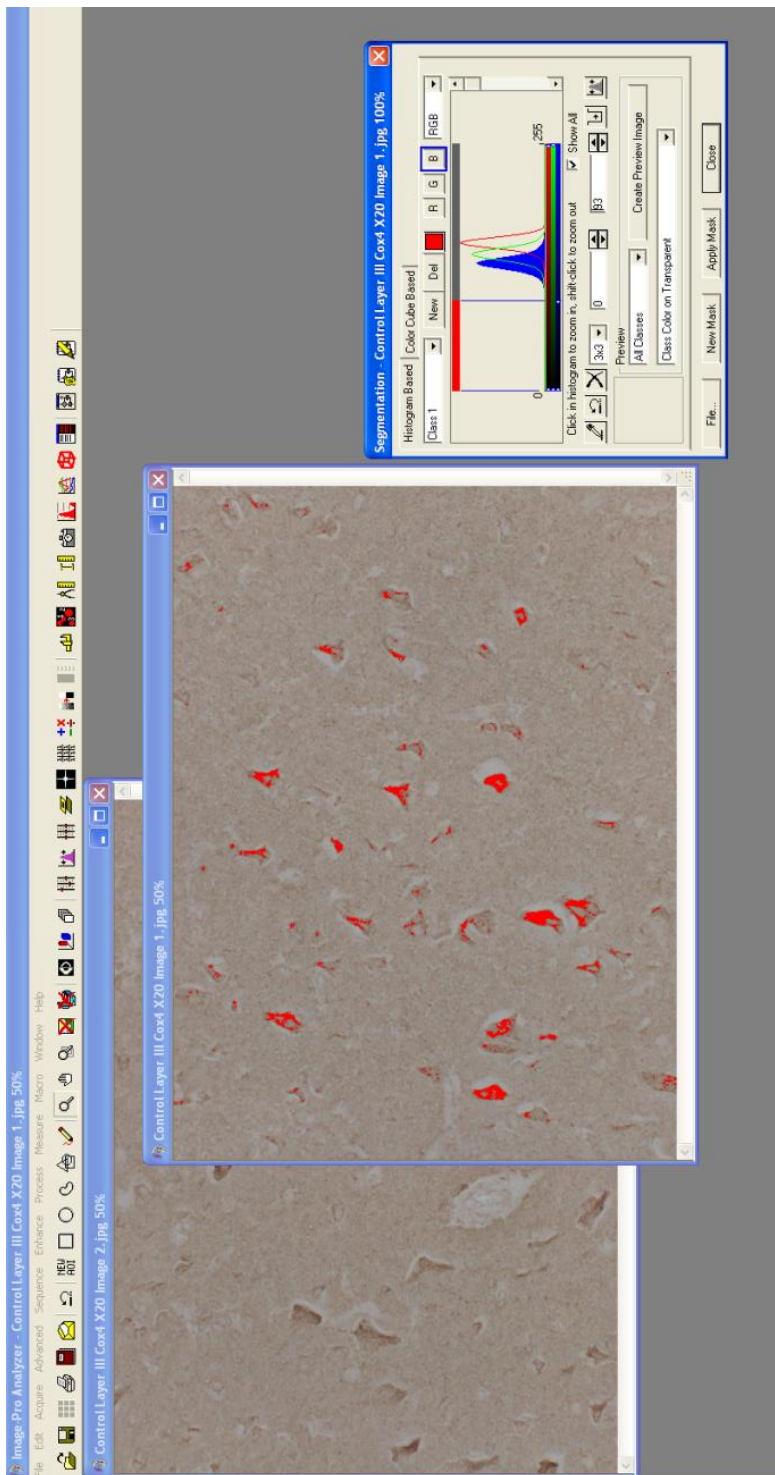


**Figure 2-4 demonstrating quantitative image analysis using the densitometric technique using Mediacybernetics Image Pro software. This screen capture demonstrates how the histogram-based analysis highlights areas immunostained in red and translates this information into a percentage of the total area analysed.**

### 2.8.3. Three dimensional stereology

Sections of thirty  $\mu\text{m}$  thickness Nissl stained were analysed using 3D stereology as described previously (Foster et al. 2014). Stereology allows for the random, unbiased, and systematic analysis of tissue (Gundersen et al. 1988; Gundersen 1988; Moller et al. 1990; West et al. 1991; Mayhew and Gundersen 1996). It is considered more reliable than traditional 2D analysis for its allowance of analysis using a 3D sampling area, making use of the x, y, and z axis for sampling. A  $4\mu\text{m}$  guard volume was removed from the top and bottom of section to remove potential mechanical damage artefact which may result from cutting. This still left a  $22\mu\text{m}$  thick section which has been shown as sufficient for this form of analysis (Harding et al. 1994). Using a wand tool, areas of interest were mapped out at 2.5x objective using Visiopharm Integrated Software (VIS). The programme then selects 25-40 frames at random from within the area of interest. Neuronal volume estimates and cell counts were performed at 100x objective from each of these randomly selected frames. Cell densities were measured using an optical disector where counts are performed on neurons within a specific disector box, and overall densities calculated using the following equation (Sterio 1984).

$$N_v = \frac{\sum p^- Q^-}{P \cdot V}$$

Where:  $N_v$  = Numerical density

$p^-$  = Disector samples

$Q^-$  = Number of objects counted

$P$  = Total number of disectors

$V$  = Disector box volume



Individual pyramidal neuron volume estimated using the nucleator method (Gundersen et al. 1988; Gundersen 1988), in which a probe is placed in the centre (or nucleolus) of a cell, from which 6 randomly orientated lines are fired. An operator then marks on screen where these probes intersect the cell boundaries. From this information the software programme can then make an estimate on neuronal volume (Figure 2-5).

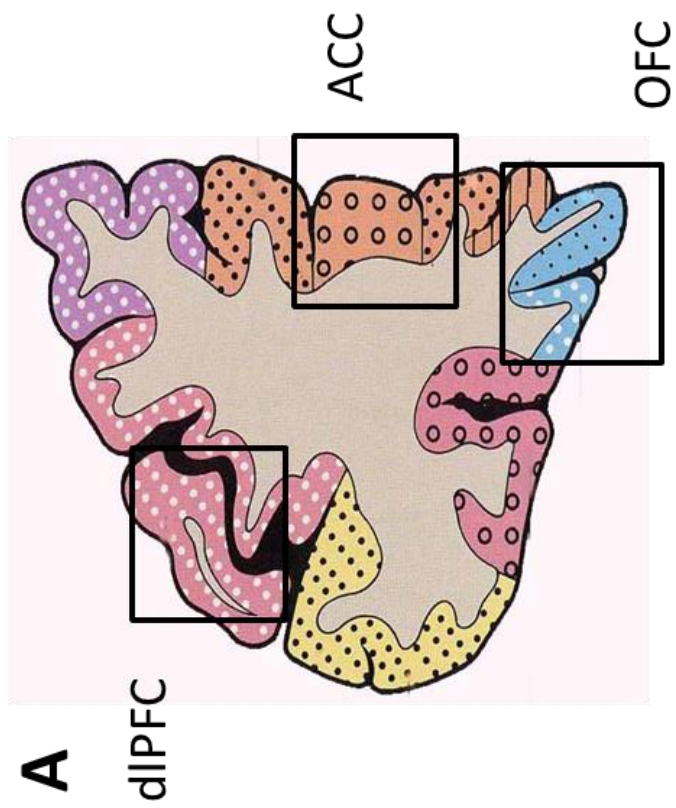
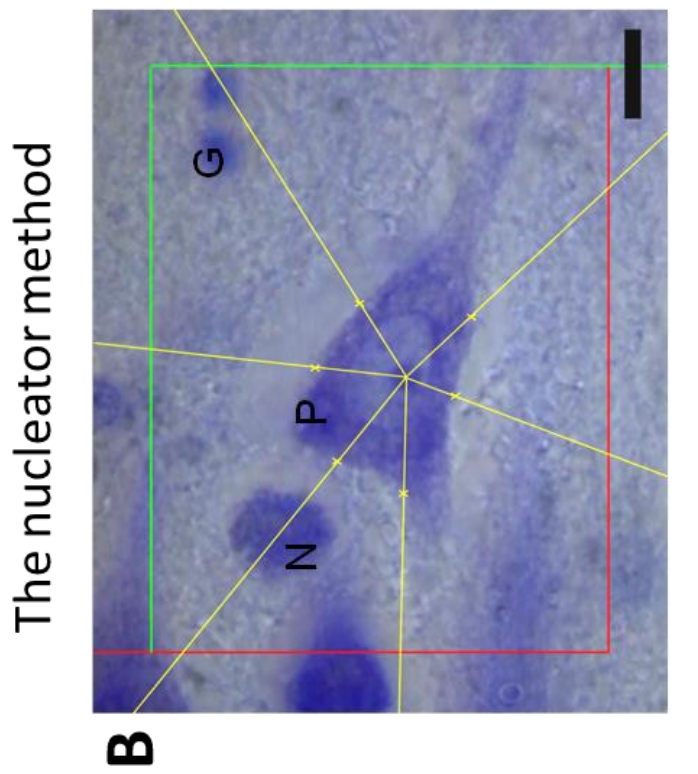


Figure 2-5 a) illustrating frontal lobe regions (O. Perry 1993) and b) image of the nucleator principle for assessing neuronal volumes.

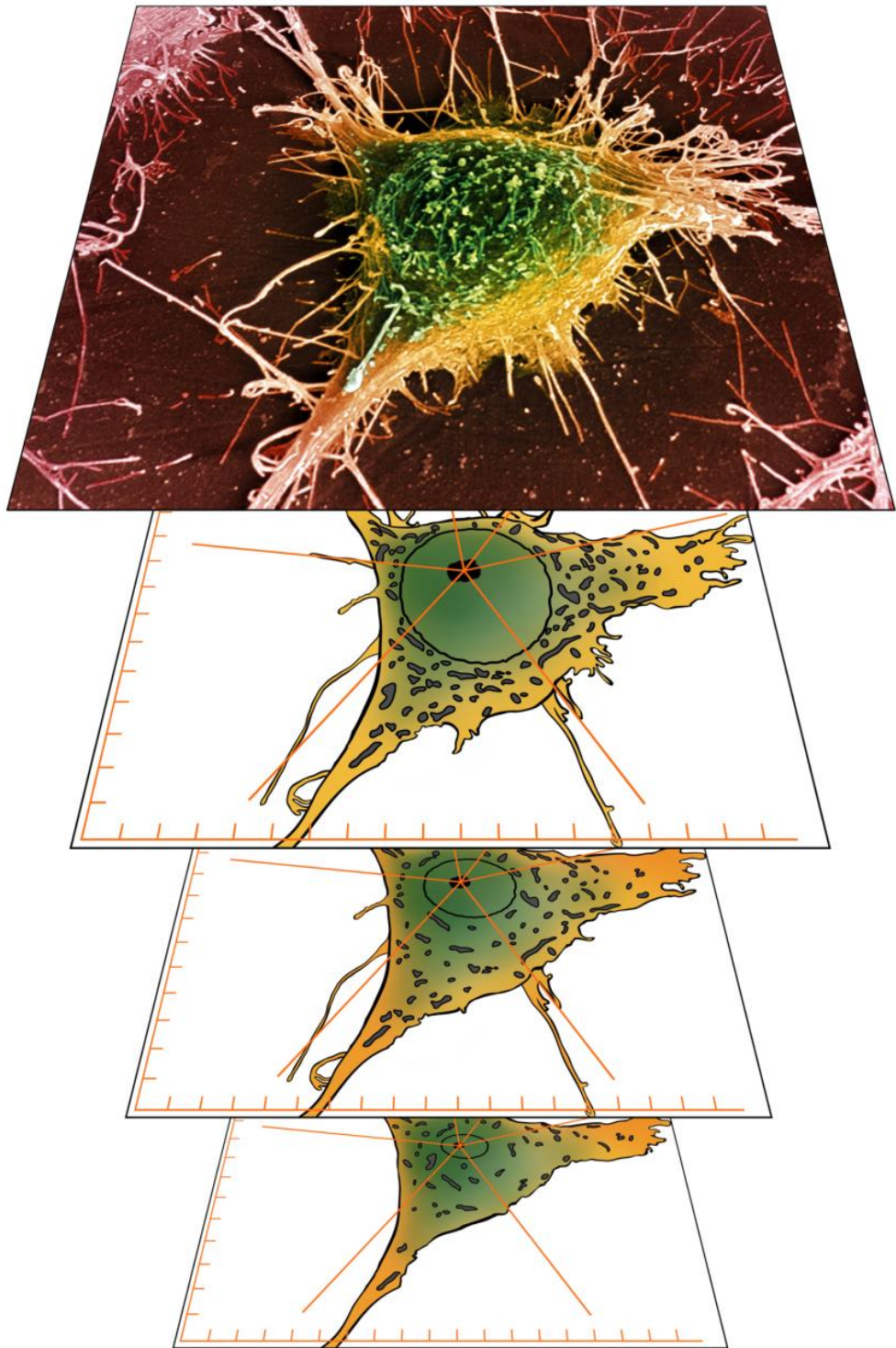


Figure 2-6 cartoon demonstrating the multi-planed, 3D nature of the stereology technique.

#### **2.8.4. 2D analysis of pyramidal neurons**

Images were taken from a selection of the Nissl stained sections used in the previous 3D stereological study which contained both the dIPFC and the OFC. From these images pyramidal neurons were randomly selected from layers III and V of the dIPFC and the OFC. On screen measurements were then used to assess the individual neurons maximum length and width. The ratio between length and width was then calculated using the following formula: ratio = length/width.

To assess neuronal volumes, these images from the dIPFC and OFC from control cases were used to calculate neuronal size. Using the wand tool to draw around these individual cells it was possible to use densitometric analysis to determine the total number of pixels within the area of the delineated cell. Neurons containing more pixels were deemed to have a larger volume than those containing fewer pixels. All images were also analysed using Image Pro analysis (Mediacybernetics, USA).

### 2.8.5. Sclerotic index measurements.

The diameters of the lumen and vessel were measured using the software, VasCal. VasCal was developed by a former member of the Neurovascular Research Group (NRG), Y. Yamamoto (Yamamoto et al. 2009). By superimposing lines onto an image of a cross sectioned vessel it is possible to calculate the lumen size, vessel diameter, and the ratio of the two, giving the sclerotic index. The line measurements are related to the actual size of the vessel as the software is previously calibrated by measuring a graticule (Figure 2-7).

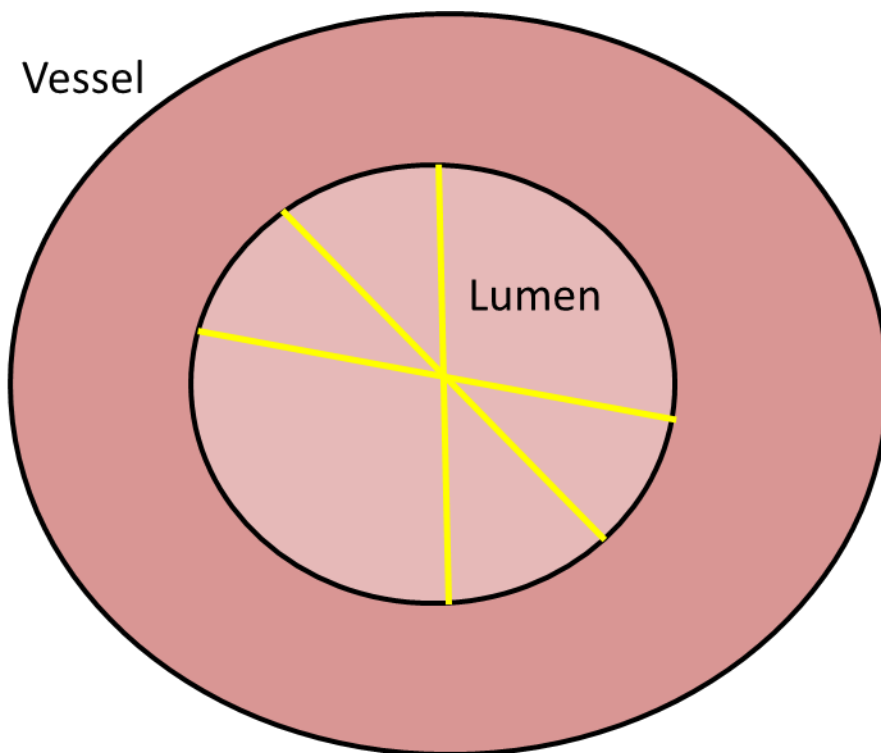


Figure 2-7 showing a cartoon of a vessel's lumen being assessed the VasCal software.

## 2.9. Atrophy analysis estimates

We measured the degree of atrophy in dlPFC of PSND brains versus those of PSD. Adapted from methods proposed by Lon White et al (Gelber et al. 2012) and correspondence with the author we investigated three markers for atrophy: the ratio of brain weight to intracranial volume, the ratio of cortical thickness to head diameter, and neuronal loss.

Brain weight was established from post mortem examination of the CogFAST cases. Intracranial volume was measured from MRI during the CogFAST study, where available.

Cortical thickness was taken from the sulcus of area 9 of the dlPFC at 2.5x objective. Three measurements were taken from each side of the sulcus and a mean calculated to remove any artefact which may result from cutting the section anything other than perfectly coronal which may cause the cortex to appear thicker than it actually is.

Head diameter was taken from a population mean as established by R. P. Ching et al (Ching 2007). Neuronal loss was scored on a 1-8 scale (1 = no loss, 8 = severe) in the region of the dlPFC.

All raw data was converted into a Z score allowing for each individual marker to be compared to one another.

$$Z = (x-u)/\sigma$$

Where: X = raw score U = mean, and  $\sigma$  = standard deviation

Each marker was assigned a percentage weight indicating how much its Z score would influence the final result (Gelber et al. 2012). Specific parameters were selected and given a percentage based on their perceived impact on cortical atrophy. The three parameters used to assess cortical atrophy were:

1. Brain weight vs. intracranial volume (50%)
2. Cortical thickness vs. head diameter (40%)
3. Neuron density (10%)

The final score for each subject group was the total Z score based on the above percentages.

### 2.9.1. **Myelin index**

Ten  $\mu\text{m}$  sections were stained using LFB and analysed using image pro as previously described by Ihara et al (Ihara et al. 2010).

An image was taken of each slide using a digital camera before being converted to grey scale images in Photoshop. Myelin loss was then determined in a large series of LFB stained serial coronal section from cases and controls. White matter was drawn around using the want tool map out the area of interest (ROI).

The detected range of grey level within the WM in each image, depicting level of staining intensity 0-115 (0, black; 115, white) was divided into quartiles for example 0-29, 30-59, 60-89, 90-119 and the median of each quartile calculated; 14.4, 43.1, 71.9, 100.6.

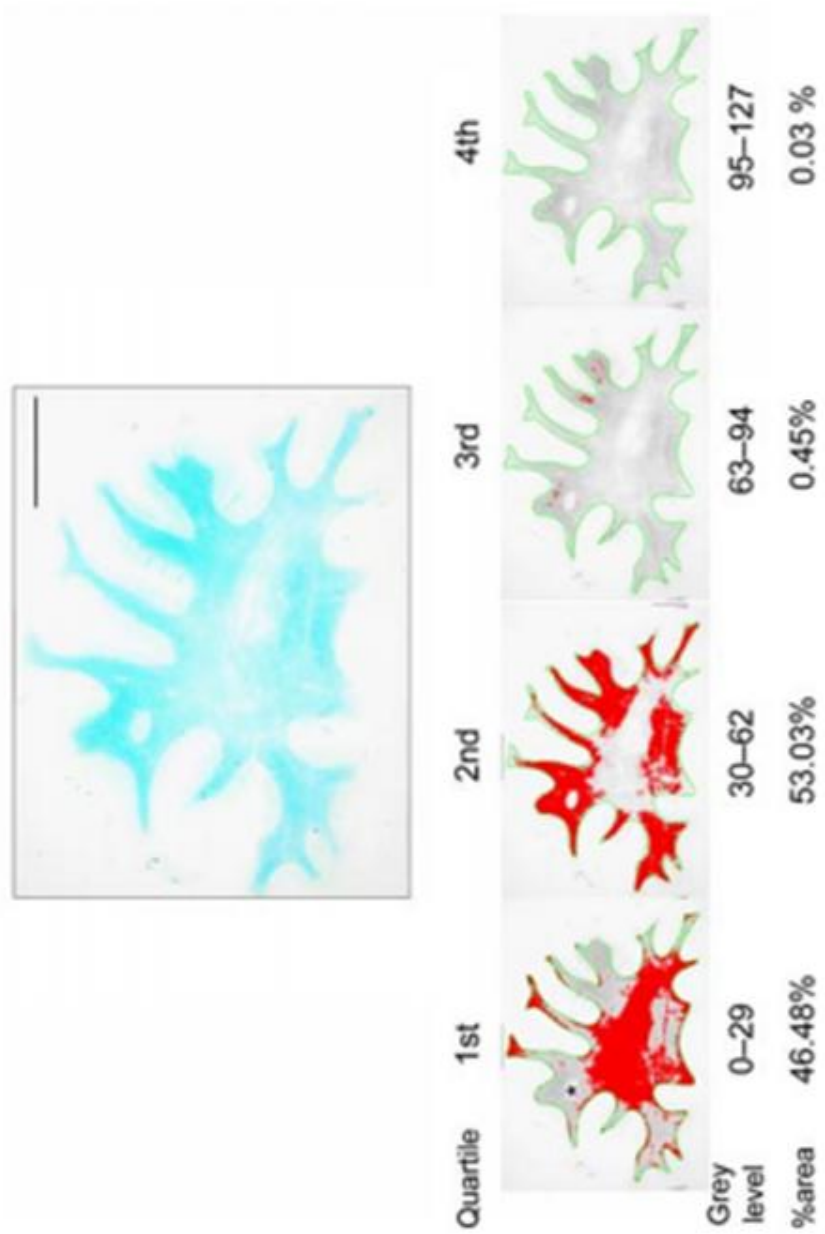


Figure 2-8 demonstrating the quartile analysis method for determining myelin index (Ihara et al. 2010).



## 2.10. **Golgi-Cox technique**

### 2.10.1. **Rapid single-section Golgi technique**

Each 200µm free floating section was placed in 4% paraformaldehyde, 0.2% picric acid in 0.1M phosphate buffer solution (pH7.4) solution, before being placed on an orbital shaker to be gently agitated for 24 hours in the dark. Sections were rinsed in 0.1M phosphate buffer before being immersed in 0.02% osmium tetroxide solution for 20 minutes. Again sections were placed in the dark on an orbital shaker. Following this sections were then rinsed in 0.1M phosphate buffer for two minutes before being immersed in 3% potassium dichromate and again placed on orbital shaker in the dark for a further 24 hours. Excess chromation was removed with a distilled water rinse, and sections were then placed between two glass coverslips, with epoxy/cyanoacrylate used as an adhesive. Sections were then immersed in 1.5% silver nitrate for 24 hours in dark, at room temperature. Coverslips were then removed and the section was rinsed in distilled water to remove excess crystals which have formed overnight. Sections were then mounted on gelatin-coated slides before drying at room temperature for one hour. Sections were then dehydrated in 95% - 100% ethanol (as previously described). Sections were then placed in two sets of xylene (5 minutes at each) before mounting section with cover slips using DPX as an adhesive. Images were then taken using brightfield microscopy. Adapted from Dall'Oglio (Dall'Oglio et al. 2010) and Gabbot (Gabbott and Somogyi 1984).

### 2.10.2. **Golgi-Kopsch technique**

Tissue sections ~1.5cm<sup>2</sup> and 0.3cm thick were cut using vibratome before being rinsed in deionised water. The section was then placed on wadded sterile cotton gauze in chromation solution of 2% potassium dichromate, 3.5% paraformaldehyde (pH). pH was checked at intervals with a pH of 4.7 indicating the need for a solution change. A total of eight solution changes were performed in 96 hours. Tissue sections were then placed in increasing concentrations of silver nitrate solutions (filtered before use): 0.2, 0.5, 0.75% for five minutes. Sections were then allowed to sit in 1% nitrate for one week in the dark. Following this incubation, tissue sections were then washed in three

changes of deionized water over 2 hours, before dehydrated in ascending alcohol concentrations. Sections were then embedded in paraffin wax from which serial sections ranging from 25um – 100um were cut using a Microtome®, before being mounted onto slides with DPX. This method was adapted from Rosoklija, G., et al (Rosoklija et al. 2003).

### 2.11. **Statistical analyses**

All statistical analysis was performed on IBM SPSS statistics 22 (IBM, USA). Distribution analysis was performed using the Shapiro-Wilk analysis, test for normality. Differences between groups were performed using either using the ANOVA or Kruskal-Wallis tests for normal and non-normally distributed data, respectively. If these tests picked up significance between groups then pairwise differences between groups were performed using Mann-Whitney U test (for normally distributed data) or Tukey (parametric testing). Significance was set at  $p < 0.05$ . Spearman's rank coefficient ( $\rho$ ) was used to test correlations between ages, fixation times, post mortem delay, and other variables. Scatter diagrams were then used to access the relationship between variables with significant correlations.

## **Chapter 3.      Pyramidal neurons of the prefrontal cortex**

### **3.1. Introduction**

The frontal lobe is classically associated with executive functions. These cortico-subcortical networks, which may span relatively vast distances throughout the brain are formed via the projections of large cortical nerve cells known as pyramidal neurons. Changes or damage to these neurons may result in selective disconnection of cortico-cortical pathways in those with vascular pathology and AD, and linked to cognitive decline and executive dysfunction (Tekin and Cummings 2002; N. Ishii et al. 1986; Wolfe et al. 1990; Stout et al. 2003; Hof and Morrison 2004, 1991; Hof et al. 1990; Hof et al. 1989; Hyman et al. 1986; Lewis et al. 1987). Frontal lobe damage is common in several disease states associated with dementia and executive function including VaD and FTLD (Deramecourt et al. 2012; Ratnavalli et al. 2002; N. Ishii et al. 1986; E. J. Burton et al. 2004), and AD (Binetti et al. 1996). Neuronal loss in the prefrontal cortex is common in AD, associated with memory loss due to temporal lobe atrophy (Khachaturian 1985; Chan et al. 2001), with symptoms beyond memory loss, such as executive function, (Morrison and Hof 1997; Hof et al. 1990; Binetti et al. 1996). It has been reported that larger pyramidal neurons, those responsible for cortico-cortical connections between the prefrontal and temporal regions have been shown to be more vulnerable than smaller neurons to pathology (Hof and Morrison 1991; Hof et al. 1990) such as hyperphosphorylated tau, which is found in high proportion in these cell types (Braak and Braak 1986). Additionally, Buee et al reported that specifically, the most vascularised areas, layers III and V, exhibited the highest burden of microvascular pathology (Buee et al. 1994). Hoff and colleagues reported reduced SMI-32 immunoreactivity (a marker for healthy neurons) in large pyramidal neurons within layers III and V of Alzheimer subjects (Hof et al. 1990). This suggests that these layers are particularly vulnerable to pathology, as indicated by the presence of fewer healthy neurons. This decline in healthy neurons may relate directly to disruption of the cortical circuits through neuronal dysfunction. In addition, those suffering depression, a disease thought to be

related to vascular pathology within the frontal lobe (Alexopoulos et al. 1997), were found to have reduced pyramidal neuronal volumes within the dlPFC when compared to aged matched controls, though no change in glial or non-pyramidal neuron number (Khundakar et al. 2009). This evidence suggests a significant relationship between vascular abnormalities and excitatory pyramidal neuron dysfunction within frontal lobe circuitry.

The dorsolateral prefrontal cortex appears to be vulnerable to vascular pathology (Deramecourt et al. 2012; N. Ishii et al. 1986), which is known to negatively impact executive functions. In those suffering depression the dlPFC has been shown to be affected by vascular pathology (Alexopoulos et al. 1997; Alexopoulos et al. 1999; Alexopoulos 2003). The OFC and ACC appear to be spared suggesting a significant role for dlPFC in the development for such disease states (Khundakar et al. 2009; Khundakar et al. 2011c, 2011b; Rajkowska et al. 1999). MRI studies have shown WMH in the frontal lobe white matter (E. Burton et al. 2003). This area contains the cortico-cortical connections emanating from pyramidal neurons of the dlPFC, ACC, and OFC, any breakdown of which may result in executive dysfunction (Tekin and Cummings 2002).

### **3.1.1. Stereological analysis of the pre-frontal cortex**

Several previous studies have relied on two-dimensional (2D) analysis to assess neuronal volumes and densities. The potential problem with this single-plane analysis is that it can result in over counting in favour of larger neurons whose profiles may appear across several serial sections leading to inaccurate and unreliable counts (Gundersen et al. 1988; Mayhew and Gundersen 1996). Historically, neuronal volume was often assessed by appearance and shape, relying heavily on the subjective assessments of the operator (West and Slomanka 2001).

Three dimensional (3D) stereology allows for a 3D interpretation of extra thick sections for accurate, quantitative analysis. Utilising random, unbiased, systematic sampling techniques, and analysing thicker tissue section (> 30um) (Harding et al. 1994), it is possible to gain reliable counts and volume estimates, as neurons can be viewed in their entirety within the tissue unlike with 2D analysis where neuroanatomical bodies are viewed at the discretion of their

topological orientation (West and Slomanka 2001; Baddeley 2001; West 1999; Schmitz and Hof 2007). Neurons are then only counted if they fulfil three criteria: size, shape, and the presence of a nucleolus. Neuronal volumes are assessed using the nucleator tool (Three dimensional stereology) (Gundersen et al. 1988), using the nucleolus as the centre-reference point for each cell.

Using 3D stereology, Bussiere et al (Bussiere, Giannakopoulos, et al. 2003) assessed SMI32 stained, pyramidal neuronal volumes in layers III and V of the dlPFC in those with AD, finding significantly lower volumes in those with dementia when compared to controls (Bussiere, Gold, et al. 2003). Khundakar et al used 3D stereology to assess neuronal volumes in the three pre-frontal circuits which control executive function in depression. Interestingly they found decreases in pyramidal neuronal volumes in the dlPFC of those suffering depression, but did not find similar changes in the OFC or the ACC, suggesting a localised and specific response in this area of the brain (Khundakar et al. 2011b, 2011c). It is plausible that vascular changes in depressive illness (Alexopoulos et al. 1997), may reflect the decreases in volumes resulting from reduced trophic factors, combined with a chronic hypoxic state affecting the functioning of these cells. This may have implications for other vascular pathology based diseases such as PSD or VaD. This correlation between cellular volumes and disease states suggest reduced neuronal size may be a reliable marker for decreased function. The dlPFC appears vulnerable to other disease processes, too. Neuronal atrophy in the dlPFC was also reported in sufferers of select autism (Courchesne et al. 2011), and schizophrenia (Pierri et al. 2001).

Though the vascular pathology may impact the frontal lobe, reduced cerebral blood flow can have a global impact, affecting other areas of the brain. Reduced neuronal volume changes are also apparent within the temporal lobe, with reduced pyramidal neuronal volume apparent in the hippocampus of AD, VaD, and post-stroke sufferers (Gemmell et al. 2012). Though the hippocampus is not traditionally associated with executive function, the complex interplay between the hippocampus and the frontal lobe means that damage to one brain region may impact on another (Tekin and Cummings 2002). However, though profound changes in pyramidal neurons have been reported in the hippocampus in post-

stroke survivors (Gemmell et al. 2012), little is known of the effect of stroke within the prefrontal cortex, or how this may impact delayed PSD.

The purpose of this study was to assess the pyramidal neuronal population within the three pre-frontal cortices; the dlPFC, OFC, and ACC, in post-stroke survivors. These would then be compared with subjects with AD, VaD, and Mixed AD/VaD and aged-matched elderly controls. Pyramidal neuron cell volume and population density were quantified and related to clinical findings gathered from the COGFAST study in an attempt to delineate the pathological substrates which determine dementia after stroke between post-stroke demented and post-stroke non-demented subjects. All brain samples from the subjects were assessed for hallmark vascular pathology and AD type pathology in an attempt to assess their respective effects.

## **3.2. Methods**

### **3.2.1. Subject demographics**

Details of the subjects are given in Table 3-1. Mean age at death and post-stroke survival times were not significantly different between groups thus dementia and executive dysfunction were the only features separating PSND and PSD (Table 3-1). Classification between PSND and PSD groups was made at a mean of 7.6 months before time of death. The location of the stroke did not appear to influence cognitive outcome, nor did the level of vascular pathology between PSND and PSD (Table 3-2). Both Alzheimer's disease and mixed dementias showed significantly higher tau and amyloid pathology when compared to all other groups.

Group ( $\pm$ SEM)	No of cases	Age, years	PMD, hours	FT, weeks	Frontal vascular score	Braak	CERAD
Control	24	81.5 (2)	35.7 (5)	11.3 (3)	N/A	2 (1)	N/A
PSND	10	83 (1)	37.9 (6)	3.8 (2)	4.5 (1)	2.3 (1)	1.6 (0.2)
PSD	11	87 (1)	40.3 (8)	1.9 (1)	4.3 (1)	2.6 (1)	1.3 (0.3)
VaD	14	83.8 (2)	46.9 (6)	4.9 (1)	5 (0.6)	2.2 (0.3)	0.8 (0.3)
Mixed	12	83.9 (2)	36.8 (6)	4.6 (2)	4 (1)	5.4 (0.2)	2.7 (0.2)
AD	12	85.6 (2)	43.4 (9)	7 (2)	1 (1)	5.4 (0.2)	3 (1)

Variable		PSND	PSD	VaD
Time from baseline- death (months)	Mean ( $\pm 2SE$ )	63.5 (22)	64.4 (14)	Dementia
Total CAMCOG score (/100)	Mean (range)	88.0 (83-98)	61.5 (24-80)	58 (36-80)
Memory sub-score (/27)	Mean (2SEM)	21.4 (2.8)	15 ( 4.3)	<15
Executive function sub-score (/28)	Mean (SEM)	16.6 (1.2)	11.1 (1.9)	<11
Clinical Dementia Rating (CDR)	Mean (2SEM)	0.1 $\pm$ 0.4	1.28 (0.25)	3.0 $\pm$ 0
Hemisphere with visible change or not on CT	None, right, left, both	4, 3, 1, 3	2, 2, 6, 3	na
OSCP stroke classification	LACS, PACS, POCS, TACS, Unknown	4, 1, 1, 1, 3	4, 3, 1, 3, 0	na

**Table 3-2 Stroke subject demographics.** OSCP = Oxford community stroke project LACS = lacunar stroke, PACS = partial anterior stroke, POCS = posterior circulation stroke, TACS = total anterior circulation stroke. Unknown = no CT report available.



### **3.2.2. Three dimensional stereological analysis of neuronal volumes and densities**

The neuronal volumes and densities of the pre-frontal cortex in three cresyl fast violet stained 30µm serial sections were measured using three-dimensional stereology. The optical dissector and nucleator techniques were used to estimate neuronal density and neuronal volume, respectively (see Three dimensional stereology). In addition to analysing PSND and PSD subjects aged- controls, VaD, mixed, and AD subjects were also analysed.

### **3.2.3. Two dimensional analysis**

Neuronal volume and dimensions of pyramidal neurons were measured in control cases in both the OFC and dlPFC using 2D dimensional densitometric analysis and onscreen measurements. The purpose of this analysis was to establish whether or not the differences between neuronal volumes detected using 3D stereology between the two regions could be detected using a less sensitive technique such as 2D analysis. All analysis was performed on CFV stained sections at a magnification of 25x (See 2D analysis of pyramidal neurons).

### **3.2.4. Sclerotic index**

SI measurements were performed using the VasCal programme as described earlier (see methods). A minimum of 10 vessels were imaged in grey matter of the dlPFC and the white matter of the prefrontal cortex. All analysis was performed on 10 µm haematoxylin and eosin stained sections.

### **3.2.5. Immunohistochemistry**

Ten µm sections were stained using immunohistological techniques as described previously. SMI31 (Alpha center, USA) (1:50,000) was utilised to stain neurofilament proteins present in damaged or struggling neurons, whereas SMI32 (Convance, USA) (1:1000) was used to highlight physically healthy, functioning neurons. AT8 antibodies (Innogetics, UK) were used to detect hyperphosphorylated tau in the dlPFC in all groups.

### 3.2.6. **Fluorescent immunohistochemistry**

10µm sections from the frontal lobe of each disease group containing the dIPFC were stained with AT8 and 4G8 (Signet, USA) antibodies for hyperphosphorylated tau and β-amyloid, respectively and visualised with dylight kit (Vector Laboratories, UK), mounted with vector shield mounting media, with DAPI (Vector Laboratories, UK) and imaged as described previously in methods.

### 3.2.7. **Cortical thickness measurements and atrophy estimates**

Cortical ribbon thickness in all cases was assessed at 2.5x magnification in 30µm Nissl stained sections. Measurements were taken from the pial surface to the edge of the WM from both sides the sulcus of area 9 containing the dIPFC. Three measurements were taken from each side of the sulcus, from the pial surface to the WM and averaged to avoid any artefact which may arise from uneven cutting of the section (see Atrophy analysis estimates).

Cortical atrophy scores of the dIPFC were estimated using an adapted formula first proposed by White et al (Gelber et al. 2012) as well as personal correspondence. Z scores were calculated from the values determined from three markers of cortical atrophy: the ratio between brain weight to intracranial volumes, cortical thickness to head diameter, and local neuronal loss (see method). Cortical thickness means were compared between layers III and V with correlations investigated using spearman's rank coefficient.

### 3.2.8. **Stroke location analysis**

Review of the pathologist's report of post-stroke subjects recruited into the CogFAST study revealed the location of the initial stroke. This data was used to investigate the relationship between stroke location and cognitive outcome.

### 3.2.9. **Statistical analysis**

All statistical analysis was performed using IBM SPSS Statistics 21 software package. Neuronal volumes and densities were found to be non-normally distributed. Group means were compared using Kruskal-Wallis test and differences in neuronal volumes and densities and SI measurements between groups were analysed using Mann-Whitney U test. Correlations between volumes and densities and other variables were established using spearman's rank coefficient. Z scores were established using the formula:  $z = (x-u)/\sigma$ .

### 3.3. Results

#### 3.3.1. Pyramidal neuronal densities

There were no significant differences between any group within layers III or V of the dlPFC (total 36 132 and 39 739 mm<sup>2</sup>), nor the ACC (43 497 and 39745 in layers III and V, respectively). When disease cases were removed from analysis in layer III of ageing controls neuronal density was calculated to be (per mm<sup>2</sup>): 35 110, 49 372, and 33 321 in the dlPFC, the ACC, and the OFC, respectively. Whilst pyramidal neuronal densities in layer V were calculated at (per mm<sup>2</sup>): 39 436, 41 057, and 30 960 in the dlPFC, ACC, and OFC, respectively.

There were no significant differences in the density of pyramidal neurons between controls and disease groups, or in the neuronal densities between post-stroke survivors in any area in either layers III or V in the dlPFC or the ACC ( $p > 0.05$ ). In the OFC pyramidal neuronal densities in layer III and V in mixed ( $p = 0.001$ , and  $p = 0.015$  respectively), and layers III of VaD were significantly lower than non-demented controls ( $p = 0.023$ ). In addition, when compared to PSD layers III and V of mixed dementia showed significantly lower densities in the OFC ( $p = 0.049$ , and  $p = 0.028$  respectively). AD was found to have significantly lower density than non-demented subjects in layer V ( $p = 0.007$ ) (Figure 3-1).

Correlation studies between neuronal densities and post-mortem reports showed no clear evidence to indicate that neuronal densities or volumes were affected by the length of fixation period ( $\sigma = -0.130$ ,  $p = 0.232$ ), post-mortem delay ( $\sigma = 0.017$ ,  $p = 0.883$ ), age ( $\sigma = 0.141$ ,  $p = 0.213$ ), Braak ( $\sigma = 0.108$ ,  $p = 0.352$ ), or CEARD ( $\sigma = 0.016$ ,  $p = 0.905$ ).

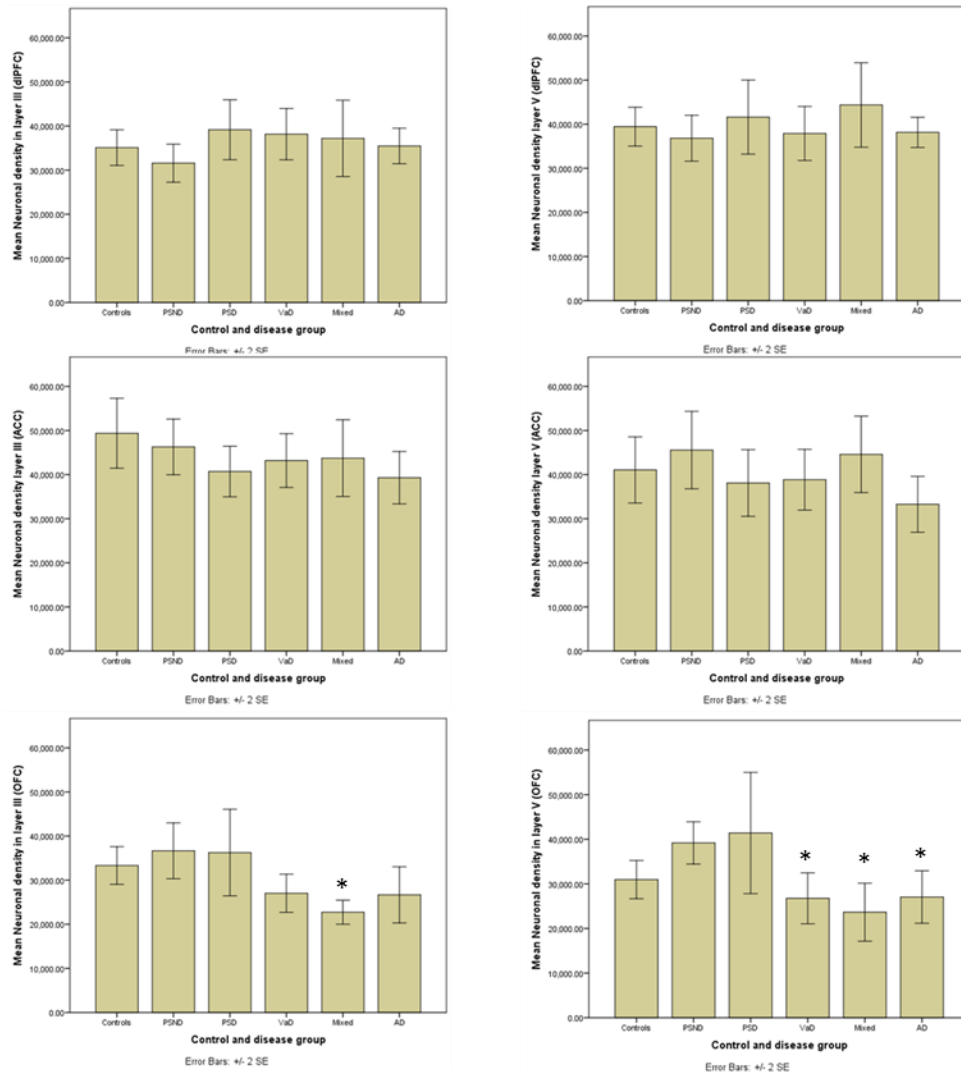


**Figure 3-1 neuronal densities in the dIPFC, ACC, and OFC. Controls = aged matched controls, PSND = post-stroke no dementia, PSD = post-stroke dementia, VaD = vascular dementia, mixed = mixed vascular and Alzheimer's disease, AD = Alzheimer's disease. \* = significance different to ageing controls ( $p < 0.05$ ). Controls vs mixed layer III and V ( $p = 0.001$ , and  $p = 0.015$  respectively), PSD vs mixed layer III and V ( $p = 0.049$ ,  $p = 0.028$  respectively), Controls vs VaD in layer III ( $p = 0.023$ ), PSND vs AD in layer III ( $p = 0.007$ ).**

### 3.3.2. Pyramidal neuronal volumes

Pyramidal neuronal volume varied largely between brain regions (Figure 3-2), with average neuronal volumes in layer III of aged controls found to be (in  $\mu\text{m}^3$ ) 1129, 1087, and 732 in the dIPFC, the ACC, and the OFC respectively.

Neuronal volumes in the ACC were significantly larger than those in both the dIPFC ( $p = 0.001$ ,  $p = 0.004$  in layers III and V, respectively) and the OFC ( $p = 0.001$ ,  $p = 0.001$  in layers III and V, respectively), across all groups. Neuronal volumes of the OFC, in both layers III and V, was significantly lower when compared all groups of the ACC, and in controls ( $p = 0.042$ ,  $p = 0.0041$  in layers III and V, respectively) and PSND ( $p = 0.001$ , and  $p = 0.002$  in layers III and V, respectively) of the dIPFC, with neuronal volumes decreasing in the following order: ACC > dIPFC > OFC. Average neuronal volumes in both layers III and V of the OFC were found to be ~50% lower than all groups in the ACC, and non-demented groups of the dIPFC ( $p = 0.001$ ).

In contrast to neuronal densities, neuronal volumes were markedly affected in demented subjects. In the dIPFC, all demented groups exhibited reduced pyramidal neuronal volumes in layer III when compared to both controls and PSND. PSD ( $p = 0.027$ ,  $p = 0.01$ ), VaD ( $p = 0.012$ ,  $p = 0.001$ ), mixed ( $p = 0.03$ ,  $p = 0.004$ ), and AD ( $p = 0.035$ ,  $p = 0.005$ ) displaying significantly smaller neurons when compared to controls and PSND, respectively. Pyramidal neuron volumes in layer V showed a similar pattern: PSD ( $p = 0.007$ ), VaD ( $p = 0.002$ ), mixed ( $p = 0.008$ ), and AD ( $p = 0.015$ ) were reduced when compared to controls. Pyramidal neuron volumes in VaD the group were also significantly lower when compared to post-stroke non-demented survivors ( $p = 0.034$ ). In both layers III and V controls exhibited similar neuronal volumes to post-stroke non-demented survivors ( $p = 0.084$  and  $p = 0.291$  in III and V respectively). There was no significant difference in neuronal volumes between control cases and PSND ( $p > 0.05$ ).

Correlation studies were implemented to assess and compare the relative rate of neuronal volume change in layers III and V of the dIPFC, seeing as this region appeared most vulnerable to the apparent neuronal changes. Layer III and V neuronal volume correlated in ageing controls and AD ( $\sigma = 0.696$ ,  $p = 0.012$  and  $\sigma = 0.695$ ,  $p = 0.026$  respectively), however in all vascular based

groups; post-stroke survivors, VaD, and mixed AD/VaD pathology layer III did not correlate with layer V (Table 3-3).

<b>Thickness (mm)</b>	Controls	PSND	PSD	VaD	Mixed	AD
Mean (SEM)	2.96 + 0.13	2.75 +0.11	2.89 +0.17	2.78 +0.10	2.98 +0.12	2.86 +0.13
<b>Volume</b>						
Layers III and V R (p value)	0.696 (0.012)	0.468 (0.172)	0.181 (0.594)	0.610 (0.061)	0.378 (0.282)	0.695 (0.026)

**Table 3-3 showing correlations between layer III and layer V pyramidal neuronal volumes in the dIPFC. Ageing controls = aged matched controls, PSND = post-stroke no dementia, PSD = post-stroke dementia, VaD = vascular dementia, mixed = mixed vascular and Alzheimer's disease, AD = Alzheimer's disease.**

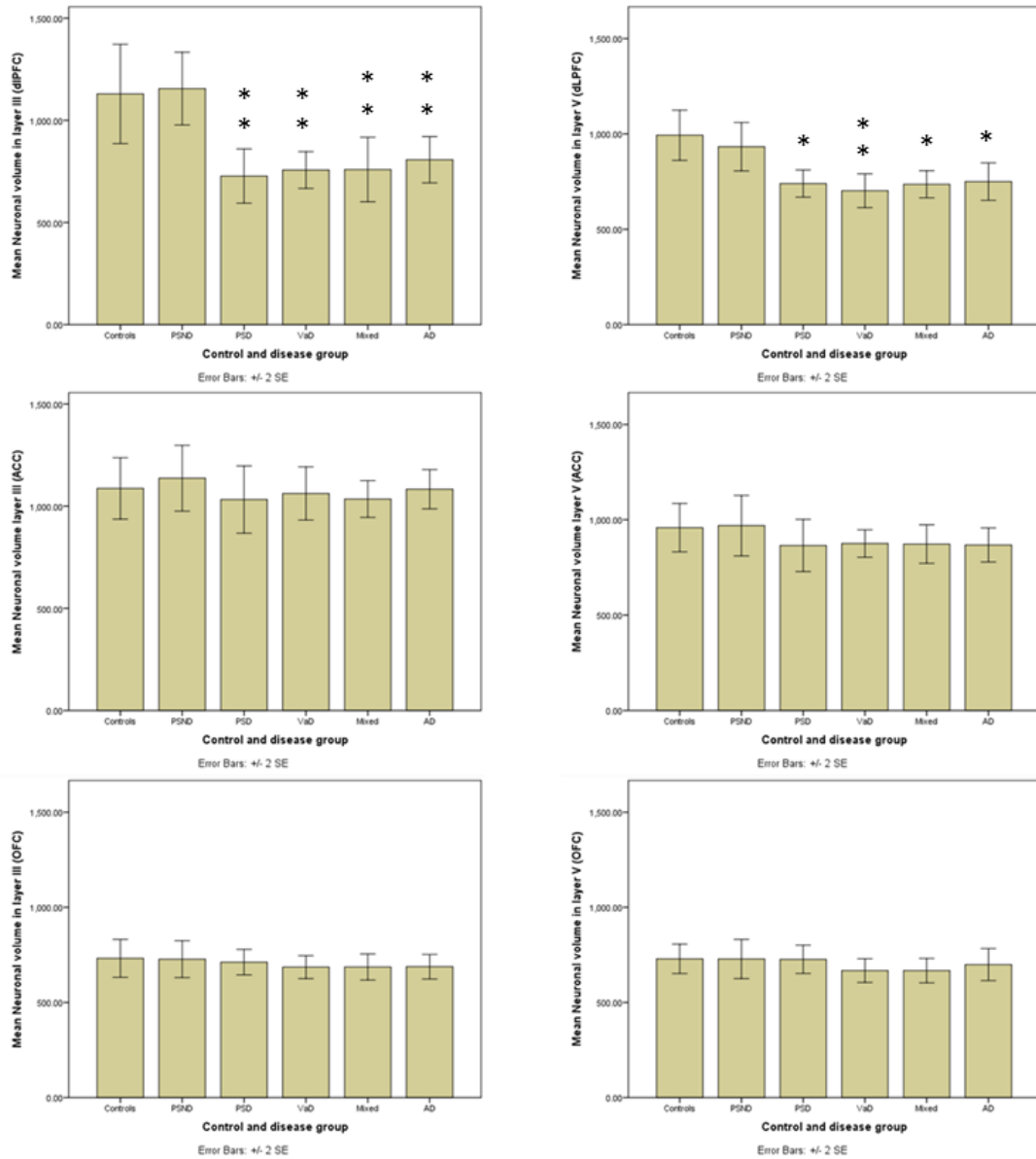


**Figure 3-2** pyramidal neuron volumes in the dlPFC, ACC, and OFC. Controls = aged matched controls, PSND = post-stroke no dementia, PSD = post-stroke dementia, VaD = vascular dementia, mixed = mixed vascular and Alzheimer’s disease, AD = Alzheimer’s disease. \* = significant to controls, \*\* = significant to controls and PSND ( $p < 0.05$ ). Controls vs PSD ( $P = 0.027$ ), VaD ( $p = 0.012$ ), mixed ( $p = 0.03$ ), and AD ( $p = 0.035$ ). PSND vs PSD ( $p = 0.01$ ), VaD ( $p = 0.01$ ), mixed ( $p = 0.004$ ), and AD ( $p = 0.005$ ) in layer III. In layer V controls vs PSD ( $p = 0.007$ ), VaD ( $p = 0.002$ ), mixed ( $p = 0.008$ ), and AD ( $p = 0.015$ ). PSND vs VaD ( $p = 0.034$ ).



### 3.3.3. Two dimensional analysis

Two dimensional analysis of pyramidal morphology was undertaken in order to a) confirm the volumetric differences between neurons in the dIPFC and the OFC, and b) assess the relative shape and dimensions of the respective pyramidal neuronal populations (if the neuronal difference detected using 3D stereology was as profound as thought, a less sensitive technique such as 2D analysis should be able to pick it up). Neuronal volumes as assessed using 2D densitometry analysis showed pyramidal volumes in the dIPFC were on average 34% and 27% larger than those of the OFC in layers III and V respectively (Figure 3-3). Analysis showed length/width ratio was significantly higher ( $p = 0.012$ ,  $p = 0.002$  layer III and V, respectively) in the OFC than pyramidal neurons in the dIPFC, suggesting those in the OFC are longer and slimmer than those in the dIPFC.

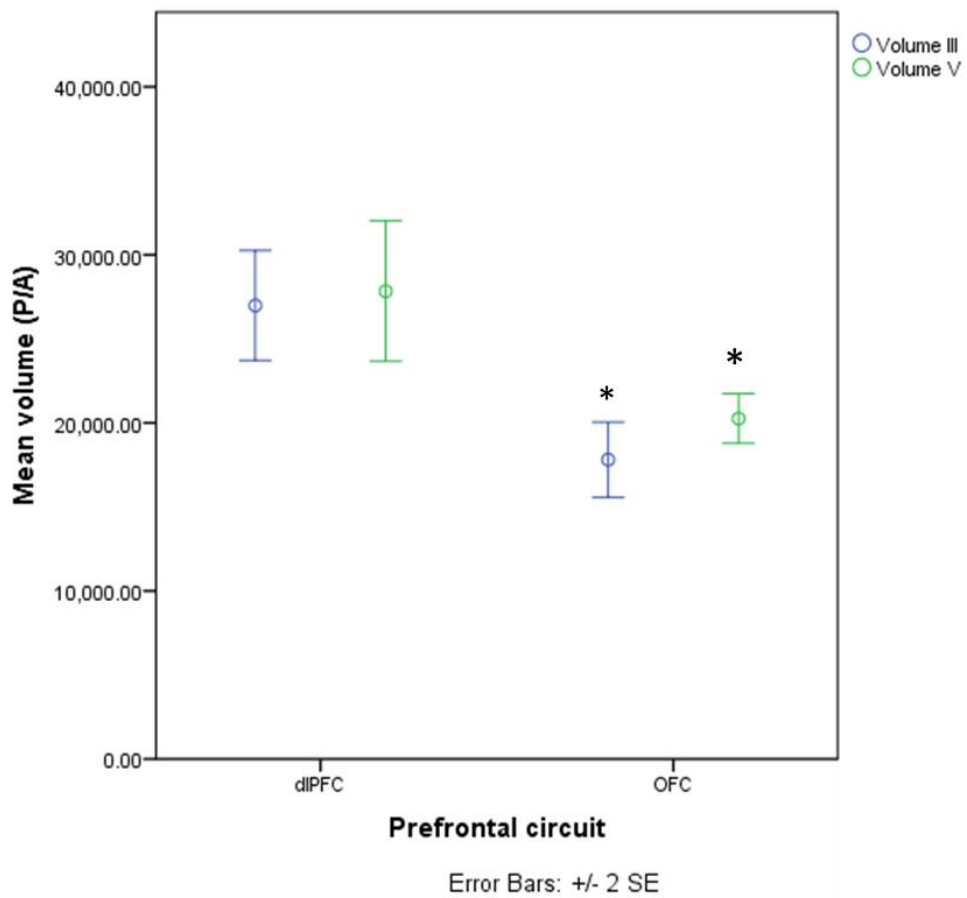


Figure 3-3 showing pyramidal neuron volumes in layers III and V in control cases of the dIPFC and OFC. P/A = per area (a count of average pixel content of each neuron). \* = significant compared to other brain region ( $p < 0.05$ ). dIPFC vs OFC layer III ( $F = 21.457$ ,  $p = 0.010$ ). layer V ( $F = 11.096$ ,  $p = 0.027$ ).

### 3.3.4. Correlations with neuropathological findings

To relate neuronal changes to cognitive function we examined the relationship between neuronal densities and volumes within the dlPFC and neuropsychometric measures which were taken as part of the CogFAST study. Neuronal volume in layer III correlated with a) total CAMCOG scores ( $\sigma = 0.707$ ,  $p = 0.0001$ ), b) MMSE ( $\sigma = 0.500$ ,  $p = 0.021$ ), and c) the CAMCOG sub score for the executive function, orientation ( $\sigma = 0.583$ ,  $p = 0.006$ ). Neuronal volumes in layer V correlated with clinical dementia rating ( $\sigma = -0.760$ ,  $p = 0.003$ ), and d) memory scores ( $\sigma = 0.444$ ,  $p = 0.044$ ) (Figure 3-4).

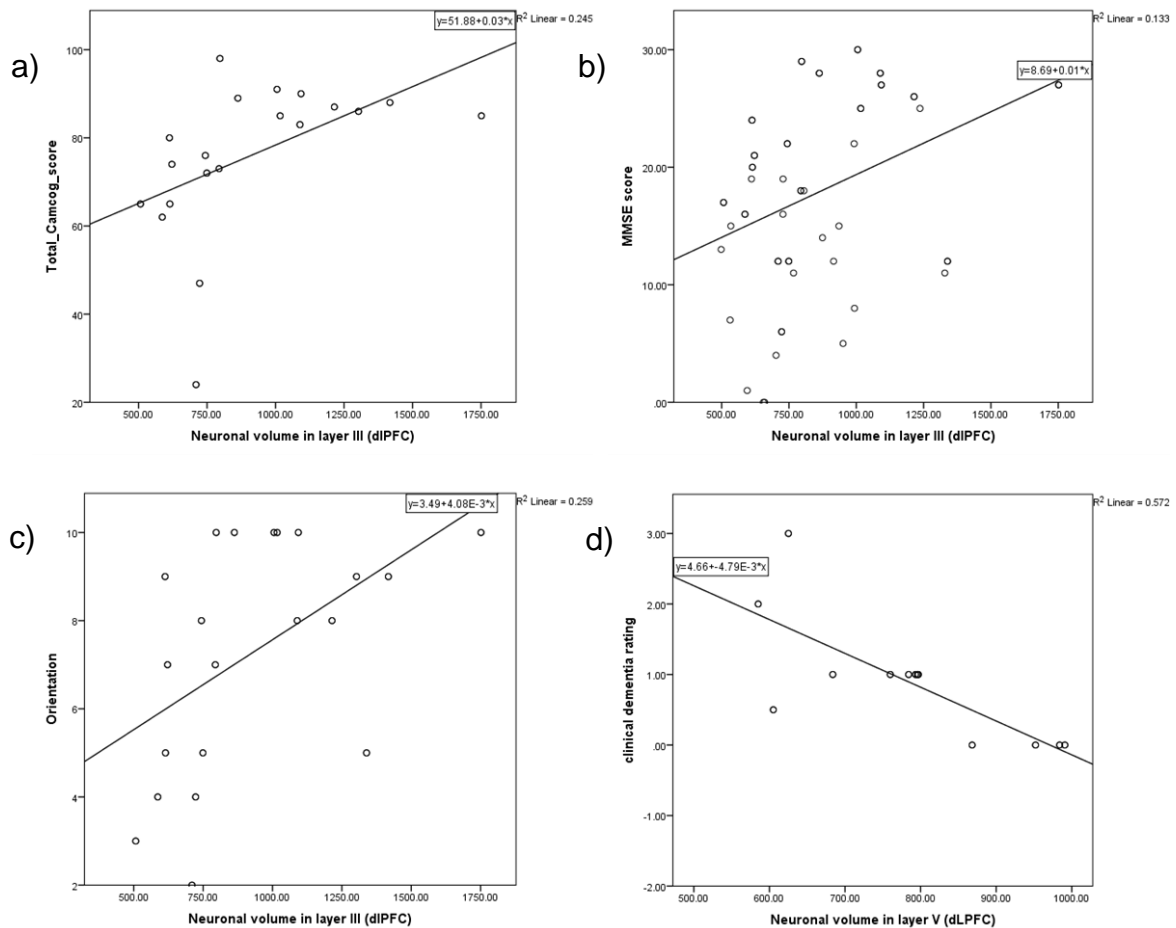


Figure 3-4 showing significant correlations between pyramidal neuronal volumes in the dlPFC and clinical variables. a)  $\sigma = 0.707$ ,  $p = 0.0001$ ), b)  $\sigma = 0.500$ ,  $p = 0.021$ , c)  $\sigma = 0.583$ ,  $p = 0.006$ , and d)  $\sigma = 0.444$ ,  $p = 0.044$ .

### 3.3.5. Clinical features in post-stroke dementia and VaD subjects

Information on the stroke type and location was collected and placed in to a table (Table 3-2). From the available clinical information of the cohort analysed in this study; nine post-stroke survivors suffered from lacunar strokes, five from partial anterior circulation stroke, two from posterior circulation strokes, and five from a total anterior circulation stroke with no relationship found between stroke type or location and the ultimate fate of the post-stroke survivor ( $p > 0.05$ ).

### 3.3.6. SMI31/32 positive cells in the dlPFC of post-stroke cases and other dementias

To further differentiate between the post-stroke cohort and the other disease groups, sections were stained for neurofilament markers SMI31 and SMI32. Neuronal counts of pyramidal neurons positively stained with SMI32 did not appear significantly different between either post-stroke groups, or between post-stroke survivors and aged-control groups in either layer III or V. Counts in VaD and AD revealed no significant differences between any groups in layers III or V. However, pyramidal neuronal counts were significantly lower in layer V of the mixed AD/VaD subjects compared with those with PSND ( $p = 0.004$ ) and PSD ( $p = 0.037$ ). There was no significant difference between mixed dementia subjects and controls ( $P > 0.05$ ). In addition, no significant difference was found in SMI32 counts between any groups in layer III ( $p < 0.05$ ) (Figure 3-5, Figure 3-7).

SMI31 counts showed significantly increased numbers of pyramidal neurons displaying positive staining in both PSD ( $p = 0.004$ ) and VaD ( $p = 0.031$ ) in layer III, but not in layer V ( $p > 0.05$ ) when compared to PSND. Additionally increased SMI31 immunoreactivity was correlated with decreased neuronal volumes in both PSD and VaD ( $\sigma = 0.573$ ,  $p = 0.016$ ) (Figure 3-6, Figure 3-8).

Further analysis showed correlation between SMI31 positive neuron counts in layer III and layer V ( $\sigma = 0.529$ ,  $p = 0.001$ ). Additionally, SMI32 positive neuron counts correlated significantly with layer III pyramidal neuronal volumes ( $\sigma = 0.733$ ,  $p = 0.016$ ), with SMI31 positive neuronal counts in layer III correlating significantly with SMI31 counts in layer V in those suffering post-stroke dementia (Figure 3-9).

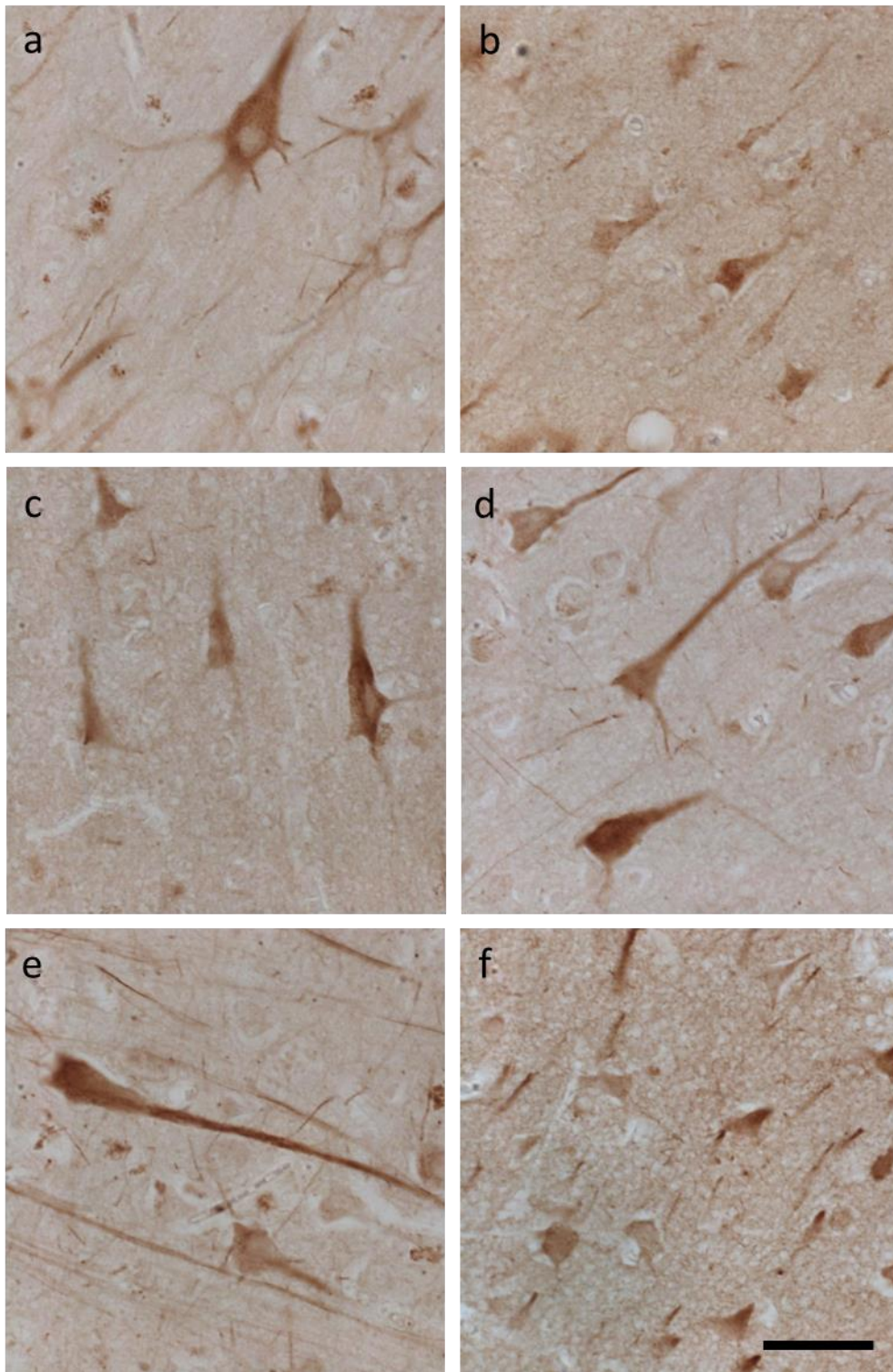


**Figure 3-5 showing SMI32 positive pyramidal neurons in layer III of the DIPFC. a) aged-controls, b) PSND c) PSD, d) VaD, e) Mixed, and f) AD. Size bar = 20 $\mu$ m.**

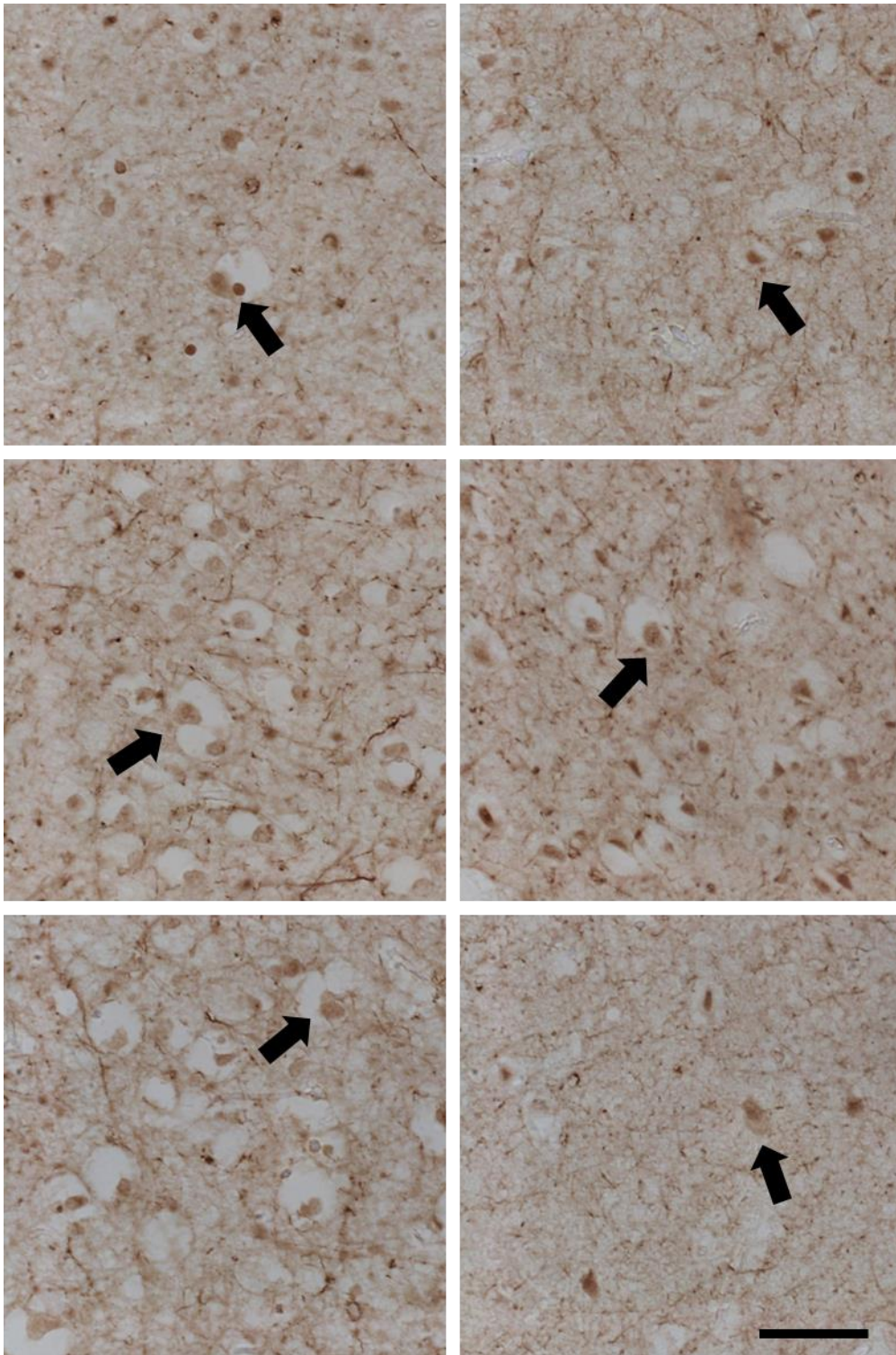


**Figure 3-6 Showing SMI31 positive neurons in layer III of the dIPFC. a) aged-controls, b) PSND, c) PSD, d) VaD, e) Mixed, and f) AD. Arrows indicates SMI31 positively stained pyramidal neurons. Size bar = 20 $\mu$ m.**

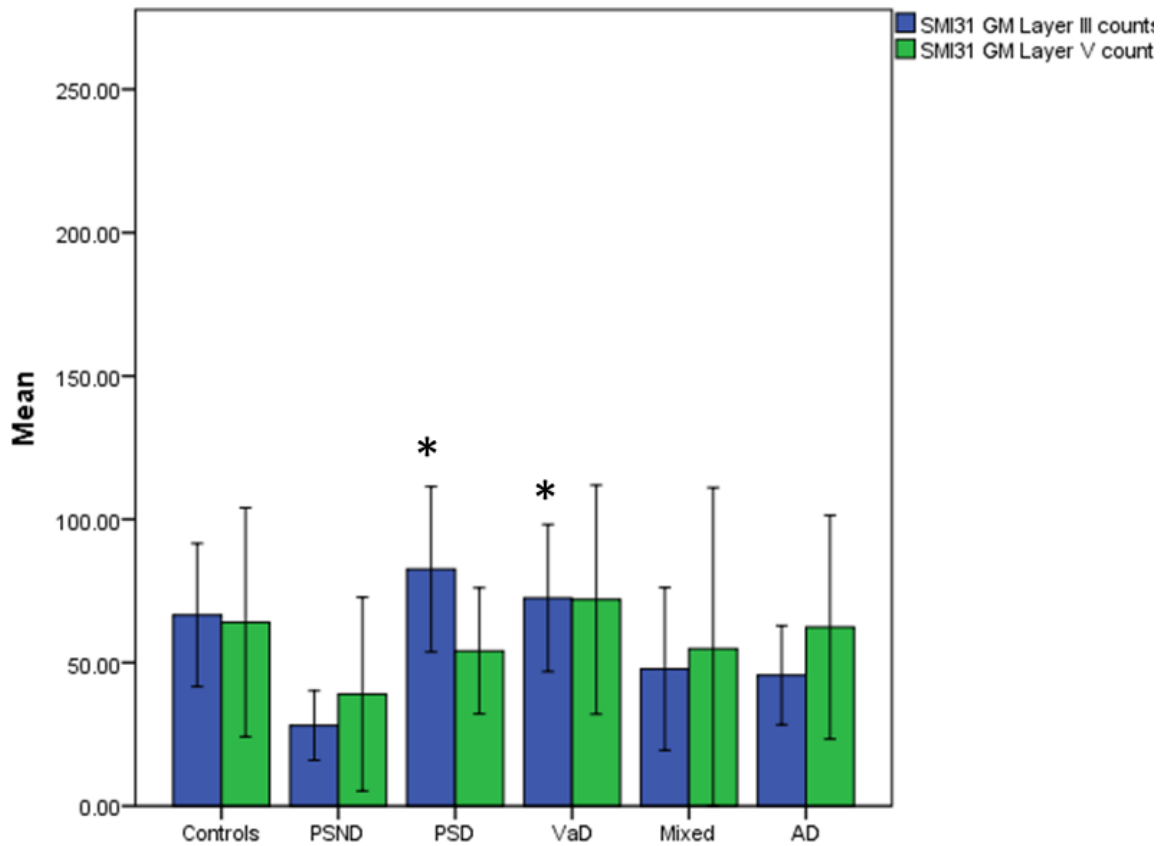


Figure 3-7 showing counts for SMI31 positive pyramidal neurons in layer III and V. Controls = aged matched controls, PSND = post-stroke no dementia, PSD = post-stroke dementia, VaD = vascular dementia, mixed = mixed vascular and Alzheimer's disease, AD = Alzheimer's disease. \* = significant to PSND. PSND vs PSD ( $p = 0.004$ ), VaD ( $P = 0.031$ ).

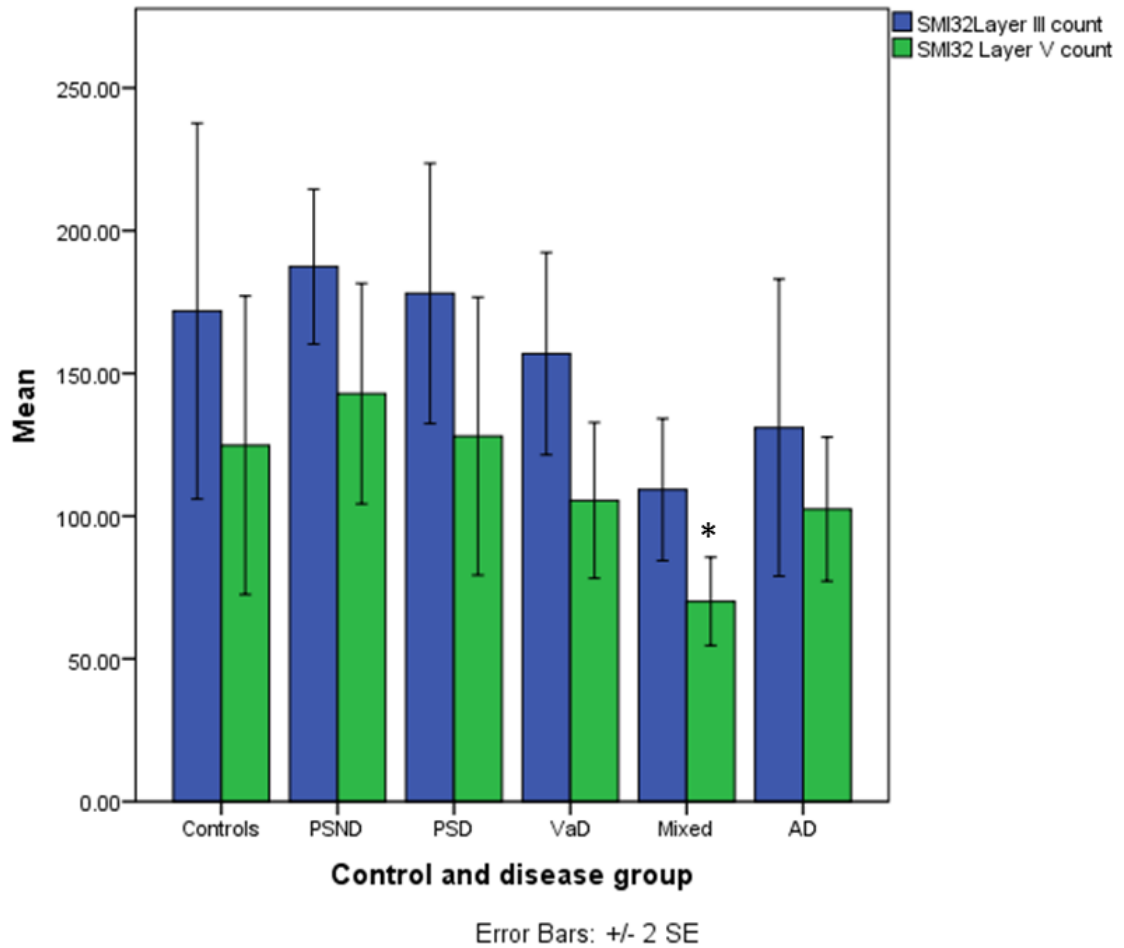
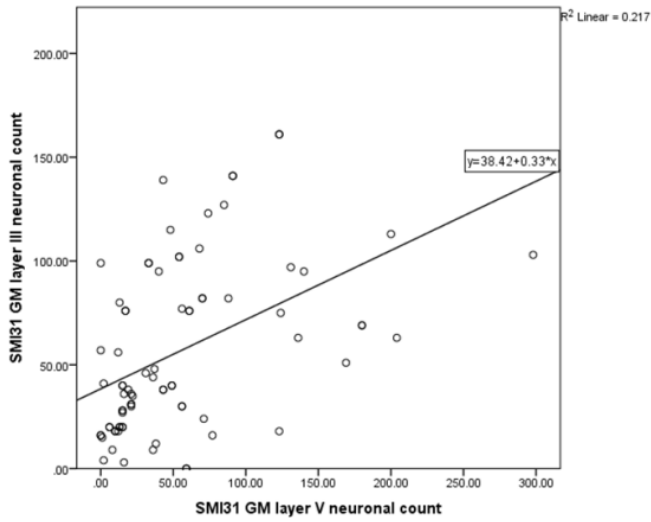


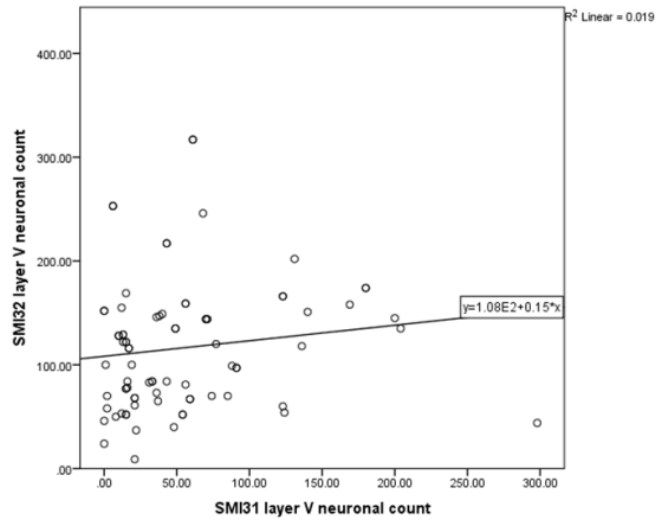
Figure 3-8 showing counts for SMI32 positive pyramidal neurons in layer III and V. Controls = aged matched controls, PSND = post-stroke no dementia, PSD = post-stroke dementia, VaD = vascular dementia, mixed = mixed vascular and Alzheimer's disease, AD = Alzheimer's disease. \* = significant to PSND and PSD. PSND vs mixed ( $p = 0.004$ ), PSD vs mixed ( $p = 0.037$ ).



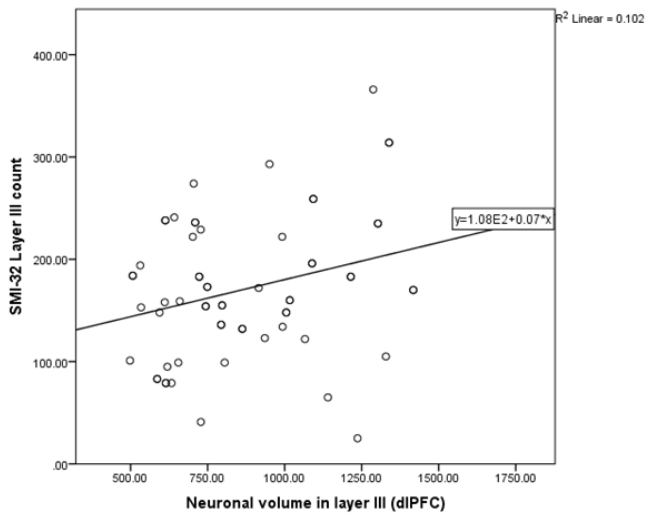
(a)



(b)



(c)



(d)

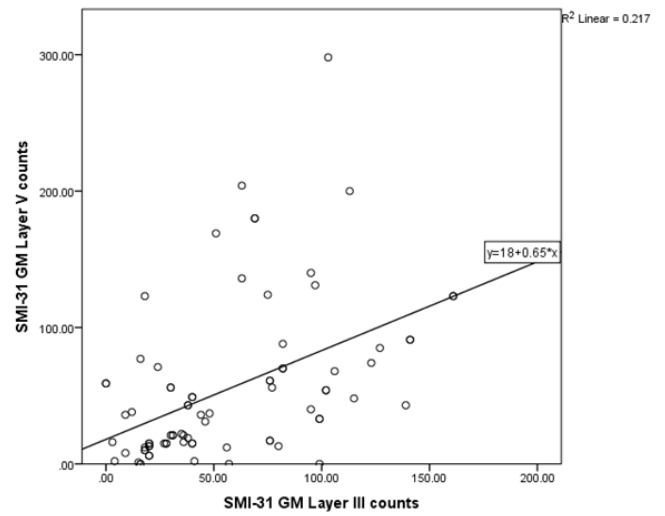


Figure 3-9 showing correlations (a) relationship between SMI31 staining in layer III vs layer V, (b) SMI32 staining in layer V vs SMI31 staining in layer V, (c) SMI32 staining vs layer III volume in post-stroke non-demented subjects, and (d) SMI31 staining in layer III vs layer V in post-stroke demented subjects. 'a' ( $\sigma = 0.529$ ,  $p = 0.001$ ), 'b' ( $\sigma =$ ), 'c' ( $\sigma = 0.733$ ,  $p = 0.016$ ), 'd' ( $\sigma = 0.259$ ,  $p = 0.020$ )

### 3.3.7. Cortical thickness and dIPFC atrophy

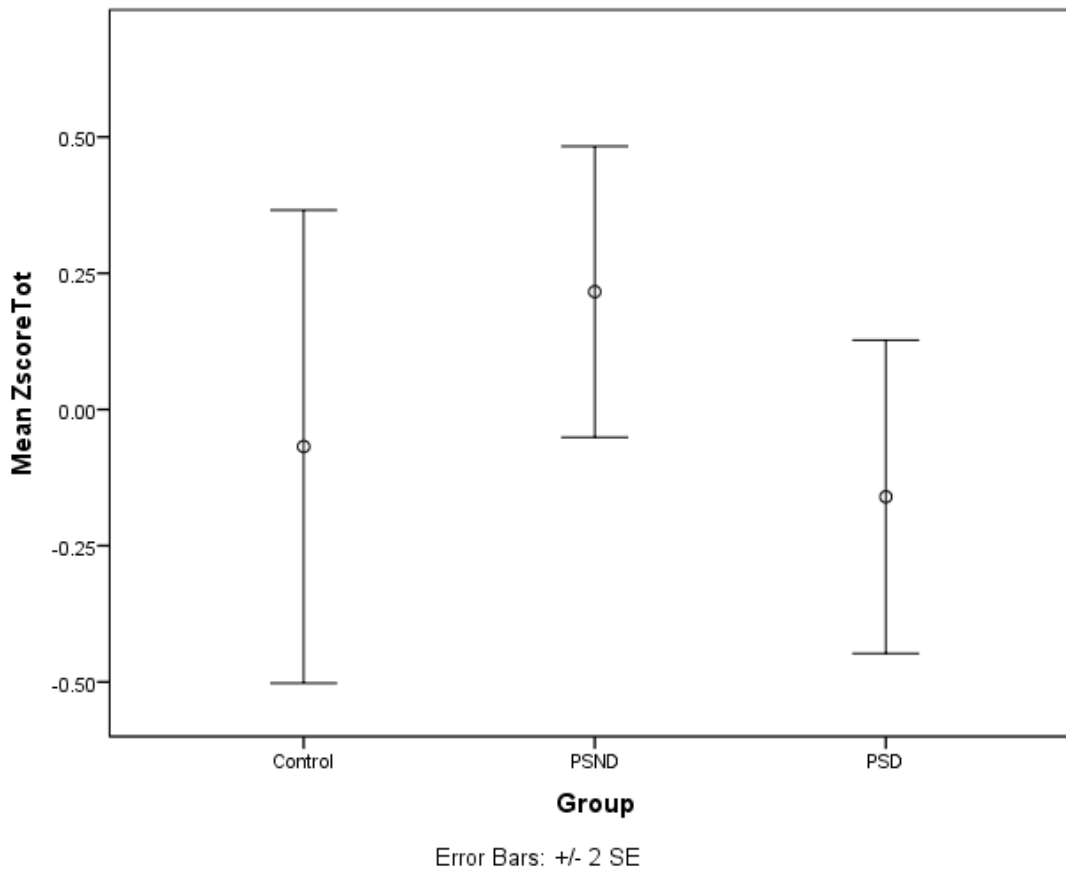
To explain if neuronal atrophy in the dIPFC of post-stroke subjects was also reflected in reduced cortical thickness we compared cortical depths in PSD, PSND and controls subjects. Global atrophy or diffuse neocortical ribbon reductions were investigated using the technique and formula already described above (see Cortical thickness measurements and atrophy estimates). Firstly, investigations into potential changes in the cortical ribbon thickness within the dIPFC revealed no significant difference in the degree of cortical thinning between demented and non-demented groups which would explain the volumetric changes (

Table 3-4). There were no significant differences found between the cortical thicknesses between any group ( $p > 0.05$ ) (Figure 3-10, Table 3-5, Table 3-6). Secondly, the clinical and post-mortem data of the CogFAST study allowed for a more detailed and in-depth cortical atrophy analysis between the two stroke survivor cohorts. Using the technique and formula adapted from White et al (correspondence) for establishing whole brain atrophy, we calculated potential atrophy of the dIPFC, as described earlier (see Cortical thickness measurements and atrophy estimates). Parametric ANOVA revealed no significant differences in dIPFC cortical atrophy between post-stroke survivors or controls ( $p = 0.193$ ). However student T-test (this test was used in place of ANOVA as we were following the protocol set out originally by Lon White et al) revealed post-stroke demented subjects did trend towards a significantly larger degree of cortical atrophy (lower Z scores) ( $p = 0.070$ ). T-test analysis of separate components of the formula found that brain weights of those suffering from post-stroke dementia were significantly lower than those of PSND ( $p = 0.022$ ). No significance was found between tissue fixation times which may have affected cortical thickness.

(SEM)	Controls	PSND	PSD	VaD	Mixed	AD
Cortical thickness	2.97 (0.13)	2.75 (0.11)	2.89 (0.17)	2.78 (0.12)	2.98 (0.12)	2.86 (0.13)
Significance to controls ( $p =$ )		0.911	0.999	0.959	1.00	0.988

**Table 3-4 displaying the mean cortical thickness of the dIPFC in each disease group and their respective significance to controls. Control = aged controls, PSND = post-stroke non-demented,**

**PSD = post-stroke demented, VaD = vascular dementia, mixed = mixed AD/VaD pathology, AD = Alzheimer's disease.**



**Figure 3-10 Cortical atrophy Z scores in the dIPFC. Controls = aged matched controls, PSND = post-stroke no dementia, PSD = post-stroke dementia.**

	Control	PSND	PSD	p value between PS groups
Weight/volume	0.00	0.55	-0.41	0.022
Cortical thickness/head diameter	-0.19	-0.015	0.014	0.303
Neuronal density	0.09	-0.43	0.39	0.056

**Table 3-5 showing weight/volume, cortical thickness/head diameter, and neuronal density ratios (z scores) within the dIPFC)**

Group	Z score	P value compared to PSD
Control	-0.016	0.731
PSND	0.216	0.070
PSD	-0.160	n/a

**Table 3-6 comparing the cortical atrophy index (z) score between non-demented controls and post-stroke dementia. Control = aged controls, PSND = post-stroke non-demented, PSD = post-stroke demented.**

### **3.3.8. Comparison of Alzheimer's type pathology between cases.**

Immunostaining for hyperphosphorylated tau (AT8), and fluorescent co-localised staining for amyloid  $\beta$  and hyperphosphorylated tau (4G8 and AT8 respectively) was conducted on the dIPFC to ensure that pathology in this area of the brain did not account for the volumetric changes reported. Dual staining made it possible to ensure that any one specific brain region was free of either pathology, through one assay. No substantial difference was found in the level of tau pathology between post-stroke survivors, nor between controls, or VaD. Mixed and AD groups, as one might expect, had significantly higher levels of hyperphosphorylated tau pathology than any other group. A qualitative analysis of hyperphosphorylated tau and amyloid burden demonstrated and reinforced this finding (Figure 3-11).

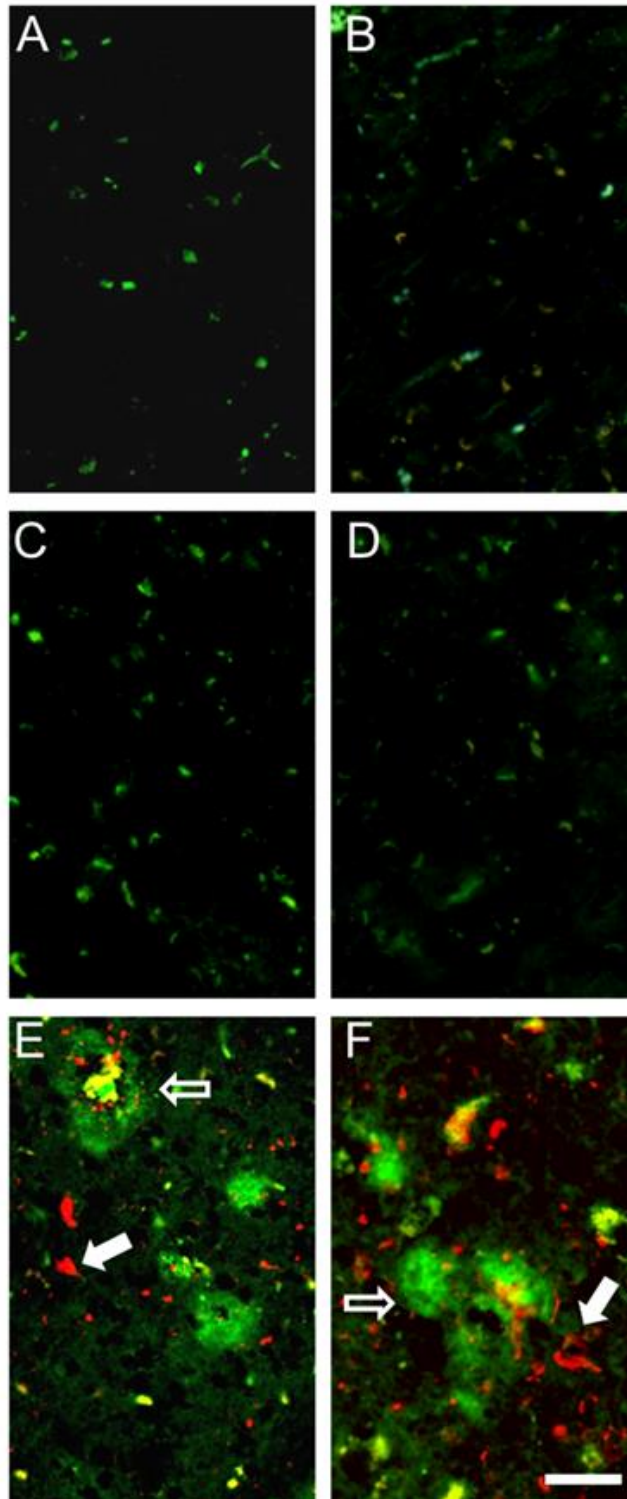


Figure 3-11 shows fluorescent stained images from the dIPFC layer III of control subjects (A), post-stroke no dementia (B), post-stroke dementia (C), vascular dementia (D), mixed dementia (E), and Alzheimer's disease (F). Background auto-fluorescence from lipofuscin and red blood cells is evident in all images. Hollow arrows = amyloid plaques (green), solid arrows = hyperphosphorylated tau (red). Scale bar 50 $\mu$ m.

### **3.4. Discussion**

#### **3.4.1. 3D stereological analysis**

3D stereological analysis revealed changes in pyramidal neuron volumes in both layers III and V of the dlPFC which may be associated with changes in cognitive function in post-stroke survivors and other ageing related dementias. Interestingly, neuronal density appears unaffected in the dlPFC, regardless of cognitive status, suggesting neurons are not necessarily lost in these disease states.

#### **3.4.2. Neuronal densities**

There were no significant changes detected in neuronal densities between any group of the dlPFC or the ACC. It has previously been suggested that cognitive dysfunction was a direct result of neuronal loss (Fiskum et al. 1999) and would have been expected in the regions believed to be pivotal in functions affected in dementia. Neuronal death within the dlPFC would be reflected in a reduction in the neuronal numbers, marked by a lower neuronal density. The lack of change in density would suggest that, although the majority of the neurons appear to be still present in diseased cases, with comparable numbers to those of the non-demented controls, these neurons are in fact not operating as they should. As discussed, the individual neuron is part of a much larger, sophisticated unit (Nedergaard et al. 2003), both in terms of operating in conjunction with other cells such as glia and other neurons and in its own far-reaching role as a connective entity (Tekin and Cummings 2002). This complexity increases the plethora of potential dysfunction which may befoul a neuron, but not result in its death. In contrast, analysis of the OFC revealed specific reductions in neuronal density in layer III of mixed dementia when compared to non-demented subjects, and VaD, mixed, and AD when in layer V. This loss may be indicative of cell death as a result of vascular or neurodegenerative pathology. This apparently specific effect in the OFC suggests particular vulnerability of these pyramidal neurons. However, no such changes were reported in the post-stroke cohort. Additionally pyramidal neurons were found to be significantly smaller in the OFC when compared to the other two regions in all groups, including non-demented controls, suggesting that although this may not be a pathological trait, the smaller size makes the neurons more susceptible to damage, and thus neuronal loss which may explain the density change. Interestingly, this effect

only appears to affect the vascular-based dementias, and is more apparent in layer V than layer III. This would suggest that the OFC is particularly vulnerable to ischemic damage. The increased susceptibility of layer V may be explained by the greater distance these projection neurons must travel in contrast to those of layer III (Khundakar et al. 2009). This is reinforced by the lack of significant difference in neuronal density between non-demented controls in the three separate regions suggesting that though reduced densities were found in the OFC of some disease states, all areas begin with a similar density of neurons. The loss of neuronal density in layer III may be a result of the synergistic effect of damage from both vascular and Alzheimer- type pathology.

These findings did not correlate with Braak or CERAD scoring, or with fixation or post-mortem delay, reinforcing the suggestion that this apparent neuronal loss is a result of vascular pathology (Figure 3-1).

#### **3.4.3. Neuronal volumes**

In contrast to neuronal densities, analyses of pyramidal neuron volumes revealed specific changes within the PFC (Figure 3-2). Within the dlPFC, pyramidal neuron volume was found to be significantly lower in all demented cases when compared to controls in both layers III and V and when compared to PSND in layer III. In layer V neuronal volumes in VaD were significantly lower than in PSND. These findings suggest an extreme vulnerability of the dlPFC to pathological insult, regardless of aetiology. There also appears to be a strong and distinct relationship between neuronal volume and cognitive function. Whether pathological insult affecting the dlPFC results in neuronal damage and dysfunction which leads to cell shrinkage, or whether naturally reduced neuronal volume (as a result of age) increases vulnerability to other risk factors which otherwise may not result in dementia in isolation, is unclear. Studies have shown a distinct relationship between WMH as seen in imaging studies and ischaemic brain pathology detected at post-mortem in subjects suffering small vessel disease (Duering et al. 2013; Yamamoto et al. 2009), suggesting vascular pathology alone is enough to impact pyramidal neuronal volume, without additional pathology. Pyramidal neuron shrinkage in the dlPFC has been reported in a number of disease states (Khundakar et al. 2009; Courchesne et al. 2011; Pierri et al. 2001) and may therefore suggest distinct vulnerability of these cell types, potentially as a result of their increased



metabolic requirements. Pyramidal neuronal shrinkage appears to occur in all disease groups, regardless of aetiology. Due to the wide-ranging nature of the pathology examined it is unlikely that morphological changes observed are triggered by the same mechanism each time. Vascular damage as that which characterises PSD, VaD and Mixed may result in reduced blood flow to the dlPFC; pyramidal neurons in this area then undergo hypoxic stress which results in their breakdown and shrinkage. Alternatively, increased WM pathology as that found in vascular pathology (Ihara et al. 2010) may disrupt neuronal axons connecting the different brain regions. This disconnection may lead to a feedback mechanism ultimately resulting in neuronal shrinkage. Those suffering from neurodegenerative disease may increasingly struggle as internal proteins such as tau (in AD) begin to build up (Goedert 1996; Mandelkow and Mandelkow 1998), placing metabolic strain on the neuron. As the tau burden increases the neuron eventually begins to dysfunction and reduce in volume. This disease related neuronal atrophy was not mirrored in the ACC nor the OFC suggesting this is an area specific affect, with the dlPFC either specifically vulnerable to such damage, or the OFC and ACC more resistant.

In aged matched controls neuronal volumes were found to be larger in the ACC, followed by the dlPFC, and smallest in the OFC, indicating significant variations across different cortices of the brain, perhaps dependent on each regions individual role in cognition, or the varying vascular patterns which may present in each brain region.

Neuronal volumes in the OFC were found to be up to 50% smaller than the dlPFC or the ACC, with neuronal volumes in the OFC consistent between groups, including aged matched controls, suggesting that this smaller volume was in fact a regional trait, and not a pathological response to underlying pathology. This finding was confirmed using 2D analysis, a less sensitive technique, with a similar margin of change (Figure 3-3).

#### **3.4.4. Neuronal volumes and cognitive impairment**

The clinical significance of this neuronal shrinkage in the dlPFC is demonstrated by correlations between neuronal volume and clinical findings. Neuronal atrophy in layer III correlated with both total CAMCOG scores, and MMSE scores (Figure 3-4) suggesting a direct relationship between neuronal volume

and cognitive dysfunction. However it is not clear whether these changes are a direct result of neuronal volume shrinkage in the dlPFC, or as a result of neuronal damage elsewhere (Firbank et al. 2007; Gemmell et al. 2012), or further along the frontal circuit (Tekin and Cummings 2002). Perhaps more significantly neuronal volume also correlated with orientation - a component of executive function controlled by the dlPFC, creating a direct link between these neuronal changes and executive dysfunction. Neuronal volumes in layer V correlated with clinical dementia ratings and memory scores. This is in keeping with our understanding of the role of these long-range projection neurons. As these projections breakdown, the pre-frontal cortex loses connection with areas of the brain such as the hippocampus which is responsible for memory.

#### 3.4.4.1. ***Stroke location***

There was no apparent correlation between stroke location and clinical outcome for post-stroke survivors or neuronal volume changes, suggesting single insult sites have little impact for prognosis (Table 3-2). When taking PSD, VaD and Mixed cases into account, long term vascular pathology appears to have a severe impact on cognitive outcomes. Damage occurring after a stroke can be mediated and limited, quelling potential long term cognitive decline. Factors such as the susceptibility of the astrocytes making up the neurovascular unit are thought to play an important role in any recovery, especially those suffering a stroke (Nedergaard and Dirnagl 2005). With this in mind, stroke sufferers with concurrent CVD are perhaps less likely to recover than those without. However, no significant differences were found between vascular pathology between PSND and PSD which suggest that another, unknown mechanism may be at play.

#### 3.4.5. **Interlaminar correlation**

Though this reduction in pyramidal neuronal volume appeared to affect layer III and V in equal measure, it was necessary to explore any potential relationship between these two sets of changes. Spearman's rank coefficient revealed significant correlations between layer III and V neuronal volume in both controls and AD subjects. There was no correlation detected between layer III and V in PSND, PSD, VaD, or mixed cases. This finding would perhaps be expected in

control cases where no change of neuronal size is apparent. The lack of correlation may suggest that layers III and V are affected differently to vascular pathology, or neurons in each layer respond varying degrees. Layer V pyramidal neurons extend their axons across greater expanses of WM, perhaps making them more vulnerable to the ischaemic damage, pathology which may be present in the WM of these cases. Conversely, layer III neurons may be less affected as their axons do not tend to project in the deep WM, remaining isolated and protected. The significant correlation between layers III and V in AD cases suggest different mechanisms may be at work than those in vascular pathology groups. The toxic impact of interneuronal tau may affect pyramidal neurons in both layers III and V to comparable degrees resulting in a similar rate of volumetric decline (Table 3-3).

#### **3.4.6. Comparison of neurofilament markers in post-stroke survivors and other groups**

Pyramidal neurons positively stained for SMI31 (a marker for cellular damage) were found in larger numbers in PSD, VaD, and mixed when compared to PSND, however this significance was not shown against aged-controls. This finding further differentiated the two post-stroke survivor groups PSND and PSD, with a higher proportion of neurons showing damage in the demented cases, following a similar pattern to neuronal volume loss, though no correlation was found between SMI31 counts and neuronal volume ( $p > 0.05$ ).

Interestingly, increased SMI31 staining was seen in both VaD and mixed dementia groups (see results), suggesting a vascular component contributing to neuronal damage. The lack of significant difference when compared to controls was unexpected. One reason may be due to the eclectic nature of the aged-control subjects. The post-stroke subjects were selected from a well characterised cohort, with well-documented clinical histories of disease progression which ensured a certain homogeneity between the characteristic shared between cases. The control groups, in contrast had very little, if any patient history, making it difficult to identify markers which may preclude underlying characteristics or pathology potentially affecting each case. In addition this made the control group much more heterogeneous when compared to post-stroke survivors. Whilst this made them an ideal group to demonstrate a wide and varied population, it also gave rise to the possibility of

very varied data, with evidence showing that even in the cognitively healthy, age can have a detrimental effect on neurons and neuronal connections (West et al. 1994; Morrison and Hof 1997). Conversely, mixed dementia showed a markedly decreased count for SMI32 positive 'healthy' pyramidal neurons within layer V when compared to post-stroke survivors, this combined with increased SMI31 counts suggests neuronal volume loss, in this group at least is a result of neuronal damage. The lack of similar SMI32 findings in other group may again pay testament to the synergistic pathology of both AD type pathology and CVD (Kalaria et al. 2012; Kalaria 2003).

Perhaps unsurprisingly, SMI31 pyramidal neuronal counts in layer III correlated positively with neuronal counts in layer V, suggesting that damage occurs simultaneously in both layers. Though when analysed individually, only in PSD did SMI31 staining in layer III correlate strongly with counts in layer V (Figure 3-9). However, this finding was not mirrored in SMI32 stained sections, suggesting a limited relationship between SMI31 and SMI32 staining. With this in mind, it is necessary to stain with both SMI31 and SMI32 to gauge an accurate count of healthy and non-healthy pyramidal neurons.

#### **3.4.7. Neuronal volume loss, cortical thinning and atrophy**

Cortical thinning can occur in normal ageing, through atrophy, fixation, dehydration, and in disease through neuronal loss (Harding et al. 1994; Kril et al. 1997; Opris and Casanova 2014) and this atrophy is thought to result in the thinning of the microcolumns which make up the dIPFC (Opris and Casanova 2014) with early changes in cortical thickness noted in cognitive impairment (Cruz et al. 2004) and related to cognitive changes in MCI and AD (Chance et al. 2011). It was therefore necessary to investigate any potential affect cortical change may have on the reported neuronal atrophy. All results were checked against fixation times and post-mortem delay for correlation where possible. Pyramidal neuronal volumes changes did not correlate with either. No correlations were found between dIPFC cortical atrophy index of PSND or PSD, or between cortical thicknesses between any groups. This suggests neuronal volume changes occur independently of cortical alterations, reinforcing the association between neuronal volume change and cognitive dysfunction. In addition, any effect of tissue shrinkage, or global atrophy affecting neuronal volumes or density changes would be expected to impact all tissue types and

regions in the same way. Brain weights were found to be significantly lower in PSD cases than PSND. This weight reduction is indicative of tissue loss. Though no cortical loss was detected in the dlPFC it does appear there is selective, but global loss in the brains of those suffering post-stroke dementia.

#### **3.4.8. Alzheimer's type and vascular type pathology in post-stroke dementia and other dementias.**

Neuronal volume changes demonstrate a stark and striking difference between the two post-stroke survivor cohorts. As discussed, this change was also found in other vascular demented cases, as well as those with high AD pathology. Qualitative AT8 analysis revealed no significant difference between the two post-stroke survivor cohorts, nor between post-stroke survivors, VaD or control groups. However, as expected both mixed and AD groups displayed significantly higher levels of hyperphosphorylated tau as detected with AT8 staining than non-neurodegenerative disease groups. Fluorescent dual staining for AT8 and 4G8 confirmed this finding. This data suggests that the clinical, cognitive, and pathophysiological differences between PSND and PSD are not the result of Alzheimer type pathology. Additionally, investigation of the vascular pathology in the frontal lobe revealed no significant difference between PSND and PSD subjects, or between any other group. These findings suggest that vascular pathology may not be the deciding factor as to why a post-stroke sufferer would decline into dementia. However, the lack of significant differences detected between any other group, including between mixed, VaD and controls would suggest that SI may not be a good predictor of vascular pathology, at least not in the frontal lobe grey matter. Furthermore, SI data did reveal greater pathology in the WM when compared to the GM in all groups, suggesting that the GM may be less susceptible to such damage, and a more sensitive technique is required to detect any potential differences between disease groups. No significant difference to PVS was reported between any groups which was also surprising. PVS have previously been associated with WMH (Yamamoto et al. 2009), which are reportedly higher in frequency in those suffering specific types of dementia, such as VaD. However, it can be suggested that MRI, due to its 2mm limited resolution, may make separating large WMH from what are in fact several vessels, all with minor PVS. Though,

the sheer number of PVS may be significant in the development of dementia, it may suggest why, in this study, no changes to PVS size was identified.

### **3.5. Conclusion**

These findings provide original and novel evidence to suggest that reduction to pyramidal neuronal volume, specific to the dlPFC, is a significant pathological substrate in the development of post-stroke dementia and other dementias. Surprisingly, neuronal loss was not evident in the PSD or other dementia groups in the dlPFC, suggesting an underlying mechanism which may result in this neuronal and cognitive dysfunction. These findings also suggest that these volume reductions in the dlPFC are independent of AD pathology and may be more in line with vascular based pathologies, with reduced blood flow resulting in neuronal atrophy. These findings are associated with increased neuronal damage in vascular cases as shown by increased SM31 staining in PSD and VaD subjects. This suggests specific damage to the cytoskeleton of pyramidal neurons in the dlPFC as a result of vascular pathology.

## **Chapter 4. Non-pyramidal neurons and glial cells within the dorsolateral prefrontal cortex in post-stroke dementia**

### **4.1. Introduction**

#### **4.1.1. Non-pyramidal neurons and disease**

Previous studies into the density of non-pyramidal neurons have been revealing to the nature of these cells. Hof et al reported that interneurons which stain positive for calretinin are resistant to degeneration in AD (Hof et al. 1993). Hoff et al also reported differential staining sensitivity of interneurons in the cortex of AD subjects, with a subset of interneurons located in layers II, III, and V displaying particularly heavy staining of calbindin (Hof and Morrison 1991; Hof et al. 1991). This suggested that interneuronal subtypes exhibit differential vulnerability in AD. Satoh et al reported parvalbumin positive interneurons in those suffering AD were significantly smaller and fewer in number when compared to controls (Satoh et al. 1991). Studies in mice have suggested that decreased parvalbumin positive neurons contribute to dysfunction in cellular networks, with possible connotation in AD subjects (Verret et al. 2012) suggesting a role for these cells in cognitive dysfunction.

Khundakar et al reported no significant changes in non-pyramidal densities in the dlPFC, despite reporting significantly smaller pyramidal neurons in elderly depressed subjects when compared to controls (Khundakar et al. 2009). This lack of change was also reported in the OFC and ACC. Rajkowska et al reported no changes in interneuronal numbers in depressed subjects, despite finding a 30% decrease in pyramidal neuron volumes in the OFC (Rajkowska et al. 2005). Bernstein et al reported partial loss of parvalbumin positive interneurons in dementia with Lewy bodies (Bernstein et al. 2011), suggesting this loss may be the result of a chronic excitatory state from increased calcium concentrations, eventually resulting in mitochondrial dysfunction and cell death in parvalbumin-expressing interneurons in the hippocampus (Bernstein et al. 2011). There are no clinicopathological studies of frontal interneurons in cases

with cerebrovascular disease. In rat models Wang et al reported that short-term cerebral ischaemia results in the dysfunction in the excitability of inhibitory interneurons, and the subsequent over excitation of pyramidal neurons (J. H. Wang 2003). This suggests a potential mechanistic link between interneuron dysfunction and pyramidal neuronal pathology in stroke subjects.

#### 4.1.2. **Glial cells**

There is strong evidence to suggest a more glial-centric aetiology to neurological disease (Lobsiger and Cleveland 2007), with astrocytes (Shin et al. 2005; Custer et al. 2006), microglia (Boillee et al. 2006), and oligodendrocytes (Tomimoto et al. 1994) all being involved. The overall roles and characteristics of glial cells have been previously described in the introduction (See Glial cells). Astrocytes form part of a network which support their neighbouring neurons, aiding the formation and maintenance of synapses, and regulating cerebral blood flow (Lobsiger and Cleveland 2007). In addition they supply various nutrients to the neuronal cell. Mutations in the genes coding for glial cells have been shown to have impaired ability to uptake excess glutamate in mice with Huntington's disease (Shin et al. 2005) and in other mouse models (Custer et al. 2006). These studies highlight the importance of glial cells role in maintaining glutamate homeostasis in protecting neurons, which can play a critical role in ischaemic damage.

As previously mentioned, microglial cells have been shown to accumulate around amyloid plaques but also around sites of ischaemic damage (Bolmont et al. 2008; Lees 1993) with mouse models showing glial cell activation and increased gliosis in the substantia nigra in association with dopaminergic neurodegeneration (Liberatore et al. 1999). Additionally, transgenic mouse models overexpressing  $\alpha$ -synuclein in oligodendrocytes resulted in a similar syndrome to multiple system atrophy (associated with neurodegeneration of specific areas of the brain) (Yazawa et al. 2005).

##### 4.1.2.1. **Glial cells and SVD**

Increased numbers of activated astrocytes (astrogliosis) have been found at lesion sites (both ischaemic and neurodegenerative), and are thought to play a role in neuronal remodelling through the release of cytokines such as tumour necrosis alpha (TNF- $\alpha$ ), which may influence the growth of synapses by



inducing the insertion of AMPA receptors at post-synaptic membranes (Sofroniew 2009; Sofroniew and Vinters 2010; Nagele et al. 2004). It is therefore apposite to infer that glia play a crucial role in both post-stroke and vascular dementia. Primate studies have found increased activation of microglia and astrocytes associated with cognitive impairment (Kemper et al. 2001) and in hypertensive rats, with enlarged astrocytes present at the site of lesions, forming around leaky sites in the vasculature (Fredriksson et al. 1988). Astrocytes form a continuous lining (glial limitans) to seal off the lesions (Giulian et al. 1994). Microglial cell numbers in Binswanger's disease, a form of vascular dementia, were found to be unchanged when compared to controls. However increased numbers of activated microglia were up to three fold higher in those suffering vascular pathology (Tomimoto et al. 1994; Akiguchi et al. 1997).

The previous chapter revealed pyramidal neuron volumes were related to dementia with CVD and AD pathology within layers III and V specific to the dlPFC, as well as being associated with cognition and executive functions. These findings are both specific and distinctive. To further understand the pathological processes which may be at work it is necessary to investigate other components which make up the dlPFC.

The aim of this study was to assess non-pyramidal neuron and glial cell density in post-stroke demented subjects and compare to aged-controls and other disease groups. 3D stereology was used to isolate specific pathologies within the dlPFC. Interneuronal sub-types were also assessed using immunohistochemistry and 2D analysis. Changes to glial cell and interneurons were related to pyramidal neuron changes reported in the previous chapter. Additionally the relationship between glial cell density and interneuronal density was also investigated to establish whether any changes occurred in unison or separately.

## 4.2. Methods

### 4.2.1. Subject demographics

(SEM)	No of cases	Age, years	PMD, hours	FT, weeks	Vascular score	Braak (I – VI)	CERAD
Control	11	81 (3)	26.6 (5)	12.6 (5)	n/a	2 (0.41)	n/a
PSND	10	83.3 (1)	42.3 (7)	3.8 (2)	4.5 (0.26)	2.3 (0.47)	1.6 (0.26)
PSD	11	87.2 (1)	35.7 (7)	1.9 (1)	4.4 (0.32)	2.8 (0.34)	1.3 (0.30)
VaD	10	83.6 (2)	47 (9)	5.3 (2)	5.5 (0.50)	2.4 (0.34)	1.2 (0.40)
Mixed	10	84.4 (2)	33.6 (7)	4.6 (3)	4.0 (1.00)	5.1 (0.31)	2.6 (0.29)
AD	10	85.8 (2)	44.1 (10)	5.5 (2)	1.20 (1.00)	5.5 (0.21)	2.9 (0.11)

**Table 4-1 Subject details. Controls = aged matched controls, PSND = post-stroke no dementia, PSD = post-stroke dementia, VaD = vascular dementia, mixed = mixed vascular and Alzheimer's disease, AD = Alzheimer's disease. FT = fixation time, PMD = post-mortem delay. Vascular score (/6). Age (F = 1.005, p = 0.423). FT (F = 2.207, p = 0.066), PMD (F = 1.029, p = 0.412).**

#### **4.2.2. Three dimensional analysis of non-pyramidal neuron and glial cell densities in layers III and V of the dIPFC.**

Non-pyramidal neuron and glial cell density was analysed using 3D stereology as described previously (See Three dimensional stereology). Glial cells were identified by their consistently round shape and size, as well as a distinctive punctate-style nucleus (Figure 2-5). Non-pyramidal neurons were identified by size (typically smaller than pyramidal neurons) and lack of large pyramidal cell soma.

#### **4.2.3. Immunohistochemical analysis of interneuronal cell populations in layers III and V the dIPFC**

Neuronal counts were performed on 10µm frontal sections containing the Brodmann 9 of the dIPFC as described previously. Three serial sections were stained with; calbindin (Sigma ,UK), parvalbumin (Sigma, UK), and calretinin (Sigma, UK) respectively. Each of these antibodies stained a specific sub-type, or range of specific sub-types, of interneurons. Individual neuronal counts were then performed. Upon analysis of IHC stained sections a sub-population of markedly darker interneurons were identified in some of the sections (see figure). These cells appeared throughout each of the three different stains and seemed to retain a higher level of pigment than the surrounding cells of the same interneuronal sub-population.

##### **4.2.3.1. *Darkly stained interneurons***

Additional counts were performed on a sub-set of cell which appeared very darkly stained (Figure 4-5). The initial hypothesis was that these darkly stained neurons were either a) expressing extraordinarily high levels of stain or, b) had shrunk in volume, thus increasing the concentration of stain within each cell, causing the neuron to appear much denser than its more 'healthy' counterparts. Hypothesis 'a' revolved around the nature of apoptosis. It is understandable to assume that in situations of extreme stress, such as hypoxia brought about by cerebral ischaemia or some other pathology, that vulnerable neurons may undergo cell death, a result of a heavy influx of calcium ions. This influx may show up as increased staining, this being a calcium-binding albumin. Theory 'b'

revolved around the idea that neurons undergoing physical stress may shrink, increasing the relative concentration of stain. To assess the true number of darker stained interneurons against the total counts, the value for total darkly stained neurons were divided against total interneuronal cell counts to give a percentage value of the total population of darkly stained neurons.

#### 4.2.4. **Statistical analysis**

Statistics were performed as described previously. ANOVA with post-hoc LSD was used for normally distributed data, or the Kruskal Wallis and the Mann-Whitney U test was used for non-normally distributed data. The Mann Whitney-U test was used to test for significant differences between groups and Spearman's rank coefficient was used to assess relationships between variables in non-normally distributed cases. ANOVA with post-hoc; lowest significant difference (LSD) was used for normally distributed cases.

##### 4.2.4.1. ***Comparing interneuronal and glial cell densities***

To highlight any potential relationship between glial cell and interneuronal densities with each other, or with clinical variables from the CogFAST study, spearman's rank coefficient was used.

### 4.3. **Results**

#### 4.3.1. **Distribution of non- pyramidal neurons**

Normality testing revealed 3D stereologically assessed non-pyramidal density and IHC based cell counts for parvalbumin, calretinin, and calbindin to be non-normally distributed in all layers except layer II.

#### 4.3.2. **Three dimensional stereological analysis of interneuronal densities in pyramidal layers III and V of the dIPFC.**

Nissl stained interneuronal densities were analysed in both layer III and V in the dIPFC. Mean densities in layer III were; (per mm<sup>3</sup>) 59298, 71348, 66474, 83412, 101393, 92563 (in aged-controls, PSND, PSD, VaD, mixed, and AD respectively), and in layer V; (per mm<sup>3</sup>) 205642, 213196, 220423, 270594, 226849, 210491(in aged-controls, PSND, PSD, VaD, mixed, and AD, respectively). There were no significant differences between PSD and PSND in

either layers III or V in the dlPFC. However, in layer II only the PSND, and PSD groups against controls were analysed. PSND and PSD showed significantly higher neuronal density when compared to control cases ( $p = 0.023$  and  $p = 0.006$ , respectively).

Interneuronal density in VaD, mixed, and AD groups was significantly increased when compared to controls in layer III ( $p = 0.017$ ,  $p = 0.003$ ,  $p = 0.017$ , respectively). In addition, mixed dementia showed significantly higher interneuronal densities when compared to both post-stroke survivors groups ( $p = 0.016$ ,  $p = 0.009$ , respectively). Conversely, no changes were found in layer V between control and disease groups. With all groups exhibiting comparable interneuronal densities. Layer II revealed no changes in interneuron density between PSND and PSD in the dlPFC ( $p > 0.05$ ) (Figure 4-4). Layer II revealed non-pyramidal neuron densities in PSND and PSD were significantly higher when compared to controls ( $p = 0.023$  and  $p = 0.006$ , respectively).

#### 4.3.2.1. ***Correlations between non-pyramidal neurons and other variables***

Non-pyramidal neuron density in layer III correlated with both CERAD and Braak scoring ( $\sigma = 0.133$ ,  $p = 0.021$  and  $\sigma = 0.231$ ,  $p = 0.001$  respectively), and MMSE score ( $\sigma = -0.205$ ,  $p = 0.009$ ). Non-pyramidal neuronal density correlated with frontal vascular pathology ( $\sigma = 0.818$ ,  $p = 0.05$ ). Non-pyramidal neuron density significantly correlated with glial cell density in layer III in both AD and control subject groups ( $\sigma = 0.758$ ,  $p = 0.011$ , and  $\sigma = 0.755$ ,  $p = 0.007$ , respectively).

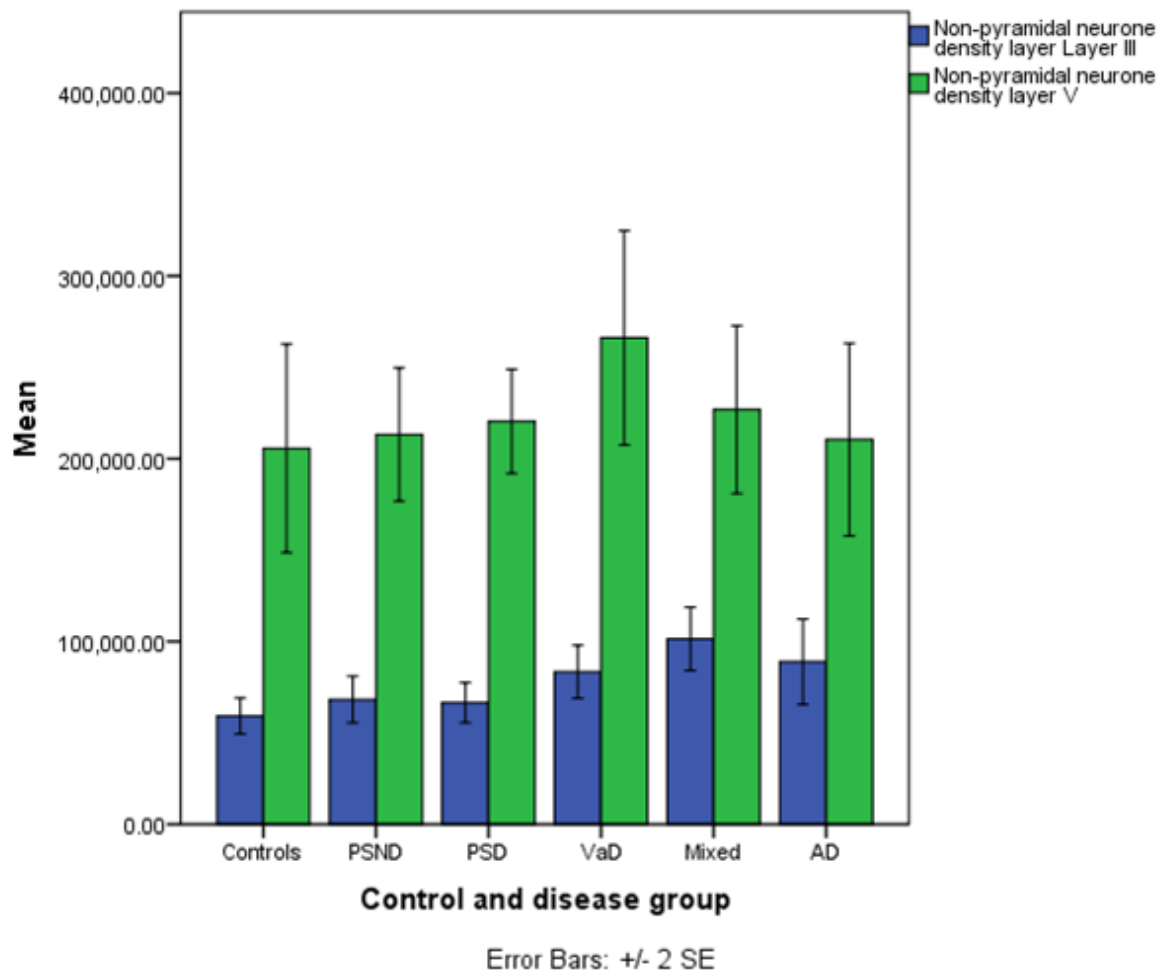
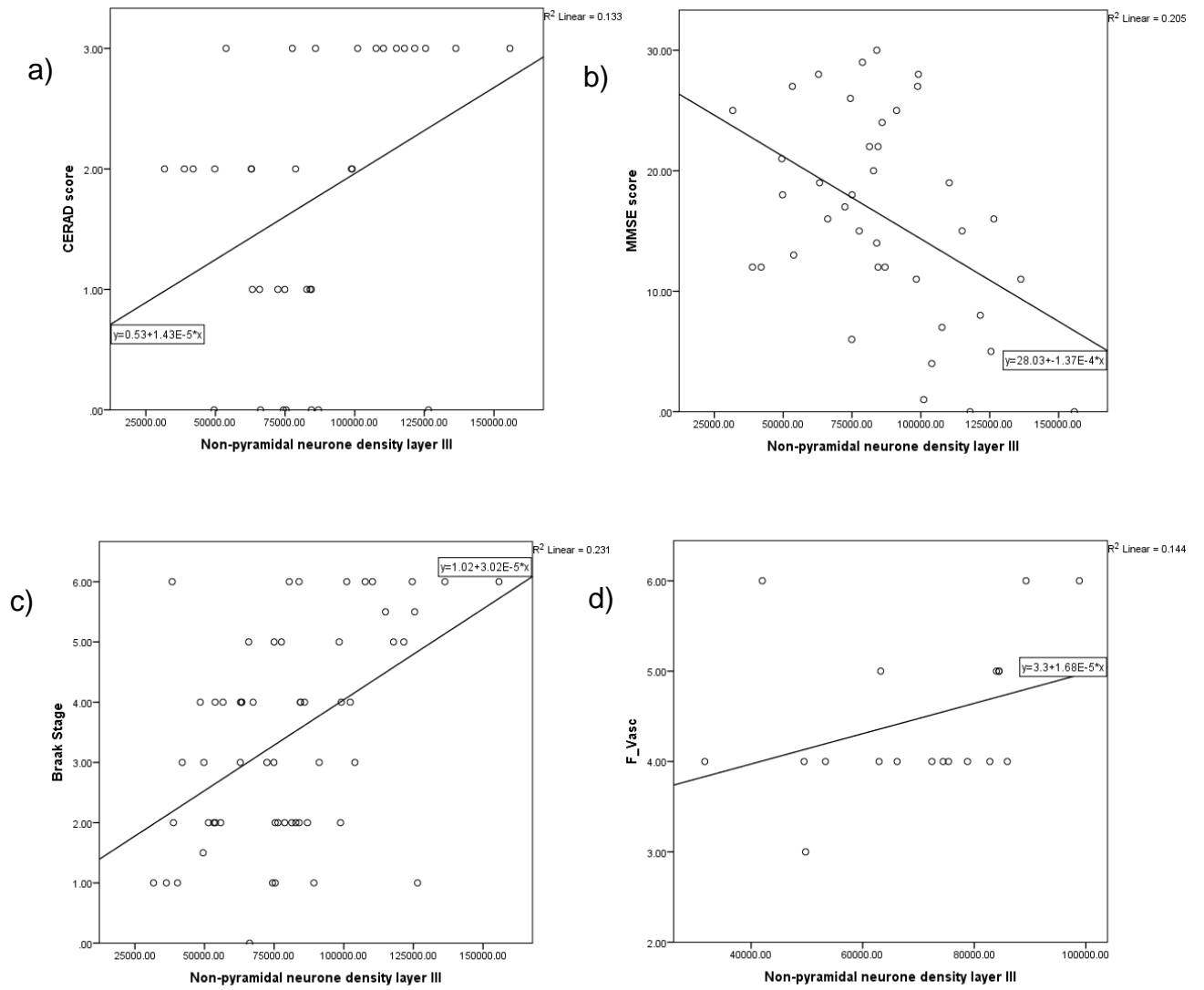


Figure 4-1 showing Nissl stained non-pyramidal neuron densities in control and disease groups in layers III and V of the dlPFC. Blue = Layer III. Green = layer V. Control = aged control, PSND = post-stroke no dementia, PSD = post-stroke dementia, VaD = vascular dementia, Mixed = mixed dementia, AD = Alzheimer's disease. Controls vs VaD ( $p = 0.017$ ), Mixed ( $p = 0.003$ ), AD ( $p = 0.017$ ). Mixed vs PSND ( $p = 0.016$ ), PSD ( $p = 0.009$ ).



**Figure 4-2 scatter graphs showing significant correlations between non-pyramidal neuronal densities in layers III and V and clinical and morphological variables. a)  $\sigma = 0.133$ ,  $p = 0.021$ , b)  $\sigma = -0.125$ ,  $p = 0.021$ , c)  $\sigma = 0.231$ ,  $p = 0.001$ , d)  $0.818$ ,  $p = 0.05$ .**

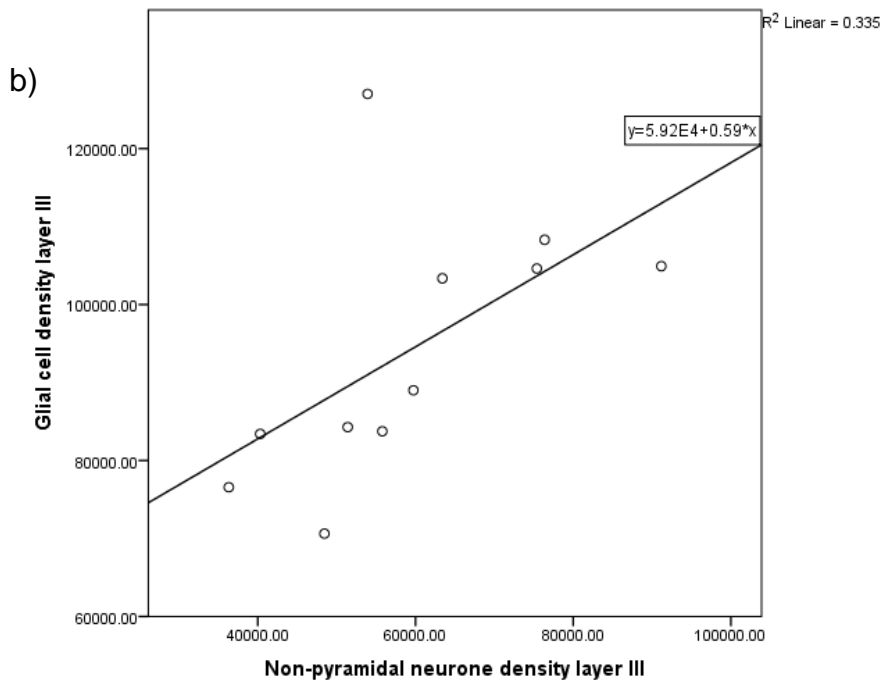
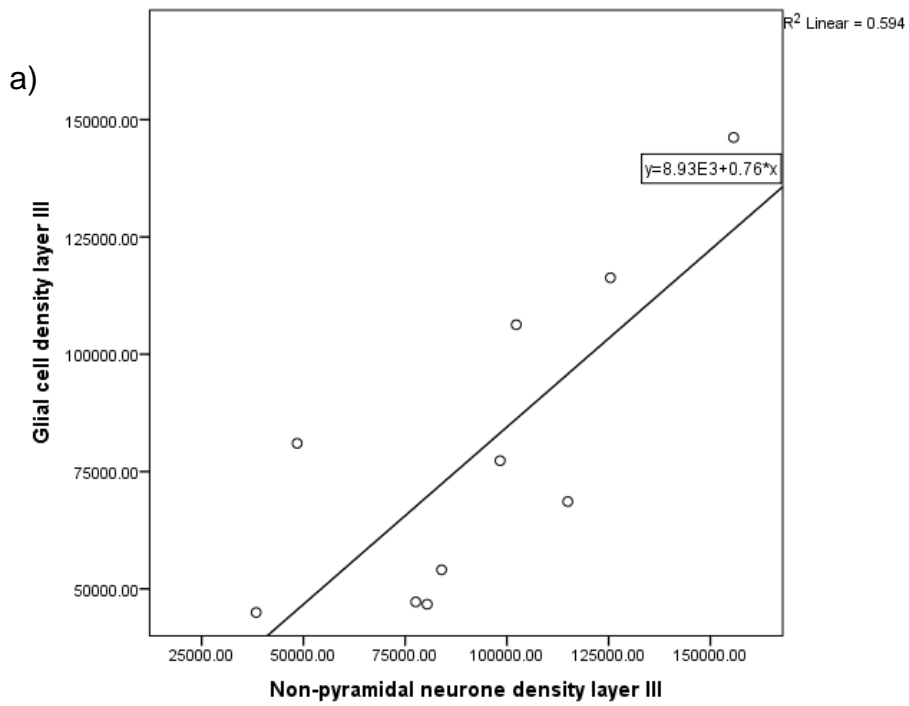
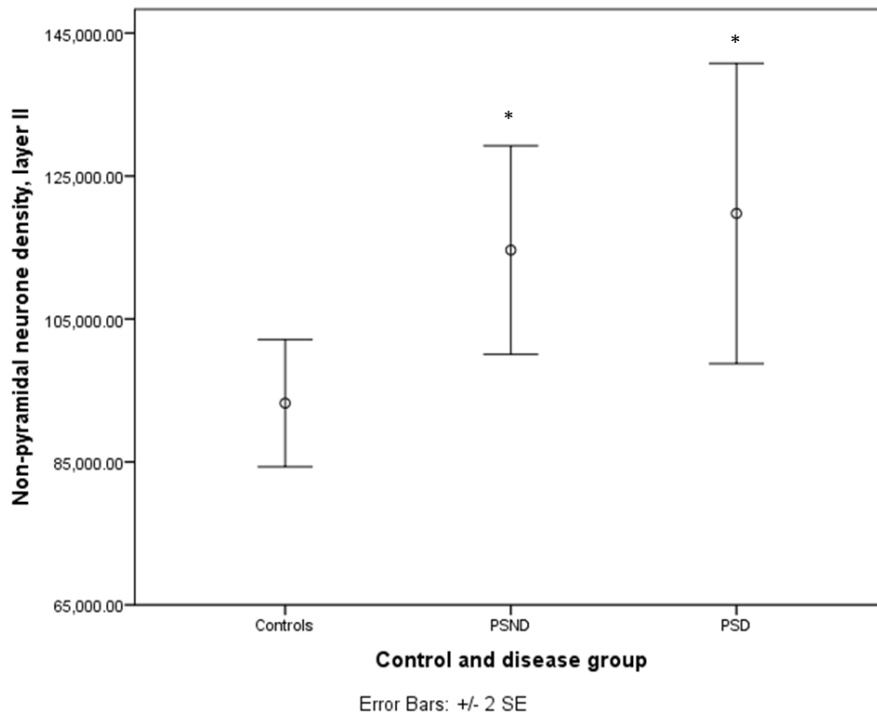


Figure 4-3 scatter graphs showing significant relationships between non-pyramidal neurons and glial cell density in layer III of the dIPFC in a) control ( $\sigma = 0.755$ ,  $p = 0.007$ ) and b) AD ( $\sigma = 0.758$ ,  $p = 0.011$ ) subjects.





**Figure 4-4** bar chart showing non-pyramidal neuron density in control, PSND, and PSD subjects in layer II of the dIPFC. Control = aged control, PSND = post-stroke no dementia, PSD = post-stroke dementia. \* = significance to controls. Controls vs PSND ( $p = 0.023$ ), PSD ( $p = 0.006$ ).

### 4.3.3. Immunohistochemical analysis of non-pyramidal neurons

#### 4.3.3.1. *Immunohistochemistry*

All antibodies showed specific staining to small cells with very little background. Parvalbumin stained section revealed the pale but very specific staining for interneurons, with few, if any, pyramidal neurons stained. In addition parvalbumin appeared to stain short lengths of dendritic process. Calbindin stained a higher proportion of neurons compared to the other two stains and was less selective, picking up pyramidal neurons as well as interneurons. Calretinin was selective for interneurons, similar to parvalbumin, calretinin appeared to stain few, if any pyramidal neurons (Figure 4-5).

#### 4.3.3.2. *Layer III*

In addition to the 3D stereological analysis of Nissl stained sections, 2D analysis was also performed to identify if there were specific changes in parvalbumin, calbindin, and calretinin positive neurons. On screen counts revealed mean total interneuronal counts in controls were; (per 10 images) 246 (parvalbumin), 276 (calbindin), 121 (calretinin).

There were no significant differences in interneuronal counts between the PSND and PSD in any stain ( $p > 0.05$ ). Total counts of parvalbumin stained interneurons showed reduced parvalbumin positive interneurons in neuronal layer III of mixed subjects when compared to control cases ( $p = 0.034$ ). There were no differences in calbindin positive cells, or calretinin positive cells between any of the groups ( $p > 0.05$ ) (Table 4-2).

#### 4.3.3.3. *Analysis of darkly stained neurons in layer III*

When darkly stained neurons were counted there were no differences between total darker stained neurons between PSND and PSD subjects ( $p > 0.05$ ). Total darkly stained neuronal counts in control groups were; 98 (parvalbumin), 53 (calretinin), and 102 (calbindin). There were no differences found between any other group in parvalbumin, calbindin, or calretinin positive cells ( $p > 0.05$ ).

When total darkly stained non-pyramidal neurons were expressed as a percentage of the total neuronal population counted there was no difference between PSND and PSD subjects. However, both PSND and VaD showed significantly lower levels of calbindin positive staining than control subjects ( $p = 0.014$ , and  $p = 0.022$  respectively) (Table 4-2, Figure 4-2).

#### 4.3.3.4. ***Layer III Correlations***

Total parvalbumin staining in layer III correlated with pyramidal neuronal volume changes in layer V ( $\sigma = 0.430$ ,  $p = 0.003$ ). In addition, frontal myelin staining loss, as measured by myelin index revealed significant correlation when compared to percentage of darkly stained PV neurons to non-stained neurons ( $\sigma = 0.376$ ,  $p = 0.011$ ). Analysis of calretinin positive section revealed a number of significant correlations.

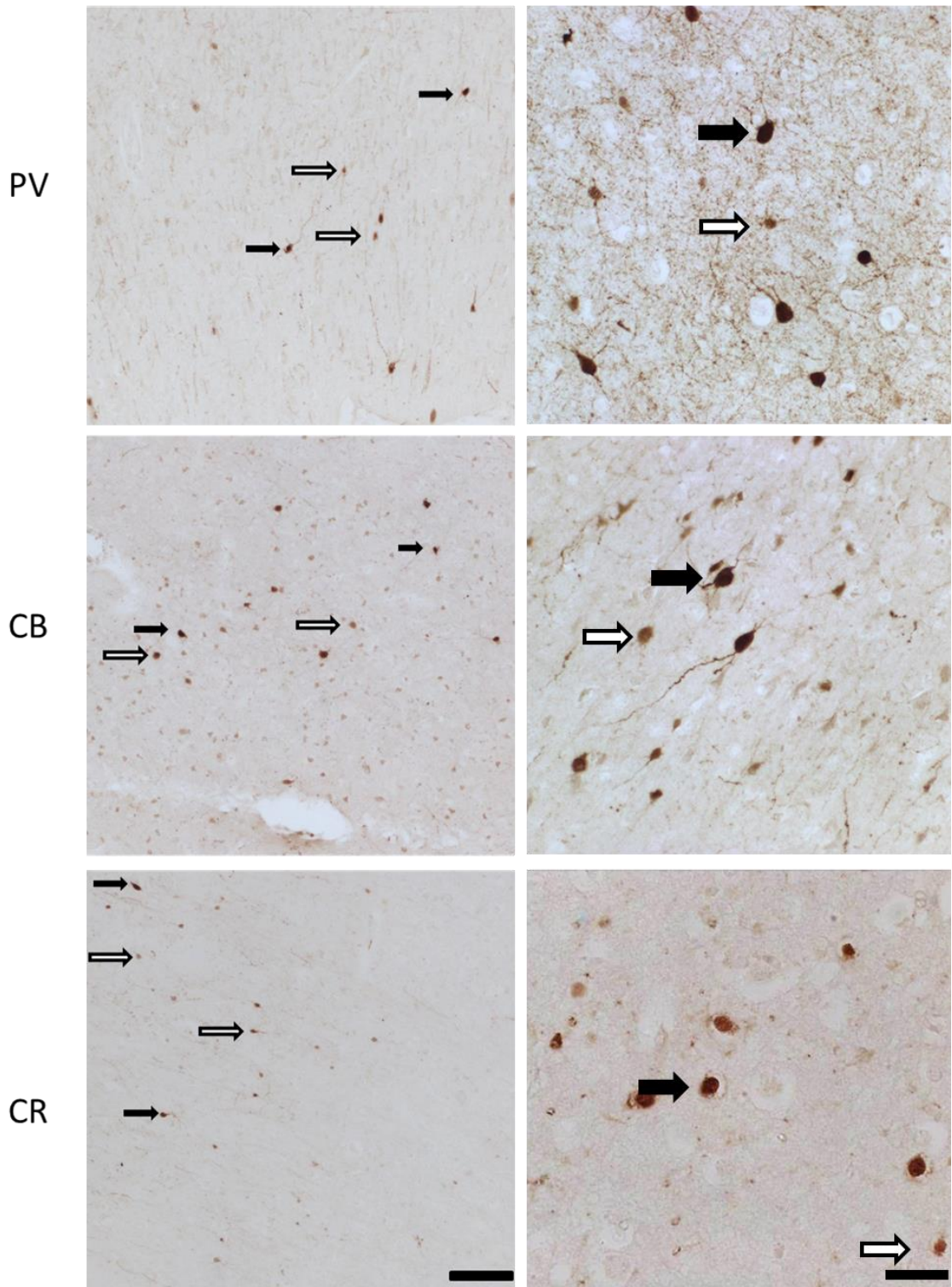


Figure 4-5 showing parvalbumin (PV), calbindin (CB), and calretinin (CR) positive neurons in layer V of the dIPFC. Solid black arrows = darkly stained neurons, hollow arrows = pale stained neurons. Left column taken at x10 magnification, right side column taken at x40 magnification. Left scale bar = 100μm. Right scale bar = 20μm

Interneuron counts (mean) layer III	Control (SEM)	PSND	PSD	VaD	Mixed	AD
Parv total	246 (19)	250 (31)	189 (22)	214 (27)	<b>186</b> <b>(22)</b>	216 (30)
Parv total dark	98 (9)	103 (21)	71 (12)	91 (10)	89 (17)	88 (17)
Parv % dark	40 (3)	39 (3)	36 (3)	44 (3)	47 (5)	39 (3)
CalB total	276 (46)	298 (59)	326 (56)	306 (55)	283 (31)	250 (70)
CalB total dark	103 (15)	84 (16)	96 (15)	93 (20)	87 (9)	88 (21)
CalB % dark	40 (5)	<b>30</b> <b>(2)</b>	32 (4)	<b>30</b> <b>(2)</b>	32 (3)	39 (4)
CalR total	122 (22)	136 (17)	96 (14)	127 (15)	101 (12)	127 (18)
CalR total dark	53 (14)	56 (11)	37 (8)	54 (8)	45 (9)	51 (13)
CalR % dark	40 (5)	41 (6)	35 (3)	42 (3)	43 (5)	40 (2)

**Table 4-2 showing mean total counts for immunohistochemical stained interneurons. Parv = parvalbumin, CalB = calbindin, CalR = calretinin. Control = aged-control, PSND = post-stroke no dementia, PSD = post-stroke dementia, VaD = vascular dementia, Mixed = mixed dementia, AD = Alzheimer's disease. Parv total: Controls vs mixed (p = 0.034). CalB % dark: controls vs PSND (p = 0.0144, and mixed (p = 0.022).**

#### 4.3.3.5. **Layer V**

Total mean counts of positively stained interneurons in controls were; (per area analysed) 225 (parvalbumin), 156 (calbindin), and 162 (calretinin).

Total counts of calretinin positive cells in layer V of the dIPFC revealed a significantly higher number of interneurons in PSND when compared to PSD ( $p = 0.049$ ). There were no significant differences between PSND and PSD subjects in either parvalbumin or calbindin positively stained interneurons (Figure 4-5)

Parvalbumin positive neurons in mixed dementia showed significantly lower mean counts than non-demented controls ( $p = 0.023$ ) and PSND subjects ( $p = 0.023$ ). In addition mixed dementia also showed significantly lower means when compared to subjects with AD ( $p = 0.049$ ). VaD sufferers also expressed higher total counts of calretinin positive cells when compared to PSD ( $p = 0.021$ ). Subjects with AD showed significantly lower total counts of calretinin positive neurons than both VaD and PSND groups ( $p = 0.049$ ) (Table 4-3).

#### 4.3.3.6. **Analysis of darkly stained neurons in layer V**

There were no significant differences between PSND or PSD when assessing total darkly stained neurons in any stain. PSND, VaD, and mixed dementia showed significantly higher total darker stained calretinin positive neuron counts when compared to aged matched controls ( $p = 0.049$ ,  $p = 0.006$ ,  $p = 0.049$  respectively). Subjects suffering VaD exhibited significantly higher darkly stained, calretinin positive neurons when compared to PSD subjects ( $p = 0.037$ ). The total counts for calbindin positive neurons revealed significantly lower total darkly stained neurons in VaD when compared to controls ( $p = 0.034$ ) and AD ( $p = 0.026$ ) (Table 4-3).

When expressed as a percentage of total cells counted, darkly stained calretinin positive non-pyramidal neurons were significantly higher in all demented groups when compared to controls ( $p = 0.023$ ,  $p = 0.019$ ,  $p = 0.002$ ,  $p = 0.013$ , and  $p = 0.010$  for PSND, PSD, VaD, Mixed, and AD respectively) (Table 4-3).

There were no significant differences in parvalbumin positive sections of either total darkly stained cell counts, or percentage darkly stained ( $p > 0.05$ ) (Table 4-3).

#### 4.3.3.7. *Layer V Correlations*

Spearman's rank coefficient revealed total non-pyramidal neuronal counts for calbindin positive cells in layer V correlated with neuronal volume in layer V of PSND, PSD, and VaD ( $\sigma = 0.456$ ,  $p = 0.018$ ,). The percentage of darkly stained neurons also correlated with neuronal volumes in subjects suffering mixed VaD and AD pathology ( $\sigma = 0.738$ ,  $p = 0.037$ ). When testing for disease groups total parvalbumin cell counts correlated with MMSE scores ( $\sigma = 0.406$ ,  $p = 0.017$ ), and calretinin correlated with MMSE scores in VaD subjects ( $\sigma = -0.900$ ,  $p = 0.037$ ) (Figure 4-6).

The percentage of darkly stained interneurons in post-stroke cases correlated with total neuronal counts in parvalbumin positive section, and PSND in calbindin stained sections.

Interneuron counts (mean) layer V	Control (SEM)	PSND	PSD	VaD	Mixed	AD
Parv total	<b>225</b> <b>(19)</b>	<b>259</b> <b>(38)</b>	205 (23)	189 (30)	<b>146</b> <b>(23)</b>	212 (26)
Parv total dark	54 (8)	71 (18)	52 (9)	54 (11)	38 (10)	45 (7)
Parv % dark	23 (3)	25 (3)	21 (3)	27 (3)	23 (4)	22 (3)
CalB total	156 (17)	117 (20)	129 (11)	126 (15)	127 (16)	162 (22)
CalB total dark	37 (5)	25 (5)	25 (3)	<b>25</b> <b>(6)</b>	27 (3)	34 (4)
CalB % dark	23 (2)	19 (3)	<b>18</b> <b>(1)</b>	<b>18</b> <b>(2)</b>	22 (1)	21 (2)
CalR total	162 (13)	170 (7)	<b>140</b> <b>(14)</b>	197 (15)	149 (13)	<b>140</b> <b>(17)</b>
CalR total dark	25 (7)	<b>46</b> <b>(6)</b>	42 (8)	<b>67</b> <b>(11)</b>	<b>45</b> <b>(8)</b>	41 (7)
CalR % dark	16 (3)	<b>27</b> <b>(3)</b>	<b>29</b> <b>(4)</b>	<b>33</b> <b>(4)</b>	<b>30</b> <b>(4)</b>	<b>28</b> <b>(3)</b>

Table 4-3 showing mean total counts for immunohistochemical stained interneurons in layer V of the dIPFC. Parv = parvalbumin, CalB = calbindin, CalR = calretinin. Control = aged control, PSND = post-stroke no dementia, PSD = post-stroke dementia, VaD = vascular dementia, Mixed = mixed dementia, AD = Alzheimer's disease. Bold + red = significant to controls. Bold + blue = significant to mixed. Bold + green = significant to PSND. CalR total: PSND vs PSD ( $p = 0.049$ ). Parv total: mixed vs control ( $p = 0.023$ ), PSND ( $p = 0.023$ ), AD ( $p = 0.049$ ). CalR total: PSD vs VaD ( $p = 0.021$ ), AD vs VaD ( $p = 0.010$ ), PSND ( $p = 0.049$ ). CalR dark: controls vs PSND ( $p = 0.049$ ), VaD (0.006), mixed ( $p = 0.049$ ). PSD vs VaD ( $p = 0.037$ ). CalB dark: VaD vs controls ( $p = 0.034$ ), AD ( $p = 0.026$ ).



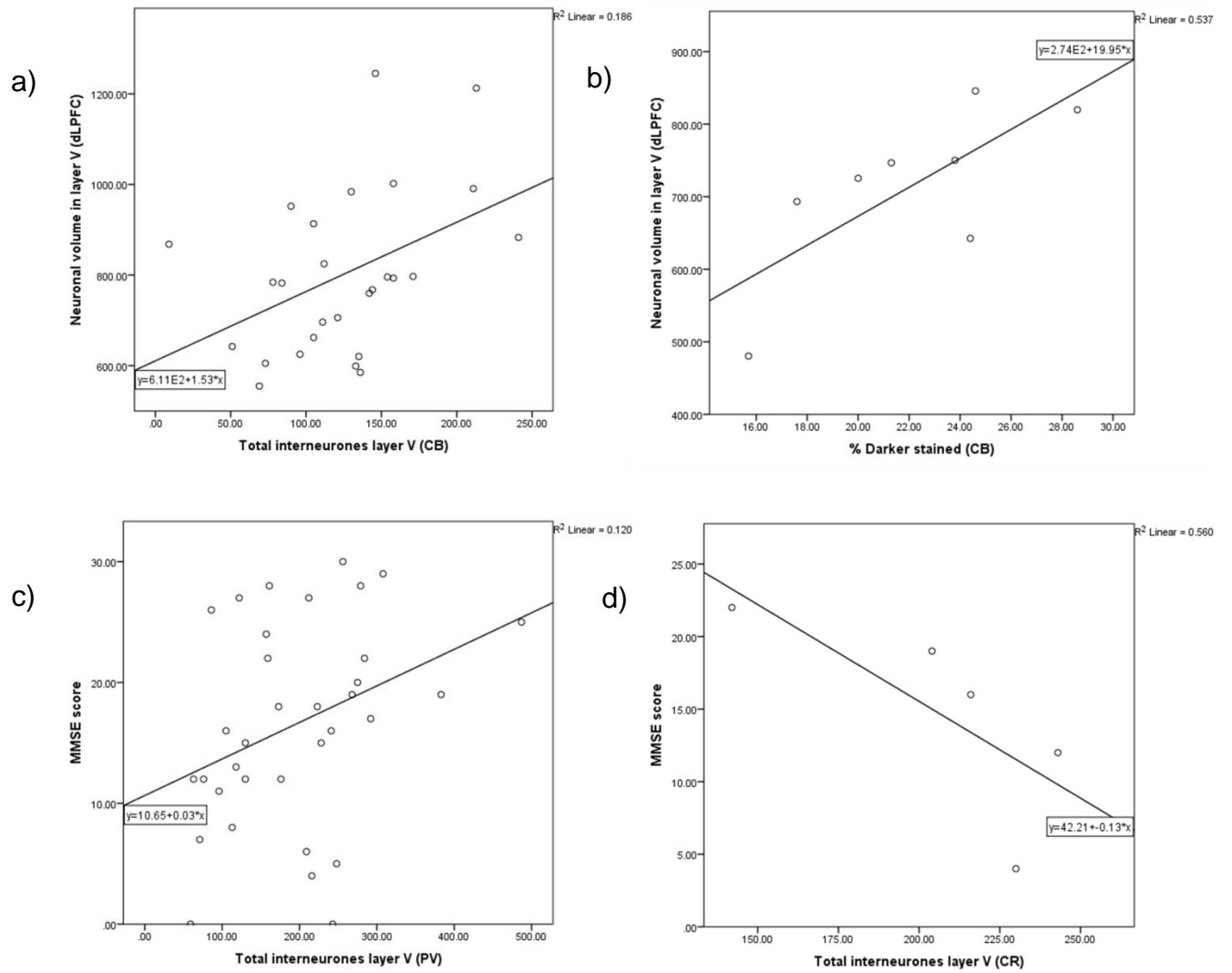


**Figure 4-6** scatter graphs showing significant correlations between non-pyramidal neuronal density in layer V and clinical variables. PV = parvalbumin, CB = calbindin, CR = calretinin. a)  $\sigma = 0.456$ ,  $p = 0.018$ , b)  $\sigma = 0.738$ ,  $p = 0.037$ , c)  $\sigma = 0.406$ ,  $p = 0.017$ , d)  $\sigma = 0.900$ ,  $p = 0.037$ .

#### 4.3.4. **Three dimensional stereological analysis of glial cell density.**

##### 4.3.4.1. **Layer III**

Three dimensional stereological analysis revealed no significant differences between PSND subjects and PSD subjects when assessing glial cell densities. When analysing post-stroke demented groups alone, glial cell density correlated with pyramidal neuronal volume in layer V ( $\sigma = 0.609$ ,  $p = 0.047$ ). Further analysis revealed significantly lower glial cell densities in VaD when compared to controls ( $p = 0.002$ ), PSND ( $p = 0.003$ ), PSD ( $p = 0.001$ ), and mixed ( $p = 0.05$ ). VaD subjects revealed a correlation between glial cell density and non-pyramidal density ( $\sigma = 0.594$ ,  $p = 0.011$ ), and glial cell density and MMSE score ( $\sigma = 0.960$ ,  $p = 0.015$ ) (Figure 4-7).

##### 4.3.4.2. **Layer V**

Similar to layer III, no significant difference was found between PSND and PSD subjects. There was no significant difference revealed in glial cell density between any group in layer V ( $p > 0.05$ ). However, glial cell density did correlate with pyramidal neuronal volumes in PSD in layer V ( $\sigma = 0.764$ ,  $p = 0.006$ ) (Figure 4-8). Additionally, glial cell density in layer V correlated with glial density in layer III. ( $\sigma = 0.535$ ,  $p = 0.001$ ) (Figure 4-7).

##### 4.3.4.3. **Layer II**

There was no significant difference between PSND or PSD in layer II of the dIPFC, or between PS subjects and aged matched controls ( $p > 0.05$ ) (Figure 4-9).

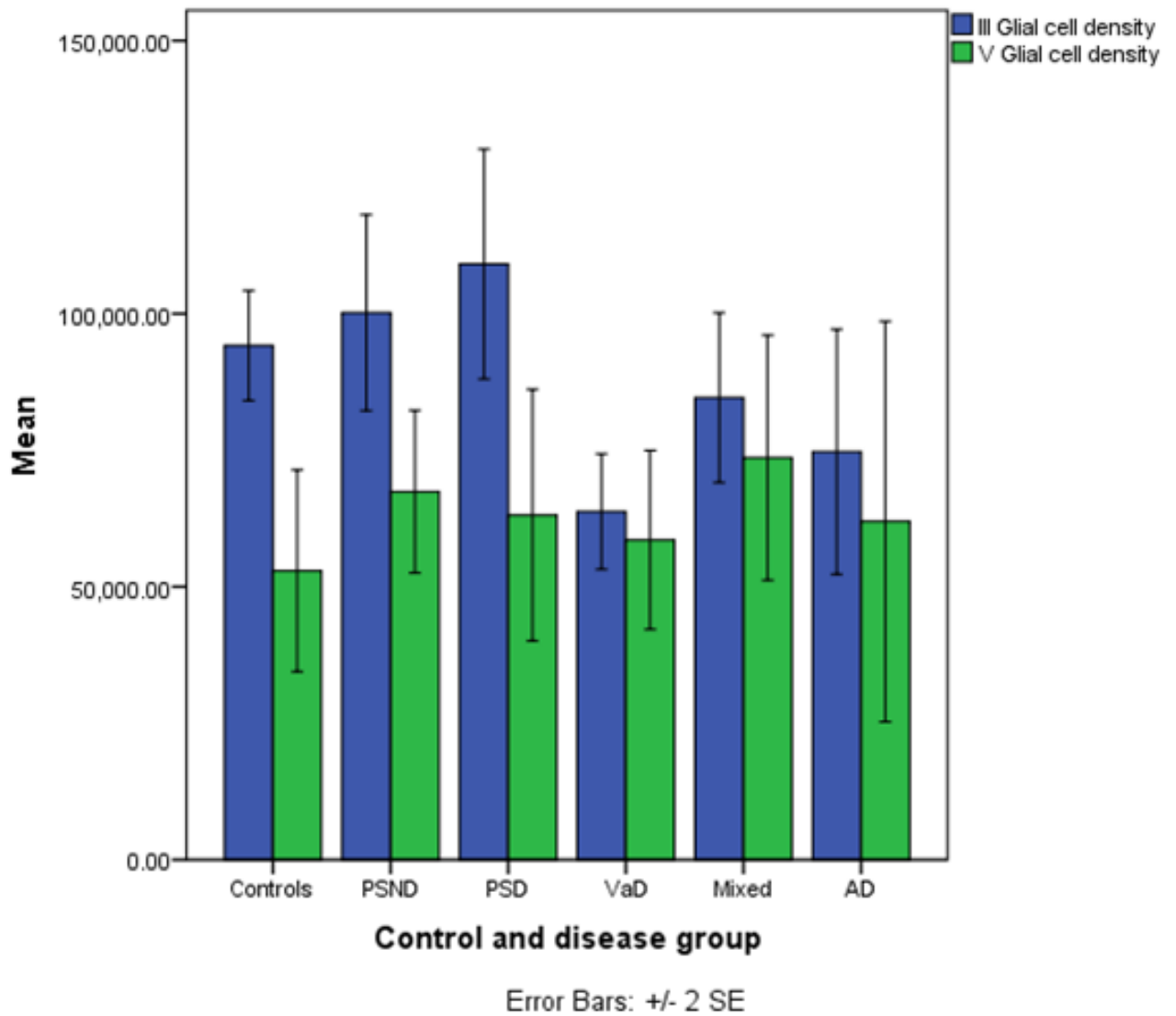


Figure 4-7 showing non-pyramidal neuron densities in control and disease groups in layers III (blue) and V (green) of the dIPFC. Control = aged control, PSND = post-stroke no dementia, PSD = post-stroke dementia, VaD = vascular dementia, Mixed = mixed dementia, AD = Alzheimer's disease. VaD vs controls ( $p = 0.002$ ), PSND ( $p = 0.003$ ), PSD ( $p = 0.001$ ), (mixed  $p = 0.05$ ) in layer III.

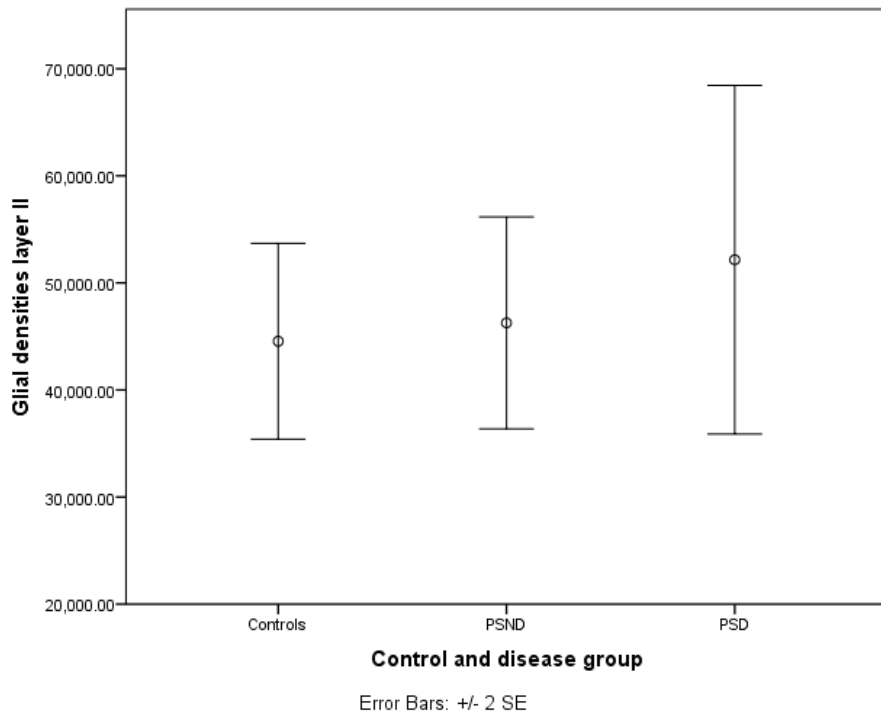


Figure 4-9 showing non-pyramidal neuron densities in control and disease groups in layer II of the dIPFC. Control = aged control, PSND = post-stroke no dementia, PSD = post-stroke dementia. No significant differences between groups ( $p < 0.05$ ).

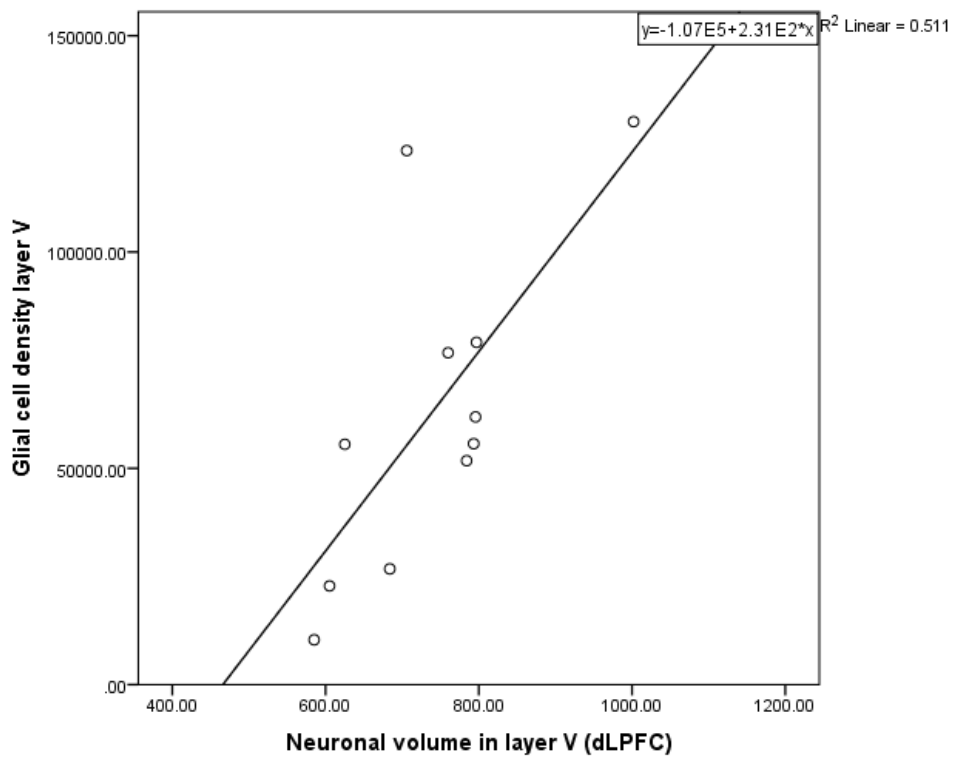


Figure 4-8 showing the correlation between pyramidal neuron volumes and glial cell densities in layer V ( $\sigma = 609$ ,  $p = 0.047$ ).

#### 4.4. Discussion

##### 4.4.1. 3D stereological analysis of non-pyramidal neuron density in the dIPFC

Non-pyramidal neuronal density in the dIPFC was assessed to establish if general atrophy of the neocortex explained the differences between PSD and PSND subjects or whether previous findings in dIPFC were specific to pyramidal neurons. Non-pyramidal neuron density were found to be higher in layer III in these subjects when compared to controls in a depression study (over 50,000 per mm<sup>3</sup> compared to under 20,000 per mm<sup>3</sup>), however findings in layer V were more comparable (Around 20,000 mm<sup>3</sup>) (Khundakar et al. 2009). There were no significant differences apparent in non-pyramidal density between PSD and PSND in either layers III or V. This finding suggests interneuronal number changes are not a key factor in the development of PSD, or explain the primary morphological differences between PSND and PSD. Additional analysis was performed in layer II of the dIPFC to assess the behavior of interneurons in a layer where pyramidal neuronal atrophy may not have such an impact. There were no significant differences between the two PS groups. However, both PS groups showed significantly increased neuronal density when compared to controls. This was unexpected as little or no cortical atrophy was found in the dIPFC. However, it does suggest that layer II of the dIPFC may be affected in stroke patients, though it does not appear to have an impact on cognitive outcome in these subjects.

When assessing other disease groups, 3D stereological analysis revealed significantly increased non-pyramidal neuron density in VaD, mixed, and AD subjects when compared to post-stroke survivors and age-matched controls in layer III ( $p < 0.05$ ) (Figure 4-1). This increased density of neurons is unlikely to be the result of an increased neuronal population. One possibility being that this density increase was the result of post-mortem fixation shrinking the tissue, and thus compacting the neurons tighter together, increasing neuronal density. This theory however, was dismissed as post-mortem processing artifact would have most likely affected all groups equally, not just those diagnosed with vascular and neurodegenerative dementias. An alternative theory, based around cortical

atrophy was proposed. Loss of tissue and thinning of the cortical ribbon would potentially result in an artificial increase in neuronal density. As the cortical ribbon decreases in thickness, the spacing between neurons becomes less abundant. This would result in a higher number of neurons being counted in a particular sampling area and thus artificially giving the impression of a higher neuronal number. This would explain why no density changes were recorded in PSND and PSD as it was previously shown that these cases do not suffer cortical atrophy in the dIPFC (Cortical thickness and dIPFC atrophy), and whilst VaD, mixed, and AD did not show signs of cortical thinning, it was impossible to assess the cortical atrophy in these subjects leaving atrophy as a potential cause for neuronal density change.

#### 4.4.1.1. *3D stereological analysis of Glial cell densities*

There were no significant differences in glial cell density between PSND and PSD subjects. There was a large difference in glial cell densities between layer III and V (means of ~ 100,000 mm<sup>3</sup> and ~ 50,000 mm<sup>3</sup> respectively) in controls. Counts in layer III were comparably high when compared to measurements of controls taken from a depression study (mean of ~ 65,000 mm<sup>3</sup>), with layer V measurement more in agreement (mean ~ 65,000 mm<sup>3</sup>) (Khundakar et al. 2009). The lack of difference between groups in this study was surprising as it has previously been shown that following a stroke these cells proliferate and may become hypertrophic in response to the insult (van Rossum and Hanisch 2004). However, bivariate analysis did reveal that glial cell densities significantly correlated with pyramidal neuron volumes in layer V, which suggests a relationship between glial cells and neurons, perhaps reinforcing the importance of the neurovascular unit in maintaining cognition (Hawkins and Davis 2005).

VaD showed significantly reduced glial cell density when compared to controls, PSND, and PSD in layer III but not in layer V, with no difference identified when compared to mixed dementia or AD groups. Glial cell decreases in VaD were not unexpected, as glial cells are damaged as a result of compromised oxygen metabolism once the vasculature is damaged (Roman et al. 2002). However, this reasoning would follow that both PSD and mixed demented subjects would follow the same pattern, which did not occur.

Glial cell densities correlated with non-pyramidal neuron densities in both control groups and AD subjects (changes in the AD subjects also correlated with both CERAD and Braak staging, suggesting a link with AD pathology), but not in VaD, or mixed subjects. The differential absence of this correlation in the vascular groups suggests differential pathological effects on different cell populations in different disease states. Indeed, this relationship between glial cell densities and interneuronal densities was expected in aged-control subjects, where no apparent changes in glial or neuronal densities were present. In AD subjects this significant correlation between glial cell and neuronal densities suggests a similar rate of density change between the two, which may be the result of cortical atrophy.

The lack of correlation between glial and neuronal densities in mixed and VaD suggest perhaps a different pathological cause than atrophy, in which damage to the vasculature may result in decreases in neuronal density in one layer at a higher rate than the other. However, in all three groups; VaD, mixed, and AD, no changes were found in pyramidal neuronal density, which would be expected if there was a global tissue alteration affecting interneurons (Harding et al. 1994).

Pyramidal neuron soma volume has been linked to the extent of a cells dendritic arbour, with larger cells commanding more processes and smaller neurons with decidedly less (Hayes and Lewis 1993; Glantz and Lewis 2000). A theory has therefore been put forward that this potential dendritic loss created additional space – gaps within the tissue with which other non-pyramidal neurons could move into, thus becoming more compact and increasing neuronal density as assessed using 3D stereology. Further investigation into neuronal dendritic arbour is needed to confirm or disprove this theory. Interestingly, this relationship between interneuron densities between the disease groups was not repeated in layer V of the dIPFC, where no significant differences in neuronal density were reported between any group ( $p > 0.05$ ). If the changes observed in layer III were a result of cortical tissue change or a result of reduced neuronal arbour, then neuronal density changes would have been expected in both layers. These findings suggest that whatever pathological substrates may be at play, they appear to be either specific to layer III, or may affect each area differently. Interestingly, when excluding AD and

mixed cases from analysis, changes in layer III significantly correlated with frontal vascular scores. Perhaps vascular pathology has a greater effect on the dendritic arbour of cells in layer III than layer V. The additional analysis of non-pyramidal layer II revealed some interesting findings with both PSND and PSD cases showing significantly higher neuronal densities when compared to controls, but no differences between each other. This finding is not consistent with either layer III or V and suggests perhaps another mechanism is at play in layer II.

#### **4.4.2. Immunohistological analysis of interneurons in the dIPFC.**

##### **4.4.2.1. Total interneuron counts**

One restriction of 3D stereological analysis of Nissl stained section is the inability to distinguish between different sub-populations of interneuronal types from each other. As previously discussed (See Interneurons and the inhibition circuits) there are several distinct sub-populations of interneurons, each with its own role within the inhibitory system of the dIPFC. Using 2D analysis to assess IHC stains for three different calcium binding proteins (calretinin, calbindin, parvalbumin), it was possible to analyse a wider range of interneuronal sub-groups.

##### **4.4.2.2. Total interneurons and post-stroke dementia**

Analysis of layer III revealed no significant difference in parvalbumin, calretinin, or calbindin-positive cell counts between either PSND or PSD. This finding suggests there is little or no impact of any sub-type of interneurons in the development of PSD. The lack of correlation between interneuronal total counts and pyramidal volume also suggests a minimum pathological relationship between the two cell types. However, the total calretinin-positive cell count was lower in PSD subjects when compared to PSND in layer V. Calretinin positive cell loss has been reported in the hippocampus of those suffering AD (Takahashi et al. 2010) and is thought to impact the progression of the disease. It is possible that decreased numbers of interneurons in layer V of the dIPFC may contribute to the progression of PSD.

##### **4.4.2.3. Interneurons and other disease groups**

Two dimensional analysis of parvalbumin positive interneurons revealed significantly fewer interneurons in mixed dementia subjects when compared to



age matched controls in both layer III and V, and PSND in layer V. Any reduction in numbers may result in a distinct over excitation of local pyramidal neurons and thus dysfunction to the local circuit (Conde et al. 1994; Daviss and Lewis 1995). This change was only observed in subjects suffering from mixed VaD/AD pathology. The lack of apparent change in other disease subjects suggest that it is the additive effect of both AD type pathology and CVD which results in reduction on parvalbumin interneurons. In parvalbumin positive interneurons in layer V of mixed dementia, there were significantly fewer parvalbumin positive cells than in AD. These data suggest the mixed pathology with both AD pathology and vascular disease affecting the interneuronal population. Total cell counts of parvalbumin positive interneurons in layer V correlated with layer V pyramidal neuronal volumes, suggesting a link between the number of parvalbumin positive interneurons and potential pyramidal neuron dysfunction in the dlPFC.

Those with AD showed significantly fewer positively stained interneurons than either VaD or PSND suggesting calretinin positive interneurons are more sensitive to neurodegenerative pathology than CVD.

#### 4.4.2.4. *Analysis of darker stained neurons in layers III and V of the dlPFC.*

Total counts of parvalbumin, calretinin, and calbindin positive interneurons revealed a specific subpopulation of very darkly stained interneurons. These cells appeared with varying frequency throughout the analysis, dependent of the case studied. It was theorised that these neurons may be a pathological substrate which may distinguish between PSND and PSD disease groups (See Darkly stained interneurons).

Neither total number of darkly stained interneurons nor the percentage total of darkly stained neurons vs. total interneurons numbers showed any significant differences between PSND and PSD subjects. These findings do not appear to support the theory that the darkly stained neurons are associated with declining cognitive ability in PSD cases.

Analysis of layer III revealed significantly lower percentage of calbindin positive cells were darkly stained in both VaD and PSND subjects when compared to

controls cases. This lower percentage of potentially diseased interneurons in VaD was interesting, as it appears that subjects with higher vascular pathology do not appear to exhibit interneuronal damage.

#### **4.5. Conclusions**

Three dimensional stereological data suggested decreased interneuronal densities in layers III and V of the dlPFC do not distinguish between the PSND and PSD subjects. However, changes in non-pyramidal density appear associated with VaD, mixed, and AD dementia. Interneuronal density does not appear to a predictor for the development of dementia in subjects who have suffered a stroke. The immunohistochemical results support the suggestion that interneuron and glial cell numbers have little impact on the progression of cognitive dysfunction after stroke. However, the relationship between glial cell density and pyramidal neuronal volumes suggests a potential mechanistic relationship between neuronal dysfunction and glial cell numbers. Additionally, darkly stained interneurons appear to have no influence on the cognitive outcome in PS subjects suggesting that this is not a specific marker of neuronal damage.

## **Chapter 5. White matter changes in the frontal lobe in post-stroke dementia.**

### **5.1. Introduction**

The decreased pyramidal neuron volumes in post-stroke demented and other demented subjects appeared to associate neuronal atrophy with specific features of executive function in PSD and other dementia subjects. These data demonstrate some involvement of the specific regions of the cortical grey matter in the development of PSD. However, it is not clear if these findings are linked to any potential pathology in the frontal underlying WM in these subjects. WM changes detected as white matter hyperintensities (WMH) on T2 weighted MRI are a common finding in CVD (DeCarli et al. 1995; O'Brien et al. 2002). Burton et al (E. J. Burton et al. 2004) reported significantly greater volumes of WMH in subjects after stroke, correlating with attention deficits. WMH have also been associated with decreased cognitive processing speed (E. J. Burton et al. 2004). Processing speed pertains to the ability to perform tasks quickly and under pressure. It may be a basic component of information processing, in those with CVD, suggesting a direct link between apparent WM damage and cognition (E. J. Burton et al. 2004). This is perhaps not surprising as WMH are thought to indicate damage, or at least disruption of the myelin or axonal tracts which connect the prefrontal circuits. However, WMH in the frontal lobe may be more significant in the current study, with executive dysfunction correlating with WMH in those suffering VaD (Cohen et al. 2002). This highlights the importance of the prefrontal circuits in executive function, and their relative vulnerability to ischaemic damage.

#### **5.1.1. Myelin and axons in post-stroke and other dementias.**

Mechanistically, loss of myelination leads to the slowing of action potentials between neurons (See Glial cells and white matter), ultimately affecting cognitive function. Though this is a logical inference, it is unclear how myelin loss relates, interacts, and influences axonal damage, and indeed how much axonal damage impacts dementia (Ferguson et al. 1997). By comparing

markers for both myelin and axonal damage it may be possible for elucidate the relationship between the two pathologies (Ferguson et al. 1997). Axon damage has been implicated in other disease processes such as multiple sclerosis (MS) following myelin damage and loss (Ferguson et al. 1997). The role of axonal damage in the development of dementia is not certain though mouse studies have found impaired axonal transport in frontotemporal dementia (Ittner et al. 2008). Axonal dysfunction has also been implicated in AD, with the build-up of hyperphosphorylated tau impairing axonal transport as demonstrated in mouse models expressing mutant forms of APP, Presenilin-1 and in tau proteins, resulting in axonal dysfunction (Gallagher et al. 2012). Potential markers for axonal damage such as APP and SMI32 can shed light on the underlying state of axons (Werner et al. 2001). APP is transported via axons, with the accumulation of the protein indicating a dysfunction in the axon's ability to transport constituents which may build in the tracts. SMI32 is a marker for non-phosphorylated neurofilaments, indicating axonal damage (Budde et al. 2008). Ferguson et al reported increases in APP as a marker of axonal damage in acute inflammation of patients suffering multiple sclerosis (Ferguson et al. 1997). Previously, conventional stains such as luxol fast blue (LFB), used to assess myelinated axons, have been used to indicate myelin loss, as a marker of WM damage in post-mortem analysis (Smallwood et al. 2012; Deramecourt et al. 2012; Ihara et al. 2010). Loss of or weaker LFB staining in these cases is interpreted as myelin loss and thus WM damage. Ihara et al also found an inverse correlation between degraded basic myelin protein (dBMP) and myelin index, reinforcing the link between LFB loss and myelin damage (Ihara et al. 2010).

#### **5.1.2. Retrograde vs. anterograde neurodegeneration.**

Though WM degeneration appears to play a major role in dementia and other cognitive disorders (Medana and Esiri 2003), it remains unclear how influential it may be in the development of post-stroke dementia. It is unknown which event precedes the other: neuronal dysfunction, or white matter loss, and to the degree with which one may influence the other. Strong evidence suggests pyramidal neuronal volumes are reduced across several disease states (Khundakar et al. 2009; Gemmell et al. 2012), and indeed, WMH have been

reported in PSD subjects (E. Burton et al. 2003). However, pyramidal neuronal volume changes in PSD and other disease cases are the result of anterograde or retrograde degeneration. From MRI or post-mortem studies, it is not possible to distinguish between cause and effect, but the degree to which neuronal damage may affect WM pathology (and vice versa), still remains a very important question.

- Wallerian, or anterograde, degeneration occurs when damage originating in neurons residing in the grey matter results in degeneration of the WM. As a neuron loses function as a result of either neurodegeneration or ischaemic injury. This loss of function is eventually passed down the axonal tract, resulting in further dysfunction. This effect may be delayed, but results in disconnection of the distal end of the axon and will appear pathologically as lesions in the WM (Mack et al. 2001; Cook and Wisniewski 1973).
- Retrograde degeneration, conversely, refers to the dying back of the cells from the axon, either due to demyelinating diseases or ischemic damage affecting the axon directly. This deafferentation results in a disruption in communication between the neuron and its target resulting in a loss of tropic support. In retrograde degeneration damage to the WM in disease's such as VaD may result in delayed transmission to connecting neurons (Cook and Wisniewski 1973; V. H. Perry et al. 1991; Mack et al. 2001).

### 5.1.3. **Vascular pathology and frontal white matter.**

Previous studies have reported high WM vascular pathology associated with cognitive dysfunction (Fernando et al. 2006; Yamamoto et al. 2009; Esiri et al. 1997). Damage to the vasculature may lead to a chronic hypoxic state. Craggs et al reported increased sclerotic index in the WM of SVD subjects, indicating increased atherosclerosis, when compared to controls (Craggs et al. 2013). This increased vulnerability of the WM in those suffering CVD suggests a potential mechanism by which the observed pyramidal neuronal volume changes are, in CVD cases as least, a result of WM damage and thus due to retrograde degeneration. Additionally, several neuroimaging studies have linked WMH with cognitive dysfunction (E. Burton et al. 2003; E. J. Burton et al. 2004; Firbank et al. 2012; K. R. Burton et al. 2014). Oligodendrocytes have been shown to be recruited in areas of WM pathology (Franklin et al. 1997) with

increased immunoreactivity in response to WM lesions (Simpson et al. 2007) most likely as response to demyelination, suggesting that this process is key in WM pathology.

The potential effect of damage to the prefrontal cortex, and its impact on the cognitive and executive function has already been outlined in previous chapters (The prefrontal cortex). This study focused on the WM underlying the PFC including myelinated axons which make up and form the major connections between the different regions of the brain. Though several studies have looked into WM pathology in PS subjects through imaging techniques, few pathological studies have attempted to assess the impact of WM pathology on neurons in PS sufferers.

It was hypothesised that differential changes in the WM may explain the neuronal volume loss in PSD compared to PSND subjects with implications for neurodegenerative disorders such as in AD and mixed dementia. The relative lack of vascular pathology in AD cases would suggest that any potential WM and/or axonal pathology would not be the result of direct CVD factors, but potentially anterograde damage originating in axons. Immunohistochemistry (IHC) and tinctorial staining methods were used to evaluate WM changes. LFB stained sections were analysed to assess the integrity of myelin in the dIPFC of post-stroke survivors and other ageing-related dementias. In addition, serial sections were stained for markers of axonal damage.

## 5.2. Methods

### 5.2.1. Details of subjects used in this study

	No of cases (SEM)	Age	PMD	FT	Frontal vascular score	Braak	CERAD
Control	10	86.5 (11)	32.3 (19)	2.9 (1)	n/a	2 (0)	n/a
PSND	10	83 (3)	42.3 (19)	3.8 (6)	4.5 (0.3)	2.3 (0.4)	1.6 (0.3)
PSD	10	87.8 (6)	36.5 (23)	2 (1)	4.4 (0.3)	2.8 (0.4)	1.3 (0.3)
VaD	10	85.5 (8)	52.1 (22)	2.7 (1)	5.5 (0.5)	2.4 (0.4)	1 (0.5)
Mixed	10	84 (8)	33.4 (19)	5.3 (9)	4 (1)	5.3 (0.3)	2.7 (0.3)
AD	10	83.5 (5)	36.8 (24)	1.5 (1)	1 (1)	5.5 (0.3)	3 (0)

**Table 5-1 Subject details. Controls = aged matched controls, PSND = post-stroke no dementia, PSD = post-stroke dementia, VaD = vascular dementia, mixed = mixed vascular and Alzheimer's disease, AD = Alzheimer's disease. FT = fixation time, PMD = post-mortem delay.**

### 5.2.2. IHC and image analysis

Immunohistochemistry was performed for SMI31, SMI32 (Convance, USA), and GRP78 (Abcam, UK) on 10µm frontal sections as described previously (Immunohistochemistry (IHC)). GRP78 was selected as an appropriate marker to stain oligodendrocytes within the WM. 2D Image analysis was performed using Image Pro as described previously, to assess both per area of staining (p/a), and the mean optical density (intensity of staining, IOD). Images were taken at 10x magnification with numerical aperture 0.3. Ten evenly distributed images were taken throughout the WM with care to avoid including any U-fibres which are unaffected in these disease states.

### 5.2.3. Myelin index assessment

Ten µm thick frontal sections from Newcastle Brain Map layers 4-8, containing the dlPFC (Brodmann area 9) were stained with LFB as described previously (See Myelin index). Myelin index was then calculated as described previously (methods section, (Yamamoto et al. 2009)) from low power stained images of the entire frontal section, with WM delineated from GM for analysis.

#### 5.2.3.1. *Undamaged myelin assessment*

Due to some degree of pathology in all groups it was deemed necessary to take specifically selected areas of undamaged myelin to use as an additional control group to assess the relative levels of pathology in each group. This is consistent with evaluating normal appearing WM from the same cases which also exhibit damaged WM (Simpson et al. 2007).



## 5.3. Results

### 5.3.1. Myelin Index

There was no significant difference in the myelin index in the frontal lobe WM between PSND and PSD subjects ( $p=0.514$ ), or combined post-stroke cases vs. controls ( $p = 0.103$ ). (Figure 5-1). Analysis showed VaD to have significantly higher myelin loss (i.e. an increased myelin index) when compared controls ( $p = 0.034$ ). VaD showed higher myelin loss when compared to PSND ( $p = 0.072$ ) though this did not reach significance. All demented cases showed comparable level of myelin loss with no significant differences found between PSD, VaD, mixed, or AD subjects.

#### 5.3.1.1. *Undamaged myelin*

Some control subjects exhibited a surprisingly high degree of WM abnormality, possibly attributed to older age, which may explain why only VaD exhibited significantly different pathology. In order to compare myelin loss in demented groups to undamaged age matched normal control with minimal WM pathology, analysis was performed on specific undamaged areas of myelin to ascertain a suitable baseline with which to compare myelin loss to other disease groups. There was no significant difference between post-stroke survivors, or between post-stroke survivors and age matched controls, or between aged matched controls and undamaged myelin ( $p > 0.05$ ). However PSD did show significantly higher WM pathology than undamaged myelin cases ( $p = 0.025$ ) (Figure 5-1). Undamaged myelin regions were not significantly different from the myelin scores of controls ( $p=0.291$ ) or non-demented post stroke cases ( $p = 0.155$ ). However, other demented groups showed increased myelin index scores (increased WM pathology) when compared to undamaged myelin: VaD ( $p = 0.001$ ), mixed ( $p = 0.003$ ), and AD ( $p = 0.002$ ).

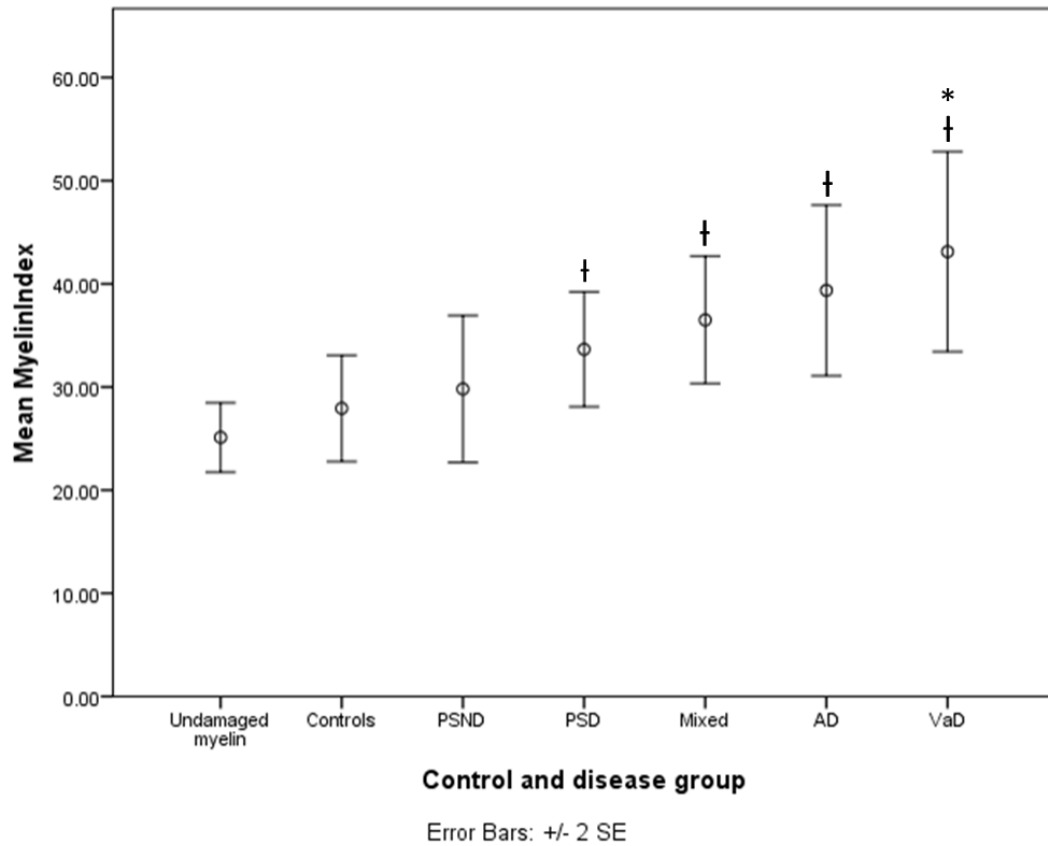


**Figure 5-1 showing the myelin index in the frontal WM of controls and disease subjects. Controls = aged controls, PSND = post-stroke non-demented, PSD = post-stroke dementia, VaD = vascular dementia, Mix = mixed dementia, AD = Alzheimer's disease. \* = significant to controls. † = significant to undamaged myelin. Mean MI: Undamaged myelin = 25, control = 28, PSND = 30, PSD = 34, VaD = 43, mixed = 36, AD = 40. Controls vs VaD ( $p = 0.034$ ). Undamaged myelin vs VaD ( $p = 0.001$ ), mixed ( $p = 0.003$ ), AD ( $p = 0.002$ ).**

#### 5.3.1.2. ***Correlations between myelin index and other variables***

To investigate the relationship between myelin index and other potential disease factors, correlations studies were undertaken. Bivariate analysis revealed myelin index (increased severity) significantly negatively correlated with MMSE and CAMCOG scores ( $\sigma = - 0.451$ ,  $p = 0.001$  and  $\sigma = - 0.320$ ,  $p = 0.02$ ), decreased learning memory ( $\sigma = 0.516$ ,  $p = 0.001$ ), attention ( $\sigma = - 0.388$ ,  $p = 0.016$ ), calculation ( $\sigma = - 0.344$ ,  $p = 0.034$ ) in PS cases. Myelin index score also correlated with SMI31 positive neurons in layer III ( $\sigma = 0.277$ ,  $p = 0.028$ ) (Figure 5-2) when looking at all groups. There was no significant between myelin index and pyramidal neuron atrophy ( $p > 0.05$ )

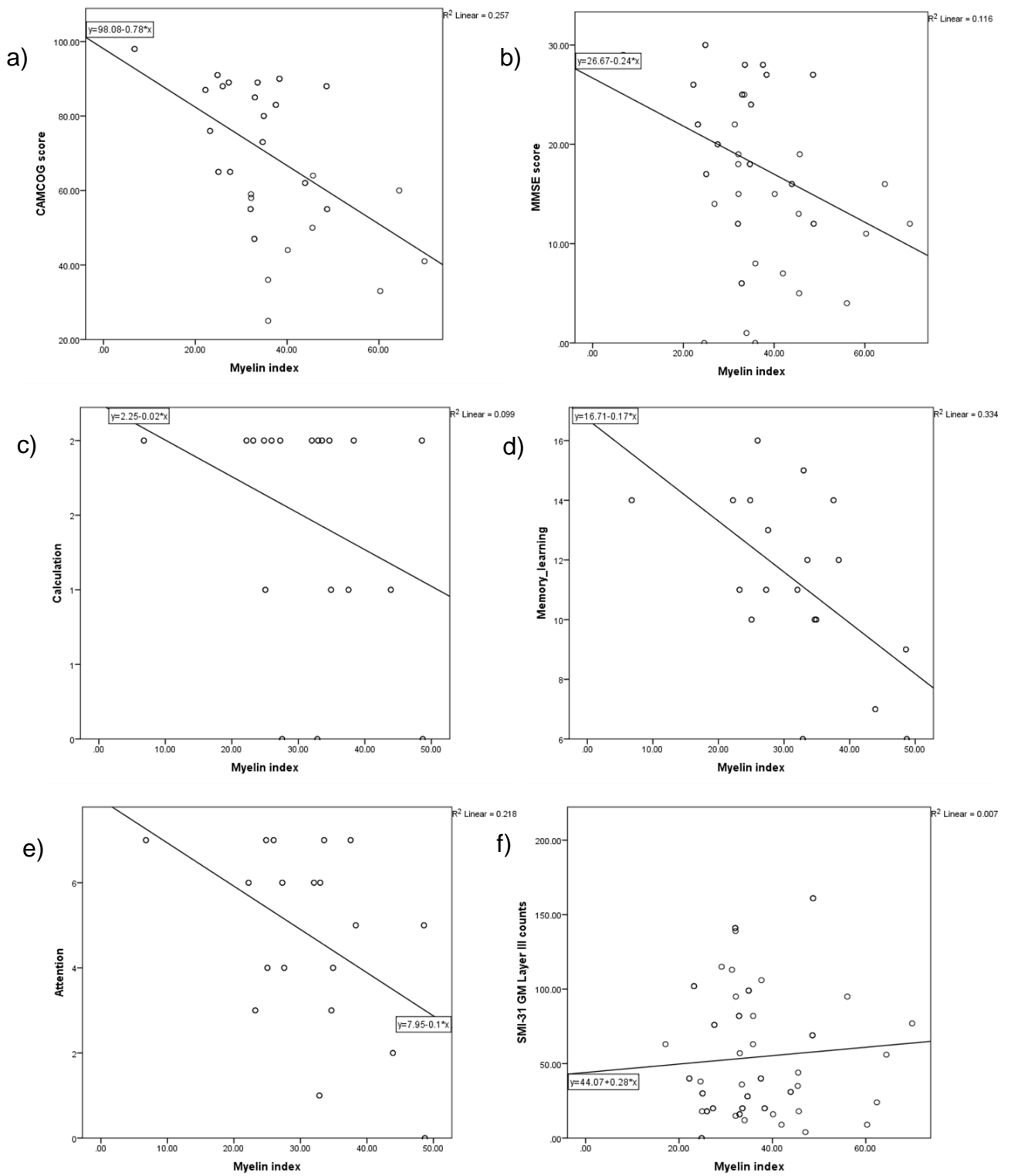


Figure 5-2 showing significant correlations between clinical variables and myelin loss index. a)  $\sigma = -0.320$ ,  $p = 0.02$ , b)  $\sigma = -0.451$ ,  $p = 0.001$ , c)  $\sigma = -0.344$ ,  $p = 0.034$ , d)  $\sigma = -0.516$ ,  $p = 0.001$ , e)  $\sigma = -0.388$ ,  $p = 0.016$ , f)  $\sigma = 0.277$ ,  $p = 0.028$ .

### 5.3.2. SMI32 analysis of axonal damage

SMI32 staining shows a variety of staining patterns between subjects, with some of the more affected subjects displaying punctate-like staining, with areas showing a build-up of SMI32 in specific areas of the frontal WM. SMI32 immunoreactivity was quantified by 2D analysis for percentage area stained (p/a) PSND, VaD, and mixed dementia had significantly higher P/A staining when compared to age matched controls ( $p = 0.018$ ,  $p = 0.041$ ,  $p = 0.001$ , respectively) and with PSD showing a trend towards significance ( $p = 0.072$ ). Mixed dementia also showed significantly higher p/a SMI32 staining when compared PSD and to AD cases ( $p = 0.041$  and  $0.005$ ). There was no significant difference between post-stroke survivors (Figure 5-4). IOD staining shared a similar pattern.

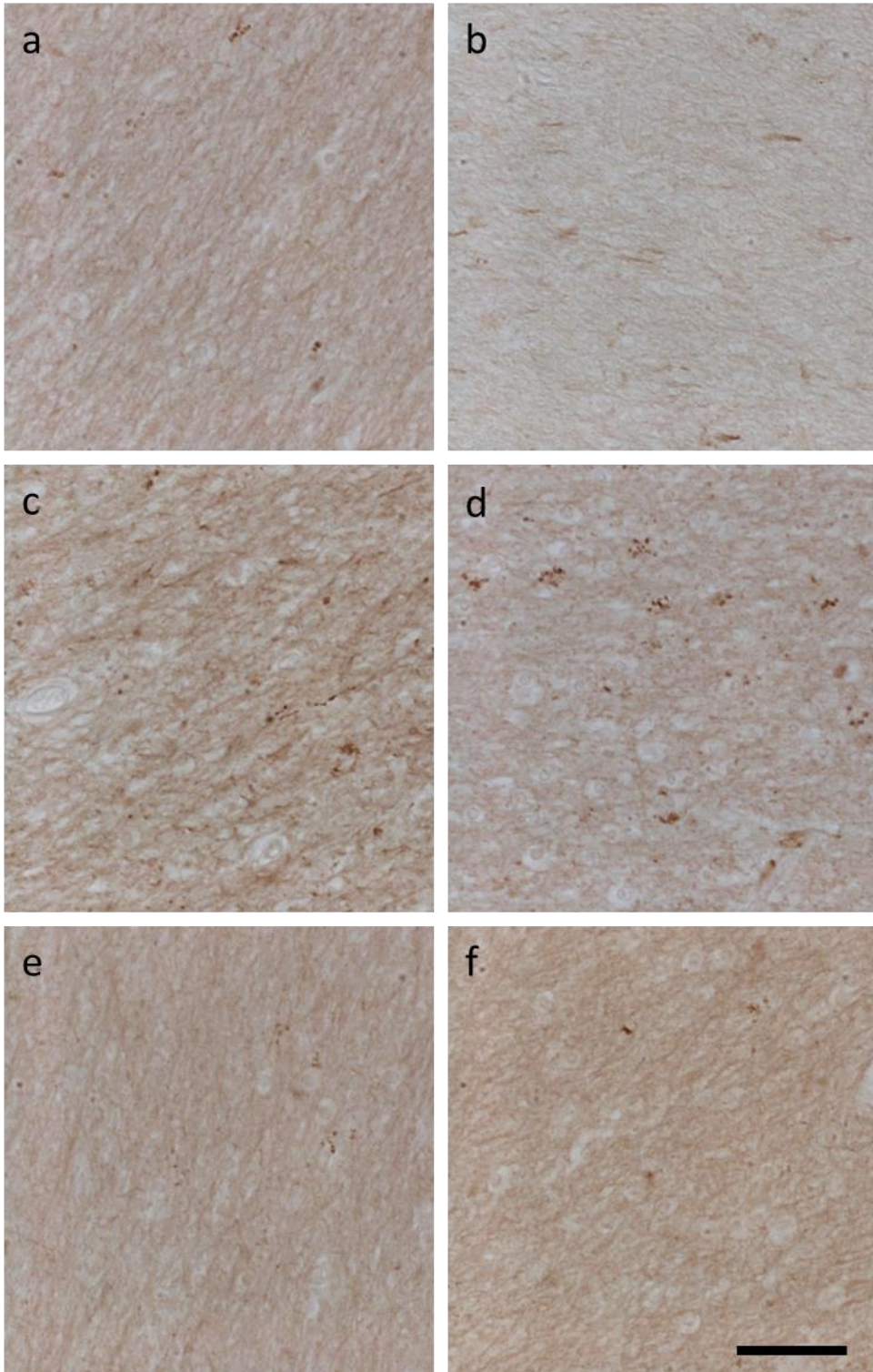


Figure 5-3 showing SMI32 positively stained axons in the frontal WM. a) aged-controls, b) PSND c) PSD, d) VaD, e) Mixed, and f) AD. Size bar = 20 $\mu$ m.

### 5.3.3. Correcting for myelin loss

To assess the relative axonal damage across the groups SMI32 values were corrected for myelin loss, as the myelin index. This was to avoid bias towards those disease states with a disposition towards myelin loss which may result in axonal damage. The aim was not only to assess the effect of myelin loss on the axons, but the effect of axonal damage on cognition as a factor independent of myelin pathology.

### 5.3.4. Adjusted SMI32 staining values

To correct for any apparent WM change, SMI32 immunoreactivity scores were normalised to myelin index scores. Additionally, one PSND case was removed, as it was deemed inadequate for reliable analysis as a large proportion of the slide had been damaged during the assay. Great care was taken to perform the assay on all slides on the same day in an attempt to minimise potential variations, which may affect staining. With this in mind it was deemed unnecessary and inappropriate to restrain the missing section as any variation may further affect results (Figure 5-4). When accounting for this correction; PSND, PSD, VaD, Mixed, and AD all show significantly increased SMI32 staining ( $p = 0.014$ ,  $p = 0.029$ ,  $p = 0.006$ ,  $p = 0.001$ ,  $p = 0.029$  respectively) when compared to controls. Mixed dementia showed increased SMI32 staining compared with PSND, PSD, and AD ( $p = 0.049$ ,  $p = 0.034$ ,  $p = 0.029$ , respectively).

#### 5.3.4.1. *Correlations between SMI32 and other clinical variables*

Including all groups, corrected SMI32 p/a staining correlated with both MMSE and CAMCOG scores for both p/a ( $\sigma = -0.319$ ,  $p = 0.020$  and  $\sigma = 0.296$ ,  $p = 0.037$ ). SMI32 staining also correlated with recent memory ( $\sigma = -0.421$ ,  $p = 0.007$ ) and language comprehension ( $\sigma = -0.339$ ,  $p = 0.033$ ) (Figure 5-5). There was no correlation between myelin index and SMI32 p/a staining or between SMI32 changes and pyramidal neuronal volumes ( $p > 0.05$ ).

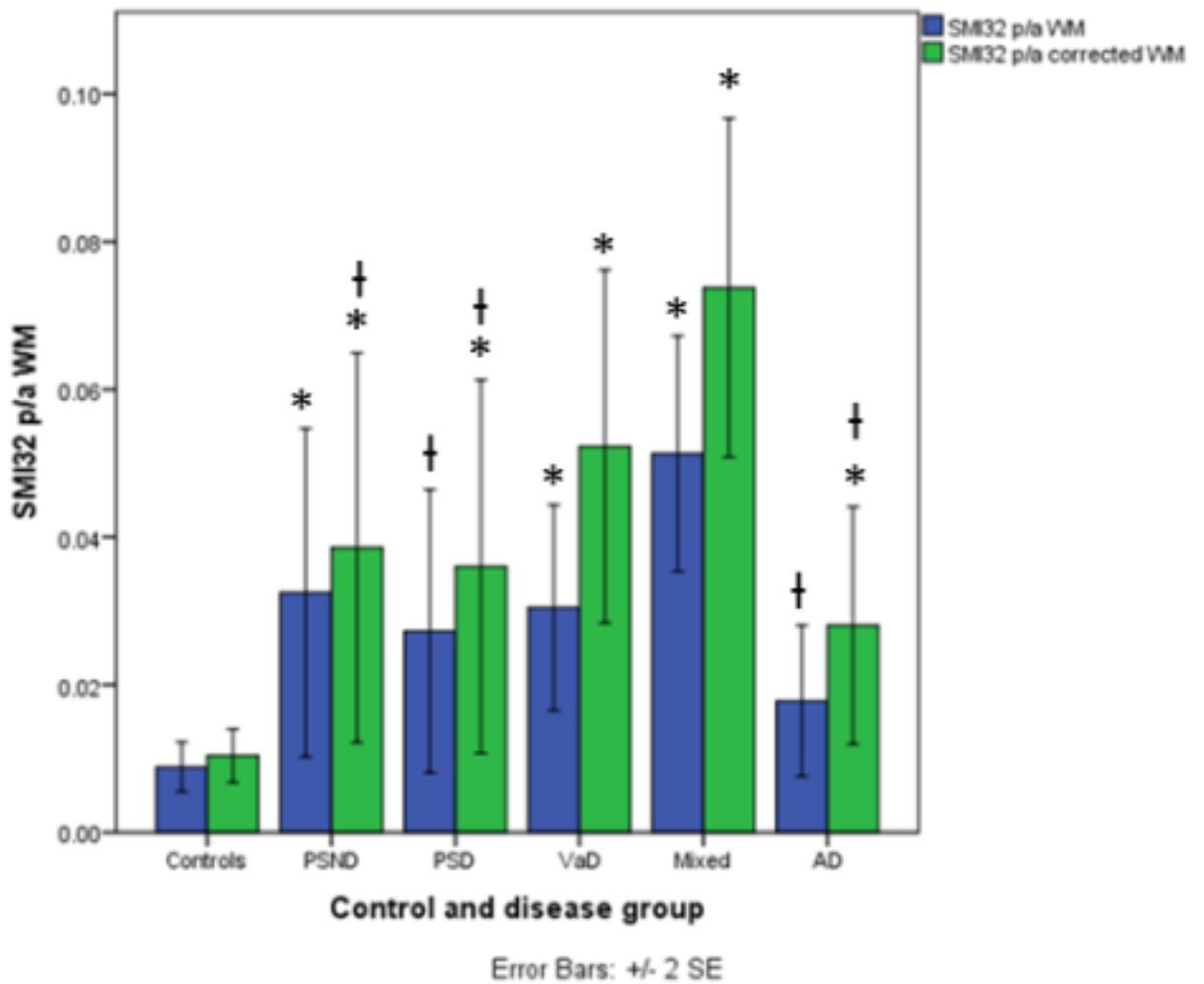


Figure 5-4 showing SMI32 staining (blue) and corrected SMI32 staining (green) in controls and disease groups. Controls = aged controls, PSND = post-stroke non-demented, PSD = post-stroke dementia, VaD = vascular dementia, Mix = mixed dementia, AD = Alzheimer's disease. \* = significant to controls. † = significant to mixed dementia. Uncorrected: Controls vs PSND ( $p = 0.018$ ), VaD ( $p = 0.041$ ), mixed ( $p = 0.001$ ). Mixed vs PSD ( $p = 0.041$ ), and AD ( $p = 0.005$ ). Corrected: Controls vs PSND ( $p = 0.014$ ), PSD ( $p = 0.029$ ), VaD ( $p = 0.006$ ), mixed ( $p = 0.001$ ), and AD ( $p = 0.029$ ). Mixed vs PSND ( $p = 0.049$ ), PSD ( $p = 0.034$ ), and AD ( $p = 0.029$ ).



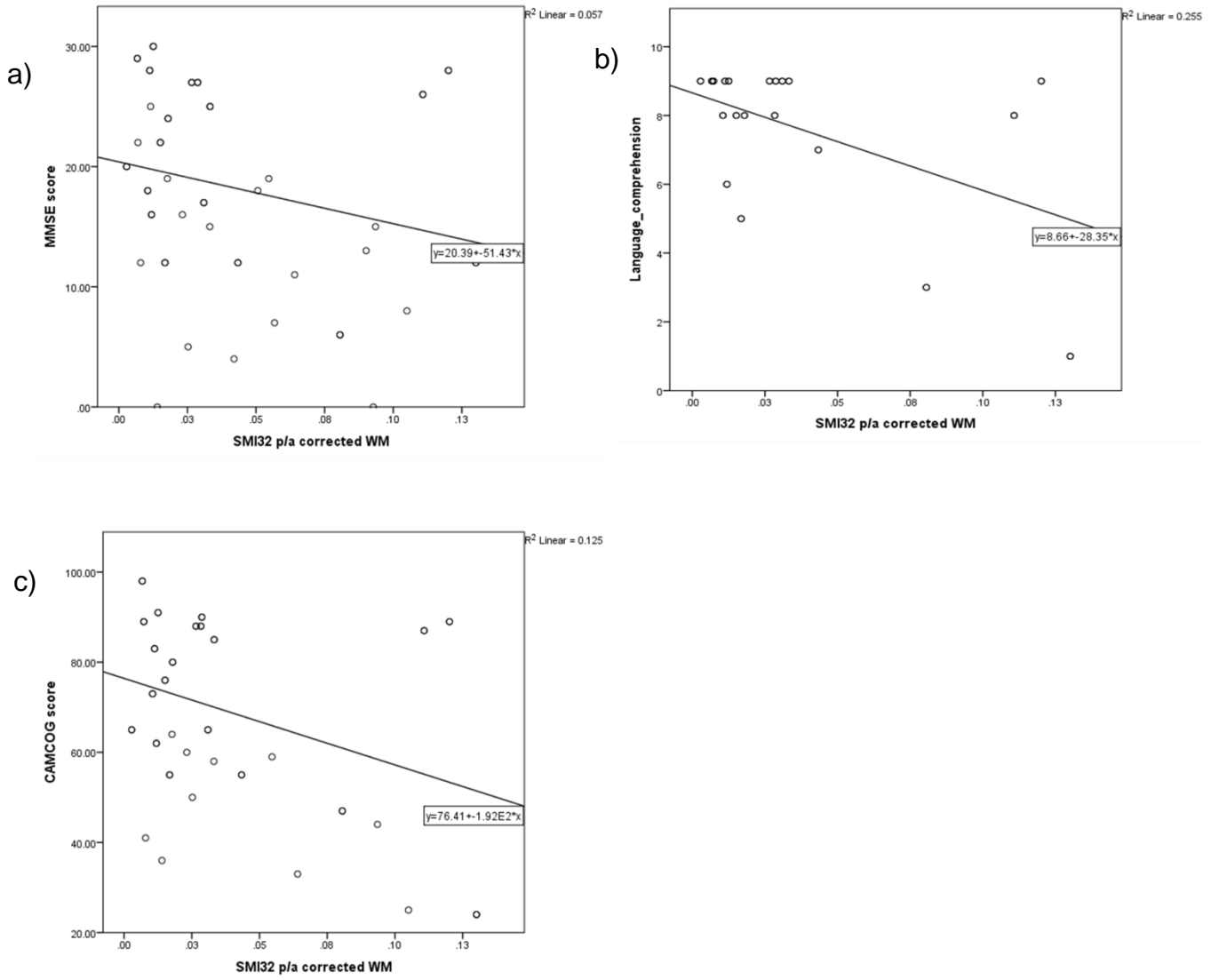


Figure 5-5 showing significant correlations between clinical variables and SMI32 frontal WM staining. a)  $\sigma = -0.319$ ,  $p = 0.020$ , b)  $\sigma = -0.339$ ,  $p = 0.033$ , c)  $\sigma = 0.296$ ,  $0.037$ .

#### **5.3.5. Analysis of SMI31 staining in the white matter.**

Per area (p/a) staining in VaD was significantly higher than controls ( $p = 0.016$ ). Mixed dementia had a very similar mean to that of VaD, however the large variation (SEM) indicated no significant differences against controls. There were no significant differences found between any other groups ( $p > 0.05$ ) (Figure 5-7).

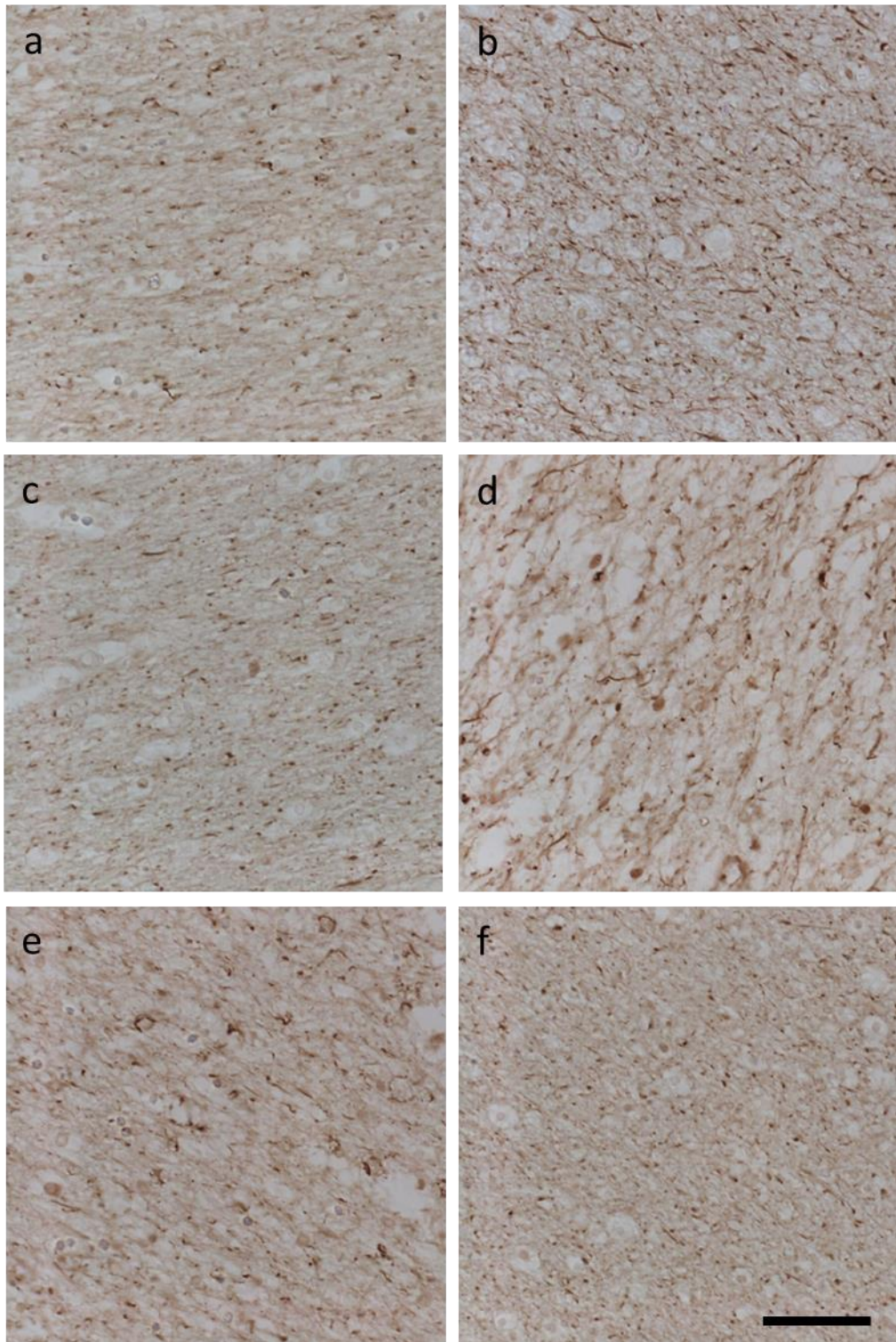


Figure 5-6 SMI31 positively stained axons in the frontal WM. a) aged-controls, b) PSND c) PSD, d) VaD, e) Mixed, and f) AD. Size bar = 20 $\mu$ m.

#### 5.3.5.1. ***SMI31 clinical variables correlations***

SMI31 p/a staining significantly correlated with CAMCOG scores ( $\sigma = -0.301$ ,  $p = 0.034$ ). SMI31 p/a also correlated with remote memory ( $\sigma = -0.335$ ,  $p = 0.035$ , respectively), praxis ( $\sigma = -0.350$ ,  $p = 0.027$ ), calculation ( $\sigma = -0.336$ ,  $p = 0.034$ ), and frontal vascular pathology ( $\sigma = 0.684$ ,  $p = 0.001$ ) (Figure 5-8). Analysis was performed on IOD staining producing no remarkable results.

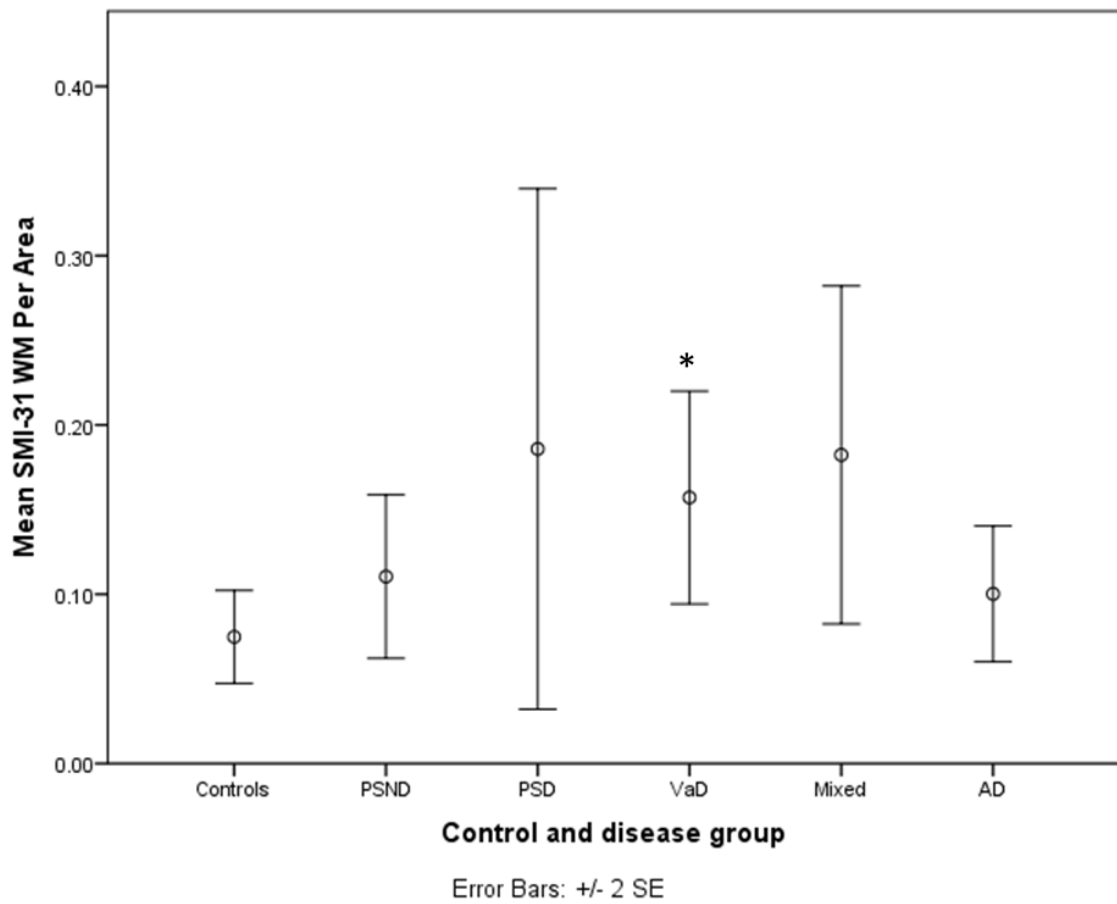


Figure 5-7 showing mean SMI31 staining in the frontal WM of controls and diseased subjects. Controls = aged controls, PSND = post-stroke non-demented, PSD = post-stroke dementia, VaD = vascular dementia, Mix = mixed dementia, AD = Alzheimer's disease. \* = significant to controls. Controls vs VaD ( $p = 0.016$ ).

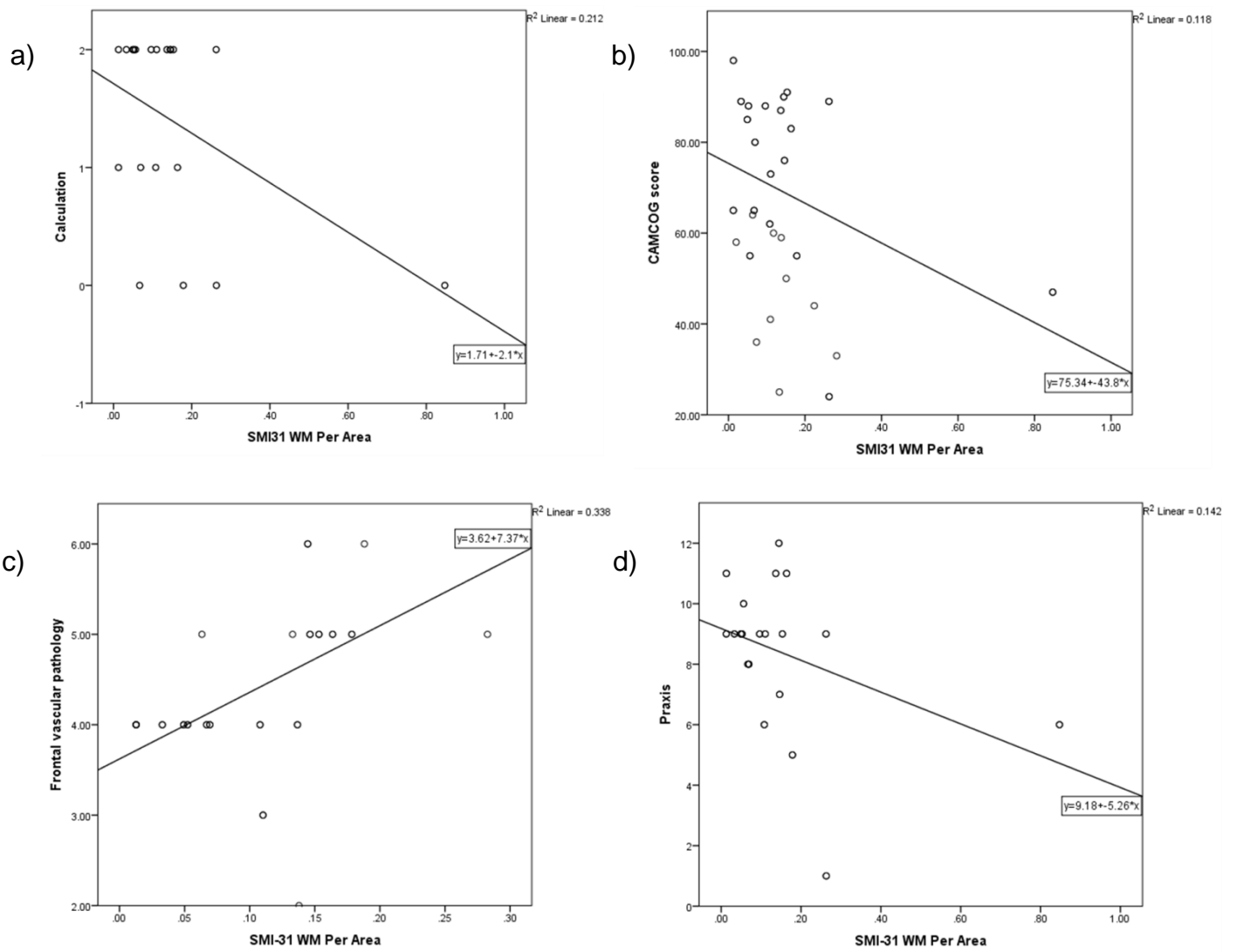
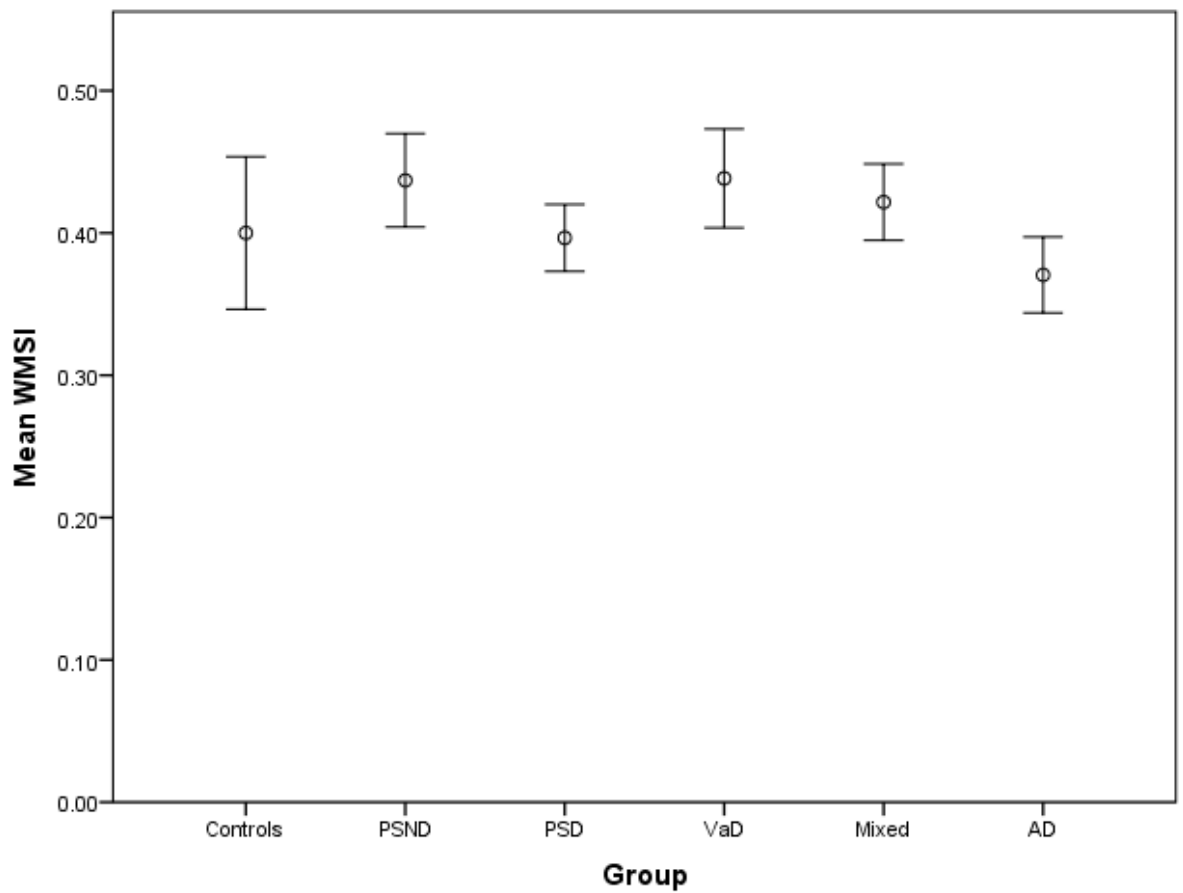


Figure 5-8 showing significant correlations between SMI31 frontal WM staining and clinical variables. a)  $\sigma = -0.336$ ,  $p = 0.034$ , b)  $\sigma = -0.301$ ,  $p = 0.034$ , c)  $\sigma = 0.684$ ,  $p = 0.001$ , d)  $\sigma = -0.350$ ,  $p = 0.027$ .

### 5.3.6. Analysis of vascular pathology in the white matter

There were no apparent differences in the SI scores of microvascular measures in the pre-frontal WM, though VaD did appear to trend towards significance when compared to AD cases ( $p = 0.07$ ). In addition, no significant changes were observed in PVS between any of the groups ( $p > 0.05$ ) (Figure 5-9).



Error Bars: +/- 2 SE

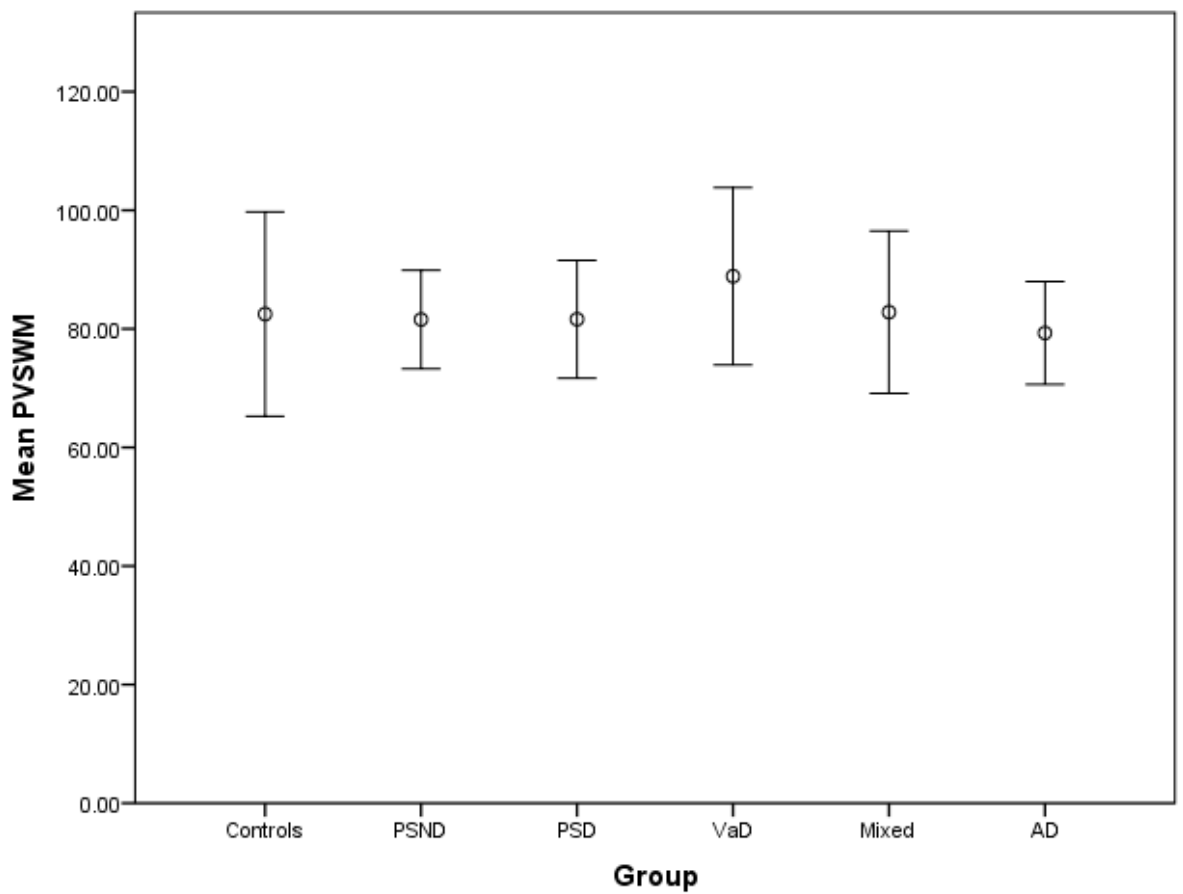


Figure 5-9 showing frontal vascular pathology in the WM of controls and disease subjects. Controls = aged controls, PSND = post-stroke non-demented, PSD = post-stroke dementia, VaD = vascular dementia, Mixed = mixed dementia, AD = Alzheimer's disease. SI = sclerotic index, PVS = perivascular space. No significance between groups: WMSI ( $p = 0.053$ ), PVSWM ( $p = 0.863$ ).



### 5.3.7. GRP78 staining of oligodendrocytes

As GRP78 also stained oligodendrocytes in the frontal WM rather specifically these cells were quantified. Visually there was a notable difference between individual subjects, however the total mean of each group remained similar (Figure 5-10). 2D densitometric analysis of GRP78 revealed no differences between any of the disease groups, or between post-stroke diseased cases and non-demented controls ( $p > 0.05$ ). GRP78 staining did not differentiate the demented and stable post-stroke survivor subjects (Figure 5-11).

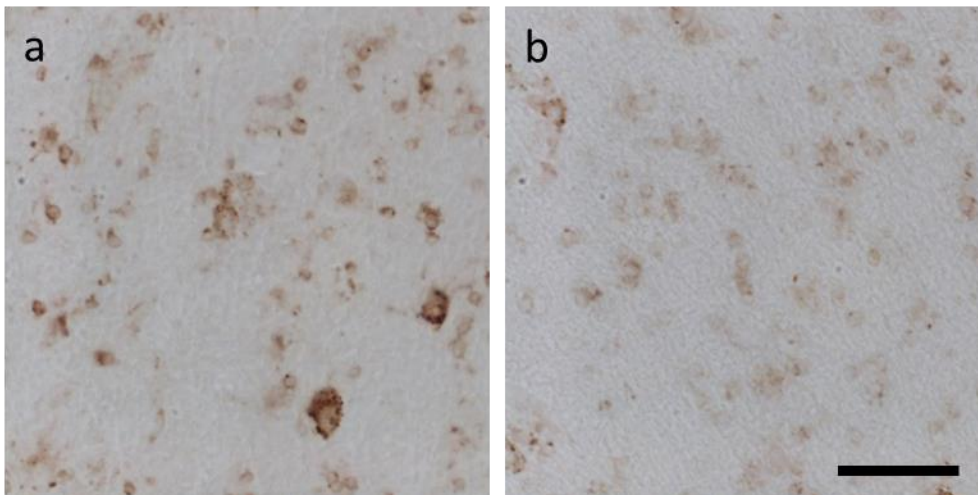


Figure 5-10 showing GRP78 staining of the WM in a) AD and b) VaD. Bar = 20 $\mu$ m.

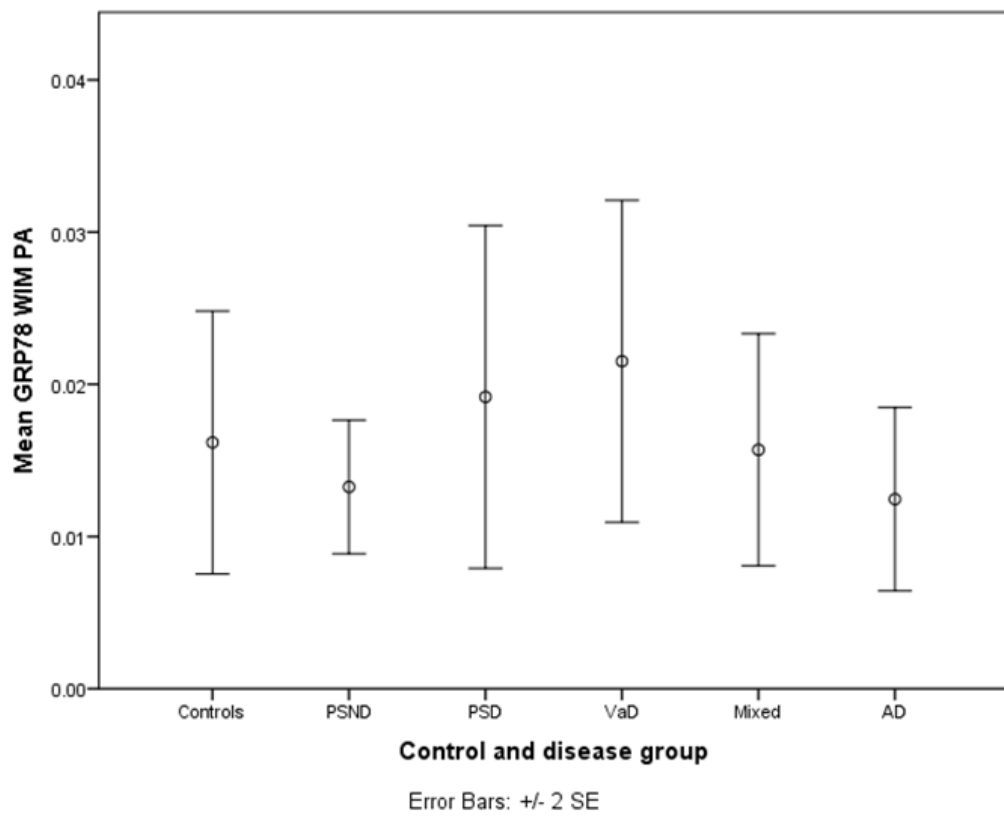


Figure 5-11 showing GRP78 staining in the frontal WM of controls and disease subjects. Controls = aged controls, PSND = post-stroke non-demented, PSD = post-stroke dementia, VaD = vascular dementia, Mix = mixed dementia, AD = Alzheimer's disease. No significance between groups ( $p = 0.868$ ).

## 5.4. Discussion

### 5.4.1. White matter loss

There was no significant difference in myelin index scores between PSND cases and PSD which would explain the cognitive deficits in PSD, and suggests myelin loss is comparable between the two groups, in turn suggesting myelin loss is not the primary cause of cognitive dysfunction in post-stroke subjects. This was surprising as previously WM damage has been shown in those with PSD (E. Burton et al. 2003). When assessing axonal damage SMI32 staining revealed no significant differences between either post stroke groups, again suggesting the cognitive dysfunction in this groups are not the result of WM damage, but possibly due to direct damage to neuronal bodies, as described previously (See Retrograde vs. anterograde neurodegeneration. ). Furthermore SMI32 staining revealed no significant difference between PSND and PSD, again suggesting little variation between the levels of non-damaged axons in each case. When compared to undamaged WM, all demented cases showed significantly higher MI though interestingly not when compared to age matched controls and non-demented post-stroke survivors.

These findings suggest two important potential consequences; (i) Underlying pathology is present in all cases, including controls. This technique may not be sensitive enough to distinguish the threshold with which WM pathology begins to affect cognition, and (ii) that there is indeed an underlying demyelinating aspect to these demented groups, regardless of aetiology, with both vascular based pathology, and AD type dementia appearing to have more severe WM damage than controls. In addition to these points, it is of interest, that no significant difference was reported between PSND and PSD ( $p > 0.05$ ), only PSD subjects were significantly difference when compared to undamaged myelin, suggesting that in fact PSD subjects have a higher degree of myelin index when compared to PSND.

When investigating the other groups, myelin index analysis revealed an increased myelin index in VaD when compared to controls, suggesting a higher level of myelin loss, and thus, white matter damage. The hypoxic state, caused by the breakdown of the vasculature in the frontal part of the brain, results in

death by excitotoxicity of the residing oligodendrocytes (Nedergaard et al. 2003) and may explain the decline in cognitive function. Indeed it has previously been shown that myelin loss may occur in conjunction with shrunken oligodendrocytes in subjects suffering from VaD (Ihara et al. 2010). These cells are very vulnerable to this type of hypoxic insult, with their death resulting in decreased myelination of the surrounding axon. The resultant dysfunction of the WM in these cases would explain the clinical cognitive affects seen in those suffering VaD. Interestingly, mixed dementia did not show significance when compared to controls ( $p > 0.05$ ), which was unexpected. Mixed cases, in this cohort, had a comparable vascular pathology when compared to VaD, and this lack of conformity between VaD and mixed is surprising. VaD also showed a trend in greater MI when compared to AD subjects. This difference helps highlight the separate aetiologies of these two diseases; despite both displaying reduced neuronal volume in the dlPFC, they do not share comparable vascular pathology. Perhaps most telling, AD subjects revealed a trend towards higher myelin loss ( $p = 0.068$ ) when compared to controls. AD pathology is well documented in the grey matter, but it also appears to play potential role in the disruption of cortical circuits via damage to the WM. This may occur as a result of CAA accumulation around the vasculature (Rose et al. 2000), resulting in oligodendrocyte death by affecting blood supply to the cells.

No significant difference was found in WM myelin index scores between the two post stroke groups. Frontal myelin index score correlated strongly with the executive function; attention. This is not surprising- cortical disruption caused by loss of myelin in the prefrontal cortex may lead to a breakdown of the one or more of the pre-frontal cortices, suggesting a direct causal link between myelin loss and cognitive dysfunction, this is reinforced by the significant correlation between myelin index and learning memory. This suggest further break down of the cortico-subcortical circuit, disrupting the link between the frontal cortex and the limbic system, inhibiting the subject's ability to form or access long-term memory.

#### 5.4.2. **Corrected SMI32 as a marker for WM damage.**

Two dimensional analysis revealed striking differences between PSND, VaD, and mixed pathology cases when compared to controls ( $p = < 0.05$ ), with PSD trending towards significance ( $p = 0.077$ ). Interestingly AD subjects did not

show similar results. This reinforces the relationship between axonal function and cognition. This increased immunoreactivity may indicate higher levels of concentrated SMI32 staining as a result of axonal transport disruption, which can occur following a stroke (Andres et al. 2011). Increased damage to the axonal tracts may interrupt action potentials between neurons which culminate in cognitive inhibition (Ferguson et al. 1997). Evidence of this relationship is further supported by the correlation between SMI32 WM staining and CAMCOG and MMSE scores, with axonal damage in the frontal lobes directly relating to global cognitive scores in PS cases. Indeed axonal damage has been shown to be reliable predictor in several other disease states (Medana and Esiri 2003). Specific functions such as recent memory and language comprehension were also significantly affected in post-stroke patients. Such damage also appears to effect the connections between areas of the brain responsible for language processing such as Broca's or Wernicke's area. However, no significantly differences were reported in location or severity of stroke between the PSND and PSD subjects, though language comprehension was found to be significantly lower in post-stroke demented patients.

#### **5.4.3. SMI31 analysis of frontal WM integrity.**

SMI31 staining was anticipated to be higher in controls and post-stroke non-demented cases when compared to demented groups. However, SMI31 staining p/a values were greater in VaD compared to age-matched controls in p/a suggesting a higher level of healthy axonal tracts in these subjects than controls which contradicted the results on SMI32 analysis. There were no significant differences observed between any other group. This was perhaps surprising, as it was postulated that SMI31 antibody would target healthy, intact axons. This result does not support this notion as it was expected for VaD to have significantly less healthy axonal tracts (Gorelick 2004). In addition, it is worth noting that mean SMI31 staining between PSD, VaD, and Mixed groups was very similar, and noticeably higher than controls, PSND, and AD. This pattern did not reach significance however, though this may be a result of rather large SEMs. Though SMI31 appeared to effectively stain axons within the WM, it appears 2D densitometric analysis is too insensitive a technique for detecting the suitable differences which may exist between post-stroke subjects.

#### **5.4.4. Myelin loss as an effective measure of axonal damage and of cognitive function.**

CAMCOG and MMSE scores correlated with both myelin loss index, and axonal damage markers. This provides a strong mechanistic pathway in which to explain the cognitive decline in post-stroke patients, suggesting that myelin loss in the frontal white matter, as measured by LFB staining intensity appears to relate with cognitive decline, and can thus be used as an effective measure for cortico-cortical circuit damage. In addition axonal damage marker SMI32 also correlated with MMSE and CAMCOG scores suggesting a direct link between axonal dysfunction and cognitive impairment. However, no correlation was observed between myelin loss and axonal damage. This lack of relationship between the two markers suggests that the two pathologies occur independently of one another and that myelin loss does not necessarily result in subsequent axonal damage as previously suggested (Ihara et al. 2010).

Interestingly, neither axonal markers nor myelin index correlated with pyramidal neuron volume changes in dIPFC ( $p > 0.05$ ). This was surprising, as it was hypothesised that the changes reported in neuronal volume of the dIPFC were potentially related to damage within the WM of the frontal lobe.

This finding, whilst unexpected, may also shed some light onto the question of anterograde vs. retrograde degeneration. Due to the apparent lack of relationship between WM changes and neuronal volume decreases, it can be argued that each pathology occurs independently of the other. Thus, if it is assumed that neuronal volume change is a pathological response, and in turn results in cognitive decline, then the lack of correlation between WM pathology would suggest that this volume change is a result of anterograde degeneration, where direct damage to the grey matter results in this decreased neuronal size, though this is hard to prove due to the widespread underlying WM pathology detected in dementia. However, pyramidal neuron damage as detected by increased SMI31 positive neuron counts does suggest a mechanistic link between damage to the frontal WM and cognitive dysfunction.

#### **5.4.5. Vascular pathology in frontal WM**

Similar to findings in the grey matter, SI analysis of WM pathology revealed no significant differences between any disease group when compared to each

other, or non-demented controls. This was unexpected as previous studies (Deramecourt et al. 2012; Craggs et al. 2013) have reported significantly increased vascular pathology in the WM in some diseases i.e. CADASIL (Cerebral Autosomal-Dominant Arteriopathy with Subcortical Infarcts and Leukoencephalopathy). Indeed, a prerequisite for a VaD diagnosis is a high burden of vascular pathology. However, the extreme age of this cohort may result in a higher level of vascular pathology in controls and non-vascular based dementias. Indeed, SI detects arteriolosclerosis, a vascular change thought to occur in the early stages of disease (Deramecourt et al. 2012) and thus may be present in all disease groups at this late stage. Perhaps a more sensitive technique would reveal any potential subtle changes in this particular type of pathology between disease groups in older subjects.

#### **5.4.6. GRP78 staining as a marker for oligodendrocyte pathology**

GRP78 is induced when cellular endoplasmic reticulum are stressed, acting as an apoptotic regulator by protecting the host cell against ER stressed induced cellular death (Rao et al. 2002; Hayashi et al. 2003). However, as GRP78 stains all cells which contain ER it is a reliable marker for staining oligodendrocytes. There were no differences in GRP78 immunostaining in the WM between any of the groups. This lack of difference in GRP78 immunostaining was surprising as it has been shown previously that oligodendrocytes are lost following stroke (Aboul-Enein et al. 2003) due to their particular vulnerability to hypoxic insult (Alberdi et al. 2005).

### **5.5. Conclusion**

This study revealed there was considerable variation in the myelin index of aged-controls and post-stroke non-demented subjects. In general all cases showed some degree of WM pathology when compared to undamaged myelin. Increased myelin index, indicating increased WM loss correlated with cognition and executive scores, suggesting myelin index is a reliable correlate of cognitive function, and that reduced cognition is likely to reflect WM damage. The SMI32 staining related strongly with disease groups, showing increased axonal damage in those suffering dementia, correlating strongly with cognitive status and features executive dysfunction. This suggests an association

between axonal damage and dysfunction of the fronto-cortical circuits. This trend was not supported by SMI31 axonal staining, which did not appear to stain for undamaged axons as postulated, not consistent with the SMI32 results. However, SMI31 staining was intense, and very strong due to the high numbers of axons present in the WM, so any changes between groups being undetectable using 2D analysis.

GRP78 immunoreactivity in the WM was an effective marker for glial cells in the WM, localising with oligodendrocytes. Its expression p/a did not differ between PSND and PSD, and did not relate to cognitive function. From these findings it is clear that WM pathology plays a strong role in the development of cognitive impairments though it is not apparent whether glial cells play a role in the development of PSD.



## **Chapter 6. Markers of metabolism in the dIPFC**

### **6.1. Introduction**

#### **6.1.1. Neuronal metabolism**

The overall health of the brain is dependent on the fulfilment of the metabolic needs of individual neurons. The vast majority of cells in the cortex are metabolically expensive excitatory (Waldvogel et al. 2000), with excitatory, glutamatergic based, action potentials using up to 47% of the energy of the cell (Attwell and Laughlin 2001). The high metabolic requirements of these cells make them vulnerable to pathology which impacts oxygen and trophic factor supplies (Spruston 2008). Changes which alter the metabolic activities of these cells may have a detrimental effect on cognition, breaking down neuronal circuits (Tekin and Cummings 2002).

Cerebral metabolism of glucose and oxygen uptake have been found to be reduced in ischaemic stroke subjects, with, 1.5T MRI revealing decreased metabolism in the infarction area four days following a stroke (Kuhl et al. 1980). Increased lactate levels in these subjects suggest neurons continue to function sometime after the initial event, though, due to poor blood circulation, struggle to obtain sufficient oxygen for metabolism which may result in gradual neuronal dysfunction (Bruhn et al. 1989). Decreased cerebral metabolism has also been reported in AD subjects. The build-up of hyperphosphorylated tau is thought to result in the gradual dysfunction of these neurons (K. Ishii et al. 1998; Blass 2001; Mosconi 2005) by disruption to cellular processes within the cell. GRP78, a glucose regulated protein which is ubiquitously expressed in all cells (Quinones et al. 2008) has been shown to increase when a cell is stressed (Rao et al. 2002), and is linked to diseases such as Parkinson's and AD (Paschen 2001). GRP78 is also thought to bind to the amyloid precursor protein and decrease  $\beta$  amyloid secretion in what is perceived as a protective mechanism (Yang et al. 1998). GRP78 has been linked to have a protective effect against glutamate excitotoxicity (Lee et al. 1999; Paschen 2001), which

may play an important role in ischaemic diseases, following stroke glutamate neurotoxicity. As mentioned previously, glial and neuron uptake systems remove glutamate released by synapses (Choi and Rothman 1990). When these systems break down, the build-up of glutamate can be lethal to the neuron as it may trigger an influx of extracellular calcium (Choi and Rothman 1990; Nedergaard and Dirnagl 2005). In more chronic hypoperfusive states, occurring in areas remote to the stroke, neurons may be subjected to a cascade of biochemical fallout. The decreased glucose and oxygen transport sets off a chain of events resulting in increased glial activation and oxidative stress. Cells switch to secondary pathways which utilise lowered oxidation of glucose and reduced cytochrome oxidation, ultimately resulting in reduced ATP production and cellular dysfunction (de la Torre 1999). These changes may be pivotal events in the development of cognitive impairment following stroke.

#### 6.1.1.1. ***Mitochondrial function***

Mitochondria are the powerhouses of the neuron, producing adenosine triphosphate (ATP) through the phosphorylation of adenosine diphosphate (ADP) via a process known as the electron transport chain (ETC). The ETC is the primary, aerobic, mechanism through which ATP is produced. Electrons are transferred through a series of electron donors and receptors, through REDOX reactions. This electron transfer is coupled with the transport of proton (H<sup>+</sup> ions) through a series of protein pumps housed in the membrane of the mitochondria (Cadenas and Davies 2000). By far the highest metabolic pressure of a neuron is the active ion transport which is initiated following an action potential, and resets the neurons, ready for more signal transduction (Attwell and Laughlin 2001). Enzymes such as cytochrome oxidase C serve as reliable indicator of neuronal oxidative capacities and energy metabolism. The tight coupling between energy metabolism and neuronal activity enable this scrutiny of cytochrome oxidase C as a sensitive neuronal marker (F. N. Wong-Riley, Robert F. Hevner, Suyan liu 1998). Cytochrome oxidase is the terminal enzyme in complex 4 of the ETC – catalysing the oxidation of cytochrome C and reduction of molecular oxygen. COX4 expression has been shown to be reduced in diseases such as AD (Parker et al. 1990) in both the frontal and temporal lobes (Kish et al. 1992). Conversely Chagnon et al reported no significant differences in COX4 expression in those suffering CVD (they did find

lower levels in AD)(Chagnon et al. 1995). However, very little is known about COX4 expression in PSD.

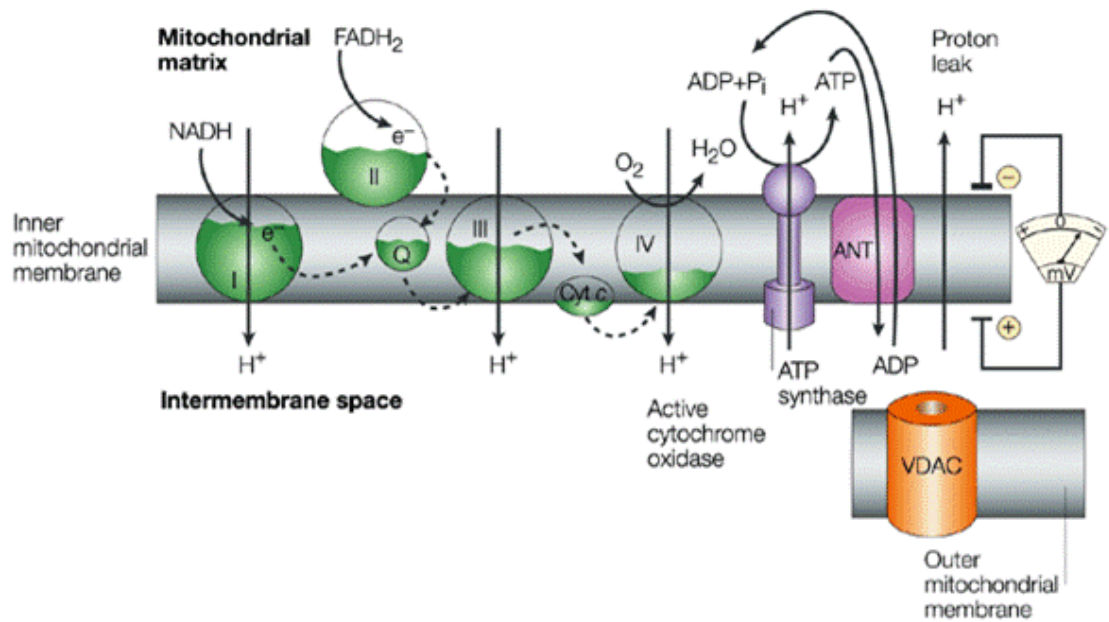


Figure 6-1 demonstrating the electron transfer chain in mitochondria (Moncada and Erusalimsky 2002).

#### 6.1.1.2. *Dendritic arbour*

Excitatory synapses have been shown to be more metabolically demanding than their inhibitory counterparts. With this in mind, any changes to pyramidal neuron metabolisms would have drastic effects of dendritic output (Waldvogel et al. 2000). This mismatch in respective energy consumption stems from the synapses of different cell types possess. Dendritic outputs from pyramidal neurons are more numerous, but less efficiently located than inhibitory synapses (Waldvogel et al. 2000). Additionally, excitatory synapses form the majority of the grey matter (Abeles 1991; Geortzel 1997) with the distribution of mitochondria suggesting that these are the major consumers of metabolic energy (M. T. Wong-Riley 1989; M. Wong-Riley et al. 1998). As previously mentioned, dendritic arbour has been linked to the soma size of the neuron (Harrison and Eastwood 2001), suggesting that any reduction in neuronal volume would indicate a reduction in the surrounding dendritic arbour. Any breakdown or reduction in dendritic arbour could theoretically impact directly on neuronal-neuronal connectivity, disrupt brain circuitry, and potentially resulting in neurological dysfunction. Post-mortem studies have found that stroke or brief ischaemia can induce changes in dendritic arbours and branch complexity and spine density (Gonzalez and Kolb 2003; C. E. Brown et al. 2007). However it is unclear how dendritic arbour remodelling differs between those suffering PSND and those who decline into dementia.

Pyramidal neurons play an important role in the development of dementia. The previous 3 chapters have gone into great detail investigating the morphological, histological, and biochemical changes which may relate to specific pathological substrates which may separate post-stroke non-demented individuals from post-stroke demented subjects. This chapter will investigate the potential mechanisms, which may result in the dysfunction of these cells.

## 6.2. Methods

### 6.2.1. Details of subjects used in this study

	No of cases (SEM)	Age	PMD	FT	Frontal vascular score	Braak	CERAD
Control	10	85.3 (16)	30.6 (17)	3 (1)	n/a	2 (1.2)	n/a
PSND	10	83.3 (3)	42.3 (19)	3.8 (6)	4.5 (0.8)	2.3 (1)	1.6 (0.7)
PSD	10	87.8 (6)	35.7 (22)	2 (1)	4.3 (0.9)	2.6 (1)	1.3 (1)
VaD	10	84.3 (9)	52.1 (22)	2.8 (1)	5 (1)	2.2 (1)	0.9 (08)
Mixed	10	83.2 (8)	33.4 (19)	5.3 (9)	4 (1.7)	5.4 (0.7)	2.7 (0.7)
AD	10	84.3 (5)	36.8 (24)	1.5 (1)	1 (0)	5.5 (0.8)	3 (0)

**Table 6-1 details of subject used in this chapter. PMD = post-mortem delay. Controls = aged matched controls, PSND = post-stroke no dementia, PSD = post-stroke dementia, VaD = vascular dementia, mixed = mixed vascular and Alzheimer's disease, AD = Alzheimer's disease. FT = fixation time, PMD = post-mortem delay.**

### 6.2.2. Immunohistochemical analysis

Ten µm Sections containing the dIPFC from all control and disease cases were stained with antibodies for COX4 (Abcam, UK) (1:200) and GRP78 (Abcam, UK) (1:2000) (using method described previously). Analysis was then performed using 2D densitometric analysis. In addition, the operator performed counts to assess the number of pyramidal neurons staining positive for each of the antibodies. To be counted, neurons must be large (as determined by operator), triangular, and show a nucleus.

### 6.2.3. Statistics

Distribution analysis was performed using SPSS. Both GRP78 and COX4 data was found to be non-normally distributed and consequently, non-parametric data analysis tests; Kruskal-Wallis and Mann-Whitney U tests were used. Bivariate correlations were tested using Spearman's rank coefficient.

## 6.3. Results

### 6.3.1. GRP78 staining in layers III and V of the dIPFC

#### 6.3.1.1. *Densitometric analysis of GRP78*

GRP78 revealed clear and specific staining of pyramidal neurons. The cortical ribbon was clear with layers III and V easily distinguishable due to the presence of large pyramidal neurons. The cell nucleus was visible within the soma and there was minimal non-specific background staining (Figure 6-2). GRP78 p/a revealed no significant difference between PSD and PSND subjects. (Figure 6-3). PSND showed significantly reduced p/a staining when compared to controls in layer V. There were no significant differences between any other groups.

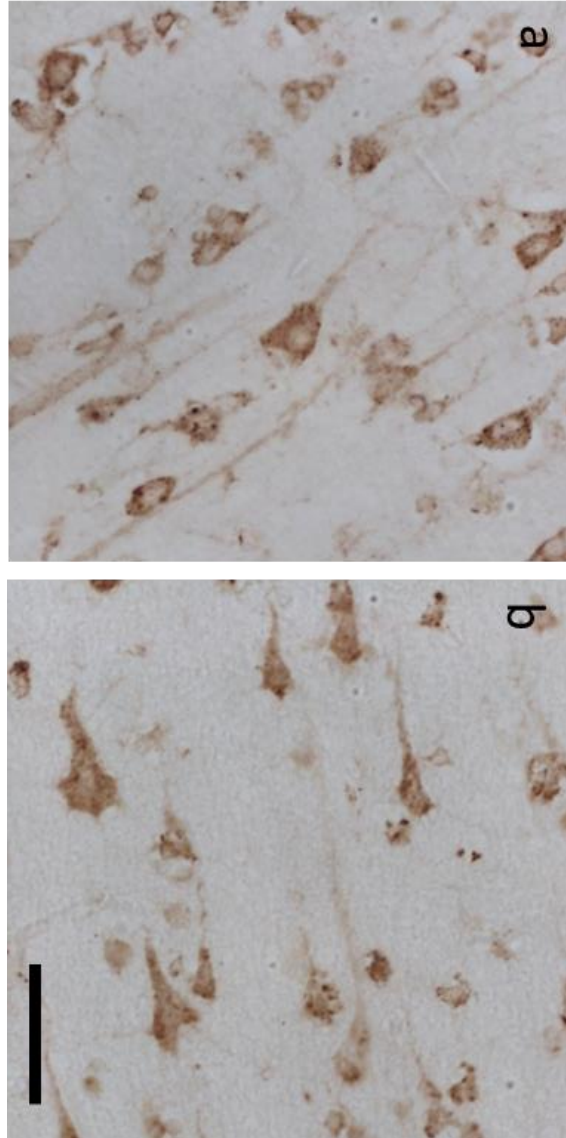


Figure 6-2 showing GRP78 staining of layer III of the dIPFC in PSND (a) and PSD (b). (scale bar = 20 $\mu$ m)



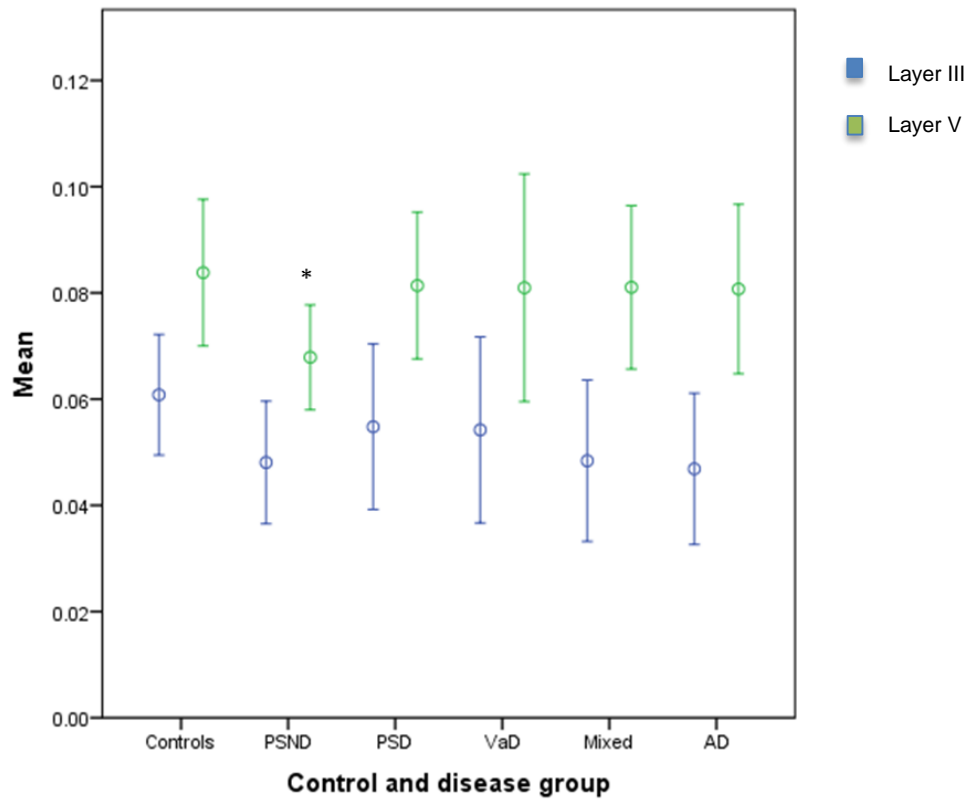


Figure 6-3 showing p/a staining of GRP78 in both layers III. Controls = aged controls, PSND = post-stroke non-demented, PSD = post-stroke demented, VaD = vascular dementia, mixed = mixed vascular and Alzheimer's disease, AD = Alzheimer's disease. Blue = layer III, Green = layer V, \* = Significant to controls. Control vs PSND (P = 0.036) in layer V.

6.3.1.2. ***GRP78 positive pyramidal neurons***

Data were found to be normally distributed in both layers ANOVA revealed significance in layer V ( $p = 0.002$ ) but this was not repeated in layer III ( $p = 0.226$ ). There were no significant differences in GRP78 positive neuronal counts between post-stroke subjects in either layers III or V. Post Hoc testing revealed significance between Controls and PSND ( $p = 0.035$ ), and PSND to AD ( $p = 0.005$ ), and VaD ( $p = 0.023$ ).

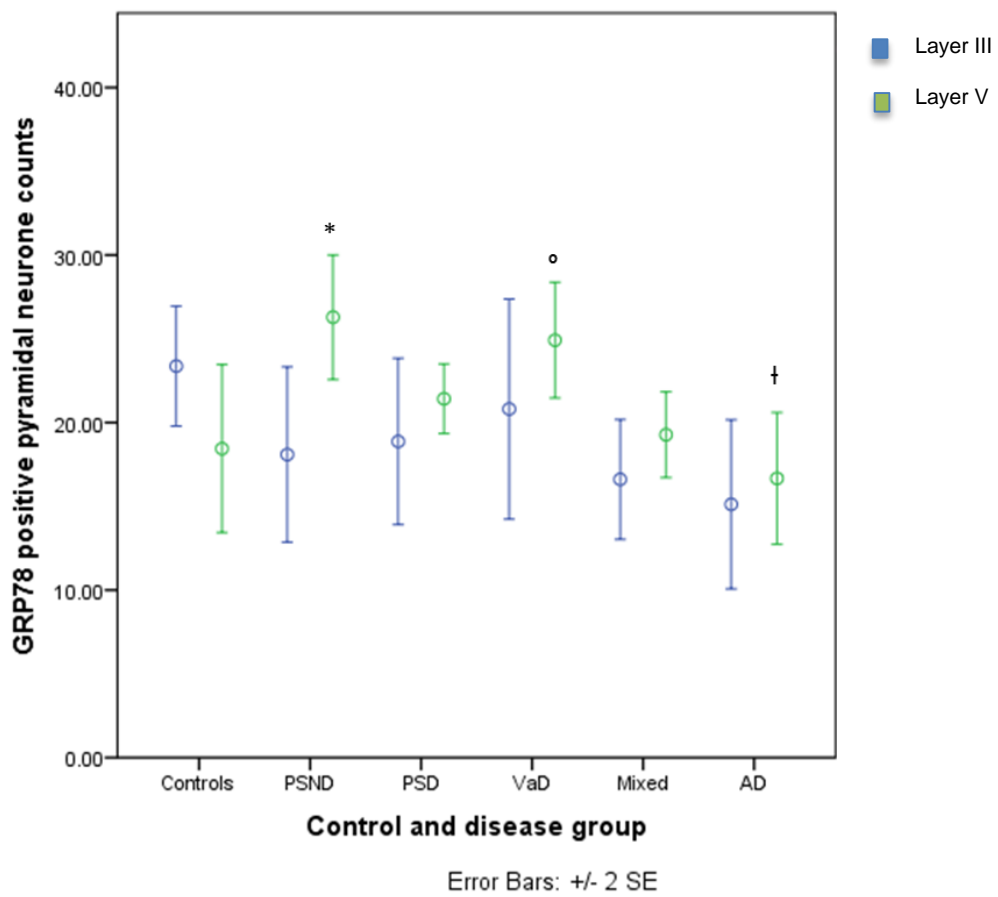
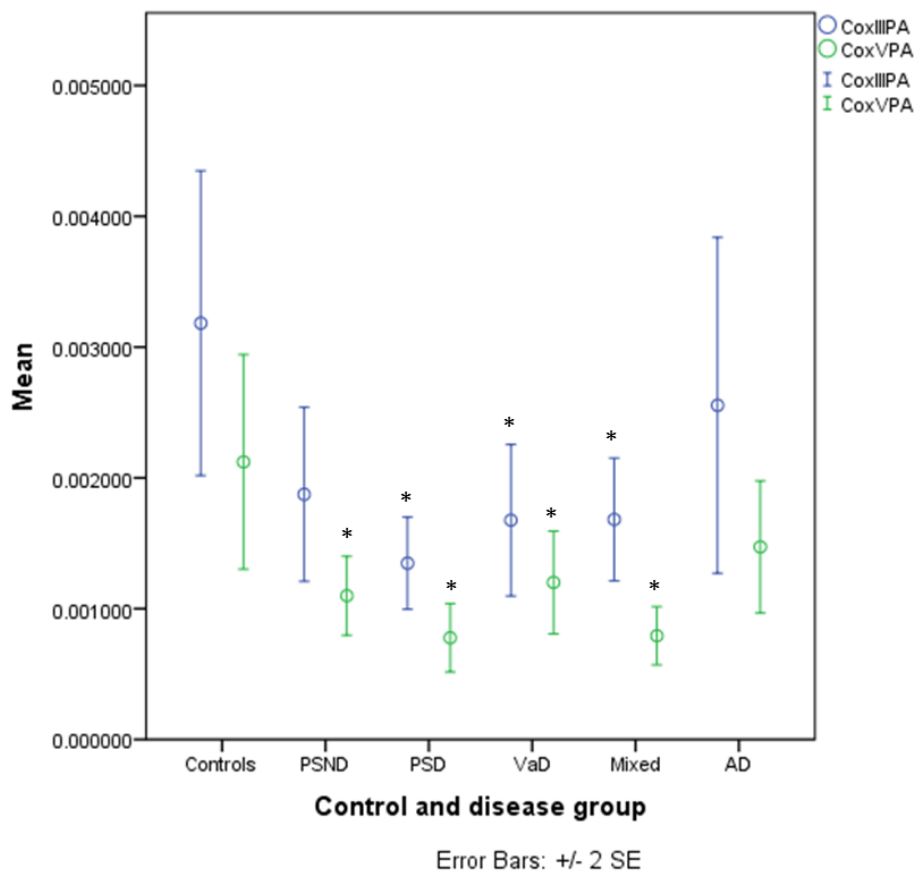


Figure 6-4 showing GRP78 counts in layers III and V of the dIPFC Controls = aged controls, PSND = post-stroke non-demented, PSD = post-stroke demented, VaD = vascular dementia, mixed = mixed vascular and Alzheimer's disease, AD = Alzheimer's disease. Blue = layer III, Green = layer V, \* = Significant to controls, ° = significant to AD, † PSND. Control vs PSND ( $p = 0.035$ ), PSND vs AD ( $p = 0.005$ ), VaD ( $p = 0.023$ ).

### 6.3.2. COX4 immunoreactivity in pyramidal neurons

COX4 revealed strong and specific staining, concentrated in the cell body of pyramidal neurons. When compared to GRP78 staining COX4 revealed a more granular staining pattern and it was evident that in several subjects that not all pyramidal neurons within layers III and V were positively stained. The nuclei of pyramidal neurons were readily visible, due to the absence of COX4. Cortical layers were easily identified as was the separation of GM and WM (Figure 6-7).

Two dimensional densitometric analysis of COX 4 antibody in the dlPFC revealed no significant difference between PSND and PSD subjects ( $p = 0.086$ ). In layer III all vascular based demented cases showed significantly reduced p/a staining when compared to controls (Figure 6-5). Interestingly, this pattern was similar in layer V with the addition of PSND showing significantly lower levels of stain when compared to controls. COX 4 positive pyramidal neuron counts in layer III revealed all diseased groups, with the exception of AD had significantly lower counts when compared to control cases. Layer V revealed significantly lower COX 4 positive neurons in all diseased cases when compared to controls (Figure 6-6). Additional analysis using IOD revealed similar findings.



**Figure 6-5 showing cytochrome oxidase 4 (COX4) p/a staining. Controls = aged controls, PSND = post-stroke non-demented, PSD = post-stroke demented, VaD = vascular dementia, mixed = mixed vascular and Alzheimer's disease, AD = Alzheimer's disease. \* = Significant to controls. Controls vs PSD ( $p = 0.019$ ), VaD ( $p = 0.028$ ), mixed ( $p = 0.034$ ) in layer III. Controls vs PSND ( $p = 0.019$ ), PSD ( $p = 0.004$ ), VaD ( $p = 0.049$ ), and mixed ( $p = 0.004$ ) in layer V.**

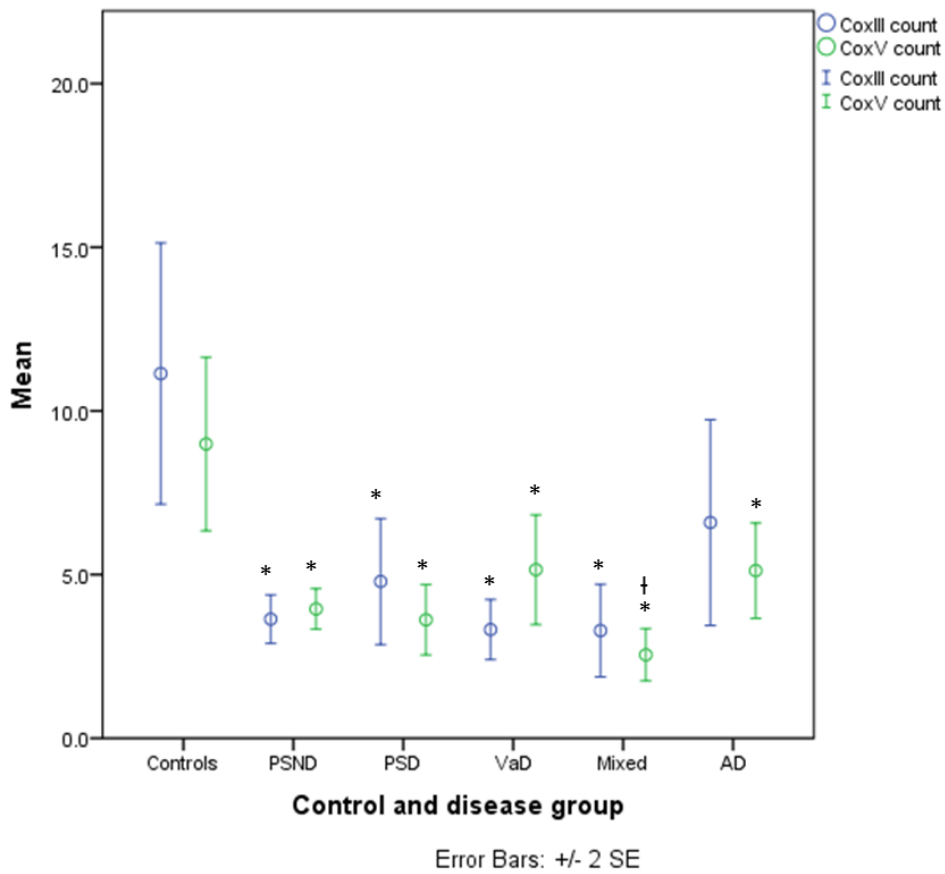


Figure 6-6 showing average COX4 positive pyramidal neuron count in layers III and V of the dIPFC. Controls = aged controls, PSND = post-stroke non-demented, PSD = post-stroke demented, VaD = vascular dementia, mixed = mixed vascular and Alzheimer's disease, AD = Alzheimer's disease. \* = Significant to controls. † = significant to AD. Controls vs PSND ( $p = 0.001$ ), PSD ( $p = 0.013$ ), VaD (0.001), and mixed (0.001) in layer III. Controls vs PSND ( $p = 0.002$ ), PSD ( $p = 0.002$ ), VaD  $p = 0.031$ , mixed ( $p = 0.002$ ), and AD (0.019). Mixed vs AD ( $p = 0.044$ ) in layer V.

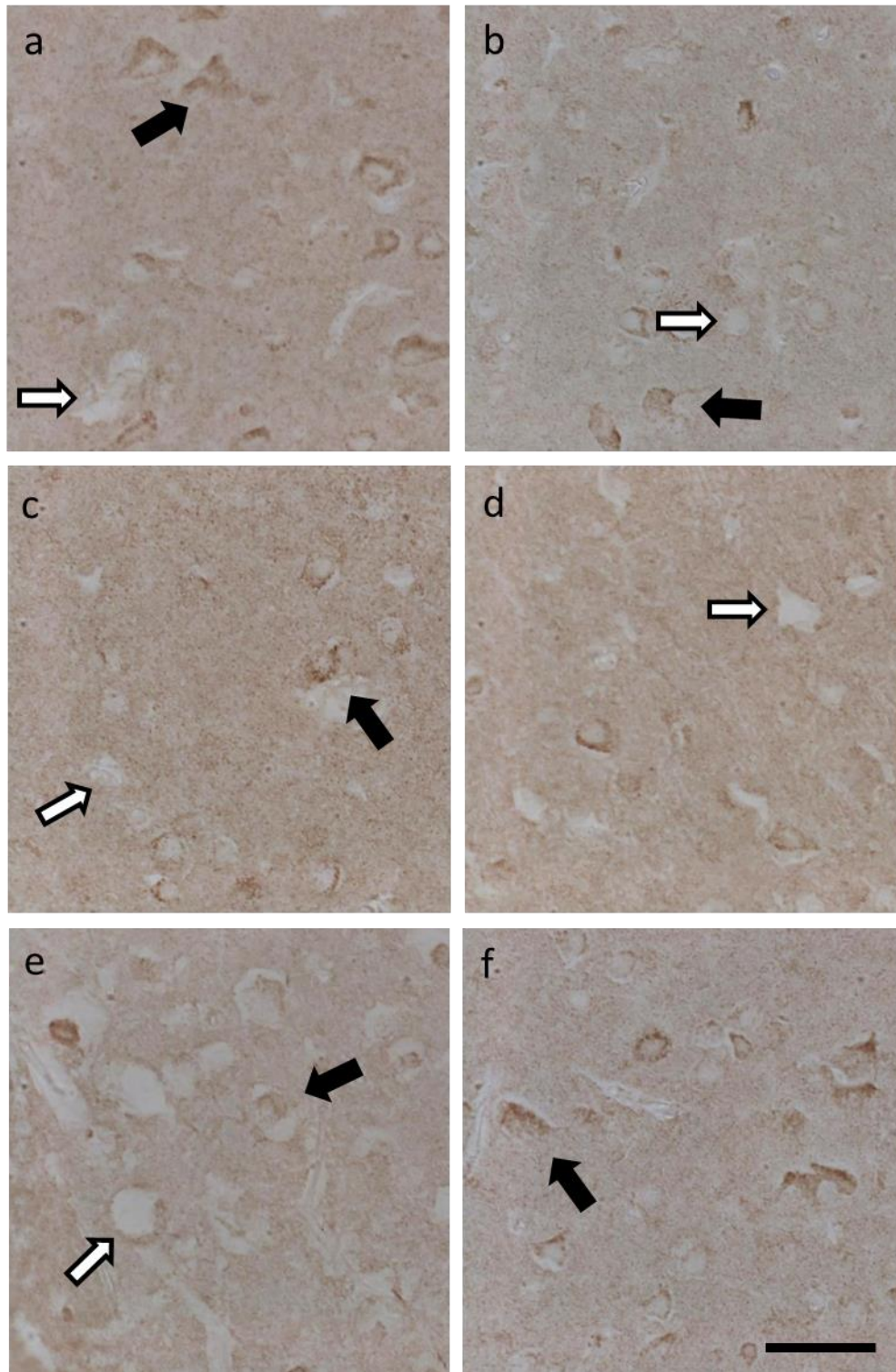


Figure 6-7 showing COX4 positive pyramidal neurons in layer V of the dIPFC. a) aged-controls, b) PSND c) PSD, d) VaD, e) Mixed, and f) AD. Solid arrows indicate positively stained pyramidal neurons, hollow arrows indicate negatively stained pyramidal neurons. Size bar = 20 $\mu$ m.

### 6.3.3. COX4 positive neurons as a percentage of total pyramidal neuron population.

ANOVA testing revealed no difference between groups in layer III ( $p = 0.258$ ), but did find significance in layer V ( $p = 0.002$ ). There was no significant difference between post-stroke demented or non-demented subjects in either layer. However, both PS subject groups (PSND  $p = 0.006$ , PSD  $p = 0.043$ ) VaD ( $p = 0.005$ ), and mixed dementia ( $p = 0.010$ ), showed significantly lower percentages of positively stained neurons when compared to controls. This finding was not repeated in AD ( $p = 0.608$ ) (Figure 6-8).

#### 6.3.3.1. *Correlations between GRP78, COX4 and clinical variables*

Layer III GRP78 counts correlated significantly with COX4 p/a staining in both layers III ( $\sigma = 0.267$ ,  $p = 0.039$ ) and V ( $\sigma = 0.275$ ,  $p = 0.035$ ). In PSD total GRP78 positive counts significantly correlated with COX4 p/a staining in layer V ( $\sigma = 0.476$ ,  $p = 0.039$ ). GRP78 counts correlated with COX4 percentage counts in layer III ( $\sigma = -0.361$ ,  $p = 0.005$ ).

In the PS cohort the percentage of COX4 positive pyramidal neurons in layers III and V correlated with both executive function ( $\sigma = -0.647$ ,  $p = 0.004$ ,  $\sigma = -0.679$ ,  $p = 0.002$  in layers III and V respectively) and vascular pathology ( $\sigma = 0.552$ ,  $p = 0.010$ ,  $\sigma = 0.568$ ,  $p = 0.007$  in layer III and V respectively). Additionally attention ( $\sigma = 0.552$ ,  $p = 0.010$ ,) and calculation ( $\sigma = 0.568$ ,  $p = 0.007$ ) in layer V.



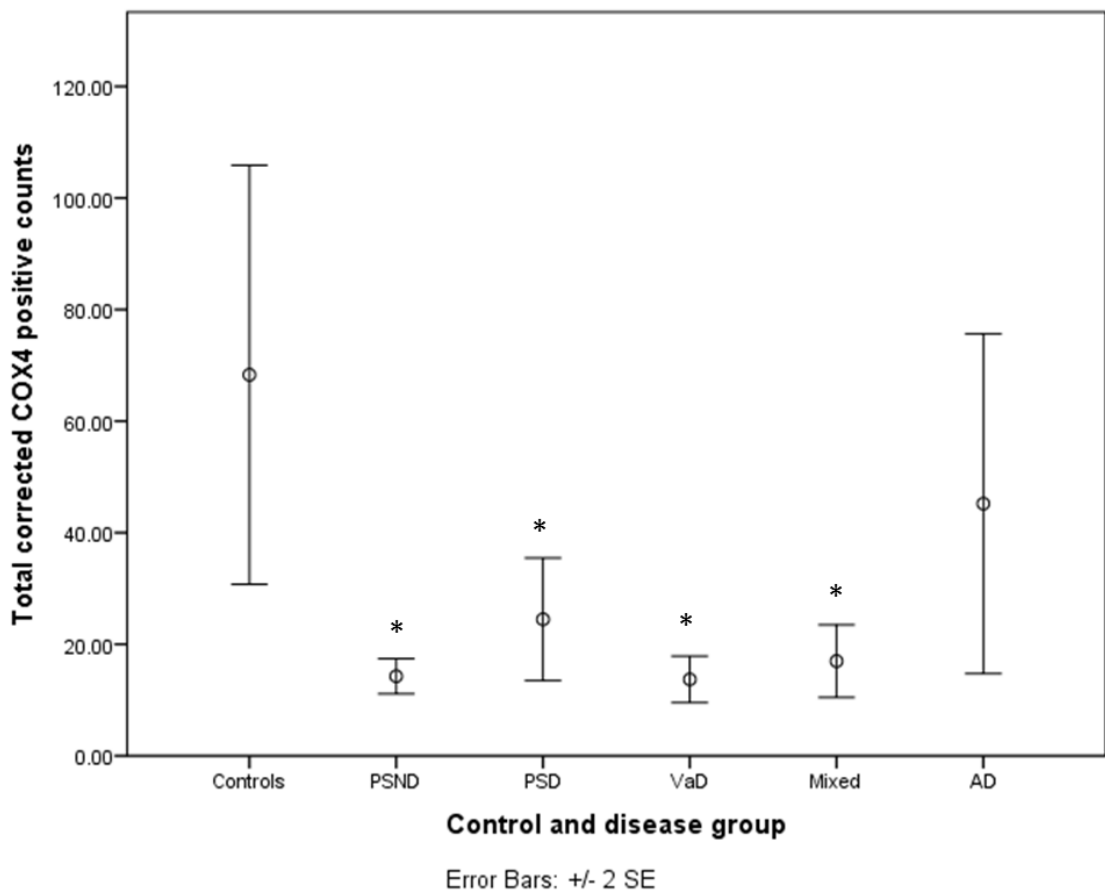


Figure 6-8 showing COX4 percentage differences of positively stained pyramidal neurons vs GRP78 total counts in layer V of the dIPFC. Controls = aged controls, PSND = post-stroke non-demented, PSD = post-stroke demented, VaD = vascular dementia, mixed = mixed vascular and Alzheimer's disease, AD = Alzheimer's disease. \* = Significant to controls. Controls vs PSND ( $p = 0.006$ ), PSD ( $p = 0.043$ ), VaD ( $p = 0.005$ ), mixed ( $p = 0.010$ ).

#### **6.3.4. Co-localisation of COX4 and GRP78**

Fluorescent imaging revealed co-localisation (yellow) of COX4 and GRP78 in both control and AD subjects. Where the two antibodies did not co-localise vessels appeared red, indicating GRP78. There was noticeably less in co-localisation in PSND, PSD, VaD, and mixed groups, though co-localised neurons were still present in these groups. Blood vessels appeared in auto-fluorescence green, or attract un-specific staining from COX4 antibody (Figure 6-9). Figure 6.9 demonstrates the increased COX4 staining (green) in aged controls, with minimal COX4 present in PSD subjects, though it is not absent. GRP78 staining appears clearly in both aged-controls and PSD subjects (Figure 6-10).

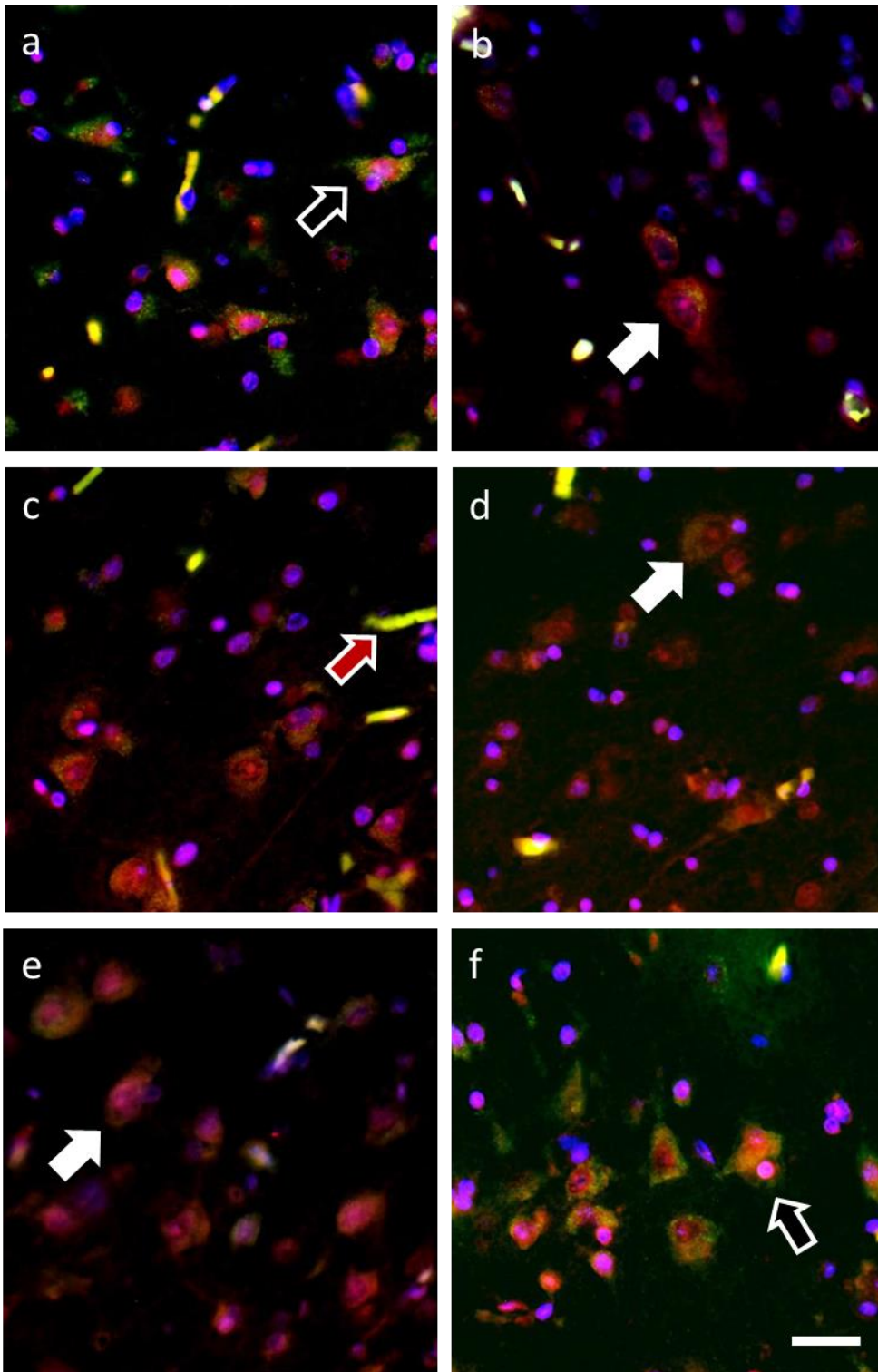


Figure 6-9 fluorescent image showing the co-localisation of COX4 antibody (green), and GRP78 (red) in pyramidal neurons in layer V of the dIPFC. Where antibodies are co-localised the image will appear yellow. Blue = DAPI. a) aged-controls, b) PSND, c) PSD, d) VaD, e) Mixed, and f) AD. Open arrows indicate co-localisation of GRP78 and COX4 within pyramidal neurons. White arrows indicate GRP78 positive, COX4 negative pyramidal neurons. Red arrows indicate vessel auto-fluorescence green. Size bar = 10µm.

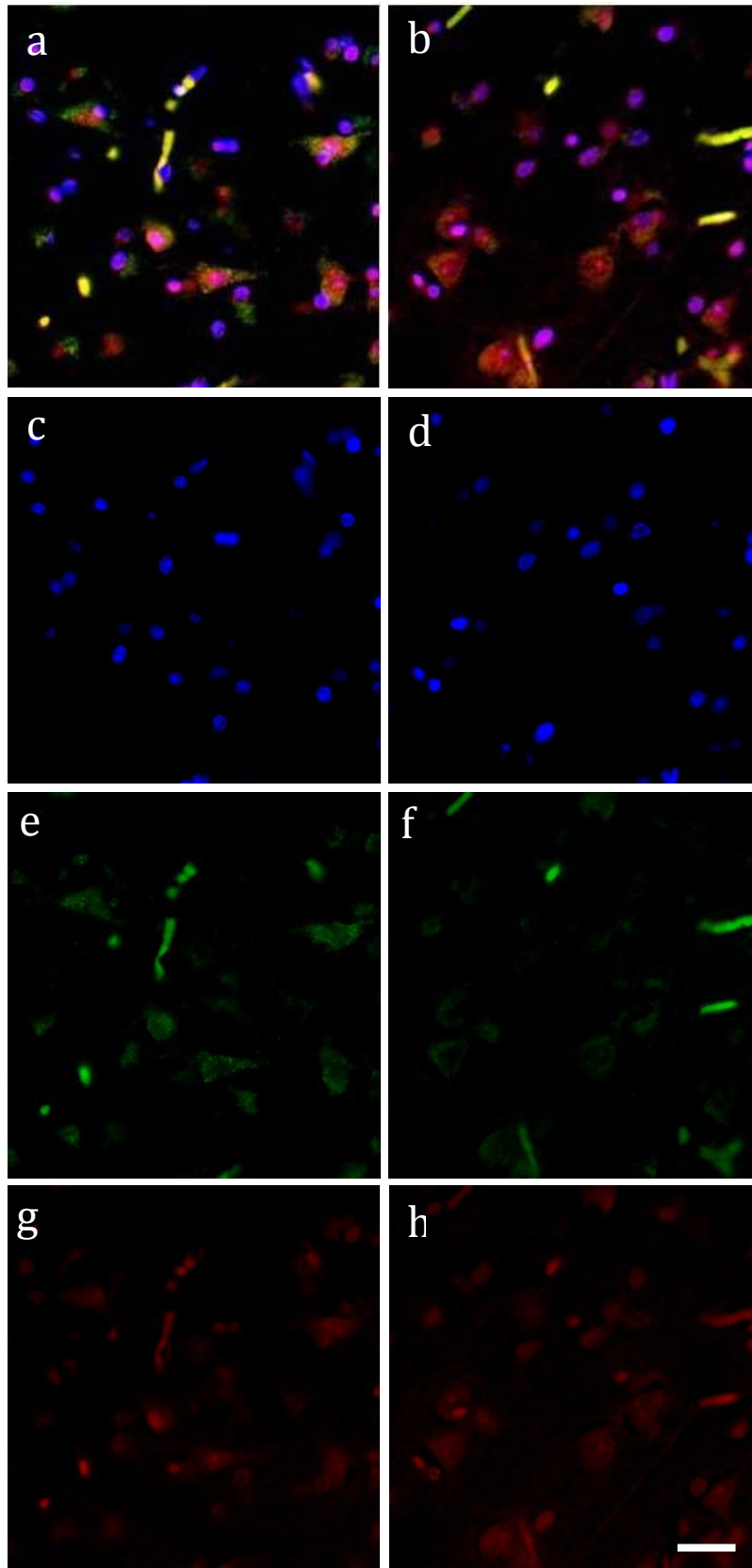


Figure 6-10 showing separate fluorescence images for DAPI (c, d), COX4 (e, f), and GRP78 (g, h) in control (left column) and PSD (right column) subjects. Images 'a' and 'b' show composite of images for control and PSD subjects, respectively. COX4 = green, GRP78 = red, DAPI = blue, co-localisation = blue Size bar = 10 $\mu$ m.

### 6.3.5. Estimation of dendritic arbour

The dendritic arbour is affected in stroke (C. E. Brown et al. 2007). To establish whether this vulnerability plays a role in the development of PSD it was necessary to investigate dendritic arbour in those with PSND and PSD. Golgi staining techniques have been used previously to stain individual dendritic branches (Gabbott and Somogyi 1984; Dall'Oglio et al. 2010). The capricious nature of the stain results in isolated dendrites which are clear enough to study. Once the dendritic arbour of individual pyramidal neurons was highlighted, 3D stereological techniques would then be used to evaluate the length density (Burke et al. 2014; Foster et al. 2014) between PSND and PSD subjects

Unfortunately, we were unable to repeat the results previously achieved by others and the Golgi staining proved too capricious and selective to allow for suitable and reliable analysis (Figure 8-1). Preliminary results are provided in the Appendix A.

## 6.4. Discussion

### 6.4.1. Analysis of GRP78 in the dIPFC

#### 6.4.1.1. *GRP78 analysis of the dIPFC*

GRP78 immunostaining revealed no significant difference between PSND and PSD in layer III of the dIPFC, however in layer V showed significantly higher in PSD when compared to PSND. GRP78 is expressed in all cell types, both on the cell surface and internally in relation to ER (Quinones et al. 2008), so any change would have to be rather profound in order to detect it using 2D densitometric analysis. Due to this high expression, the changes in cell counts would suggest fewer neurons were present in PSND subjects which was surprising as 3D analysis did not reveal any changes to pyramidal neuron density. Though increased GRP78 has been found in a range of disease states (Quinones et al. 2008; Yang et al. 1998), a more subtle method may be required. However, this method did confirm that GRP78 staining is ubiquitously present in all pyramidal neurons. It has however been reported that

endoplasmic reticulum associated GRP78 is increased in disease states such as tumour growth in an attempt to protect the cell against the undesirable environment the disease creates. The lower levels found in the two post-stroke subjects groups when compared to aged controls may suggest that perhaps this protective mechanism is not functional in these cases, increasing the burden of pathology. However, this would not explain the low levels of GRP78 p/a staining in PSND.

It has been shown in cell culture that increased expression of GRP78 protects against oxidative stress and excitotoxicity (Yu et al. 1999), and GRP78 has also been associated with the up regulation of cytokines such as interleukin-6 and tumour necrosis factor- $\alpha$  as well as increasing the activity of microglia (Kakimura et al. 2001). The increased expression shown in PSND when compared to controls may be a result of this increased neuroprotective response, and possibly relates to why these subjects have not developed PSD. The PSD cohort expressed comparable levels to that of controls and therefore appears not to have developed an adequate enough response to starve the cell damage.

#### 6.4.1.2. ***GRP78 positive pyramidal neuron counts***

Interestingly, individual neuronal counts did not follow the same pattern as that for p/a staining. PSND revealed significantly higher GRP78 positive neurons than controls and PSD, with VaD also significantly higher than AD within layer V. As it is understood that GRP78 is expressed in all cells in the human body, this data suggest that there are a higher number of pyramidal neurons present in the layer V of the dIPFC in PSND and VaD. This data was unexpected and contradicts our original findings regarding 3D stereological estimates of neurons in layer V.

#### 6.4.2. **COX4 analysis of pyramidal neuron metabolism**

##### 6.4.2.1. ***COX4 Immunoreactivity in pyramidal neurons.***

There were no significant differences observed between the PSND and PSD in COX4 immunoreactive neurons in layers III and V of the dIPFC despite quite marked differences observed between disease subjects and control groups. The smaller pyramidal neurons observed in demented subjects may explain the

reduced area expressing COX4, with neurons physically unable to express a higher degree of immunoreactivity, however, this does not explain why lower immunoreactivity was also observed in PSND, where pyramidal neuron volume was comparable to aged-controls. It has been put forward that COX4 is a reliable surrogate marker for decreased metabolic activity within a cell (F. N. Wong-Riley, Robert F. Hevner, Suyan Liu 1998; M. T. Wong-Riley 1989). If this is the case it may suggest a potential mechanism for decreased pyramidal neuronal volumes within demented subjects, however, the findings in PSND does not support this. Though interesting, metabolism is a dynamic process and it is unlikely that COX4 expression within pyramidal neurons is the whole story. However, it does suggest a possible protein or structural change which may have some impact on the cells function.

#### 6.4.2.2. ***COX4 counts***

The next step was to establish whether this apparent decrease in COX4 immunoreactivity staining was representing changes in mitochondria within individual pyramidal neurons, or whether it was due to a reduction in the gross number of pyramidal neurons expressing the protein. To elucidate which, the number of individual pyramidal neurons expressing positive staining for COX4 in each case were counted. COX4 positive pyramidal neuron counts revealed a similar pattern to immunoreactivity expression with all disease groups showing decreased positively stained pyramidal neurons when compared to controls (with the exception of AD in layer III). There was no significant difference between the number of COX4 positive pyramidal neurons between PSND and PSD, which again suggests that pyramidal mitochondrial dysfunction is not involved in the development of PSD, or the cause of decreased pyramidal neuronal volumes in the dlPFC. These data suggested that the lower immunoreactivity was due to fewer pyramidal neurons expressing COX4. There was no change in pyramidal neuron density in layers III or V as measured using 3D stereology, so it would appear these neurons were present, but absence of COX4.

#### 6.4.2.3. ***COX4 counts corrected with GRP78 total neuronal counts.***

This finding suggests the initial decreases in immunoreactivity are likely a result of decreased COX4 expression in individual neurons. However, it is unknown which proportion of the total neuronal population are COX4 positive. To

elaborate on these results, total pyramidal neuron counts were performed on GRP78 stained sections. GRP78 ubiquitously throughout the brain and will therefore mark each pyramidal neuron clearly (Quinones et al. 2008). By relating COX4 positive pyramidal neuron counts to the total pyramidal neuron population it may be possible to establish whether or not there is a decrease in healthy, metabolically active pyramidal neurons in the dlPFC.

There were a significantly lower percentage of COX4 positive neurons in PSND (14%), PSD (25%), VaD (14%), and mixed subjects (17%) when compared to aged-controls in layer V of the dlPFC. This change was not apparent in layer III. These data directly contradicts those reported previously on decreases in AD but not CVD (Chagnon et al. 1995). However, studies in rat models have found that in ischaemic disease reduced COX activity in the CA1 and other brain regions is a predictor of neuronal damage, preempting damage to the cell soma (de la Torre et al. 1997; Cafe et al. 1994) and suggest that COX4 expression may play a role in neuronal soma volume changes, as those previously reported in the dlPFC. The current study found the percentage of pyramidal neurons expressing COX4 significantly correlated with vascular pathology in those who had suffered a stroke. This data provides evidence that CVD may have a profound effect on mitochondrial and cognitive function. It appears the dysfunction of mitochondria has a profound effect on pyramidal neurons, impacting cognitive decline. Indeed in post-stroke subjects COX4 expression correlated with executive function, suggesting that lower COX4 expression may be a marker of reduced pyramidal neuron activity in layer V in the dlPFC, influencing the clinical outcomes in those suffering a stroke.

a) Only pyramidal neurons in layer V appear to be affected with dysfunctional 'power units' in disease groups, suggesting that those neurons which are responsible for long range projections throughout the brain (Khundakar et al. 2009; Tekin and Cummings 2002). It is plausible these neurons, have a very high metabolic demand (Attwell and Laughlin 2001) due to their crucial roles within the brain and would struggle to function correctly, if they have fewer, or less functional mitochondrial units. This stress may result in gradual dysfunction of the neuron, potentially affecting the dendritic arbour processes and other cellular processes



b) That only vascular based pathology appears to be affected in this way. This finding separates the vascular based pathologies from the neurodegenerative disease states and suggests a separate pathway, or disease progression between these diseases. In turn it reinforces the concept that different triggers, resulting from a arranged of pathologies, may have similar impacts on the brain (Wardlaw et al. 2003). In this case, this impact is shrunken pyramidal neurons.

COX4 expression in AD was expected to follow a similar pattern to that of VaD and mixed, however it was more comparable to that of control subjects. As previously mentioned, AD has been shown to express significantly lower levels of COX4 when compared to controls (F. N. Wong-Riley, Robert F. Hevner, Suyan liu 1998). Given the findings in other disease groups, this omission is unexpected. Additionally, the previous findings reported in chapter 3 would have led to the assumption that COX4 would follow a similar pattern in AD subjects, as CVD subjects

Interestingly, the correlation between GRP78 counts and COX4 counts in layer III suggest there is a distinct relationship between the two proteins, reinforcing the concept that COX4, like GRP78 is, under usual circumstances, active and present in the majority of pyramidal neurons. This finding was not repeated in layer V of the dlPFC, were not all pyramidal neurons appeared to expressed COX4, but did express GRP78. Together these correlations suggest GRP78 as a suitable marker for marking pyramidal neurons.

#### **6.5. GRP78 and COX4 co-localisation.**

The above findings suggest that a population of pyramidal neurons in demented subjects express GRP78 but not COX4 and that a higher population of pyramidal neurons expressing both COX4 and GRP78 would be found in aged-controls and AD subjects when compared to PSND, PSD, VaD, and mixed dementia. Immunofluorescence revealed a higher proportion of GRP78 and COX4 co-localisation in aged-control and AD subjects as suggested by the higher incidence of yellow fluorescence demonstrating a combination of both green (COX4) and red (GRP78). Figure 6.9 demonstrates the individual fluorescent staining of GRP78 and COX4 separately in aged-control (high levels of COX4 immunoreactivity) and PSD subjects (low COX4 immunoreactivity). GRP78 is comparable between the two groups which suggests its ubiquitous

nature. Though great effort went into suppressing the autofluorescing of lipofuscin (which can be an inherent issue when using human tissue) it is possible that some of this was picked up in the green and may have given the appearance of COX4 positive staining. However, the uniform nature of the green fluorescence does not support this theory (lipofuscin appears more granular and punctate). Though qualitative, this data does appear to support the notion that some pyramidal neurons within the dIPFC do in fact not express COX4, whilst GRP78 appears to be ubiquitous throughout the cortex.

### **6.6. Golgi analysis of the dendritic arbour**

Unfortunately the nature of the Golgi stain resulted in no reliable analyses with which to assess dendritic arbour in the dIPFC (Figure 8-3). The apparent random nature of the staining would have made unbiased analysis impossible, and the clustering nature of the stain compounded this issue by making the image distorted, making the selection of individual dendritic limbs very difficult.

#### **6.6.1. Conclusion**

GRP78 appears to be ubiquitously expressed in control and demented subjects and therefore a reliable cellular marker, though the unexpected lower expression in PSD subjects should be taken into account. Decreased COX4 does appear to be markedly reduced in disease subjects, suggesting it may be a potential marker for an underlying pathological process. Layer V appeared to be most impacted in CVD subjects, suggesting the long axonal projections of the dIPFC are most affected and vulnerable. COX4 counts did suggest that specific populations of pyramidal neurons appear to express the protein whilst others did not, and that this was the reason for lower immunostaining in VaD, Mixed, and AD cases. This data was supported by accompanying fluorescent staining. Unfortunately Golgi staining revealed sections which were inappropriate to analyses. However, the Golgi is a proven technique for staining dendrites and it is necessary for further work to be done to quantify dendrites and to establish their role in the development of PSD.

## **Chapter 7. Discussion**

### **7.1. Introduction**

The aim of this project was to establish the neuropathological substrates of post-stroke dementia (PSD), and what role the frontal lobe plays in the development of executive dysfunction. Using clinically well characterised post-mortem tissue, we investigated neuronal morphology and density, glial cell populations, and WM pathology to achieve a better understanding of the underlying causes of cognitive impairment including executive dysfunction which might be attributed to the frontal lobe in PSD. The study involved the use of 88 brains from post-stroke subjects which have come to autopsy in addition to those collected from other dementias from our prospective clinical cohorts. The use of a large brain sample, including those from neurodegenerative disease, allowed for the comparison of disease processes and demonstrate specificity for changes relating to vascular aetiology.

### **7.2. Morphological changes in the dIPFC**

Three-dimension stereology revealed significant (about 30-40%) cell volume reduction of pyramidal neurons in the dIPFC of PSD subjects and in other dementias (AD, Mixed, and VAD) in both layers III and V, when compared to PSND and aged controls. This was not evident in the ACC or the OFC. These results suggest the decrease in neuronal volume is a regional specific pathological response to dementia in dIPFC. Investigations into cortical atrophy revealed that there was little or no atrophy with the dIPFC which would explain the neuronal shrinkage in these subjects.

Pyramidal neuron atrophy correlated with global cognitive and executive dysfunction scores in the post-stroke group suggesting smaller, atrophied neurons may not be functioning normally and contribute to the cognitive impairment. Previous studies on PSD have also found reduced pyramidal neuronal volumes in the hippocampus (Gemmell et al. 2012). The hippocampus has a range of connections with the frontal lobe, with a strong interplay between

the two areas which may explain the reduced global function and reduced memory scores (Laroche et al. 2000; Tekin and Cummings 2002) which builds the complexity of the disease process. These connections may underlie the correlations between memory scores and pyramidal neuron changes in the prefrontal cortex.

Damage to the frontal lobe has been previously related to executive dysfunction (S. W. Anderson et al. 1991), with stroke affecting fronto-subcortical circuitry (E. Burton et al. 2003; E. J. Burton et al. 2004; Pohjasvaara et al. 2002). Other disease states affecting the frontal lobes, such as FTD, (Huey et al. 2009) also result in executive dysfunction. There was no apparent relationship between AD type pathology and reduced pyramidal volumes in PSD, which was also evident in the hippocampus (Gemmell et al. 2012) suggesting either a) the neuronal volume reductions are the result of a common pathology between the demented groups, i.e. vascular disease pathology; present in all disease cases including AD (Jellinger 2002; Jellinger and Attems 2003; Kalaria 2003) or b) pyramidal volume changes are a common end point to multiple triggers (from stroke to Alzheimer-type disease (Wardlaw et al. 2003; Vaux 1993). Evidence suggested the latter b) is more likely, with similar findings amongst other disease types, such as depression, schizophrenia, and autism (Courchesne et al. 2011; Pierri et al. 2001; Khundakar et al. 2009). Indeed studies attempting to link the processes which precede the development of AD and schizophrenia have suggested that schizophrenia may be a form of premature dementia (Douaud et al. 2014), occurring at a different end of the age spectrum compared to AD, affecting younger individuals.

The pathological complexity of diseases such as AD and vascular pathology make it very unlikely that the underlying mechanism which resulted in pyramidal volume reductions and cognitive impairments in PSD, VaD, mixed dementia, and AD are the same. A previous study (Regeur et al. 1994) has suggested that the neuronal volume reduction was an artefact resulting from the selective vulnerability of larger neurons to disease. Once these neurons succumbed to the disease state only smaller neurons were left, thus reducing the average size of the population. However, there were no changes in neuronal density in any disease group, an observation which suggests that at least in the dlPFC the majority of neurons are still present. These findings, along with previous

hippocampal data suggest that neuronal atrophy is not a global process with neurons in different areas of the brain responding differently to pathological stress.

The lack of neuronal volume changes in the OFC or the ACC was surprising and unexpected. It is possible other factors prevent global deterioration, preserving some brain regions even when connected in the same frontal circuits. Further investigations into other components making up the cortex, and the cortical circuits are necessary to develop a greater understanding of the environmental factors which contribute to dementia, in PS subjects and other dementias.

### **7.2.1. The causes of cognitive dysfunction**

Overall, the above findings have some interesting implications: Firstly, that most neurons are preserved in dementia. Secondly, affected neurons appear to atrophy as detected by reduced volumes. Thirdly, that these atrophied neurons appear to dysfunction to such an extent that they result in cognitive impairment. This association of pyramidal neuronal volume with cognitive dysfunction may be key to deciphering why some post-stroke subjects develop cognitive decline in the form of PSD and others do not. In this respect, four hypotheses can be proposed that provide theories as potential links between pyramidal neuron atrophy and dementia; decreases in pyramidal neuron volume may represent:

1. The neurocentric hypothesis for the breakdown of the neurovascular unit.
2. The degeneration of the white matter and disruption of cortical circuitry.
3. Decreased metabolic output, dysfunctional ineffective neuron.
4. The collapse of the dendritic arbour.

These theories are explored below.

### **7.2.2. The neurocentric hypothesis for the breakdown of the neurovascular unit**

Traditionally, the theory behind cognitive impairment has been largely neurocentric, with pathology and dysfunction of the neuron at the centre of cognitive dysfunction and glial cells relegated to supporting roles (Verkhatsky et al. 2012). However, it is now well understood that the intricate nature of brain

function and cell survival is created in part through the cooperation between a wide range of cells, particularly the neurovascular unit (Giaume et al. 2007; Verkhratsky et al. 2012).

Investigations into glial cell density suggested astroglial numbers were not significantly reduced in PSD and other dementias when compared with controls, in either layers III or V. Given that astrocytes have a role in controlling homeostasis within the CNS (Danbolt 2001; Walz 2000) it is surprising that there was not a more prominent change in their numbers post-stroke.

Some subtle relationships between pyramidal neuron atrophy and glial cell density were detected. In PS cases, glial cell density positively correlated with pyramidal neuronal atrophy. These data suggest that though pyramidal neuron atrophy appears to play a role in executive dysfunction, glial cells appear to have some involvement. Though this finding is suggestive of glial cell involvement, supporting the glialcentric view to disease progression (Smith 2010; LoPachin and Aschner 1993; Mutch 2010), further work into the role of astroglia, and other cells, needs to be embarked upon to shed light in this area. If the susceptibility of glial cells to excitotoxicity (Nedergaard and Dirnagl 2005) plays a significant role in cognitive decline, treatments targeted at the protection of these cells may be a viable treatment against the development of dementia. Indeed, it has been shown that the condition of neighbouring glial cells following a stroke can have a great impact on the outcome of the subject (Nedergaard and Dirnagl 2005). Astrocytes control synaptogenesis and synaptic pruning, shaping the architecture of connections within the GM during development and throughout adulthood (Nedergaard et al. 2003; Pfrieger 2009, 2010) which can be crucial in recovery following stroke (Nudo 2003), as previously mentioned, dendritic arbour may have a critical impact on pyramidal neuron volume (Harrison and Eastwood 2001). Though astroglia did not appear to be reduced in number it is possible that individual cell function and morphology is affected in dementia. Further study into the biochemistry and morphology of astroglia will shed more light on the role these cells play in the development of PSD.

In addition to the neurovascular unit, the prefrontal cortex relies on an intricate arrangement of neurons known as minicolumns (Opris and Casanova 2014). These minicolumns consist of neurons sending and receiving signals to

each other as they control executive and behavioural functions, with executive abilities arising from cortico-cortico interactions within the prefrontal cortex, in microcircuits. Damage to these circuits, which has been reported in AD may result in dysfunction of this intricate network (Opris and Casanova 2014). Breakdown of pyramidal neuron connection within this circuit in PSD may well contribute to the executive dysfunction observed in these subjects.

### **7.2.3. WM pathology and pyramidal volume change in the frontal lobe**

Previous imaging studies have found significant levels of WM hyperintensities in this post-stroke cohort (E. Burton et al. 2003; E. J. Burton et al. 2004; O'Brien et al. 2002). These are often indicative of underlying WM pathology, which, if present, would help explain the pyramidal neuronal atrophy. Both studies into axonal myelination changes, as well as direct axonal damage did not reveal any significant changes between PSND and PSD subjects. Some myelin pathology was observed in the vascular cohort, which agreed with previous findings (Ihara et al. 2010). These data were unexpected as it was hypothesised that WM damage may explain why pyramidal neurons in the dlPFC were atrophied through retrograde degeneration (V. H. Perry et al. 1991; Richardson et al. 1982; Spöndlin 1975). However, changes in the WM which would just impact the dlPFC would have to be subtle, and specific, as to not also impact the pyramidal neurons in the OFC or the ACC. Axonal connections from each of the three pre-frontal cortices, though originating in different locations, eventually come together as they share similar circuitry as each other (Abeles 1991; Lichter and Cummings 2001; Tekin and Cummings 2002), so it is likely that any gross, non-specific pathological changes, i.e. those occurring due to a stroke or breakdown of a nearby vessel within the WM, would result in unbiased damage to each of the axonal tracts. This in turn may then result in decreased pyramidal neuronal volume in both the ACC and the OFC. With this in mind, any potential WM changes which only affect the dlPFC may be too subtle to be picked up by this method, as any disease related pathology may be lost in the overall pathology resulting from age (Kalaria 1996). However, results on WM changes within the VaD subjects do not support this.

The lack of correlation between axonal damage and myelin degeneration to morphological changes within the GM in PS subjects may suggest that there is indeed a minimal relationship between WM pathology and the GM neuronal

atrophy in PSD in this cohort. This would reinforce the concept of pathology originating within the GM. These data do appear to suggest little correspondence between MRI data and detectable WM changes at post-mortem. However, if atrophy begins further down the circuit, for example the lateral dorsomedial aspect of the globus pallidus, this may result in retrograde damage, with connected areas of the circuit eventually being affected as well. The death of neurons in the globus pallidus would result in feedback to the connecting pyramidal neurons in the dlPFC, and not the OFC or the ACC (Tekin and Cummings 2002)

#### **7.2.4. Mechanisms for pathology in the dlPFC and cognitive dysfunction**

The evidence so far argues a neurocentric view to pyramidal neuron volume changes and the subsequent progression of PSD. From the evidence obtained neither WM, nor glial cell pathology appear to have a strong impact on the neuronal changes observed through the different disease groups. Therefore, it is unclear how these volumetric changes may result in cognitive impairment or indeed how the morphological changes occur in the first place. Analysis showed no clear association between GM and WM pathology in PS subjects despite suggesting that both PSND and PSD exhibit significantly higher pathology than aged-control subjects, suggesting pathology originates in the GM, affecting selective neurons, particularly pyramidal neurons. COX4 immunoreactivity suggested reduced immunoreactivity in both PSND and PSD subjects suggesting the mitochondrial units in these subjects have undergone some chemical or structural change. This finding was compounded by similar findings in VaD, mixed, and AD subjects. Reduced COX4 immunoreactivity. However, the PSND showed a similar pattern of COX4 staining, and raising the question as to why these neurons are not, too, atrophied.

It is unknown whether pyramidal neurons in demented cases are atrophied as a result of stroke, or that subjects begin life with smaller neurons than their non-demented counterparts, and are thusly more susceptible to developing dementia. This is an important distinction, though one which may be very difficult to prove in human subjects as it is impractical to assess pyramidal neuron volumes in the living. However, COX4 immunoreactivity was reduced between PSND and PSD as well as VaD and mixed dementia, with mixed dementia expressing an even greater degree of change. Therefore, COX4



immunoreactivity may be reduced in all demented cases as a result of hypoperfusion, which would explain why AD subjects did not follow the same pattern. It is therefore possible that PSND subjects, had they lived longer, would have eventually succumbed to PSD. However, due to comorbidity factors, they died before cognitive dysfunction became apparent.

COX4 expression was greatly reduced in diseased subjects. Though no correlation was found between pyramidal volume and COX4 staining, it can be suggested that smaller pyramidal neurons (those mainly present in the dlPFC of demented subjects) may have fewer fully functional mitochondria. Previous studies have found metabolic reduction in subjects following stroke, (Bruhn et al. 1989), VaD (Pascual et al. 2010), CVD (Kuczynski et al. 2009), and neurodegenerative diseases (K. Ishii et al. 1998; Blass 2001) suggesting a relation between metabolism and cognitive function, and may be related to the reduced COX4 staining reported here.

#### **7.2.5. Cognitive brain reserve.**

The findings reported in this study suggest several other factors which could contribute towards the development of dementia. The volumetric changes suggest that neuronal atrophy may result in PSD. However, if it is assumed that those cases with PSD (and other subjects who go onto develop dementia) are not suffering from atrophy of the pyramidal neurons, but initially begin life with smaller neurons in the first place, then different theory become prominent. Cognitive brain reserve, as described previously regards the brain's threshold capacity to resist pathology, and remain cognitively functional. Those with a higher cognitive reserve can withstand more than those with a lower reserve. With this in mind, those with smaller pyramidal neurons may only be able to withstand a specific level of CVD than those with larger neurons, and go on to develop PSD. Those with larger neurons starve of PSD until much later in life, and may well die before developing the syndrome. However, it is unknown whether all subjects would eventually go on to develop the disease or not.

### **7.3. Strengths and limitations of the study**

#### **7.3.1. The CogFAST study**

The CogFAST study offered this study access not only to processed and well characterised post-stroke brains, but the clinicopathological detail which was collected during the last years of life offered unique insight into to the clinical and cognitive state of the post-stroke subjects allowing for the comparison between pathological findings which can only be investigated after death with cognitive changes during life. Additionally, the CogFAST study provided two well characterised groups. The longitudinal ascertainment of dementia status enabled us to compare the brains of those who did develop dementia after a stroke with those who did not develop dementia after a stroke, providing a unique insight into post-stroke processes and PSD development. However, with all human cohort based studies, every desirable and ideal variable cannot be assessed and often longitudinal studies are limited when it comes to post-mortem analysis. The cut off age for inclusion in this study was 75 years old, with many much older. These subjects had all lived long, full lives, filled with varying degrees of risk factors, environmental factors, and personal factors. Each one of these factors is unaccounted for and may have an impact on our pathological findings.

#### **7.3.2. Additional disease subjects and aged-controls**

The inclusion of aged-controls, VaD, mixed, and AD allowed insight into the complex processes which may be compared with PSD. By comparing the findings of the PS cohort to these groups it was possible to identify whether changes were pathologically distinct from CVD or neurodegenerative process, or if PSD shared characteristics with a range of disease types. Though the insight gained from these cases was invaluable, only limited information could be learned from the disease states themselves. Though it was possible to relate pathological changes within the dlPFC to executive and cognitive functions, these data were not available to make such comparisons in other disease groups. Additionally, VaD, mixed, and AD groups were recruited into other studies with strict pathological criteria, aged controls were not. Elderly brains can have varying degrees of pathological changes which may impact findings in this study. Though this makes the aged-controls a realistic cross section of society, the use of clinically 'clean' brains in future studies may provide more

insight into disease states. However, it is important to include aged-controls as it provides a baseline of age-induced changes from which are representative of the general population and can tell us a lot about the relationship between pathology, and normal ageing. Other characteristics of post-mortem tissue are issues such as post-mortem delay (PMD), and fixation time (FT), though these were taken into account and it was ensured that neither FT nor PMD were factors in this study.

#### 7.3.2.1. ***Additional frontal pathology cases – Frontal temporal dementia***

In addition to the six groups analysed in this study, 3D stereology was also performed on the dIPFC of 4 subjects diagnosed with FTD. These subjects were analysed to investigate pyramidal neuron volumes in a disease group which specifically suffers from frontal pathology, and whether these subjects would follow a similar pattern to other dementia groups. The details of this study can be found in the appendix [Frontotemporal Dementia (FTD)]

### 7.4. **Future directions**

#### 7.4.1. **Morphological investigations**

This study has identified and outlined specific changes within the prefrontal cortex and related these changes to clinical occurrences and the outcome of dementia. Changes in dIPFC pyramidal neurons are clearly a relevant aspect of PSD, however, these changes can only ever be a small part of what must be a greater pathological process within the cortical circuits. It would be beneficial to our understanding of the prefrontal circuits in dementia to investigate further the components of the dIPFC. Whether the reported changes occur within cortex or whether the subcortical regions such as the caudate or the globus pallidus and thalamus (Tekin and Cummings 2002) is unknown. Further investigation would perhaps make the aetiology of the dIPFC GM changes, clearer.

It is important to understand the progression of the circuit's dysfunction. Are the pathological processes which originate and connect to the sub-cortical structures such as the globus pallidus of thalamus (critical areas in stroke)(Tatemichi et al. 1995) affected to the same extent as the cortical region of the dIPFC? As several sub-cortical regions are shared between the prefrontal circuits (Tekin and Cummings 2002) it would be interesting to establish at which

level the distinction between healthy and non-healthy circuits becomes apparent. Additionally, along the same vein, connections between the prefrontal circuits and the temporal lobe are potentially a key aspect to the development of dementia. With similar changes to pyramidal neuron morphology reported in PSD and other dementias within the hippocampus (Gemmell et al. 2012), the interplay between the two areas requires additional attention.

Though this study included a large range of disease groups, it is important to establish the pathology present in groups which are not affected by the ageing process. The 3D stereology should be conducted on the dIPFC in CADASIL subjects. This disease of pure vascular aetiology, which largely affects younger individuals, will help to eliminate the effect of age-related CVD and AD pathology and aid in clarifying the role of pure vascular pathology in the development of dementia (Craggs et al. 2013).

#### **7.4.2. Dendritic arbour and cognition**

The dendritic arbour is crucial in cellular communication within the CNS and is perhaps the most metabolically demanding structure of the neuron. Any changes to the metabolism within the brain may have a significant impact on these spines. Previous studies using Golgi methods have identified stunted dendritic arbour in those with dementia (Buell and Coleman 1979; Scheibel and Tomiyasu 1978), with decreased dendritic spines found on cortical pyramidal neurons (Catala et al. 1988). These findings, point towards an intricate relationship between dendritic arbour and cognition. Unfortunately, it was not possible to assess dendritic arbour in this cohort, as the Golgi stain was not sufficient to make accurate estimates of dendritic length, or condition. However, neuronal size has been linked to dendritic arbour (Harrison and Eastwood 2001) and is a potential clue as to the state of neuronal connectivity within the dIPFC. With this assumption, it would appear that dendritic arbour is significantly reduced in all demented subjects in this study, but perhaps most significantly; it appears to be intact in PSND and non-demented aged-controls. This distinction between the two PS cohorts perhaps highlights one of the most important findings which can be proposed, that the states of dendrites within the dIPFC may have a significant impact on the cognitive outcome of those suffering a stroke. However, further investigation will be required to confirm this hypothesis. It will be crucial to either establish a more effective Golgi-procedure

or develop a different technique to isolate the dendritic arbour in dementia. Once an effective method for dendritic staining has been established, quantification techniques such as 3D stereology can be used to accurately determine the state of the arbour between diseases.

#### **7.4.3. Biochemical basis for neuronal dysfunction**

The importance of the prefrontal circuits as a whole cannot be over expressed, however this study has reinforced the significance of the pyramidal neuron as a key individual component in the development of PSD and other dementias. Early biochemical changes should be investigated. The mechanism of apoptosis, which incorporates both cell death and cell shrinkage (Majno and Joris 1995), and how cellular mechanism affect the neuron would be valuable to understanding underlying cause of the shrinkage. In addition, cellular autophagy, the controlled destruction of cells may also play a role in neuronal atrophy. If a common apoptotic or autophagic mechanism was established as the main cause for cell shrinkage and dysfunction it would explain why disease groups with different aetiologies have similar morphological traits. Apoptotic mechanisms may be triggered by a range of pathologies, and it would be important to decipher if this mechanism is in operation in PSD.

#### **7.4.4. Genomics of the CogFAST cohort**

The CogFAST cohort, as a clinically well characterised post-mortem brains resource, has provided much information. There are still several factors and substrates which may be uncovered to explain how cognitive impairment occurs following a stroke. The next step may be to begin profiling the DNA of individual's within the cohort, with the aim to isolate potential risk genes which may be present in those developing PSD. The identification of these genes would allow for more targeted analysis of proteins, if a particular mutation is identified, for example, tracing the regulated protein further downstream may highlight previously overlooked proteins which could play a crucial role in PSD development. Indeed it may be possible to uncover a common pathway which is affected by a range of disease types, from vascular pathology, AD, to autism, and through to schizophrenia and depression. If a common gateway protein can be discovered it may open the way for targeted therapies and drug treatments, open up the understanding between the different disease groups, and help take the mystery out of varying types of dementia.

## 7.5. Conclusion

This study has highlighted several novel findings which outline potential pathological substrates which may ultimately result in dementia post-stroke (Foster et al. 2014). Pyramidal neuronal volumes were reduced in the dlPFC in PSD and other demented groups in both layers III and V when compared to PSND and aged-controls. These findings provide an insight into the potential mechanism responsible for the disruption of the prefrontal circuits which ultimately leads to executive dysfunctions within demented subjects. The lack of relationship between neuron volume changes and Alzheimer type pathology suggests an underlying vascular basis for cognitive dysfunction. The presence of atrophied neurons and lack of neuronal density changes suggest neurons in demented subjects are not lost, but dysfunctional, leaving some potential opportunity for future therapeutic targets.

Cortical glial cell densities were not significantly altered. This suggests that dementia resulting after stroke is a largely neuronal phenomenon. However, previous literature is in contradiction to this finding and it remains likely that glial cells play a central role in this disease state. Though 3D stereology is perhaps the best method for assessing the density of glial cells, further investigation with immunohistochemical and protein based analysis is required to further clarify the role of glial cells within PSD. Astrocytes have been reported to express large numbers of processes which interact with neurons, following a stroke, as well as having an important role in controlling glutamate regulation (Nedergaard and Dirnagl 2005). It will be necessary to understand the role this processes may have in the development of PSD.

Although some findings alluded to specific relationships between WM pathology in some disease states, it is not possible to link cognitive dysfunction and pyramidal neuronal volume changes in PSD. These data suggests PSD may be centred around pyramidal neuronal atrophy, with decreased neuronal connections potentially playing a large part in cognitive dysfunction following stroke.

Future studies will need to investigate the mechanisms which result in individual pyramidal neuron dysfunction between disease groups and to investigate whether these mechanisms can be suitable targets for therapy. Additionally,

further work into the dendritic arbour with the dIPFC, and its association to pyramidal neuron volume may be crucial to understanding PSD.

## Chapter 8. Appendix

### 8.1. Golgi staining

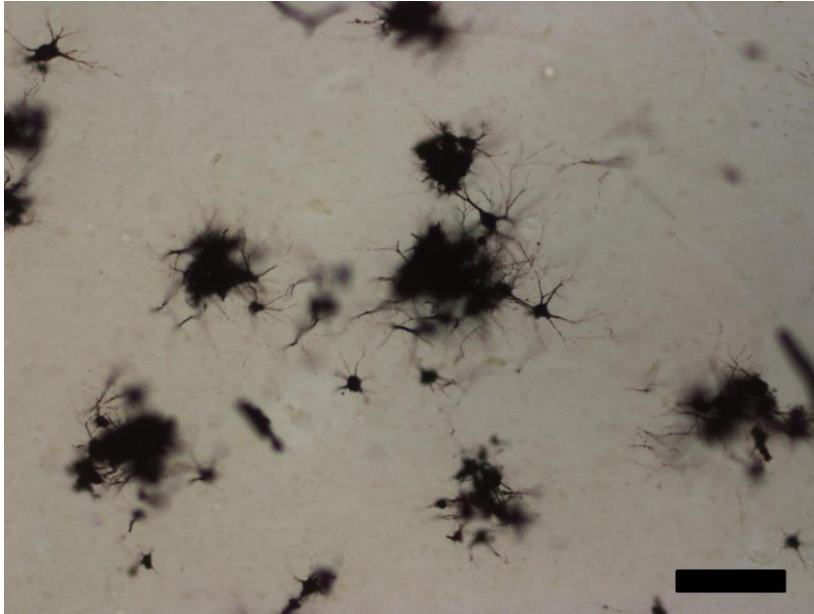


Figure 8-1 demonstrating the clustering nature of the Golgi-Kopsch technique on pyramidal neurons within layer III the dIPFC. Scale bar = 100 $\mu$ m.

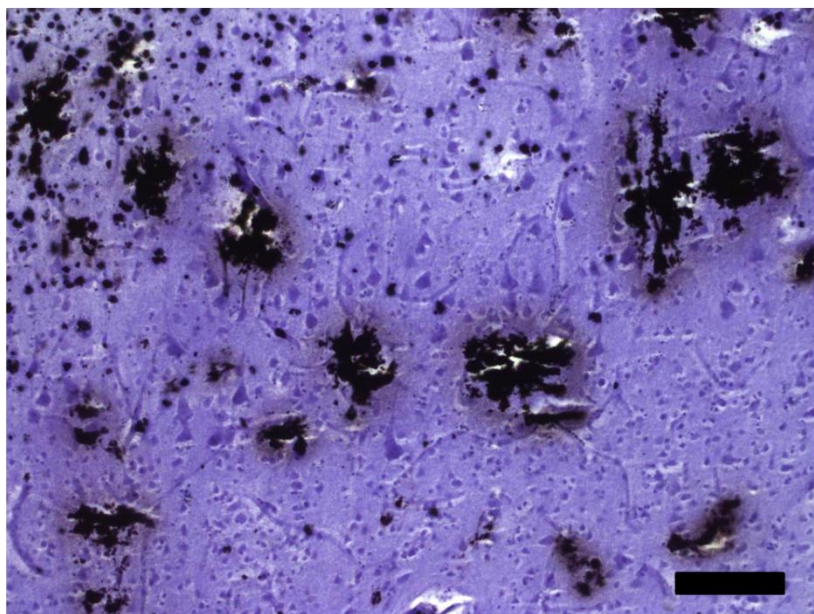


Figure 8-2 demonstrating the clustering nature of the golgi-kopsh technique. The section had been counterstained with nissl to demonstrate a specific sub-population of pyramidal neurons within layer III of the dIPFC have been unaffected by the stain. Scale bar = 100 $\mu$ m.





Figure 8-3 showing the Golgi techniques uniform staining of blood vessels within the frontal lobe.  
Scale bar = 100 $\mu$ m.

## 8.2. Frontotemporal Dementia (FTD)

Frontotemporal dementia is the second most common, early onset, dementia characterised by progressive behavioural changes, frontal executive dysfunction and language deficits (Ratnavalli et al. 2002). Frontotemporal dementia (FTD) is widely used to describe the clinical onset and characterisation of the disease, with the term frontotemporal lobar degeneration (FTLD) used to describe the pathological presentation and diagnosis. The disease classically presents with frontal and temporal atrophy and hypometabolism which can often be detected via MRI scans (Ratnavalli et al. 2002; Pickering-Brown 2007, 2010).

Relatively few studies have been conducted into the prevalence of frontotemporal dementia but it is thought that it affects between 15-22 per 100,000 of the population aged between 45-64 (half the prevalence of AD in this age group) with an average age of onset between 50-60 years of age (Ratnavalli et al. 2002; Harvey et al. 2003; Borroni et al. 2010).

Several variants for FTD exist: The behavioural variant (bvFTD), language or semantic variant (SD), and progressive non-fluent aphasia variant (PNFA). The progression of each FTD dementia presents with an insidious onset followed by a gradual decline in cognitive faculties with individual clinical syndrome indicative of different topographical cortical involvement (Ratnavalli et al. 2002; Pickering-Brown 2010): bvFTD with associated with symmetrical frontal and anterior temporal atrophy, PNFA with left frontotemporal dysfunction, and SD with anterior temporal deficits. The majority of FTD symptoms resolve around frontal lobe dysfunction. Despite this heterogeneity of cortical involvement each variant shares some similar symptoms: emotional blunting, apathy, loss of empathy and selfishness are symptoms shared by all variants though are indicative of bvFTD (Bathgate et al. 2001) making FTD an ideal clinical example of frontal lobe syndrome. Apathy has been associated with involvement of the anterior cingulate cortex (ACC), dis-inhibition with the orbitofrontal cortex (OFC), and executive dysfunction with the dorsolateral prefrontal cortex (DLPFC) (Huey et al. 2009) suggesting involvement of the three frontal cortical circuits.

When Theory of Mind (ToM) tasks are used to assess social cognition and empathy of early stage FTD, the test is thought to focus on deficits largely within the OFC. As the disease progresses additional frontal areas become increasingly involved. In late stage FTD ToM scores correlate with executive function deficits indicating increased pathology within the dlPFC (Libon et al. 2009; Eslinger et al. 2007).

MRI studies have shown involvement of both the frontal (including the Prefrontal circuits) and paralimbic areas in bvFTD with pathological studies finding high burdens of Tau in these areas (Pickering-Brown 2010). This atrophy spreads to more lateral frontal, more posterior temporal and more anterior parietal areas as the disease progresses, though the tauopathy variant of FTD appear more symmetrical and is restricted to the frontal and temporal lobes (Whitwell et al. 2007; Whitwell et al. 2009).

FTD offers a useful model for investigating neuronal networks in the frontal lobes. Underlying pathologies of FTD are heterogeneous though a third of FTD sufferers possess an autosomal dominant mutation (Pickering-Brown 2007). Mutations in the gene controlling microtubule-associated protein tau (MAPT) is thought to account for a high proportion of cases in which hyperphosphorylated tau builds up inside neurons of the frontal lobe, echoing AD (Pickering-Brown 2010, 2007). Patients with MAPT mutations frequently present with the bvFTD variant of the disease with executive dysfunction and episodic memory deficits (Pickering-Brown et al. 2008; Pickering-Brown 2010).

### **8.2.1. Three dimensional stereological analysis of the dIPFC in FTD subjects**

There were no apparent changes in pyramidal neuron densities in either layers III or V, separately or, when compared to control cases ( $p = 0.514$ , and  $p = 0.433$ , respectively). In addition no significant changes in pyramidal neuronal volumes were detected when compared to control groups ( $p = 0.151$ ,  $p = 0.151$ , respectively). However, when layer III and V were combined, total pyramidal neuronal volumes was significantly lower in FTD cases when compared to control cases ( $p = 0.044$ ). Total pyramidal neuronal densities were not significantly different between the two groups ( $p = 0.708$ ) (Figure 8-4, Figure 8-5).

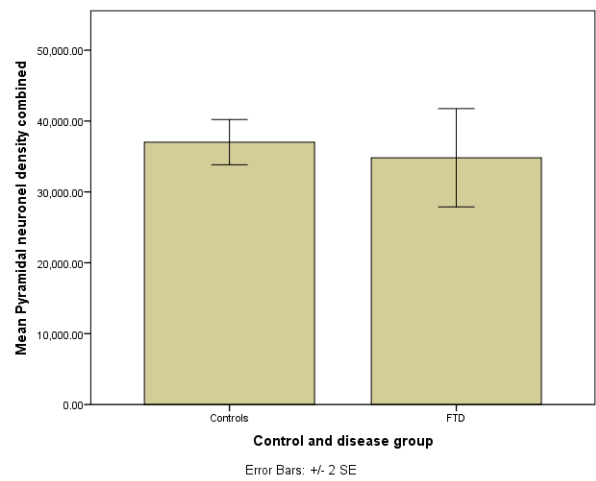
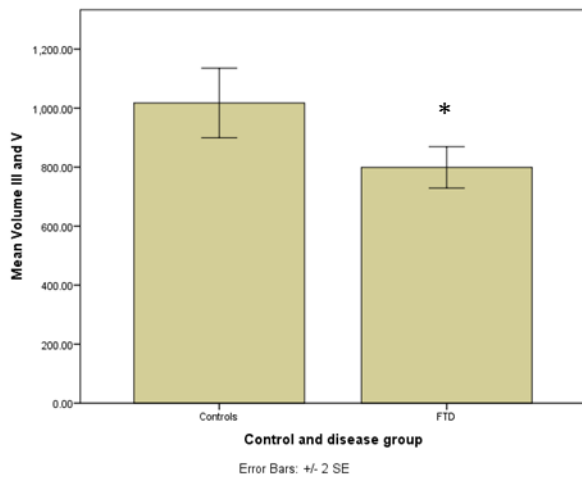


Figure 8-5 showing combined layer III and V pyramidal neuronal volume in the dIPFC in FTD subjects. \* = significant compared to controls ( $p < 0.044$ ).

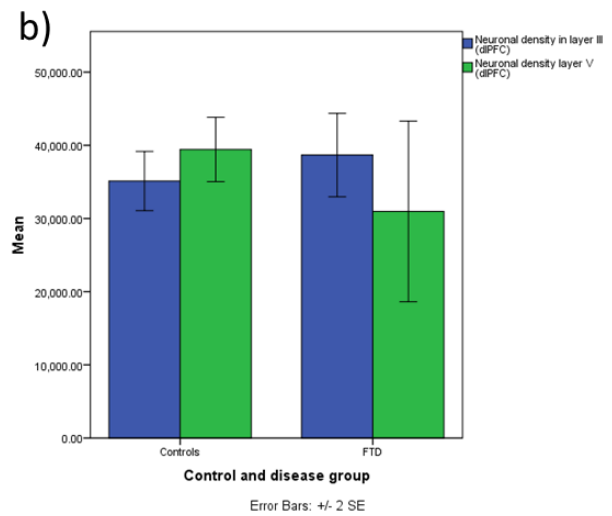
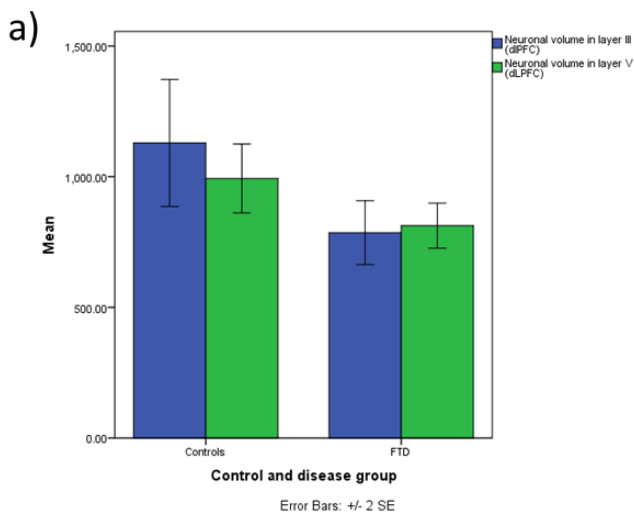


Figure 8-4 showing (a) pyramidal neuronal volumes, and b) pyramidal neuron densities in the dIPFC of FTD subjects in both layers III and V.

### 8.2.2. Additional analysis of the FTD subjects

The reduction in pyramidal neuronal volumes appeared to be a shared trait between several different types of dementia. It was unexpected to uncover such homogenous findings in range of disease states; from largely vascular based pathologies, to those suffering from the neurodegenerative effects of amyloid and tau. By analysing the dIPFC of a disease group characterised by frontal lobe tau-based pathology, perhaps some light could be shed on the direct effect of tau on pyramidal neurons. Interestingly, FTD cases showed no significant difference in pyramidal neuron densities when compared to controls, following the same pattern as other disease groups. Perhaps surprisingly, no significant difference was detected between neuronal volumes in the dIPFC of FTD cases when compared to controls. With FTD characterised by high levels of frontal pathology it was hypothesised that pyramidal neuronal volume would be significantly reduced, as those in other disease groups. This finding could suggest that pure tauopathies such as that suffered by this FTD cohort does not affect pyramidal neurons as those of vascular pathologies, however if this was the case one would expect similar findings in the dIPFC of AD cases, which was not found. It is therefore likely that this particular group was underpowered to detect significance. A total of 4 groups were analysed, compared to the 10 or more analysed in each of the other groups. This point is supported by the fact that when layers III and V are combined, effectively increasing the amount of neurons being analysed, FTD shows significantly lower volumes when compared to controls cases.

### 8.3. List of publications

- **June 2014** - Pyramidal neurons of the prefrontal cortex in post-stroke, vascular and other ageing-related dementias. *Brain*- **Foster, V.**, A. E. Oakley, J. Y. Slade, R. Hall, T. M. Polvikoski, M. Burke, A. J. Thomas, A. Khundakar, L. M. Allan and R. N. Kalaria (Foster et al. 2014).
- **June 2014** - Seminar of my work at the Institute for Ageing and Health, Newcastle University.
- **June 2013** - Presentation of research at the International Society of Vascular Behavioural and Cognitive Disorders, Toronto.
- **January 2013** - Presentation of my research at the British Neuropathological society, London.

- **January 2012** - Poster presentation at the European Congress of Neuropathology 2012. My poster was subsequently selected for special mention and I was invited to speak.

## References

- Abeles, M. (1991) *Corticongs: Neural circuits of the cerebral cortex*. Cambridge University Press.
- Aboul-Enein, F., H. Rauschka, B. Kornek, C. Stadelmann, A. Stefferl, W. Bruck, C. Lucchinetti, M. Schmidbauer, K. Jellinger and H. Lassmann (2003) Preferential loss of myelin-associated glycoprotein reflects hypoxia-like white matter damage in stroke and inflammatory brain diseases. *J Neuropathol Exp Neurol* 62/1: 25-33. Available at <http://www.ncbi.nlm.nih.gov/pubmed/12528815>.
- Akiguchi, I., H. Tomimoto, T. Suenaga, H. Wakita and H. Budka (1997) Alterations in glia and axons in the brains of Binswanger's disease patients. *Stroke* 28/7: 1423-1429. Available at <http://www.ncbi.nlm.nih.gov/pubmed/9227695>.
- Alafuzoff, I., R. Adolfsson, G. Bucht and B. Winblad (1983) Albumin and immunoglobulin in plasma and cerebrospinal fluid, and blood-cerebrospinal fluid barrier function in patients with dementia of Alzheimer type and multi-infarct dementia. *J Neurol Sci* 60/3: 465-472. Available at <http://www.ncbi.nlm.nih.gov/pubmed/6631444>.
- Alberdi, E., M. V. Sanchez-Gomez and C. Matute (2005) Calcium and glial cell death. *Cell Calcium* 38/3-4: 417-425. Available at <http://www.ncbi.nlm.nih.gov/pubmed/16095689>.
- Alexopoulos, G. S. (2003) Vascular disease, depression, and dementia. *J Am Geriatr Soc* 51/8: 1178-1180. Available at <http://www.ncbi.nlm.nih.gov/pubmed/12890087>.
- Alexopoulos, G. S., M. L. Bruce, D. Silbersweig, B. Kalayam and E. Stern (1999) Vascular depression: a new view of late-onset depression. *Dialogues Clin Neurosci* 1/2: 68-80. Available at <http://www.ncbi.nlm.nih.gov/pubmed/22033775>.
- Alexopoulos, G. S., B. S. Meyers, R. C. Young, T. Kakuma, D. Silbersweig and M. Charlson (1997) Clinically defined vascular depression. *Am J Psychiatry* 154/4: 562-565. Available at <http://www.ncbi.nlm.nih.gov/pubmed/9090349>.
- Allan, L. M., E. N. Rowan, M. J. Firbank, A. J. Thomas, S. W. Parry, T. M. Polvikoski, J. T. O'Brien and R. N. Kalara (2011) Long term incidence of dementia, predictors of mortality and pathological diagnosis in older stroke survivors. *Brain* 134/Pt 12: 3716-3727. Available at <http://www.ncbi.nlm.nih.gov/pubmed/22171356>.
- Alonso, A. C., B. Li, I. Grundke-Iqbal and K. Iqbal (2008) Mechanism of tau-induced neurodegeneration in Alzheimer disease and related tauopathies. *Curr Alzheimer Res* 5/4: 375-384. Available at <http://www.ncbi.nlm.nih.gov/pubmed/18690834>.
- Alonzo, N. C., B. T. Hyman, G. W. Rebeck and S. M. Greenberg (1998) Progression of cerebral amyloid angiopathy: accumulation of amyloid-beta40 in affected vessels. *J Neuropathol Exp Neurol* 57/4: 353-359. Available at <http://www.ncbi.nlm.nih.gov/pubmed/9600229>.
- Anderson, C. M. and R. A. Swanson (2000) Astrocyte glutamate transport: review of properties, regulation, and physiological functions. *Glia* 32/1: 1-14. Available at <http://www.ncbi.nlm.nih.gov/pubmed/10975906>.



- Anderson, S. W., H. Damasio, R. D. Jones and D. Tranel (1991) Wisconsin Card Sorting Test performance as a measure of frontal lobe damage. *J Clin Exp Neuropsychol* 13/6: 909-922. Available at <http://www.ncbi.nlm.nih.gov/pubmed/1779030>.
- Andres, R. H., N. Horie, W. Slikker, H. Keren-Gill, K. Zhan, G. Sun, N. C. Manley, M. P. Pereira, L. A. Sheikh, E. L. McMillan, B. T. Schaar, C. N. Svendsen, T. M. Bliss and G. K. Steinberg (2011) Human neural stem cells enhance structural plasticity and axonal transport in the ischaemic brain. *Brain* 134/Pt 6: 1777-1789. Available at <http://www.ncbi.nlm.nih.gov/pubmed/21616972>.
- Apaydin, H., J. E. Ahlskog, J. E. Parisi, B. F. Boeve and D. W. Dickson (2002) Parkinson disease neuropathology: later-developing dementia and loss of the levodopa response. *Arch Neurol* 59/1: 102-112. Available at <http://www.ncbi.nlm.nih.gov/pubmed/11790237>.
- Attems, J., K. Jellinger, D. R. Thal and W. Van Nostrand (2011) Review: sporadic cerebral amyloid angiopathy. *Neuropathol Appl Neurobiol* 37/1: 75-93. Available at <http://www.ncbi.nlm.nih.gov/pubmed/20946241>.
- Attwell, D. and S. B. Laughlin (2001) An energy budget for signaling in the grey matter of the brain. *J Cereb Blood Flow Metab* 21/10: 1133-1145. Available at <http://www.ncbi.nlm.nih.gov/pubmed/11598490>.
- Baddeley, A. (2001) Is stereology 'unbiased'? *Trends Neurosci* 24/7: 375-376; author reply 378-380. Available at <http://www.ncbi.nlm.nih.gov/pubmed/11467287>.
- Baldo, J. V., A. P. Shimamura, D. C. Delis, J. Kramer and E. Kaplan (2001) Verbal and design fluency in patients with frontal lobe lesions. *J Int Neuropsychol Soc* 7/5: 586-596. Available at <http://www.ncbi.nlm.nih.gov/pubmed/11459110>.
- Ballard, C., I. McKeith, J. O'Brien, R. Kalaria, E. Jaros, P. Ince and R. Perry (2000) Neuropathological substrates of dementia and depression in vascular dementia, with a particular focus on cases with small infarct volumes. *Dement Geriatr Cogn Disord* 11/2: 59-65. Available at <http://www.ncbi.nlm.nih.gov/pubmed/10705161>.
- Ballard, C., E. Rowan, S. Stephens, R. Kalaria and R. A. Kenny (2003) Prospective follow-up study between 3 and 15 months after stroke: improvements and decline in cognitive function among dementia-free stroke survivors >75 years of age. *Stroke* 34/10: 2440-2444. Available at <http://www.ncbi.nlm.nih.gov/pubmed/14512580>.
- Barcelo, F. and R. T. Knight (2002) Both random and perseverative errors underlie WCST deficits in prefrontal patients. *Neuropsychologia* 40/3: 349-356. Available at <http://www.ncbi.nlm.nih.gov/pubmed/11684168>.
- Barulli, D. and Y. Stern (2013) Efficiency, capacity, compensation, maintenance, plasticity: emerging concepts in cognitive reserve. *Trends Cogn Sci* 17/10: 502-509. Available at <http://www.ncbi.nlm.nih.gov/pubmed/24018144>.
- Bathgate, D., J. S. Snowden, A. Varma, A. Blackshaw and D. Neary (2001) Behaviour in frontotemporal dementia, Alzheimer's disease and vascular dementia. *Acta Neurol Scand* 103/6: 367-378. Available at <http://www.ncbi.nlm.nih.gov/pubmed/11421849>.
- Bernstein, H. G., M. Johnson, R. H. Perry, F. E. LeBeau, H. Dobrowolny, B. Bogerts and E. K. Perry (2011) Partial loss of parvalbumin-containing hippocampal interneurons in dementia with Lewy bodies. *Neuropathology* 31/1: 1-10. Available at <http://www.ncbi.nlm.nih.gov/pubmed/20487308>.

- Binetti, G., E. Magni, A. Padovani, S. F. Cappa, A. Bianchetti and M. Trabucchi (1996) Executive dysfunction in early Alzheimer's disease. *J Neurol Neurosurg Psychiatry* 60/1: 91-93. Available at <http://www.ncbi.nlm.nih.gov/pubmed/8558161>.
- Blake, H., M. McKinney, K. Treece, E. Lee and N. B. Lincoln (2002) An evaluation of screening measures for cognitive impairment after stroke. *Age Ageing* 31/6: 451-456. Available at <http://www.ncbi.nlm.nih.gov/pubmed/12446291>.
- Blass, J. P. (2001) Brain metabolism and brain disease: is metabolic deficiency the proximate cause of Alzheimer dementia? *J Neurosci Res* 66/5: 851-856. Available at <http://www.ncbi.nlm.nih.gov/pubmed/11746411>.
- Blennow, K., A. Wallin and J. K. Chong (1995) Cerebrospinal fluid 'neuronal thread protein' comes from serum by passage over the blood-brain barrier. *Neurodegeneration* 4/2: 187-193. Available at <http://www.ncbi.nlm.nih.gov/pubmed/7583683>.
- Blennow, K., A. Wallin, P. Fredman, I. Karlsson, C. G. Gottfries and L. Svennerholm (1990) Blood-brain barrier disturbance in patients with Alzheimer's disease is related to vascular factors. *Acta Neurol Scand* 81/4: 323-326. Available at <http://www.ncbi.nlm.nih.gov/pubmed/2360400>.
- Boillee, S., K. Yamanaka, C. S. Lobsiger, N. G. Copeland, N. A. Jenkins, G. Kassiotis, G. Kollias and D. W. Cleveland (2006) Onset and progression in inherited ALS determined by motor neurons and microglia. *Science* 312/5778: 1389-1392. Available at <http://www.ncbi.nlm.nih.gov/pubmed/16741123>.
- Bolmont, T., F. Haiss, D. Eicke, R. Radde, C. A. Mathis, W. E. Klunk, S. Kohsaka, M. Jucker and M. E. Calhoun (2008) Dynamics of the microglial/amyloid interaction indicate a role in plaque maintenance. *J Neurosci* 28/16: 4283-4292. Available at <http://www.ncbi.nlm.nih.gov/pubmed/18417708>.
- Bonita, R. (1992) Epidemiology of stroke. *Lancet* 339/8789: 342-344. Available at <http://www.ncbi.nlm.nih.gov/pubmed/1346420>.
- Bornstein, M. H. and M. D. Sigman (1986) Continuity in mental development from infancy. *Child Dev* 57/2: 251-274. Available at <http://www.ncbi.nlm.nih.gov/pubmed/3956312>.
- Borroni, B., A. Alberici, M. Grassi, M. Turla, O. Zanetti, A. Bianchetti, G. Dalla Volta, R. Rozzini, N. Gilberti, G. Bellelli and A. Padovani (2010) Is frontotemporal lobar degeneration a rare disorder? Evidence from a preliminary study in Brescia county, Italy. *J Alzheimers Dis* 19/1: 111-116. Available at <http://www.ncbi.nlm.nih.gov/pubmed/20061630>.
- Braak, H. and E. Braak (1986) Ratio of pyramidal cells versus non-pyramidal cells in the human frontal isocortex and changes in ratio with ageing and Alzheimer's disease. *Prog Brain Res* 70: 185-212. Available at <http://www.ncbi.nlm.nih.gov/pubmed/3575748>.
- Braak, H. and E. Braak (1991) Neuropathological staging of Alzheimer-related changes. *Acta Neuropathol* 82/4: 239-259. Available at <http://www.ncbi.nlm.nih.gov/pubmed/1759558>.
- Braak, H. and E. Braak (1996) Evolution of the neuropathology of Alzheimer's disease. *Acta Neurologica Scandinavica, Supplement* 93/165: 3-12. Available at <http://www.scopus.com/inward/record.url?eid=2-s2.0-0029686696&partnerID=40&md5=948d58ff4a0928b2c54cb43111d4f92d>.
- Braak, H. and E. Braak (1998) Evolution of neuronal changes in the course of Alzheimer's disease. *J Neural Transm Suppl* 53: 127-140. Available at <http://www.ncbi.nlm.nih.gov/pubmed/9700651>.

- Braak, H., E. Braak, J. Bohl and H. Bratzke (1998) Evolution of Alzheimer's disease related cortical lesions. *J Neural Transm Suppl* 54: 97-106. Available at <http://www.ncbi.nlm.nih.gov/pubmed/9850918>.
- Breteler, M. M. (2000) Vascular involvement in cognitive decline and dementia. Epidemiologic evidence from the Rotterdam Study and the Rotterdam Scan Study. *Ann N Y Acad Sci* 903: 457-465. Available at <http://www.ncbi.nlm.nih.gov/pubmed/10818538>.
- Brockmann, M. D., M. Kukovic, M. Schonfeld, J. Sedlacik and I. L. Hanganu-Opatz (2013) Hypoxia-ischemia disrupts directed interactions within neonatal prefrontal-hippocampal networks. *PLoS One* 8/12: e83074. Available at <http://www.ncbi.nlm.nih.gov/pubmed/24376636>.
- Brown, A. M. and B. R. Ransom (2007) Astrocyte glycogen and brain energy metabolism. *Glia* 55/12: 1263-1271. Available at <http://www.ncbi.nlm.nih.gov/pubmed/17659525>.
- Brown, C. E., P. Li, J. D. Boyd, K. R. Delaney and T. H. Murphy (2007) Extensive turnover of dendritic spines and vascular remodeling in cortical tissues recovering from stroke. *J Neurosci* 27/15: 4101-4109. Available at <http://www.ncbi.nlm.nih.gov/pubmed/17428988>.
- Bruhn, H., J. Frahm, M. L. Gyngell, K. D. Merboldt, W. Hanicke and R. Sauter (1989) Cerebral metabolism in man after acute stroke: new observations using localized proton NMR spectroscopy. *Magn Reson Med* 9/1: 126-131. Available at <http://www.ncbi.nlm.nih.gov/pubmed/2540394>.
- Brun, A. (1994) Pathology and pathophysiology of cerebrovascular dementia: pure subgroups of obstructive and hypoperfusive etiology. *Dementia* 5/3-4: 145-147. Available at <http://www.ncbi.nlm.nih.gov/pubmed/8087169>.
- Bucks, R. S. and J. Haworth (2002) Bristol Activities of Daily Living Scale: a critical evaluation. *Expert Rev Neurother* 2/5: 669-676. Available at <http://www.ncbi.nlm.nih.gov/pubmed/19810983>.
- Budde, M. D., J. H. Kim, H. F. Liang, J. H. Russell, A. H. Cross and S. K. Song (2008) Axonal injury detected by in vivo diffusion tensor imaging correlates with neurological disability in a mouse model of multiple sclerosis. *NMR Biomed* 21/6: 589-597. Available at <http://www.ncbi.nlm.nih.gov/pubmed/18041806>.
- Buee, L., P. R. Hof, C. Bouras, A. Delacourte, D. P. Perl, J. H. Morrison and H. M. Fillit (1994) Pathological alterations of the cerebral microvasculature in Alzheimer's disease and related dementing disorders. *Acta Neuropathol* 87/5: 469-480. Available at <http://www.ncbi.nlm.nih.gov/pubmed/8059599>.
- Buell, S. J. and P. D. Coleman (1979) Dendritic growth in the aged human brain and failure of growth in senile dementia. *Science* 206/4420: 854-856. Available at <http://www.ncbi.nlm.nih.gov/pubmed/493989>.
- Buhl, E. H., K. Halasy and P. Somogyi (1994) Diverse sources of hippocampal unitary inhibitory postsynaptic potentials and the number of synaptic release sites. *Nature* 368/6474: 823-828. Available at <http://www.ncbi.nlm.nih.gov/pubmed/8159242>.
- Bullock, R. (2002) New drugs for Alzheimer's disease and other dementias. *Br J Psychiatry* 180: 135-139. Available at <http://www.ncbi.nlm.nih.gov/pubmed/11823323>.
- Burke, M. J., L. Nelson, J. Y. Slade, A. E. Oakley, A. A. Khundakar and R. N. Kaloria (2014) Morphometry of the hippocampal microvasculature in post-stroke

- and age-related dementias. *Neuropathol Appl Neurobiol* 40/3: 284-295. Available at <http://www.ncbi.nlm.nih.gov/pubmed/24003901>.
- Burton, E., C. Ballard, S. Stephens, R. A. Kenny, R. Kalaria, R. Barber and J. O'Brien (2003) Hyperintensities and fronto-subcortical atrophy on MRI are substrates of mild cognitive deficits after stroke. *Dement Geriatr Cogn Disord* 16/2: 113-118. Available at <http://www.ncbi.nlm.nih.gov/pubmed/12784036>.
- Burton, E. J., R. A. Kenny, J. O'Brien, S. Stephens, M. Bradbury, E. Rowan, R. Kalaria, M. Firbank, K. Wesnes and C. Ballard (2004) White matter hyperintensities are associated with impairment of memory, attention, and global cognitive performance in older stroke patients. *Stroke* 35/6: 1270-1275. Available at <http://www.ncbi.nlm.nih.gov/pubmed/15118186>.
- Burton, K. R., N. Perlis, R. I. Aviv, A. R. Moody, M. K. Kapral, M. D. Krahn and A. Laupacis (2014) Systematic review, critical appraisal, and analysis of the quality of economic evaluations in stroke imaging. *Stroke* 45/3: 807-814. Available at <http://www.ncbi.nlm.nih.gov/pubmed/24519409>.
- Bussiere, T., P. Giannakopoulos, C. Bouras, D. P. Perl, J. H. Morrison and P. R. Hof (2003) Progressive degeneration of nonphosphorylated neurofilament protein-enriched pyramidal neurons predicts cognitive impairment in Alzheimer's disease: stereologic analysis of prefrontal cortex area 9. *J Comp Neurol* 463/3: 281-302. Available at <http://www.ncbi.nlm.nih.gov/pubmed/12820162>.
- Bussiere, T., G. Gold, E. Kovari, P. Giannakopoulos, C. Bouras, D. P. Perl, J. H. Morrison and P. R. Hof (2003) Stereologic analysis of neurofibrillary tangle formation in prefrontal cortex area 9 in aging and Alzheimer's disease. *Neuroscience* 117/3: 577-592. Available at <http://www.ncbi.nlm.nih.gov/pubmed/12617964>.
- Butler, R W., IA; Rorsman, J M. Hill and R Tuma (1993) The effects of frontal brain impairment on fluency: Simple and complex paradigms. *Neuropsychology* 7/4: 519-529.
- Cadenas, E. and K. J. Davies (2000) Mitochondrial free radical generation, oxidative stress, and aging. *Free Radic Biol Med* 29/3-4: 222-230. Available at <http://www.ncbi.nlm.nih.gov/pubmed/11035250>.
- Cafe, C., C. Torri, S. Gatti, D. Adinolfi, P. Gaetani, Y. Baena R. Rodriguez and F. Marzatico (1994) Changes in non-synaptosomal and synaptosomal mitochondrial membrane-linked enzymatic activities after transient cerebral ischemia. *Neurochem Res* 19/12: 1551-1555. Available at <http://www.ncbi.nlm.nih.gov/pubmed/7877728>.
- Catala, I., I. Ferrer, E. Galofre and I. Fabregues (1988) Decreased numbers of dendritic spines on cortical pyramidal neurons in dementia. A quantitative Golgi study on biopsy samples. *Hum Neurobiol* 6/4: 255-259. Available at <http://www.ncbi.nlm.nih.gov/pubmed/3350705>.
- Chagnon, P., C. Betard, Y. Robitaille, A. Cholette and D. Gauvreau (1995) Distribution of brain cytochrome oxidase activity in various neurodegenerative diseases. *Neuroreport* 6/5: 711-715. Available at <http://www.ncbi.nlm.nih.gov/pubmed/7605932>.
- Chan, D., N. C. Fox, R. Jenkins, R. I. Scahill, W. R. Crum and M. N. Rossor (2001) Rates of global and regional cerebral atrophy in AD and frontotemporal dementia. *Neurology* 57/10: 1756-1763. Available at <http://www.ncbi.nlm.nih.gov/pubmed/11723259>.

- Chance, S. A., L. Clover, H. Cousijn, L. Currah, R. Pettingill and M. M. Esiri (2011) Microanatomical correlates of cognitive ability and decline: normal ageing, MCI, and Alzheimer's disease. *Cereb Cortex* 21/8: 1870-1878. Available at <http://www.ncbi.nlm.nih.gov/pubmed/21239393>.
- Chen, J. J., H. D. Rosas and D. H. Salat (2011) Age-associated reductions in cerebral blood flow are independent from regional atrophy. *Neuroimage* 55/2: 468-478. Available at <http://www.ncbi.nlm.nih.gov/pubmed/21167947>.
- Ching, Randal P. (2007) Relationship between head mass and circumference in human adults. *Technical report*.
- Choi, D. W. and S. M. Rothman (1990) The role of glutamate neurotoxicity in hypoxic-ischemic neuronal death. *Annu Rev Neurosci* 13: 171-182. Available at <http://www.ncbi.nlm.nih.gov/pubmed/1970230>.
- Christiansen, P., H. B. Larsson, C. Thomsen, S. B. Wieslander and O. Henriksen (1994) Age dependent white matter lesions and brain volume changes in healthy volunteers. *Acta Radiol* 35/2: 117-122. Available at <http://www.ncbi.nlm.nih.gov/pubmed/8172734>.
- Coffey, C. E., G. S. Figiel, W. T. Djang and R. D. Weiner (1990) Subcortical hyperintensity on magnetic resonance imaging: a comparison of normal and depressed elderly subjects. *Am J Psychiatry* 147/2: 187-189. Available at <http://www.ncbi.nlm.nih.gov/pubmed/2301657>.
- Cohen, R. A., R. H. Paul, B. R. Ott, D. J. Moser, T. M. Zawacki, W. Stone and N. Gordon (2002) The relationship of subcortical MRI hyperintensities and brain volume to cognitive function in vascular dementia. *J Int Neuropsychol Soc* 8/6: 743-752. Available at <http://www.ncbi.nlm.nih.gov/pubmed/12240738>.
- Conde, F., J. S. Lund, D. M. Jacobowitz, K. G. Baimbridge and D. A. Lewis (1994) Local circuit neurons immunoreactive for calretinin, calbindin D-28k or parvalbumin in monkey prefrontal cortex: distribution and morphology. *J Comp Neurol* 341/1: 95-116. Available at <http://www.ncbi.nlm.nih.gov/pubmed/8006226>.
- Cook, R. D. and H. M. Wisniewski (1973) The role of oligodendroglia and astroglia in Wallerian degeneration of the optic nerve. *Brain Res* 61: 191-206. Available at <http://www.ncbi.nlm.nih.gov/pubmed/4204124>.
- Coria, F. and I. Rubio (1996) Cerebral amyloid angiopathies. *Neuropathol Appl Neurobiol* 22/3: 216-227. Available at <http://www.ncbi.nlm.nih.gov/pubmed/8804023>.
- Courchesne, E., P. R. Mouton, M. E. Calhoun, K. Semendeferi, C. Ahrens-Barbeau, M. J. Hallet, C. C. Barnes and K. Pierce (2011) Neuron number and size in prefrontal cortex of children with autism. *JAMA* 306/18: 2001-2010. Available at <http://www.ncbi.nlm.nih.gov/pubmed/22068992>.
- Craggs, L. J., C. Hagel, G. Kuhlenbaeumer, A. Borjesson-Hanson, O. Andersen, M. Viitanen, H. Kalimo, C. A. McLean, J. Y. Slade, R. A. Hall, A. E. Oakley, Y. Yamamoto, V. Deramecourt and R. N. Kalaria (2013) Quantitative Vascular Pathology and Phenotyping Familial and Sporadic Cerebral Small Vessel Diseases. *Brain Pathol*. Available at <http://www.ncbi.nlm.nih.gov/pubmed/23387519>.
- Crow, T. J., A. J. Cross, S. J. Cooper, J. F. Deakin, I. N. Ferrier, J. A. Johnson, M. H. Joseph, F. Owen, M. Poulter, R. Lofthouse and et al. (1984) Neurotransmitter receptors and monoamine metabolites in the brains of patients with Alzheimer-type dementia and depression, and suicides. *Neuropharmacology*

- 23/12B: 1561-1569. Available at <http://www.ncbi.nlm.nih.gov/pubmed/6084823>.
- Cruz, L., D. L. Roe, B. Urbanc, H. Cabral, H. E. Stanley and D. L. Rosene (2004) Age-related reduction in microcolumnar structure in area 46 of the rhesus monkey correlates with behavioral decline. *Proc Natl Acad Sci U S A* 101/45: 15846-15851. Available at <http://www.ncbi.nlm.nih.gov/pubmed/15520373>.
- Cumming, T. B. and A. Brodtmann (2011) Can stroke cause neurodegenerative dementia? *Int J Stroke* 6/5: 416-424. Available at <http://www.ncbi.nlm.nih.gov/pubmed/21951407>.
- Custer, S. K., G. A. Garden, N. Gill, U. Rueb, R. T. Libby, C. Schultz, S. J. Guyenet, T. Deller, L. E. Westrum, B. L. Sopher and A. R. La Spada (2006) Bergmann glia expression of polyglutamine-expanded ataxin-7 produces neurodegeneration by impairing glutamate transport. *Nat Neurosci* 9/10: 1302-1311. Available at <http://www.ncbi.nlm.nih.gov/pubmed/16936724>.
- Dall'Oglio, A., D. Ferme, J. Brusco, J. E. Moreira and A. A. Rasia-Filho (2010) The "single-section" Golgi method adapted for formalin-fixed human brain and light microscopy. *J Neurosci Methods* 189/1: 51-55. Available at <http://www.ncbi.nlm.nih.gov/pubmed/20347871>.
- Danbolt, N. C. (2001) Glutamate uptake. *Prog Neurobiol* 65/1: 1-105. Available at <http://www.ncbi.nlm.nih.gov/pubmed/11369436>.
- Davalos, D., J. Grutzendler, G. Yang, J. V. Kim, Y. Zuo, S. Jung, D. R. Littman, M. L. Dustin and W. B. Gan (2005) ATP mediates rapid microglial response to local brain injury in vivo. *Nat Neurosci* 8/6: 752-758. Available at <http://www.ncbi.nlm.nih.gov/pubmed/15895084>.
- Daviss, S. R. and D. A. Lewis (1995) Local circuit neurons of the prefrontal cortex in schizophrenia: selective increase in the density of calbindin-immunoreactive neurons. *Psychiatry Res* 59/1-2: 81-96. Available at <http://www.ncbi.nlm.nih.gov/pubmed/8771223>.
- de la Torre, J. C. (1999) Critical threshold cerebral hypoperfusion causes Alzheimer's disease? *Acta Neuropathol* 98/1: 1-8. Available at <http://www.ncbi.nlm.nih.gov/pubmed/10412794>.
- de la Torre, J. C., A. Cada, N. Nelson, G. Davis, R. J. Sutherland and F. Gonzalez-Lima (1997) Reduced cytochrome oxidase and memory dysfunction after chronic brain ischemia in aged rats. *Neurosci Lett* 223/3: 165-168. Available at <http://www.ncbi.nlm.nih.gov/pubmed/9080458>.
- de Leeuw, F. E., J. C. de Groot, E. Achten, M. Oudkerk, L. M. Ramos, R. Heijboer, A. Hofman, J. Jolles, J. van Gijn and M. M. Breteler (2001) Prevalence of cerebral white matter lesions in elderly people: a population based magnetic resonance imaging study. The Rotterdam Scan Study. *J Neurol Neurosurg Psychiatry* 70/1: 9-14. Available at <http://www.ncbi.nlm.nih.gov/pubmed/11118240>.
- DeCarli, C., D. G. Murphy, M. Tranh, C. L. Grady, J. V. Haxby, J. A. Gillette, J. A. Salerno, A. Gonzales-Aviles, B. Horwitz, S. I. Rapoport and et al. (1995) The effect of white matter hyperintensity volume on brain structure, cognitive performance, and cerebral metabolism of glucose in 51 healthy adults. *Neurology* 45/11: 2077-2084. Available at <http://www.ncbi.nlm.nih.gov/pubmed/7501162>.
- DeFelipe, J. (1997) Types of neurons, synaptic connections and chemical characteristics of cells immunoreactive for calbindin-D28K, parvalbumin

- and calretinin in the neocortex. *J Chem Neuroanat* 14/1: 1-19. Available at <http://www.ncbi.nlm.nih.gov/pubmed/9498163>.
- DeFelipe, J. and I. Farinas (1992) The pyramidal neuron of the cerebral cortex: morphological and chemical characteristics of the synaptic inputs. *Prog Neurobiol* 39/6: 563-607. Available at <http://www.ncbi.nlm.nih.gov/pubmed/1410442>.
- Deng, Y., B. Li, Y. Liu, K. Iqbal, I. Grundke-Iqbal and C. X. Gong (2009) Dysregulation of insulin signaling, glucose transporters, O-GlcNAcylation, and phosphorylation of tau and neurofilaments in the brain: Implication for Alzheimer's disease. *Am J Pathol* 175/5: 2089-2098. Available at <http://www.ncbi.nlm.nih.gov/pubmed/19815707>.
- Deramecourt, V., J. Y. Slade, A. E. Oakley, R. H. Perry, P. G. Ince, C. A. Maurage and R. N. Kalaria (2012) Staging and natural history of cerebrovascular pathology in dementia. *Neurology* 78/14: 1043-1050. Available at <http://www.ncbi.nlm.nih.gov/pubmed/22377814>.
- Desmond, D. W., J. T. Moroney, M. C. Paik, M. Sano, J. P. Mohr, S. Aboumatar, C. L. Tseng, S. Chan, J. B. Williams, R. H. Remien, W. A. Hauser and Y. Stern (2000) Frequency and clinical determinants of dementia after ischemic stroke. *Neurology* 54/5: 1124-1131. Available at <http://www.ncbi.nlm.nih.gov/pubmed/10720286>.
- Dienel, G. A. and L. Hertz (2005) Astrocytic contributions to bioenergetics of cerebral ischemia. *Glia* 50/4: 362-388. Available at <http://www.ncbi.nlm.nih.gov/pubmed/15846808>.
- Dirnagl, U., C. Iadecola and M. A. Moskowitz (1999) Pathobiology of ischaemic stroke: an integrated view. *Trends Neurosci* 22/9: 391-397. Available at <http://www.ncbi.nlm.nih.gov/pubmed/10441299>.
- Donmez, G., D. Wang, D. E. Cohen and L. Guarente (2010) SIRT1 suppresses beta-amyloid production by activating the alpha-secretase gene ADAM10. *Cell* 142/2: 320-332. Available at <http://www.ncbi.nlm.nih.gov/pubmed/20655472>.
- Douaud, G., A. R. Groves, C. K. Tamnes, L. T. Westlye, E. P. Duff, A. Engvig, K. B. Walhovd, A. James, A. Gass, A. U. Monsch, P. M. Matthews, A. M. Fjell, S. M. Smith and H. Johansen-Berg (2014) A common brain network links development, aging, and vulnerability to disease. *Proc Natl Acad Sci U S A*. Available at <http://www.ncbi.nlm.nih.gov/pubmed/25422429>.
- DSM-IV (1994) Diagnostic and statistical manual of mental disorders DSM-IV. *American Psychiatric Association*.
- Duering, M., E. Csanadi, B. Gesierich, E. Jouvent, D. Herve, S. Seiler, B. Belaroussi, S. Ropele, R. Schmidt, H. Chabriat and M. Dichgans (2013) Incident lacunes preferentially localize to the edge of white matter hyperintensities: insights into the pathophysiology of cerebral small vessel disease. *Brain* 136/Pt 9: 2717-2726. Available at <http://www.ncbi.nlm.nih.gov/pubmed/23864274>.
- Elovaara, I., J. Palo, T. Erkinjuntti and R. Sulkava (1987) Serum and cerebrospinal fluid proteins and the blood-brain barrier in Alzheimer's disease and multi-infarct dementia. *Eur Neurol* 26/4: 229-234. Available at <http://www.ncbi.nlm.nih.gov/pubmed/3595662>.
- Erkinjuntti, T. (1994) Clinical criteria for vascular dementia: the NINDS-AIREN criteria. *Dementia* 5/3-4: 189-192. Available at <http://www.ncbi.nlm.nih.gov/pubmed/8087178>.

- Ertekin-Taner, N. (2010) Genetics of Alzheimer disease in the pre- and post-GWAS era. *Alzheimers Res Ther* 2/1: 3. Available at <http://www.ncbi.nlm.nih.gov/pubmed/20236449>.
- Esiri, M. M., Z. Nagy, M. Z. Smith, L. Barnetson and A. D. Smith (1999) Cerebrovascular disease and threshold for dementia in the early stages of Alzheimer's disease. *Lancet* 354/9182: 919-920. Available at <http://www.ncbi.nlm.nih.gov/pubmed/10489957>.
- Esiri, M. M., G. K. Wilcock and J. H. Morris (1997) Neuropathological assessment of the lesions of significance in vascular dementia. *J Neurol Neurosurg Psychiatry* 63/6: 749-753. Available at <http://www.ncbi.nlm.nih.gov/pubmed/9416809>.
- Eslinger, P. J. and L. M. Grattan (1993) Frontal lobe and frontal-striatal substrates for different forms of human cognitive flexibility. *Neuropsychologia* 31/1: 17-28. Available at <http://www.ncbi.nlm.nih.gov/pubmed/8437679>.
- Eslinger, P. J., P. Moore, V. Troiani, S. Antani, K. Cross, S. Kwok and M. Grossman (2007) Oops! Resolving social dilemmas in frontotemporal dementia. *J Neurol Neurosurg Psychiatry* 78/5: 457-460. Available at <http://www.ncbi.nlm.nih.gov/pubmed/17012339>.
- Farkas, E. and P. G. Luiten (2001) Cerebral microvascular pathology in aging and Alzheimer's disease. *Prog Neurobiol* 64/6: 575-611. Available at <http://www.ncbi.nlm.nih.gov/pubmed/11311463>.
- Farrall, A. J. and J. M. Wardlaw (2009) Blood-brain barrier: ageing and microvascular disease--systematic review and meta-analysis. *Neurobiol Aging* 30/3: 337-352. Available at <http://www.ncbi.nlm.nih.gov/pubmed/17869382>.
- Fein, G., V. Di Sclafani, J. Tanabe, V. Cardenas, M. W. Weiner, W. J. Jagust, B. R. Reed, D. Norman, N. Schuff, L. Kusdra, T. Greenfield and H. Chui (2000) Hippocampal and cortical atrophy predict dementia in subcortical ischemic vascular disease. *Neurology* 55/11: 1626-1635. Available at <http://www.ncbi.nlm.nih.gov/pubmed/11113215>.
- Ferguson, B., M. K. Matyszak, M. M. Esiri and V. H. Perry (1997) Axonal damage in acute multiple sclerosis lesions. *Brain* 120 ( Pt 3): 393-399. Available at <http://www.ncbi.nlm.nih.gov/pubmed/9126051>.
- Fernando, M. S., J. E. Simpson, F. Matthews, C. Brayne, C. E. Lewis, R. Barber, R. N. Kalaria, G. Forster, F. Esteves, S. B. Wharton, P. J. Shaw, J. T. O'Brien, P. G. Ince, M. R. C. Cognitive Function and Group Ageing Neuropathology Study (2006) White matter lesions in an unselected cohort of the elderly: molecular pathology suggests origin from chronic hypoperfusion injury. *Stroke* 37/6: 1391-1398. Available at <http://www.ncbi.nlm.nih.gov/pubmed/16627790>.
- Fetler, L. and S. Amigorena (2005) Neuroscience. Brain under surveillance: the microglia patrol. *Science* 309/5733: 392-393. Available at <http://www.ncbi.nlm.nih.gov/pubmed/16020721>.
- Firbank, M. J., L. M. Allan, E. J. Burton, R. Barber, J. T. O'Brien and R. N. Kalaria (2012) Neuroimaging predictors of death and dementia in a cohort of older stroke survivors. *J Neurol Neurosurg Psychiatry* 83/3: 263-267. Available at <http://www.ncbi.nlm.nih.gov/pubmed/22114300>.
- Firbank, M. J., E. J. Burton, R. Barber, S. Stephens, R. A. Kenny, C. Ballard, R. N. Kalaria and J. T. O'Brien (2007) Medial temporal atrophy rather than white matter hyperintensities predict cognitive decline in stroke survivors.



- Neurobiol Aging* 28/11: 1664-1669. Available at <http://www.ncbi.nlm.nih.gov/pubmed/16934370>.
- Firbank, M. J., J. He, A. M. Blamire, B. Singh, P. Danson, R. N. Kalaria and J. T. O'Brien (2011) Cerebral blood flow by arterial spin labeling in poststroke dementia. *Neurology* 76/17: 1478-1484. Available at <http://www.ncbi.nlm.nih.gov/pubmed/21518997>.
- Fiskum, G., A. N. Murphy and M. F. Beal (1999) Mitochondria in neurodegeneration: acute ischemia and chronic neurodegenerative diseases. *J Cereb Blood Flow Metab* 19/4: 351-369. Available at <http://www.ncbi.nlm.nih.gov/pubmed/10197505>.
- Folstein, M. F., S. E. Folstein and P. R. McHugh (1975) "Mini-mental state". A practical method for grading the cognitive state of patients for the clinician. *J Psychiatr Res* 12/3: 189-198. Available at <http://www.ncbi.nlm.nih.gov/pubmed/1202204>.
- Foster, V., A. E. Oakley, J. Y. Slade, R. Hall, T. M. Polvikoski, M. Burke, A. J. Thomas, A. Khundakar, L. M. Allan and R. N. Kalaria (2014) Pyramidal neurons of the prefrontal cortex in post-stroke, vascular and other ageing-related dementias. *Brain*. Available at <http://www.ncbi.nlm.nih.gov/pubmed/24974383>.
- Franklin, R. J., J. M. Gilson and W. F. Blakemore (1997) Local recruitment of remyelinating cells in the repair of demyelination in the central nervous system. *J Neurosci Res* 50/2: 337-344. Available at <http://www.ncbi.nlm.nih.gov/pubmed/9373042>.
- Fredriksson, K., H. Kalimo, C. Nordborg, Y. Olsson and B. B. Johansson (1988) Cyst formation and glial response in the brain lesions of stroke-prone spontaneously hypertensive rats. *Acta Neuropathol* 76/5: 441-450. Available at <http://www.ncbi.nlm.nih.gov/pubmed/3188837>.
- Fujikawa, T., S. Yamawaki and Y. Touhoda (1993) Incidence of silent cerebral infarction in patients with major depression. *Stroke* 24/11: 1631-1634. Available at <http://www.ncbi.nlm.nih.gov/pubmed/8236334>.
- Gabbott, P. L. and J. Somogyi (1984) The 'single' section Golgi-impregnation procedure: methodological description. *J Neurosci Methods* 11/4: 221-230. Available at <http://www.ncbi.nlm.nih.gov/pubmed/6392756>.
- Gallagher, J. J., X. Zhang, G. J. Ziomek, R. E. Jacobs and E. L. Bearer (2012) Deficits in axonal transport in hippocampal-based circuitry and the visual pathway in APP knock-out animals witnessed by manganese enhanced MRI. *Neuroimage* 60/3: 1856-1866. Available at <http://www.ncbi.nlm.nih.gov/pubmed/22500926>.
- Gamblin, T. C., F. Chen, A. Zambrano, A. Abraha, S. Lagalwar, A. L. Guillozet, M. Lu, Y. Fu, F. Garcia-Sierra, N. LaPointe, R. Miller, R. W. Berry, L. I. Binder and V. L. Cryns (2003) Caspase cleavage of tau: linking amyloid and neurofibrillary tangles in Alzheimer's disease. *Proc Natl Acad Sci U S A* 100/17: 10032-10037. Available at <http://www.ncbi.nlm.nih.gov/pubmed/12888622>.
- Gehrmann, J. and G. W. Kreutzberg (1994) Experimental models to study microglial in vivo. The activated microglia: an early response element in the injured CNS? *Neuropathol Appl Neurobiol* 20/2: 180-182. Available at <http://www.ncbi.nlm.nih.gov/pubmed/8072650>.
- Gelber, R. P., L. J. Launer and L. R. White (2012) The Honolulu-Asia Aging Study: epidemiologic and neuropathologic research on cognitive impairment. *Curr Alzheimer Res* 9/6: 664-672. Available at <http://www.ncbi.nlm.nih.gov/pubmed/22471866>.

- Gemmell, E., H. Bosomworth, L. Allan, R. Hall, A. Khundakar, A. E. Oakley, V. Deramecourt, T. M. Polvikoski, J. T. O'Brien and R. N. Kalaria (2012) Hippocampal neuronal atrophy and cognitive function in delayed poststroke and aging-related dementias. *Stroke* 43/3: 808-814. Available at <http://www.ncbi.nlm.nih.gov/pubmed/22207507>.
- Geortzel, Ben (1997) *From complexity to creativity*. 11. Springer US.
- Ghashghaei, H. T. and H. Barbas (2002) Pathways for emotion: interactions of prefrontal and anterior temporal pathways in the amygdala of the rhesus monkey. *Neuroscience* 115/4: 1261-1279. Available at <http://www.ncbi.nlm.nih.gov/pubmed/12453496>.
- Giaume, C., F. Kirchhoff, C. Matute, A. Reichenbach and A. Verkhratsky (2007) Glia: the fulcrum of brain diseases. *Cell Death Differ* 14/7: 1324-1335. Available at <http://www.ncbi.nlm.nih.gov/pubmed/17431421>.
- Gilbert, C. D. (1993) Circuitry, architecture, and functional dynamics of visual cortex. *Cereb Cortex* 3/5: 373-386. Available at <http://www.ncbi.nlm.nih.gov/pubmed/8260807>.
- Gittins, R. A. and P. J. Harrison (2011) A morphometric study of glia and neurons in the anterior cingulate cortex in mood disorder. *J Affect Disord* 133/1-2: 328-332. Available at <http://www.ncbi.nlm.nih.gov/pubmed/21497910>.
- Giulian, D., J. Li, X. Li, J. George and P. A. Rutecki (1994) The impact of microglia-derived cytokines upon gliosis in the CNS. *Dev Neurosci* 16/3-4: 128-136. Available at <http://www.ncbi.nlm.nih.gov/pubmed/7535679>.
- Glantz, L. A. and D. A. Lewis (2000) Decreased dendritic spine density on prefrontal cortical pyramidal neurons in schizophrenia. *Arch Gen Psychiatry* 57/1: 65-73. Available at <http://www.ncbi.nlm.nih.gov/pubmed/10632234>.
- Goedert, M. (1996) Tau protein and the neurofibrillary pathology of Alzheimer's disease. *Ann N Y Acad Sci* 777: 121-131. Available at <http://www.ncbi.nlm.nih.gov/pubmed/8624074>.
- Gold, G., P. Giannakopoulos, C. Montes-Paixao Junior, F. R. Herrmann, R. Mulligan, J. P. Michel and C. Bouras (1997) Sensitivity and specificity of newly proposed clinical criteria for possible vascular dementia. *Neurology* 49/3: 690-694. Available at <http://www.ncbi.nlm.nih.gov/pubmed/9305324>.
- Gonzalez, C. L. and B. Kolb (2003) A comparison of different models of stroke on behaviour and brain morphology. *Eur J Neurosci* 18/7: 1950-1962. Available at <http://www.ncbi.nlm.nih.gov/pubmed/14622227>.
- Gorelick, P. B. (2004) Risk factors for vascular dementia and Alzheimer disease. *Stroke* 35/11 Suppl 1: 2620-2622. Available at <http://www.ncbi.nlm.nih.gov/pubmed/15375299>.
- Grafman, J., B. Jonas and A. Salazar (1990) Wisconsin Card Sorting Test performance based on location and size of neuroanatomical lesion in Vietnam veterans with penetrating head injury. *Percept Mot Skills* 71/3 Pt 2: 1120-1122. Available at <http://www.ncbi.nlm.nih.gov/pubmed/2087366>.
- Grinberg, L. T. and D. R. Thal (2010) Vascular pathology in the aged human brain. *Acta Neuropathol* 119/3: 277-290. Available at <http://www.ncbi.nlm.nih.gov/pubmed/20155424>.
- Gundersen, H. J. (1988) The nucleator. *J Microsc* 151/Pt 1: 3-21. Available at <http://www.ncbi.nlm.nih.gov/pubmed/3193456>.
- Gundersen, H. J., P. Bagger, T. F. Bendtsen, S. M. Evans, L. Korbo, N. Marcussen, A. Moller, K. Nielsen, J. R. Nyengaard, B. Pakkenberg and et al. (1988) The new stereological tools: disector, fractionator, nucleator and point sampled intercepts and their use in pathological research and diagnosis. *APMIS*

- 96/10: 857-881. Available at <http://www.ncbi.nlm.nih.gov/pubmed/3056461>.
- Haight, T. J., S. M. Landau, O. Carmichael, C. Schwarz, C. DeCarli, W. J. Jagust and Initiative Alzheimer's Disease Neuroimaging (2013) Dissociable effects of Alzheimer disease and white matter hyperintensities on brain metabolism. *JAMA Neurol* 70/8: 1039-1045. Available at <http://www.ncbi.nlm.nih.gov/pubmed/23779022>.
- Hampel, H., F. Muller-Spahn, C. Berger, A. Haberl, M. Ackenheil and C. Hock (1995) Evidence of blood-cerebrospinal fluid-barrier impairment in a subgroup of patients with dementia of the Alzheimer type and major depression: a possible indicator for immunoactivation. *Dementia* 6/6: 348-354. Available at <http://www.ncbi.nlm.nih.gov/pubmed/8563789>.
- Harding, A. J., G. M. Halliday and K. Cullen (1994) Practical considerations for the use of the optical disector in estimating neuronal number. *J Neurosci Methods* 51/1: 83-89. Available at <http://www.ncbi.nlm.nih.gov/pubmed/8189753>.
- Hardy, J. (1997) Amyloid, the presenilins and Alzheimer's disease. *Trends Neurosci* 20/4: 154-159. Available at <http://www.ncbi.nlm.nih.gov/pubmed/9106355>.
- Hardy, J. A. and G. A. Higgins (1992) Alzheimer's disease: the amyloid cascade hypothesis. *Science* 256/5054: 184-185. Available at <http://www.ncbi.nlm.nih.gov/pubmed/1566067>.
- Harrison, P. J. and S. L. Eastwood (2001) Neuropathological studies of synaptic connectivity in the hippocampal formation in schizophrenia. *Hippocampus* 11/5: 508-519. Available at <http://www.ncbi.nlm.nih.gov/pubmed/11732704>.
- Harvey, R. J., M. Skelton-Robinson and M. N. Rossor (2003) The prevalence and causes of dementia in people under the age of 65 years. *J Neurol Neurosurg Psychiatry* 74/9: 1206-1209. Available at <http://www.ncbi.nlm.nih.gov/pubmed/12933919>.
- Hawkins, B. T. and T. P. Davis (2005) The blood-brain barrier/neurovascular unit in health and disease. *Pharmacol Rev* 57/2: 173-185. Available at <http://www.ncbi.nlm.nih.gov/pubmed/15914466>.
- Hayashi, T., A. Saito, S. Okuno, M. Ferrand-Drake and P. H. Chan (2003) Induction of GRP78 by ischemic preconditioning reduces endoplasmic reticulum stress and prevents delayed neuronal cell death. *J Cereb Blood Flow Metab* 23/8: 949-961. Available at <http://www.ncbi.nlm.nih.gov/pubmed/12902839>.
- Hayes, T. L. and D. A. Lewis (1993) Hemispheric differences in layer III pyramidal neurons of the anterior language area. *Arch Neurol* 50/5: 501-505. Available at <http://www.ncbi.nlm.nih.gov/pubmed/8489407>.
- Henon, H., I. Durieu, D. Guerouaou, F. Lebert, F. Pasquier and D. Leys (2001) Poststroke dementia: incidence and relationship to prestroke cognitive decline. *Neurology* 57/7: 1216-1222. Available at <http://www.ncbi.nlm.nih.gov/pubmed/11591838>.
- Henon, H., I. Durieu, C. Lucas, O. Godefroy, F. Pasquier and D. Leys (1996) Dementia in stroke. *Neurology* 47/3: 852-853. Available at <http://www.ncbi.nlm.nih.gov/pubmed/8797503>.
- Henon, H., O. Godefroy, C. Lucas, J. P. Pruvo and D. Leys (1996) Risk factors and leukoaraiosis in stroke patients. *Acta Neurol Scand* 94/2: 137-144. Available at <http://www.ncbi.nlm.nih.gov/pubmed/8891060>.

- Hof, P. R., C. Bouras, J. Constantinidis and J. H. Morrison (1989) Balint's syndrome in Alzheimer's disease: specific disruption of the occipito-parietal visual pathway. *Brain Res* 493/2: 368-375. Available at <http://www.ncbi.nlm.nih.gov/pubmed/2765903>.
- Hof, P. R., K. Cox and J. H. Morrison (1990) Quantitative analysis of a vulnerable subset of pyramidal neurons in Alzheimer's disease: I. Superior frontal and inferior temporal cortex. *J Comp Neurol* 301/1: 44-54. Available at <http://www.ncbi.nlm.nih.gov/pubmed/2127598>.
- Hof, P. R., K. Cox, W. G. Young, M. R. Celio, J. Rogers and J. H. Morrison (1991) Parvalbumin-immunoreactive neurons in the neocortex are resistant to degeneration in Alzheimer's disease. *J Neuropathol Exp Neurol* 50/4: 451-462. Available at <http://www.ncbi.nlm.nih.gov/pubmed/2061713>.
- Hof, P. R. and J. H. Morrison (1991) Neocortical neuronal subpopulations labeled by a monoclonal antibody to calbindin exhibit differential vulnerability in Alzheimer's disease. *Exp Neurol* 111/3: 293-301. Available at <http://www.ncbi.nlm.nih.gov/pubmed/1999232>.
- Hof, P. R. and J. H. Morrison (2004) The aging brain: morphomolecular senescence of cortical circuits. *Trends Neurosci* 27/10: 607-613. Available at <http://www.ncbi.nlm.nih.gov/pubmed/15374672>.
- Hof, P. R., E. A. Nimchinsky, M. R. Celio, C. Bouras and J. H. Morrison (1993) Calretinin-immunoreactive neocortical interneurons are unaffected in Alzheimer's disease. *Neurosci Lett* 152/1-2: 145-148. Available at <http://www.ncbi.nlm.nih.gov/pubmed/8515868>.
- Huang, K. L., K. J. Lin, M. Y. Ho, Y. J. Chang, C. H. Chang, S. P. Wey, C. J. Hsieh, T. C. Yen, I. T. Hsiao and T. H. Lee (2012) Amyloid deposition after cerebral hypoperfusion: evidenced on [(18)F]AV-45 positron emission tomography. *J Neurol Sci* 319/1-2: 124-129. Available at <http://www.ncbi.nlm.nih.gov/pubmed/22572706>.
- Huey, E. D., E. N. Goveia, S. Paviol, M. Pardini, F. Krueger, G. Zamboni, M. C. Tierney, E. M. Wassermann and J. Grafman (2009) Executive dysfunction in frontotemporal dementia and corticobasal syndrome. *Neurology* 72/5: 453-459. Available at <http://www.ncbi.nlm.nih.gov/pubmed/19188577>.
- Hulette, C., D. Nochlin, D. McKeel, J. C. Morris, S. S. Mirra, S. M. Sumi and A. Heyman (1997) Clinical-neuropathologic findings in multi-infarct dementia: a report of six autopsied cases. *Neurology* 48/3: 668-672. Available at <http://www.ncbi.nlm.nih.gov/pubmed/9065545>.
- Huppert, F. A., C. Brayne, C. Gill, E. S. Paykel and L. Beardsall (1995) CAMCOG--a concise neuropsychological test to assist dementia diagnosis: socio-demographic determinants in an elderly population sample. *Br J Clin Psychol* 34 ( Pt 4): 529-541. Available at <http://www.ncbi.nlm.nih.gov/pubmed/8563660>.
- Hyman, B. T., G. W. Van Hoesen, L. J. Kromer and A. R. Damasio (1986) Perforant pathway changes and the memory impairment of Alzheimer's disease. *Ann Neurol* 20/4: 472-481. Available at <http://www.ncbi.nlm.nih.gov/pubmed/3789663>.
- Iadecola, C. (2004) Neurovascular regulation in the normal brain and in Alzheimer's disease. *Nat Rev Neurosci* 5/5: 347-360. Available at <http://www.ncbi.nlm.nih.gov/pubmed/15100718>.
- Ihara, M., T. M. Polvikoski, R. Hall, J. Y. Slade, R. H. Perry, A. E. Oakley, E. Englund, J. T. O'Brien, P. G. Ince and R. N. Kalaria (2010) Quantification of myelin loss in frontal lobe white matter in vascular dementia, Alzheimer's disease, and

- dementia with Lewy bodies. *Acta Neuropathol* 119/5: 579-589. Available at <http://www.ncbi.nlm.nih.gov/pubmed/20091409>.
- Iqbal, K., F. Liu, C. X. Gong and I. Grundke-Iqbal (2010) Tau in Alzheimer disease and related tauopathies. *Curr Alzheimer Res* 7/8: 656-664. Available at <http://www.ncbi.nlm.nih.gov/pubmed/20678074>.
- Ishii, K., T. Imamura, M. Sasaki, S. Yamaji, S. Sakamoto, H. Kitagaki, M. Hashimoto, N. Hirono, T. Shimomura and E. Mori (1998) Regional cerebral glucose metabolism in dementia with Lewy bodies and Alzheimer's disease. *Neurology* 51/1: 125-130. Available at <http://www.ncbi.nlm.nih.gov/pubmed/9674790>.
- Ishii, N., Y. Nishihara and T. Imamura (1986) Why do frontal lobe symptoms predominate in vascular dementia with lacunes? *Neurology* 36/3: 340-345. Available at <http://www.ncbi.nlm.nih.gov/pubmed/3951700>.
- Ittner, L. M., T. Fath, Y. D. Ke, M. Bi, J. van Eersel, K. M. Li, P. Gunning and J. Gotz (2008) Parkinsonism and impaired axonal transport in a mouse model of frontotemporal dementia. *Proc Natl Acad Sci U S A* 105/41: 15997-16002. Available at <http://www.ncbi.nlm.nih.gov/pubmed/18832465>.
- Jagust, W. J., J. P. Seab, R. H. Huesman, P. E. Valk, C. A. Mathis, B. R. Reed, P. G. Coxson and T. F. Budinger (1991) Diminished glucose transport in Alzheimer's disease: dynamic PET studies. *J Cereb Blood Flow Metab* 11/2: 323-330. Available at <http://www.ncbi.nlm.nih.gov/pubmed/1997504>.
- Jellinger, K. A. (2002) Alzheimer disease and cerebrovascular pathology: an update. *J Neural Transm* 109/5-6: 813-836. Available at <http://www.ncbi.nlm.nih.gov/pubmed/12111471>.
- Jellinger, K. A. (2013) Pathology and pathogenesis of vascular cognitive impairment-a critical update. *Front Aging Neurosci* 5: 17. Available at <http://www.ncbi.nlm.nih.gov/pubmed/23596414>.
- Jellinger, K. A. and J. Attems (2003) Incidence of cerebrovascular lesions in Alzheimer's disease: a postmortem study. *Acta Neuropathol* 105/1: 14-17. Available at <http://www.ncbi.nlm.nih.gov/pubmed/12471455>.
- Jobst, K. A., L. P. Barnetson and B. J. Shepstone (1998) Accurate prediction of histologically confirmed Alzheimer's disease and the differential diagnosis of dementia: the use of NINCDS-ADRDA and DSM-III-R criteria, SPECT, X-ray CT, and Apo E4 in medial temporal lobe dementias. Oxford Project to Investigate Memory and Aging. *Int Psychogeriatr* 10/3: 271-302. Available at <http://www.ncbi.nlm.nih.gov/pubmed/9785148>.
- Johnson, V. E., W. Stewart and D. H. Smith (2012) Widespread tau and amyloid-beta pathology many years after a single traumatic brain injury in humans. *Brain Pathol* 22/2: 142-149. Available at <http://www.ncbi.nlm.nih.gov/pubmed/21714827>.
- Jorm, A. F. and D. Jolley (1998) The incidence of dementia: a meta-analysis. *Neurology* 51/3: 728-733. Available at <http://www.ncbi.nlm.nih.gov/pubmed/9748017>.
- Joseph, J., B. Shukitt-Hale, N. A. Denisova, A. Martin, G. Perry and M. A. Smith (2001) Copernicus revisited: amyloid beta in Alzheimer's disease. *Neurobiol Aging* 22/1: 131-146. Available at <http://www.ncbi.nlm.nih.gov/pubmed/11164287>.
- Kakimura, J., Y. Kitamura, T. Taniguchi, S. Shimohama and P. J. Gebicke-Haerter (2001) Bip/GRP78-induced production of cytokines and uptake of amyloid-beta(1-42) peptide in microglia. *Biochem Biophys Res Commun* 281/1: 6-10. Available at <http://www.ncbi.nlm.nih.gov/pubmed/11178952>.

- Kalaria, R. N. (1992) The blood-brain barrier and cerebral microcirculation in Alzheimer disease. *Cerebrovasc Brain Metab Rev* 4/3: 226-260. Available at <http://www.ncbi.nlm.nih.gov/pubmed/1389957>.
- Kalaria, R. N. (1996) Cerebral vessels in ageing and Alzheimer's disease. *Pharmacol Ther* 72/3: 193-214. Available at <http://www.ncbi.nlm.nih.gov/pubmed/9364575>.
- Kalaria, R. N. (2002) Similarities between Alzheimer's disease and vascular dementia. *J Neurol Sci* 203-204: 29-34. Available at <http://www.ncbi.nlm.nih.gov/pubmed/12417353>.
- Kalaria, R. N. (2003) Vascular factors in Alzheimer's disease. *Int Psychogeriatr* 15 Suppl 1: 47-52. Available at <http://www.ncbi.nlm.nih.gov/pubmed/16191216>.
- Kalaria, R. N. (2010) Vascular basis for brain degeneration: faltering controls and risk factors for dementia. *Nutr Rev* 68 Suppl 2: S74-87. Available at <http://www.ncbi.nlm.nih.gov/pubmed/21091952>.
- Kalaria, R. N. (2012) Cerebrovascular disease and mechanisms of cognitive impairment: evidence from clinicopathological studies in humans. *Stroke* 43/9: 2526-2534. Available at <http://www.ncbi.nlm.nih.gov/pubmed/22879100>.
- Kalaria, R. N., R. Akinyemi and M. Ihara (2012) Does vascular pathology contribute to Alzheimer changes? *J Neurol Sci* 322/1-2: 141-147. Available at <http://www.ncbi.nlm.nih.gov/pubmed/22884479>.
- Kalaria, R. N. and C. Ballard (1999) Overlap between pathology of Alzheimer disease and vascular dementia. *Alzheimer Dis Assoc Disord* 13 Suppl 3: S115-123. Available at <http://www.ncbi.nlm.nih.gov/pubmed/10609690>.
- Kalaria, R. N. and C. Ballard (2001) Stroke and cognition. *Curr Atheroscler Rep* 3/4: 334-339. Available at <http://www.ncbi.nlm.nih.gov/pubmed/11389800>.
- Kalaria, R. N., D. L. Cohen, D. R. Premkumar, S. Nag, J. C. LaManna and W. D. Lust (1998) Vascular endothelial growth factor in Alzheimer's disease and experimental cerebral ischemia. *Brain Res Mol Brain Res* 62/1: 101-105. Available at <http://www.ncbi.nlm.nih.gov/pubmed/9795165>.
- Kalaria, R. N. and M. Ihara (2013) Dementia: Vascular and neurodegenerative pathways-will they meet? *Nat Rev Neurol* 9/9: 487-488. Available at <http://www.ncbi.nlm.nih.gov/pubmed/23938746>.
- Kalaria, R. N., R. A. Kenny, C. G. Ballard, R. Perry, P. Ince and T. Polvikoski (2004) Towards defining the neuropathological substrates of vascular dementia. *J Neurol Sci* 226/1-2: 75-80. Available at <http://www.ncbi.nlm.nih.gov/pubmed/15537525>.
- Kalimo, H., M. Kaste and M. Haltia (2002) Greenfield's Chapter 6: Vascular diseases. 310-311.
- Karran, E., M. Mercken and B. De Strooper (2011) The amyloid cascade hypothesis for Alzheimer's disease: an appraisal for the development of therapeutics. *Nat Rev Drug Discov* 10/9: 698-712. Available at <http://www.ncbi.nlm.nih.gov/pubmed/21852788>.
- Kemper, T. L., G. J. Blatt, R. J. Killiany and M. B. Moss (2001) Neuropathology of progressive cognitive decline in chronically hypertensive rhesus monkeys. *Acta Neuropathol* 101/2: 145-153. Available at <http://www.ncbi.nlm.nih.gov/pubmed/11271369>.
- Khachaturian, Z. S. (1985) Diagnosis of Alzheimer's disease. *Arch Neurol* 42/11: 1097-1105. Available at <http://www.ncbi.nlm.nih.gov/pubmed/2864910>.

- Khundakar, A., C. M. Morris, A. E. Oakley and A. J. Thomas (2011a) Cellular pathology within the anterior cingulate cortex of patients with late-life depression: a morphometric study. *Psychiatry Res* 194/2: 184-189. Available at <http://www.ncbi.nlm.nih.gov/pubmed/21924875>.
- Khundakar, A., C. Morris, A. Oakley, W. McMeekin and A. J. Thomas (2009) Morphometric analysis of neuronal and glial cell pathology in the dorsolateral prefrontal cortex in late-life depression. *Br J Psychiatry* 195/2: 163-169. Available at <http://www.ncbi.nlm.nih.gov/pubmed/19648551>.
- Khundakar, A., C. Morris, A. Oakley and A. J. Thomas (2011b) Morphometric analysis of neuronal and glial cell pathology in the caudate nucleus in late-life depression. *Am J Geriatr Psychiatry* 19/2: 132-141. Available at <http://www.ncbi.nlm.nih.gov/pubmed/20808096>.
- Khundakar, A., C. Morris, A. Oakley and A. J. Thomas (2011c) A morphometric examination of neuronal and glial cell pathology in the orbitofrontal cortex in late-life depression. *Int Psychogeriatr* 23/1: 132-140. Available at <http://www.ncbi.nlm.nih.gov/pubmed/20561380>.
- Kimelberg, H. K. (2005) Astrocytic swelling in cerebral ischemia as a possible cause of injury and target for therapy. *Glia* 50/4: 389-397. Available at <http://www.ncbi.nlm.nih.gov/pubmed/15846797>.
- Kish, S. J., C. Bergeron, A. Rajput, S. Dozic, F. Mastrogiacomo, L. J. Chang, J. M. Wilson, L. M. DiStefano and J. N. Nobrega (1992) Brain cytochrome oxidase in Alzheimer's disease. *J Neurochem* 59/2: 776-779. Available at <http://www.ncbi.nlm.nih.gov/pubmed/1321237>.
- Kling, M. A., J. Q. Trojanowski, D. A. Wolk, V. M. Lee and S. E. Arnold (2013) Vascular disease and dementias: paradigm shifts to drive research in new directions. *Alzheimers Dement* 9/1: 76-92. Available at <http://www.ncbi.nlm.nih.gov/pubmed/23183137>.
- Klunk, W. E., H. Engler, A. Nordberg, Y. Wang, G. Blomqvist, D. P. Holt, M. Bergstrom, I. Savitcheva, G. F. Huang, S. Estrada, B. Ausen, M. L. Debnath, J. Barletta, J. C. Price, J. Sandell, B. J. Lopresti, A. Wall, P. Koivisto, G. Antoni, C. A. Mathis and B. Langstrom (2004) Imaging brain amyloid in Alzheimer's disease with Pittsburgh Compound-B. *Ann Neurol* 55/3: 306-319. Available at <http://www.ncbi.nlm.nih.gov/pubmed/14991808>.
- Knudsen, K. A., J. Rosand, D. Karluk and S. M. Greenberg (2001) Clinical diagnosis of cerebral amyloid angiopathy: validation of the Boston criteria. *Neurology* 56/4: 537-539. Available at <http://www.ncbi.nlm.nih.gov/pubmed/11222803>.
- Koehler, R. C., R. J. Roman and D. R. Harder (2009) Astrocytes and the regulation of cerebral blood flow. *Trends Neurosci* 32/3: 160-169. Available at <http://www.ncbi.nlm.nih.gov/pubmed/19162338>.
- Kokmen, E., J. P. Whisnant, W. M. O'Fallon, C. P. Chu and C. M. Beard (1996) Dementia after ischemic stroke: a population-based study in Rochester, Minnesota (1960-1984). *Neurology* 46/1: 154-159. Available at <http://www.ncbi.nlm.nih.gov/pubmed/8559366>.
- Kreutzberg, G. W. (1996) Microglia: a sensor for pathological events in the CNS. *Trends Neurosci* 19/8: 312-318. Available at <http://www.ncbi.nlm.nih.gov/pubmed/8843599>.
- Kril, J. J., G. M. Halliday, M. D. Svoboda and H. Cartwright (1997) The cerebral cortex is damaged in chronic alcoholics. *Neuroscience* 79/4: 983-998. Available at <http://www.ncbi.nlm.nih.gov/pubmed/9219961>.

- Krishnan, K. R., V. Goli, E. H. Ellinwood, R. D. France, D. G. Blazer and C. B. Nemeroff (1988) Leukoencephalopathy in patients diagnosed as major depressive. *Biol Psychiatry* 23/5: 519-522. Available at <http://www.ncbi.nlm.nih.gov/pubmed/3345325>.
- Kuczynski, B., W. Jagust, H. C. Chui and B. Reed (2009) An inverse association of cardiovascular risk and frontal lobe glucose metabolism. *Neurology* 72/8: 738-743. Available at <http://www.ncbi.nlm.nih.gov/pubmed/19237703>.
- Kuhl, D. E., M. E. Phelps, A. P. Kowell, E. J. Metter, C. Selin and J. Winter (1980) Effects of stroke on local cerebral metabolism and perfusion: mapping by emission computed tomography of 18FDG and 13NH3. *Ann Neurol* 8/1: 47-60. Available at <http://www.ncbi.nlm.nih.gov/pubmed/6967712>.
- Laakso, M. P., K. Partanen, P. Riekkinen, M. Lehtovirta, E. L. Helkala, M. Hallikainen, T. Hanninen, P. Vainio and H. Soininen (1996) Hippocampal volumes in Alzheimer's disease, Parkinson's disease with and without dementia, and in vascular dementia: An MRI study. *Neurology* 46/3: 678-681. Available at <http://www.ncbi.nlm.nih.gov/pubmed/8618666>.
- Lamb, B. T. (1997) Presenilins, amyloid-beta and Alzheimer's disease. *Nat Med* 3/1: 28-29. Available at <http://www.ncbi.nlm.nih.gov/pubmed/8986735>.
- Lammie, G. A. (2000) Pathology of small vessel stroke. *Br Med Bull* 56/2: 296-306. Available at <http://www.ncbi.nlm.nih.gov/pubmed/11092081>.
- Laroche, S., S. Davis and T. M. Jay (2000) Plasticity at hippocampal to prefrontal cortex synapses: dual roles in working memory and consolidation. *Hippocampus* 10/4: 438-446. Available at <http://www.ncbi.nlm.nih.gov/pubmed/10985283>.
- Larsen, G. A., H. K. Skjellegrind, J. Berg-Johnsen, M. C. Moe and M. L. Vinje (2006) Depolarization of mitochondria in isolated CA1 neurons during hypoxia, glucose deprivation and glutamate excitotoxicity. *Brain Res* 1077/1: 153-160. Available at <http://www.ncbi.nlm.nih.gov/pubmed/16480964>.
- Leal, J., R. Luengo-Fernandez, A. Gray, S. Petersen and M. Rayner (2006) Economic burden of cardiovascular diseases in the enlarged European Union. *Eur Heart J* 27/13: 1610-1619. Available at <http://www.ncbi.nlm.nih.gov/pubmed/16495286>.
- Lee, J., A. J. Bruce-Keller, Y. Kruman, S. L. Chan and M. P. Mattson (1999) 2-Deoxy-D-glucose protects hippocampal neurons against excitotoxic and oxidative injury: evidence for the involvement of stress proteins. *J Neurosci Res* 57/1: 48-61. Available at <http://www.ncbi.nlm.nih.gov/pubmed/10397635>.
- Leeds, L., R. J. Meara, R. Woods and J. P. Hobson (2001) A comparison of the new executive functioning domains of the CAMCOG-R with existing tests of executive function in elderly stroke survivors. *Age Ageing* 30/3: 251-254. Available at <http://www.ncbi.nlm.nih.gov/pubmed/11443027>.
- Lees, G. J. (1993) The possible contribution of microglia and macrophages to delayed neuronal death after ischemia. *J Neurol Sci* 114/2: 119-122. Available at <http://www.ncbi.nlm.nih.gov/pubmed/8445391>.
- Leis, J. A., L. K. Bekar and W. Walz (2005) Potassium homeostasis in the ischemic brain. *Glia* 50/4: 407-416. Available at <http://www.ncbi.nlm.nih.gov/pubmed/15846795>.
- Letinic, K., R. Zoncu and P. Rakic (2002) Origin of GABAergic neurons in the human neocortex. *Nature* 417/6889: 645-649. Available at <http://www.ncbi.nlm.nih.gov/pubmed/12050665>.
- Lewis, D. A., M. J. Campbell, R. D. Terry and J. H. Morrison (1987) Lamina and regional distributions of neurofibrillary tangles and neuritic plaques in



- Alzheimer's disease: a quantitative study of visual and auditory cortices. *J Neurosci* 7/6: 1799-1808. Available at <http://www.ncbi.nlm.nih.gov/pubmed/2439665>.
- Leys, D., H. Henon, M. A. Mackowiak-Cordoliani and F. Pasquier (2005) Poststroke dementia. *Lancet Neurol* 4/11: 752-759. Available at <http://www.ncbi.nlm.nih.gov/pubmed/16239182>.
- Leys, D., H. Henon and F. Pasquier (1998) White matter changes and poststroke dementia. *Dement Geriatr Cogn Disord* 9 Suppl 1: 25-29. Available at <http://www.ncbi.nlm.nih.gov/pubmed/9716241>.
- Liberatore, G. T., V. Jackson-Lewis, S. Vukosavic, A. S. Mandir, M. Vila, W. G. McAuliffe, V. L. Dawson, T. M. Dawson and S. Przedborski (1999) Inducible nitric oxide synthase stimulates dopaminergic neurodegeneration in the MPTP model of Parkinson disease. *Nat Med* 5/12: 1403-1409. Available at <http://www.ncbi.nlm.nih.gov/pubmed/10581083>.
- Libon, D. J., S. X. Xie, X. Wang, L. Massimo, P. Moore, L. Vesely, A. Khan, A. Chatterjee, H. B. Coslett, H. I. Hurtig, T. W. Liang and M. Grossman (2009) Neuropsychological decline in frontotemporal lobar degeneration: a longitudinal analysis. *Neuropsychology* 23/3: 337-346. Available at <http://www.ncbi.nlm.nih.gov/pubmed/19413447>.
- Lichter, D. G. and J. L. Cummings (2001) Frontal-Subcortical Circuits in Psychiatric and Neurological Disorders.
- Lobsiger, C. S. and D. W. Cleveland (2007) Glial cells as intrinsic components of non-cell-autonomous neurodegenerative disease. *Nat Neurosci* 10/11: 1355-1360. Available at <http://www.ncbi.nlm.nih.gov/pubmed/17965655>.
- LoPachin, R. M., Jr. and M. Aschner (1993) Glial-neuronal interactions: relevance to neurotoxic mechanisms. *Toxicol Appl Pharmacol* 118/2: 141-158. Available at <http://www.ncbi.nlm.nih.gov/pubmed/8441994>.
- Ly, J. and P. Maquet (2014) [Stroke and aging]. Translation of Accident vasculaire cerebral du sujet age. *Rev Med Liege* 69/5-6: 315-317. Available at <http://www.ncbi.nlm.nih.gov/pubmed/25065238>.
- Mack, T. G., M. Reiner, B. Beirowski, W. Mi, M. Emanuelli, D. Wagner, D. Thomson, T. Gillingwater, F. Court, L. Conforti, F. S. Fernando, A. Tarlton, C. Andressen, K. Addicks, G. Magni, R. R. Ribchester, V. H. Perry and M. P. Coleman (2001) Wallerian degeneration of injured axons and synapses is delayed by a Ube4b/Nmnat chimeric gene. *Nat Neurosci* 4/12: 1199-1206. Available at <http://www.ncbi.nlm.nih.gov/pubmed/11770485>.
- Maelicke, A. (2001) The pharmacological rationale for treating vascular dementia with galantamine (Reminyl). *Int J Clin Pract Suppl* /120: 24-28. Available at <http://www.ncbi.nlm.nih.gov/pubmed/11406923>.
- Magistretti, P. J. (2006) Neuron-glia metabolic coupling and plasticity. *J Exp Biol* 209/Pt 12: 2304-2311. Available at <http://www.ncbi.nlm.nih.gov/pubmed/16731806>.
- Magistretti, P. J. and L. Pellerin (1999) Cellular mechanisms of brain energy metabolism and their relevance to functional brain imaging. *Philos Trans R Soc Lond B Biol Sci* 354/1387: 1155-1163. Available at <http://www.ncbi.nlm.nih.gov/pubmed/10466143>.
- Majno, G. and I. Joris (1995) Apoptosis, oncosis, and necrosis. An overview of cell death. *Am J Pathol* 146/1: 3-15. Available at <http://www.ncbi.nlm.nih.gov/pubmed/7856735>.

- Mandelkow, E. M. and E. Mandelkow (1998) Tau in Alzheimer's disease. *Trends Cell Biol* 8/11: 425-427. Available at <http://www.ncbi.nlm.nih.gov/pubmed/9854307>.
- Mangialasche, F., A. Solomon, B. Winblad, P. Mecocci and M. Kivipelto (2010) Alzheimer's disease: clinical trials and drug development. *Lancet Neurol* 9/7: 702-716. Available at <http://www.ncbi.nlm.nih.gov/pubmed/20610346>.
- Mann, D. M., B. Marcyniuk, P. O. Yates, D. Neary and J. S. Snowden (1988) The progression of the pathological changes of Alzheimer's disease in frontal and temporal neocortex examined both at biopsy and at autopsy. *Neuropathol Appl Neurobiol* 14/3: 177-195. Available at <http://www.ncbi.nlm.nih.gov/pubmed/3405392>.
- Mapstone, M., A. K. Cheema, M. S. Fiandaca, X. Zhong, T. R. Mhyre, L. H. MacArthur, W. J. Hall, S. G. Fisher, D. R. Peterson, J. M. Haley, M. D. Nazar, S. A. Rich, D. J. Berlau, C. B. Peltz, M. T. Tan, C. H. Kawas and H. J. Federoff (2014) Plasma phospholipids identify antecedent memory impairment in older adults. *Nat Med* 20/4: 415-418. Available at <http://www.ncbi.nlm.nih.gov/pubmed/24608097>.
- Marin-Padilla, M. (1969) Origin of the pericellular baskets of the pyramidal cells of the human motor cortex: a Golgi study. *Brain Res* 14/3: 633-646. Available at <http://www.ncbi.nlm.nih.gov/pubmed/4186210>.
- Markram, H., M. Toledo-Rodriguez, Y. Wang, A. Gupta, G. Silberberg and C. Wu (2004) Interneurons of the neocortical inhibitory system. *Nat Rev Neurosci* 5/10: 793-807. Available at <http://www.ncbi.nlm.nih.gov/pubmed/15378039>.
- Marner, L., J. R. Nyengaard, Y. Tang and B. Pakkenberg (2003) Marked loss of myelinated nerve fibers in the human brain with age. *J Comp Neurol* 462/2: 144-152. Available at <http://www.ncbi.nlm.nih.gov/pubmed/12794739>.
- Masliah, E. (1995) Mechanisms of synaptic dysfunction in Alzheimer's disease. *Histol Histopathol* 10/2: 509-519. Available at <http://www.ncbi.nlm.nih.gov/pubmed/7599445>.
- Masliah, E. (1998) Mechanisms of synaptic pathology in Alzheimer's disease. *J Neural Transm Suppl* 53: 147-158. Available at <http://www.ncbi.nlm.nih.gov/pubmed/9700653>.
- Masson, C., D. Leys and L. Buee (2000) [Cerebral amyloid angiopathies]. Translation of Les angiopathies amyloides cerebrales. *Presse Med* 29/31: 1717-1722. Available at <http://www.ncbi.nlm.nih.gov/pubmed/11094619>.
- Mayhew, T. M. and H. J. Gundersen (1996) If you assume, you can make an ass out of u and me': a decade of the disector for stereological counting of particles in 3D space. *J Anat* 188 ( Pt 1): 1-15. Available at <http://www.ncbi.nlm.nih.gov/pubmed/8655396>.
- Medana, I. M. and M. M. Esiri (2003) Axonal damage: a key predictor of outcome in human CNS diseases. *Brain* 126/Pt 3: 515-530. Available at <http://www.ncbi.nlm.nih.gov/pubmed/12566274>.
- Moller, A., P. Strange and H. J. Gundersen (1990) Efficient estimation of cell volume and number using the nucleator and the disector. *J Microsc* 159/Pt 1: 61-71. Available at <http://www.ncbi.nlm.nih.gov/pubmed/2204703>.
- Moncada, S. and J. D. Erusalimsky (2002) Does nitric oxide modulate mitochondrial energy generation and apoptosis? *Nat Rev Mol Cell Biol* 3/3: 214-220. Available at <http://www.ncbi.nlm.nih.gov/pubmed/11994742>.

- Montine, T. J., C. H. Phelps, T. G. Beach, E. H. Bigio, N. J. Cairns, D. W. Dickson, C. Duyckaerts, M. P. Frosch, E. Masliah, S. S. Mirra, P. T. Nelson, J. A. Schneider, D. R. Thal, J. Q. Trojanowski, H. V. Vinters, B. T. Hyman, Aging National Institute on and Association Alzheimer's (2012) National Institute on Aging-Alzheimer's Association guidelines for the neuropathologic assessment of Alzheimer's disease: a practical approach. *Acta Neuropathol* 123/1: 1-11. Available at <http://www.ncbi.nlm.nih.gov/pubmed/22101365>.
- Moody, D. M., C. R. Thore, J. A. Anstrom, V. R. Challa, C. D. Langefeld and W. R. Brown (2004) Quantification of afferent vessels shows reduced brain vascular density in subjects with leukoariosis. *Radiology* 233/3: 883-890. Available at <http://www.ncbi.nlm.nih.gov/pubmed/15564412>.
- Moroney, J. T., E. Bagiella, D. W. Desmond, M. C. Paik, Y. Stern and T. K. Tatemichi (1997) Cerebral hypoxia and ischemia in the pathogenesis of dementia after stroke. *Ann N Y Acad Sci* 826: 433-436. Available at <http://www.ncbi.nlm.nih.gov/pubmed/9329718>.
- Moroney, J. T. and D. W. Desmond (1997) Predictors in stroke outcome. *Neurology* 48/5: 1475-1476; author reply 1476-1477. Available at <http://www.ncbi.nlm.nih.gov/pubmed/9153509>.
- Morris, C. M., C. G. Ballard, L. Allan, E. Rowan, S. Stephens, M. Firbank, G. A. Ford, R. A. Kenny, J. T. O'Brien and R. N. Kalaria (2011) NOS3 gene rs1799983 polymorphism and incident dementia in elderly stroke survivors. *Neurobiol Aging* 32/3: 554 e551-556. Available at <http://www.ncbi.nlm.nih.gov/pubmed/20691505>.
- Morrison, J. H. and P. R. Hof (1997) Life and death of neurons in the aging brain. *Science* 278/5337: 412-419. Available at <http://www.ncbi.nlm.nih.gov/pubmed/9334292>.
- Mosconi, L. (2005) Brain glucose metabolism in the early and specific diagnosis of Alzheimer's disease. FDG-PET studies in MCI and AD. *Eur J Nucl Med Mol Imaging* 32/4: 486-510. Available at <http://www.ncbi.nlm.nih.gov/pubmed/15747152>.
- Mountcastle, V. B. (1997) The columnar organization of the neocortex. *Brain* 120 (Pt 4): 701-722. Available at <http://www.ncbi.nlm.nih.gov/pubmed/9153131>.
- Mutch, W. A. (2010) New concepts regarding cerebral vasospasm: glial-centric mechanisms. *Can J Anaesth* 57/5: 479-489. Available at <http://www.ncbi.nlm.nih.gov/pubmed/20131107>.
- Nagele, R. G., J. Wegiel, V. Venkataraman, H. Imaki, K. C. Wang and J. Wegiel (2004) Contribution of glial cells to the development of amyloid plaques in Alzheimer's disease. *Neurobiol Aging* 25/5: 663-674. Available at <http://www.ncbi.nlm.nih.gov/pubmed/15172746>.
- Nave, K. A. (2010a) Myelination and support of axonal integrity by glia. *Nature* 468/7321: 244-252. Available at <http://www.ncbi.nlm.nih.gov/pubmed/21068833>.
- Nave, K. A. (2010b) Myelination and the trophic support of long axons. *Nat Rev Neurosci* 11/4: 275-283. Available at <http://www.ncbi.nlm.nih.gov/pubmed/20216548>.
- Nedergaard, M. and U. Dirnagl (2005) Role of glial cells in cerebral ischemia. *Glia* 50/4: 281-286. Available at <http://www.ncbi.nlm.nih.gov/pubmed/15846807>.

- Nedergaard, M., B. Ransom and S. A. Goldman (2003) New roles for astrocytes: redefining the functional architecture of the brain. *Trends Neurosci* 26/10: 523-530. Available at <http://www.ncbi.nlm.nih.gov/pubmed/14522144>.
- Nelson, P. T., I. Alafuzoff, E. H. Bigio, C. Bouras, H. Braak, N. J. Cairns, R. J. Castellani, B. J. Crain, P. Davies, K. Del Tredici, C. Duyckaerts, M. P. Frosch, V. Haroutunian, P. R. Hof, C. M. Hulette, B. T. Hyman, T. Iwatsubo, K. A. Jellinger, G. A. Jicha, E. Kovari, W. A. Kukull, J. B. Leverenz, S. Love, I. R. Mackenzie, D. M. Mann, E. Masliah, A. C. McKee, T. J. Montine, J. C. Morris, J. A. Schneider, J. A. Sonnen, D. R. Thal, J. Q. Trojanowski, J. C. Troncoso, T. Wisniewski, R. L. Woltjer and T. G. Beach (2012) Correlation of Alzheimer disease neuropathologic changes with cognitive status: a review of the literature. *J Neuropathol Exp Neurol* 71/5: 362-381. Available at <http://www.ncbi.nlm.nih.gov/pubmed/22487856>.
- Nimmerjahn, A., F. Kirchhoff and F. Helmchen (2005) Resting microglial cells are highly dynamic surveillants of brain parenchyma in vivo. *Science* 308/5726: 1314-1318. Available at <http://www.ncbi.nlm.nih.gov/pubmed/15831717>.
- Nudo, R. J. (2003) Adaptive plasticity in motor cortex: implications for rehabilitation after brain injury. *J Rehabil Med* /41 Suppl: 7-10. Available at <http://www.ncbi.nlm.nih.gov/pubmed/12817650>.
- O'Brien, J. T., T. Erkinjuntti, B. Reisberg, G. Roman, T. Sawada, L. Pantoni, J. V. Bowler, C. Ballard, C. DeCarli, P. B. Gorelick, K. Rockwood, A. Burns, S. Gauthier and S. T. DeKosky (2003) Vascular cognitive impairment. *Lancet Neurol* 2/2: 89-98. Available at <http://www.ncbi.nlm.nih.gov/pubmed/12849265>.
- O'Brien, J. T., R. Wiseman, E. J. Burton, B. Barber, K. Wesnes, B. Saxby and G. A. Ford (2002) Cognitive associations of subcortical white matter lesions in older people. *Ann N Y Acad Sci* 977: 436-444. Available at <http://www.ncbi.nlm.nih.gov/pubmed/12480784>.
- Ohm, T. G., H. Muller, H. Braak and J. Bohl (1995) Close-meshed prevalence rates of different stages as a tool to uncover the rate of Alzheimer's disease-related neurofibrillary changes. *Neuroscience* 64/1: 209-217. Available at <http://www.ncbi.nlm.nih.gov/pubmed/7708206>.
- Okamoto, Y., T. Yamamoto, R. N. Kalaria, H. Senzaki, T. Maki, Y. Hase, A. Kitamura, K. Washida, M. Yamada, H. Ito, H. Tomimoto, R. Takahashi and M. Ihara (2012) Cerebral hypoperfusion accelerates cerebral amyloid angiopathy and promotes cortical microinfarcts. *Acta Neuropathol* 123/3: 381-394. Available at <http://www.ncbi.nlm.nih.gov/pubmed/22170742>.
- Opris, I. and M. F. Casanova (2014) Prefrontal cortical minicolumn: from executive control to disrupted cognitive processing. *Brain* 137/Pt 7: 1863-1875. Available at <http://www.ncbi.nlm.nih.gov/pubmed/24531625>.
- Parker, W. D., Jr., C. M. Filley and J. K. Parks (1990) Cytochrome oxidase deficiency in Alzheimer's disease. *Neurology* 40/8: 1302-1303. Available at <http://www.ncbi.nlm.nih.gov/pubmed/2166249>.
- Paschen, W. (2001) Dependence of vital cell function on endoplasmic reticulum calcium levels: implications for the mechanisms underlying neuronal cell injury in different pathological states. *Cell Calcium* 29/1: 1-11. Available at <http://www.ncbi.nlm.nih.gov/pubmed/11133351>.
- Pascual, B., E. Prieto, J. Arbizu, J. Marti-Climent, J. Olier and J. C. Masdeu (2010) Brain glucose metabolism in vascular white matter disease with dementia: differentiation from Alzheimer disease. *Stroke* 41/12: 2889-2893. Available at <http://www.ncbi.nlm.nih.gov/pubmed/21051671>.

- Pasquier, F. and D. Leys (1997) Why are stroke patients prone to develop dementia? *J Neurol* 244/3: 135-142. Available at <http://www.ncbi.nlm.nih.gov/pubmed/9050953>.
- Pendlebury, S. T. and P. M. Rothwell (2009) Prevalence, incidence, and factors associated with pre-stroke and post-stroke dementia: a systematic review and meta-analysis. *Lancet Neurol* 8/11: 1006-1018. Available at <http://www.ncbi.nlm.nih.gov/pubmed/19782001>.
- Perret, E. (1974) The left frontal lobe of man and the suppression of habitual responses in verbal categorical behaviour. *Neuropsychologia* 12/3: 323-330. Available at <http://www.ncbi.nlm.nih.gov/pubmed/4421777>.
- Perry, E. K., G. Blessed, B. E. Tomlinson, R. H. Perry, T. J. Crow, A. J. Cross, G. J. Dockray, R. Dimaline and A. Arregui (1981) Neurochemical activities in human temporal lobe related to aging and Alzheimer-type changes. *Neurobiol Aging* 2/4: 251-256. Available at <http://www.ncbi.nlm.nih.gov/pubmed/6174877>.
- Perry, Oakley (1993) Newcastle brain map. *Neuropsychiatric Disorders*.
- Perry, V. H., M. C. Brown and E. R. Lunn (1991) Very Slow Retrograde and Wallerian Degeneration in the CNS of C57BL/Ola Mice. *Eur J Neurosci* 3/1: 102-105. Available at <http://www.ncbi.nlm.nih.gov/pubmed/12106273>.
- Pfeiffer, S. E., A. E. Warrington and R. Bansal (1993) The oligodendrocyte and its many cellular processes. *Trends Cell Biol* 3/6: 191-197. Available at <http://www.ncbi.nlm.nih.gov/pubmed/14731493>.
- Pfriege, F. W. (2009) Roles of glial cells in synapse development. *Cell Mol Life Sci* 66/13: 2037-2047. Available at <http://www.ncbi.nlm.nih.gov/pubmed/19308323>.
- Pfriege, F. W. (2010) Role of glial cells in the formation and maintenance of synapses. *Brain Res Rev* 63/1-2: 39-46. Available at <http://www.ncbi.nlm.nih.gov/pubmed/19931561>.
- Pickering-Brown, S. M. (2007) The complex aetiology of frontotemporal lobar degeneration. *Exp Neurol* 206/1: 1-10. Available at <http://www.ncbi.nlm.nih.gov/pubmed/17509568>.
- Pickering-Brown, S. M. (2010) Review: Recent progress in frontotemporal lobar degeneration. *Neuropathol Appl Neurobiol* 36/1: 4-16. Available at <http://www.ncbi.nlm.nih.gov/pubmed/19821908>.
- Pickering-Brown, S. M., S. Rollinson, D. Du Plessis, K. E. Morrison, A. Varma, A. M. Richardson, D. Neary, J. S. Snowden and D. M. Mann (2008) Frequency and clinical characteristics of progranulin mutation carriers in the Manchester frontotemporal lobar degeneration cohort: comparison with patients with MAPT and no known mutations. *Brain* 131/Pt 3: 721-731. Available at <http://www.ncbi.nlm.nih.gov/pubmed/18192287>.
- Pierri, J. N., C. L. Volk, S. Auh, A. Sampson and D. A. Lewis (2001) Decreased somal size of deep layer 3 pyramidal neurons in the prefrontal cortex of subjects with schizophrenia. *Arch Gen Psychiatry* 58/5: 466-473. Available at <http://www.ncbi.nlm.nih.gov/pubmed/11343526>.
- Pohjasvaara, T., T. Erkinjuntti, R. Ylikoski, M. Hietanen, R. Vataja and M. Kaste (1998) Clinical determinants of poststroke dementia. *Stroke* 29/1: 75-81. Available at <http://www.ncbi.nlm.nih.gov/pubmed/9445332>.
- Pohjasvaara, T., M. Leskela, R. Vataja, H. Kalska, R. Ylikoski, M. Hietanen, A. Leppavuori, M. Kaste and T. Erkinjuntti (2002) Post-stroke depression, executive dysfunction and functional outcome. *Eur J Neurol* 9/3: 269-275. Available at <http://www.ncbi.nlm.nih.gov/pubmed/11985635>.

- Quinones, Q. J., G. G. de Ridder and S. V. Pizzo (2008) GRP78: a chaperone with diverse roles beyond the endoplasmic reticulum. *Histol Histopathol* 23/11: 1409-1416. Available at <http://www.ncbi.nlm.nih.gov/pubmed/18785123>.
- Rajkowska, G., J. J. Miguel-Hidalgo, P. Dubey, C. A. Stockmeier and K. R. R. Krishnan (2005) Prominent reduction in pyramidal neurons density in the orbitofrontal cortex of elderly depressed patients. *Biological Psychiatry* 58/4: 297-306. Available at <http://www.scopus.com/inward/record.url?eid=2-s2.0-23644453791&partnerID=40&md5=662d1716c90730f3d945b61499ac8a1d>.
- Rajkowska, G., J. J. Miguel-Hidalgo, J. Wei, G. Dilley, S. D. Pittman, H. Y. Meltzer, J. C. Overholser, B. L. Roth and C. A. Stockmeier (1999) Morphometric evidence for neuronal and glial prefrontal cell pathology in major depression. *Biol Psychiatry* 45/9: 1085-1098. Available at <http://www.ncbi.nlm.nih.gov/pubmed/10331101>.
- Rao, R. V., A. Peel, A. Logvinova, G. del Rio, E. Hermel, T. Yokota, P. C. Goldsmith, L. M. Ellerby, H. M. Ellerby and D. E. Bredesen (2002) Coupling endoplasmic reticulum stress to the cell death program: role of the ER chaperone GRP78. *FEBS Lett* 514/2-3: 122-128. Available at <http://www.ncbi.nlm.nih.gov/pubmed/11943137>.
- Ratnavalli, E., C. Brayne, K. Dawson and J. R. Hodges (2002) The prevalence of frontotemporal dementia. *Neurology* 58/11: 1615-1621. Available at <http://www.ncbi.nlm.nih.gov/pubmed/12058088>.
- Reed, B. R., J. L. Eberling, D. Mungas, M. Weiner, J. H. Kramer and W. J. Jagust (2004) Effects of white matter lesions and lacunes on cortical function. *Arch Neurol* 61/10: 1545-1550. Available at <http://www.ncbi.nlm.nih.gov/pubmed/15477508>.
- Regeur, L., G. B. Jensen, H. Pakkenberg, S. M. Evans and B. Pakkenberg (1994) No global neocortical nerve cell loss in brains from patients with senile dementia of Alzheimer's type. *Neurobiol Aging* 15/3: 347-352. Available at <http://www.ncbi.nlm.nih.gov/pubmed/7936059>.
- Richardson, P. M., V. M. Issa and S. Shemie (1982) Regeneration and retrograde degeneration of axons in the rat optic nerve. *J Neurocytol* 11/6: 949-966. Available at <http://www.ncbi.nlm.nih.gov/pubmed/7153791>.
- Roman, G. C. (2002a) Vascular dementia may be the most common form of dementia in the elderly. *J Neurol Sci* 203-204: 7-10. Available at <http://www.ncbi.nlm.nih.gov/pubmed/12417349>.
- Roman, G. C. (2002b) Vascular dementia revisited: diagnosis, pathogenesis, treatment, and prevention. *Med Clin North Am* 86/3: 477-499. Available at <http://www.ncbi.nlm.nih.gov/pubmed/12168556>.
- Roman, G. C., T. Erkinjuntti, A. Wallin, L. Pantoni and H. C. Chui (2002) Subcortical ischaemic vascular dementia. *Lancet Neurol* 1/7: 426-436. Available at <http://www.ncbi.nlm.nih.gov/pubmed/12849365>.
- Roman, G. C. and D. R. Royall (1999) Executive control function: a rational basis for the diagnosis of vascular dementia. *Alzheimer Dis Assoc Disord* 13 Suppl 3: S69-80. Available at <http://www.ncbi.nlm.nih.gov/pubmed/10609685>.
- Rose, S. E., F. Chen, J. B. Chalk, F. O. Zelaya, W. E. Strugnell, M. Benson, J. Semple and D. M. Doddrell (2000) Loss of connectivity in Alzheimer's disease: an evaluation of white matter tract integrity with colour coded MR diffusion tensor imaging. *J Neurol Neurosurg Psychiatry* 69/4: 528-530. Available at <http://www.ncbi.nlm.nih.gov/pubmed/10990518>.

- Rosoklija, G., B. Mancevski, B. Ilievski, T. Perera, S. H. Lisanby, J. D. Coplan, A. Duma, T. Serafimova and A. J. Dwork (2003) Optimization of Golgi methods for impregnation of brain tissue from humans and monkeys. *J Neurosci Methods* 131/1-2: 1-7. Available at <http://www.ncbi.nlm.nih.gov/pubmed/14659818>.
- Rouach, N., E. Avignone, W. Meme, A. Koulakoff, L. Venance, F. Blomstrand and C. Giaume (2002) Gap junctions and connexin expression in the normal and pathological central nervous system. *Biol Cell* 94/7-8: 457-475. Available at <http://www.ncbi.nlm.nih.gov/pubmed/12566220>.
- Sanchez-Gomez, M. V., E. Alberdi, G. Ibarretxe, I. Torre and C. Matute (2003) Caspase-dependent and caspase-independent oligodendrocyte death mediated by AMPA and kainate receptors. *J Neurosci* 23/29: 9519-9528. Available at <http://www.ncbi.nlm.nih.gov/pubmed/14573531>.
- Satoh, J., T. Tabira, M. Sano, H. Nakayama and J. Tateishi (1991) Parvalbumin-immunoreactive neurons in the human central nervous system are decreased in Alzheimer's disease. *Acta Neuropathol* 81/4: 388-395. Available at <http://www.ncbi.nlm.nih.gov/pubmed/2028743>.
- Savva, G. M., B. C. Stephan and Group Alzheimer's Society Vascular Dementia Systematic Review (2010) Epidemiological studies of the effect of stroke on incident dementia: a systematic review. *Stroke* 41/1: e41-46. Available at <http://www.ncbi.nlm.nih.gov/pubmed/19910553>.
- Scarborough, Peter, Vito Peto, Prachi Bhatnagar, Asha Kaur, Jose Leal, Ramon Luengo-Fernandez, Alastair Gray and Mike Rayner (2009) Stroke statistics 2009. *Stroke statistics*.
- Scheibel, A. B. and U. Tomiyasu (1978) Dendritic sprouting in Alzheimer's presenile dementia. *Exp Neurol* 60/1: 1-8. Available at <http://www.ncbi.nlm.nih.gov/pubmed/350599>.
- Schmitz, C. and P. R. Hof (2007) Design-Based Stereology in Brain Aging Research. In D. R. Riddle, ed. *Brain Aging: Models, Methods, and Mechanisms*. In series *Frontiers in Neuroscience*. Boca Raton (FL). Available at <http://www.ncbi.nlm.nih.gov/pubmed/21204353>.
- Schousboe, A., H. M. Sickmann, A. B. Walls, L. K. Bak and H. S. Waagepetersen (2010) Functional importance of the astrocytic glycogen-shunt and glycolysis for maintenance of an intact intra/extracellular glutamate gradient. *Neurotox Res* 18/1: 94-99. Available at <http://www.ncbi.nlm.nih.gov/pubmed/20306167>.
- Seshadri, S., A. Beiser, M. Kelly-Hayes, C. S. Kase, R. Au, W. B. Kannel and P. A. Wolf (2006) The lifetime risk of stroke: estimates from the Framingham Study. *Stroke* 37/2: 345-350. Available at <http://www.ncbi.nlm.nih.gov/pubmed/16397184>.
- Sherman, D. L. and P. J. Brophy (2005) Mechanisms of axon ensheathment and myelin growth. *Nat Rev Neurosci* 6/9: 683-690. Available at <http://www.ncbi.nlm.nih.gov/pubmed/16136172>.
- Shin, J. Y., Z. H. Fang, Z. X. Yu, C. E. Wang, S. H. Li and X. J. Li (2005) Expression of mutant huntingtin in glial cells contributes to neuronal excitotoxicity. *J Cell Biol* 171/6: 1001-1012. Available at <http://www.ncbi.nlm.nih.gov/pubmed/16365166>.
- Silver, J. and J. H. Miller (2004) Regeneration beyond the glial scar. *Nat Rev Neurosci* 5/2: 146-156. Available at <http://www.ncbi.nlm.nih.gov/pubmed/14735117>.

- Simard, M., G. Arcuino, T. Takano, Q. S. Liu and M. Nedergaard (2003) Signaling at the gliovascular interface. *J Neurosci* 23/27: 9254-9262. Available at <http://www.ncbi.nlm.nih.gov/pubmed/14534260>.
- Simpson, J. E., M. S. Fernando, L. Clark, P. G. Ince, F. Matthews, G. Forster, J. T. O'Brien, R. Barber, R. N. Kalaria, C. Brayne, P. J. Shaw, C. E. Lewis, S. B. Wharton, M. R. C. Cognitive Function and Group Ageing Neuropathology Study (2007) White matter lesions in an unselected cohort of the elderly: astrocytic, microglial and oligodendrocyte precursor cell responses. *Neuropathol Appl Neurobiol* 33/4: 410-419. Available at <http://www.ncbi.nlm.nih.gov/pubmed/17442062>.
- Skoog, I., R. N. Kalaria and M. M. Breteler (1999) Vascular factors and Alzheimer disease. *Alzheimer Dis Assoc Disord* 13 Suppl 3: S106-114. Available at <http://www.ncbi.nlm.nih.gov/pubmed/10609689>.
- Skoog, I., A. Wallin, P. Fredman, C. Hesse, O. Aevansson, I. Karlsson, C. G. Gottfries and K. Blennow (1998) A population study on blood-brain barrier function in 85-year-olds: relation to Alzheimer's disease and vascular dementia. *Neurology* 50/4: 966-971. Available at <http://www.ncbi.nlm.nih.gov/pubmed/9566380>.
- Smallwood, A., A. Oulhaj, C. Joachim, S. Christie, C. Sloan, A. D. Smith and M. Esiri (2012) Cerebral subcortical small vessel disease and its relation to cognition in elderly subjects: a pathological study in the Oxford Project to Investigate Memory and Ageing (OPTIMA) cohort. *Neuropathol Appl Neurobiol* 38/4: 337-343. Available at <http://www.ncbi.nlm.nih.gov/pubmed/21951164>.
- Smith, K. (2010) Neuroscience: Settling the great glia debate. *Nature* 468/7321: 160-162. Available at <http://www.ncbi.nlm.nih.gov/pubmed/21068805>.
- Snowdon, D. A., L. H. Greiner, J. A. Mortimer, K. P. Riley, P. A. Greiner and W. R. Markesbery (1997) Brain infarction and the clinical expression of Alzheimer disease: The Nun Study. *Journal of the American Medical Association* 277/10: 813-817. Available at <http://www.scopus.com/inward/record.url?eid=2-s2.0-0031054674&partnerID=40&md5=89cc9e7b1546feb74064da1935da3a46>
- Sofroniew, M. V. (2009) Molecular dissection of reactive astrogliosis and glial scar formation. *Trends Neurosci* 32/12: 638-647. Available at <http://www.ncbi.nlm.nih.gov/pubmed/19782411>.
- Sofroniew, M. V. and H. V. Vinters (2010) Astrocytes: biology and pathology. *Acta Neuropathol* 119/1: 7-35. Available at <http://www.ncbi.nlm.nih.gov/pubmed/20012068>.
- Sojkova, J., L. Beason-Held, Y. Zhou, Y. An, M. A. Kraut, W. Ye, L. Ferrucci, C. A. Mathis, W. E. Klunk, D. F. Wong and S. M. Resnick (2008) Longitudinal cerebral blood flow and amyloid deposition: an emerging pattern? *J Nucl Med* 49/9: 1465-1471. Available at <http://www.ncbi.nlm.nih.gov/pubmed/18703614>.
- Spoendlin, H. (1975) Retrograde degeneration of the cochlear nerve. *Acta Otolaryngol* 79/3-4: 266-275. Available at <http://www.ncbi.nlm.nih.gov/pubmed/1094788>.
- Spruston, N. (2008) Pyramidal neurons: dendritic structure and synaptic integration. *Nat Rev Neurosci* 9/3: 206-221. Available at <http://www.ncbi.nlm.nih.gov/pubmed/18270515>.



- Stephens, S., R. A. Kenny, E. Rowan, L. Allan, R. N. Kalaria, M. Bradbury and C. G. Ballard (2004) Neuropsychological characteristics of mild vascular cognitive impairment and dementia after stroke. *Int J Geriatr Psychiatry* 19/11: 1053-1057. Available at <http://www.ncbi.nlm.nih.gov/pubmed/15481073>.
- Sterio, D. C. (1984) The unbiased estimation of number and sizes of arbitrary particles using the disector. *J Microsc* 134/Pt 2: 127-136. Available at <http://www.ncbi.nlm.nih.gov/pubmed/6737468>.
- Stern, Y., B. Gurland, T. K. Tatemichi, M. X. Tang, D. Wilder and R. Mayeux (1994) Influence of education and occupation on the incidence of Alzheimer's disease. *JAMA* 271/13: 1004-1010. Available at <http://www.ncbi.nlm.nih.gov/pubmed/8139057>.
- Stout, J. C., M. F. Wyman, S. A. Johnson, G. M. Peavy and D. P. Salmon (2003) Frontal behavioral syndromes and functional status in probable Alzheimer disease. *Am J Geriatr Psychiatry* 11/6: 683-686. Available at <http://www.ncbi.nlm.nih.gov/pubmed/14609810>.
- Stuss, D. T., M. P. Alexander, L. Hamer, C. Palumbo, R. Dempster, M. Binns, B. Levine and D. Izukawa (1998) The effects of focal anterior and posterior brain lesions on verbal fluency. *J Int Neuropsychol Soc* 4/3: 265-278. Available at <http://www.ncbi.nlm.nih.gov/pubmed/9623001>.
- Stuss, D. T., D. Floden, M. P. Alexander, B. Levine and D. Katz (2001) Stroop performance in focal lesion patients: dissociation of processes and frontal lobe lesion location. *Neuropsychologia* 39/8: 771-786. Available at <http://www.ncbi.nlm.nih.gov/pubmed/11369401>.
- Sultzer, D. L., H. S. Levin, M. E. Mahler, W. M. High and J. L. Cummings (1993) A comparison of psychiatric symptoms in vascular dementia and Alzheimer's disease. *Am J Psychiatry* 150/12: 1806-1812. Available at <http://www.ncbi.nlm.nih.gov/pubmed/8238634>.
- Takahashi, H., I. Brasnjevic, B. P. Rutten, N. Van Der Kolk, D. P. Perl, C. Bouras, H. W. Steinbusch, C. Schmitz, P. R. Hof and D. L. Dickstein (2010) Hippocampal interneuron loss in an APP/PS1 double mutant mouse and in Alzheimer's disease. *Brain Struct Funct* 214/2-3: 145-160. Available at <http://www.ncbi.nlm.nih.gov/pubmed/20213270>.
- Takeda, A., E. Loveman, A. Clegg, J. Kirby, J. Picot, E. Payne and C. Green (2006) A systematic review of the clinical effectiveness of donepezil, rivastigmine and galantamine on cognition, quality of life and adverse events in Alzheimer's disease. *Int J Geriatr Psychiatry* 21/1: 17-28. Available at <http://www.ncbi.nlm.nih.gov/pubmed/16323253>.
- Tang, W. K., S. S. Chan, H. F. Chiu, G. S. Ungvari, K. S. Wong and T. C. Kwok (2004) Emotional incontinence in Chinese stroke patients--diagnosis, frequency, and clinical and radiological correlates. *J Neurol* 251/7: 865-869. Available at <http://www.ncbi.nlm.nih.gov/pubmed/15258791>.
- Tatemichi, T. K. (1990) How acute brain failure becomes chronic: a view of the mechanisms of dementia related to stroke. *Neurology* 40/11: 1652-1659. Available at <http://www.ncbi.nlm.nih.gov/pubmed/2234420>.
- Tatemichi, T. K., D. W. Desmond and I. Prohovnik (1995) Strategic infarcts in vascular dementia. A clinical and brain imaging experience. *Arzneimittelforschung* 45/3A: 371-385. Available at <http://www.ncbi.nlm.nih.gov/pubmed/7763329>.
- Tatemichi, T. K., M. Paik, E. Bagiella, D. W. Desmond, Y. Stern, M. Sano, W. A. Hauser and R. Mayeux (1994) Risk of dementia after stroke in a hospitalized

- cohort: results of a longitudinal study. *Neurology* 44/10: 1885-1891. Available at <http://www.ncbi.nlm.nih.gov/pubmed/7936242>.
- Tekin, S. and J. L. Cummings (2002) Frontal-subcortical neuronal circuits and clinical neuropsychiatry: an update. *J Psychosom Res* 53/2: 647-654. Available at <http://www.ncbi.nlm.nih.gov/pubmed/12169339>.
- Teodorczuk, A., J. T. O'Brien, M. J. Firbank, L. Pantoni, A. Poggesi, T. Erkinjuntti, A. Wallin, L. O. Wahlund, A. Gouw, G. Waldemar, R. Schmidt, J. M. Ferro, H. Chabriat, H. Bazner, D. Inzitari and Ladis Group (2007) White matter changes and late-life depressive symptoms: longitudinal study. *Br J Psychiatry* 191: 212-217. Available at <http://www.ncbi.nlm.nih.gov/pubmed/17766760>.
- Thal, D. R., U. Rub, M. Orantes and H. Braak (2002) Phases of A beta-deposition in the human brain and its relevance for the development of AD. *Neurology* 58/12: 1791-1800. Available at <http://www.ncbi.nlm.nih.gov/pubmed/12084879>.
- Thind, K. and M. N. Sabbagh (2007) Pathological correlates of cognitive decline in Alzheimer's disease. *Panminerva Med* 49/4: 191-195. Available at <http://www.ncbi.nlm.nih.gov/pubmed/18091671>.
- Tomimoto, H., I. Akiguchi, H. Wakita and J. Kimura (1994) [Changes in glial cells in Binswanger-type infarction]. *No To Shinkei* 46/8: 771-779. Available at <http://www.ncbi.nlm.nih.gov/pubmed/7946634>.
- Trendelenburg, G. and U. Dirnagl (2005) Neuroprotective role of astrocytes in cerebral ischemia: focus on ischemic preconditioning. *Glia* 50/4: 307-320. Available at <http://www.ncbi.nlm.nih.gov/pubmed/15846804>.
- van Rossum, D. and U. K. Hanisch (2004) Microglia. *Metab Brain Dis* 19/3-4: 393-411. Available at <http://www.ncbi.nlm.nih.gov/pubmed/15554430>.
- Vaux, D. L. (1993) Toward an understanding of the molecular mechanisms of physiological cell death. *Proc Natl Acad Sci U S A* 90/3: 786-789. Available at <http://www.ncbi.nlm.nih.gov/pubmed/8430086>.
- Verkhatsky, A., M. V. Sofroniew, A. Messing, N. C. deLanerolle, D. Rempe, J. J. Rodriguez and M. Nedergaard (2012) Neurological diseases as primary gliopathies: a reassessment of neurocentrism. *ASN Neuro* 4/3. Available at <http://www.ncbi.nlm.nih.gov/pubmed/22339481>.
- Verret, L., E. O. Mann, G. B. Hang, A. M. Barth, I. Cobos, K. Ho, N. Devidze, E. Masliah, A. C. Kreitzer, I. Mody, L. Mucke and J. J. Palop (2012) Inhibitory interneuron deficit links altered network activity and cognitive dysfunction in Alzheimer model. *Cell* 149/3: 708-721. Available at <http://www.ncbi.nlm.nih.gov/pubmed/22541439>.
- Vinters, H. V., W. G. Ellis, C. Zarow, B. W. Zaias, W. J. Jagust, W. J. Mack and H. C. Chui (2000) Neuropathologic substrates of ischemic vascular dementia. *J Neuropathol Exp Neurol* 59/11: 931-945. Available at <http://www.ncbi.nlm.nih.gov/pubmed/11089571>.
- Wada, H. (1998) Blood-brain barrier permeability of the demented elderly as studied by cerebrospinal fluid-serum albumin ratio. *Intern Med* 37/6: 509-513. Available at <http://www.ncbi.nlm.nih.gov/pubmed/9678683>.
- Waldvogel, D., P. van Gelderen, W. Muellbacher, U. Ziemann, I. Immisch and M. Hallett (2000) The relative metabolic demand of inhibition and excitation. *Nature* 406/6799: 995-998. Available at <http://www.ncbi.nlm.nih.gov/pubmed/10984053>.

- Walter, J. (2012) gamma-Secretase, apolipoprotein E and cellular cholesterol metabolism. *Curr Alzheimer Res* 9/2: 189-199. Available at <http://www.ncbi.nlm.nih.gov/pubmed/21605030>.
- Walz, W. (2000) Role of astrocytes in the clearance of excess extracellular potassium. *Neurochem Int* 36/4-5: 291-300. Available at <http://www.ncbi.nlm.nih.gov/pubmed/10732996>.
- Wang, J. H. (2003) Short-term cerebral ischemia causes the dysfunction of interneurons and more excitation of pyramidal neurons in rats. *Brain Res Bull* 60/1-2: 53-58. Available at <http://www.ncbi.nlm.nih.gov/pubmed/12725892>.
- Wang, Y., A. Gupta, M. Toledo-Rodriguez, C. Z. Wu and H. Markram (2002) Anatomical, physiological, molecular and circuit properties of nest basket cells in the developing somatosensory cortex. *Cereb Cortex* 12/4: 395-410. Available at <http://www.ncbi.nlm.nih.gov/pubmed/11884355>.
- Wardlaw, J. M., P. A. Sandercock, M. S. Dennis and J. Starr (2003) Is breakdown of the blood-brain barrier responsible for lacunar stroke, leukoaraiosis, and dementia? *Stroke* 34/3: 806-812. Available at <http://www.ncbi.nlm.nih.gov/pubmed/12624314>.
- Weller, R. O., D. Boche and J. A. Nicoll (2009) Microvasculature changes and cerebral amyloid angiopathy in Alzheimer's disease and their potential impact on therapy. *Acta Neuropathol* 118/1: 87-102. Available at <http://www.ncbi.nlm.nih.gov/pubmed/19234858>.
- Werner, P., D. Pitt and C. S. Raine (2001) Multiple sclerosis: altered glutamate homeostasis in lesions correlates with oligodendrocyte and axonal damage. *Ann Neurol* 50/2: 169-180. Available at <http://www.ncbi.nlm.nih.gov/pubmed/11506399>.
- West, M. J. (1999) Stereological methods for estimating the total number of neurons and synapses: issues of precision and bias. *Trends Neurosci* 22/2: 51-61. Available at <http://www.ncbi.nlm.nih.gov/pubmed/10092043>.
- West, M. J., P. D. Coleman, D. G. Flood and J. C. Troncoso (1994) Differences in the pattern of hippocampal neuronal loss in normal ageing and Alzheimer's disease. *Lancet* 344/8925: 769-772. Available at <http://www.scopus.com/inward/record.url?eid=2-s2.0-0028122463&partnerID=40&md5=7619e473d09b6eb888a758febca0c0da>.
- West, M. J. and L. Slomanka (2001) 2-D versus 3-D cell counting--a debate. What is an optical disector? *Trends Neurosci* 24/7: 374; author reply 378-380. Available at <http://www.ncbi.nlm.nih.gov/pubmed/11467286>.
- West, M. J., L. Slomianka and H. J. Gundersen (1991) Unbiased stereological estimation of the total number of neurons in the subdivisions of the rat hippocampus using the optical fractionator. *Anat Rec* 231/4: 482-497. Available at <http://www.ncbi.nlm.nih.gov/pubmed/1793176>.
- Whitwell, J. L., C. R. Jack, Jr., M. Baker, R. Rademakers, J. Adamson, B. F. Boeve, D. S. Knopman, J. F. Parisi, R. C. Petersen, D. W. Dickson, M. L. Hutton and K. A. Josephs (2007) Voxel-based morphometry in frontotemporal lobar degeneration with ubiquitin-positive inclusions with and without progranulin mutations. *Arch Neurol* 64/3: 371-376. Available at <http://www.ncbi.nlm.nih.gov/pubmed/17353379>.
- Whitwell, J. L., C. R. Jack, Jr., B. F. Boeve, M. L. Senjem, M. Baker, R. Rademakers, R. J. Ivnik, D. S. Knopman, Z. K. Wszolek, R. C. Petersen and K. A. Josephs (2009) Voxel-based morphometry patterns of atrophy in FTL D with mutations in

- MAPT or PGRN. *Neurology* 72/9: 813-820. Available at <http://www.ncbi.nlm.nih.gov/pubmed/19255408>.
- Wimo, A., L. Jonsson, J. Bond, M. Prince, B. Winblad and International Alzheimer Disease (2013) The worldwide economic impact of dementia 2010. *Alzheimers Dement* 9/1: 1-11 e13. Available at <http://www.ncbi.nlm.nih.gov/pubmed/23305821>.
- Wolfe, N., R. Linn, V. L. Babikian, J. E. Knoefel and M. L. Albert (1990) Frontal systems impairment following multiple lacunar infarcts. *Arch Neurol* 47/2: 129-132. Available at <http://www.ncbi.nlm.nih.gov/pubmed/2302084>.
- Wong-Riley, Feng Nigh, Robert F. Hevner, Suyan liu (1998) *Cytochrome oxidase in neuronal metabolism and Alzheimer's disease*.
- Wong-Riley, M., B. Anderson, W. Liebl and Z. Huang (1998) Neurochemical organization of the macaque striate cortex: correlation of cytochrome oxidase with Na<sup>+</sup>K<sup>+</sup>ATPase, NADPH-diaphorase, nitric oxide synthase, and N-methyl-D-aspartate receptor subunit 1. *Neuroscience* 83/4: 1025-1045. Available at <http://www.ncbi.nlm.nih.gov/pubmed/9502244>.
- Wong-Riley, M. T. (1989) Cytochrome oxidase: an endogenous metabolic marker for neuronal activity. *Trends Neurosci* 12/3: 94-101. Available at <http://www.ncbi.nlm.nih.gov/pubmed/2469224>.
- Yamamoto, Y., M. Ihara, C. Tham, R. W. Low, J. Y. Slade, T. Moss, A. E. Oakley, T. Polvikoski and R. N. Kalaria (2009) Neuropathological correlates of temporal pole white matter hyperintensities in CADASIL. *Stroke* 40/6: 2004-2011. Available at <http://www.ncbi.nlm.nih.gov/pubmed/19359623>.
- Yang, Y., R. S. Turner and J. R. Gaut (1998) The chaperone BiP/GRP78 binds to amyloid precursor protein and decreases Abeta40 and Abeta42 secretion. *J Biol Chem* 273/40: 25552-25555. Available at <http://www.ncbi.nlm.nih.gov/pubmed/9748217>.
- Yazawa, I., B. I. Giasson, R. Sasaki, B. Zhang, S. Joyce, K. Uryu, J. Q. Trojanowski and V. M. Lee (2005) Mouse model of multiple system atrophy alpha-synuclein expression in oligodendrocytes causes glial and neuronal degeneration. *Neuron* 45/6: 847-859. Available at <http://www.ncbi.nlm.nih.gov/pubmed/15797547>.
- Yu, Z., H. Luo, W. Fu and M. P. Mattson (1999) The endoplasmic reticulum stress-responsive protein GRP78 protects neurons against excitotoxicity and apoptosis: suppression of oxidative stress and stabilization of calcium homeostasis. *Exp Neurol* 155/2: 302-314. Available at <http://www.ncbi.nlm.nih.gov/pubmed/10072306>.
- Zlokovic, B. V. (2011) Neurovascular pathways to neurodegeneration in Alzheimer's disease and other disorders. *Nat Rev Neurosci* 12/12: 723-738. Available at <http://www.ncbi.nlm.nih.gov/pubmed/22048062>.